DEGRADABILITY OF BAMBOO FIBRE REINFORCED POLYESTER COMPOSITES

A dissertation submitted by

Noor Azwa Zulkarnain

006 10 293 55

For the award of

Doctor of Philosophy

2014

Abstract

Fibre reinforced polymer composites made up of synthetic fibres such as glass and carbon have shown outstanding performance in civil engineering load bearing applications. Development in replacing these fibres with natural fibres from plants has recently gained much attention due to the promotion of green-technology. However, the current applications of natural fibre/polymer composites in civil engineering are mostly concentrated on non-load bearing indoor components due to their vulnerability to environmental attack. Their ease to biodegrade becomes a main challenge in the widespread use of these types of materials. In this study, fibre treatment through alkalisation and the application of commercial weather protection coating are suggested to enhance outdoor performance of natural fibre/polymer composite. Bamboo fibre reinforced polyester composites are selected for the current work due to their potential in civil applications. The study is divided into two stages: optimisation of sodium hydroxide (NaOH) treatment on bamboo fibre/polyester composite and the degradability of bamboo fibre/polyester composite. The degradation study involves material exposure to heat, moisture and the combination of both heat and moisture to provide hygrothermal effect.

The test samples comprised of untreated fibre/polyester composite, treated fibre/polyester composite, coated fibre/polyester composite and neat polyester. All composite samples were fabricated using vacuum bagging process on randomly oriented bamboo fibres. To study the optimum fibre treatment using NaOH, bamboo fibres were treated with 0, 4, 6 and 8 wt. % NaOH. Through tensile testing of both fibre and composite, as well as interfacial shear strength study, it was revealed that alkali treatment results in improvement in strength of fibres and fibre/matrix adhesion up to 6 wt. % NaOH concentration due to the decrease in microfibril angle and rougher fibre surface for better interlocking with neat polyester. At higher NaOH concentrations, fibrils were found damaged causing deterioration in these properties. Thus, the optimum concentration of NaOH for bamboo fibre treatment is considered to be at 6%, with 181% and 22% of improvement in fibre tensile strength and interfacial shear strength, respectively. The coating product selected is an acrylic-based weather protection coat, commercially available for outdoor use and it is applied on the optimised NaOH treated composite. The study has shown that the coating provided improved mechanical properties of the composite up to 15.5% for tensile strength and 5.5% for stiffness at room temperature as well as added durability against heat and moisture below 80^0C. Generally, the thermal degradation study involves the use of thermo gravimetric analysis (TGA), dynamic mechanical analysis (DMA) and thermo-mechanical test. From the TGA, it was found that alkali treated fibres decomposed at lower temperatures than the untreated fibres due to the reduction in thermal stability of the cellulosic component of the fibres. For the composites, the decomposition temperature decreased by approximately 7.7% with the addition of the thermally less stable bamboo fibres in the neat polyester, but an approximately 90% increase in charring was observed. The glass transition temperature (T_g) for the composites is approximately 120^0C obtained through DMA. The visco-elastic properties of the composites were found to be better than neat polyester above T_g as the bamboo fibres restrict the molecular movements of the softened resin. Similar findings were observed through the thermo-mechanical test, which was conducted at 40, 80 and 120^0C. As the exposure temperature approaches T_g, the strength of the composites, although reduced, becomes better than neat

polyester, with 331% higher for treated composite due to the presence of fibres which provide restriction to molecular movements of the resin. In comparison with the tensile behaviour of the composites at room temperature, the strength of the composites were found to improve up to 23% at 80^0C, which through scanning electron microscopy (SEM) observations, attributed this to better fibre/matrix adhesion. With the immersion of samples in water, the changes in physical and mechanical properties were observed. Without the addition of fibres into the neat polyester, the resin sample showed better resistance to moisture, with less than 1% of moisture absorption observed in 60 days. The voids observed on alkali treated fibres have influenced the increment on moisture absorption of individual bamboo fibres. However, with better interlocking with neat polyester, the moisture gain and absorption rate of the composites were found to decrease with NaOH treatment, whereby 6% NaOH treated composite achieved 60% less moisture gain than untreated composite. The thickness swelling of the untreated composites showed comparable result with treated composites but a notable improvement was observed with the application of the coating layer, providing 40% additional barrier against swelling. However, the strength of moisture degraded treated and untreated composites were comparable at 22 MPa, both approximately 2% higher than dry samples. This is due to the plasticising effect by free water molecules which was advantageous to the strength of cellulose fibres and also to the increased in interfacial shear strength by fibre swelling which filled the voids at the fibre/matrix interface. With the influence of both moisture and thermal exposure, the Tg was found to decrease which was attributed to the hydrolytic depolymerisation of neat polyester whereby the entanglement between the ester links were cleaved by chemical reaction with water, reducing its T_g from 112^0C to 103^0C. The rate of absorption and swelling were higher in hygrothermal condition for all samples while the strength experienced a 13.6% reduction compared to immersion at room temperature. Through SEM, this was explained by the presence of microcracks on the resin and deterioration of fibre/matrix adhesion. NaOH treatment and coating layer did not play a major role on the moisture absorption and swelling behaviour of the composites in hygrothermal condition.

From this study, it can be concluded that alkali treatment of fibres has the potential to improve the resistance of bamboo fibre/polyester composites against the effects of heat and moisture, depending on how the degradation parameters alter the condition of the fibre/matrix interface. The presence of a good coating system may help increase the durability of the composite but it must be designed specifically for a certain exposure condition to ensure its effectiveness.

Certification of Dissertation

I certify that the ideas, designs and experimental work, results, analyses and conclusions set out in this thesis are entirely my own effort, except where otherwise indicated and acknowledged.

I further certify that the work is original and has not been previously submitted for assessment in any other course or institution, except where specifically stated.

Noor Azwa Zulkarnain
006 10 293 35

_____   _____

Signature of Candidate   Date

Endorsement

_____   _____
Signature of Principal Supervisor Signature of Associate Supervisor

_____   _____
Date   Date

_____
Signature of Associate Supervisor

_____
Date

Acknowledgements

I would like to express my deepest gratitude to all those who were involved in the completion of this thesis. First and foremost, I would like to thank God Almighty for giving me this opportunity and the strength to endure all challenges throughout the completion of this project.

I am deeply indebted to my supervisor, Dr. Belal Yousif whose help, guidance, stimulating suggestions and encouragement had helped me in all the time of the research, experiments and in writing of this thesis. To my associate supervisor, Dr. Allan Manalo, a big thank you for your time and fruitful discussion on the development of the composite fabrication and testing methods which has formed the basis of this research. I would also like to extend my gratitude to my second associate supervisor, Assoc. Prof. Dr. Karu Karunasena for his suggestions and technical support in filling the gaps throughout this study.

To the members of the Centre of Excellence in Engineered Fibre Composites (CEEFC), I greatly appreciate your support, suggestion and friendship. Many thanks to Wayne Crowell, Martin Geach, Mohan Trada, Adrian Blockland and Dr. Francisco Cardona, whose administrative and technical support have made this research possible. The knowledge and experience that they have passed on to me are greatly appreciated.

To my husband, Hizam Shah, whose help and support throughout this project had lightened my burden and worries, and without him, all this might not be possible. A special thanks to him. Last but not least, I would like to thank my beloved parents and sons, whose love and encouragement had enabled me to complete this work. To those whom I failed to mention but have been a great part of this endeavour, thank you very much.

List of Publications

Journals

Azwa, Z. N., Yousif, B. F., Manalo, A. C., & Karunasena, W. (2013). A review on the degradability of polymeric composites based on natural fibres. *Materials & Design*, *47*, 424-442.

Azwa, Z. N., & Yousif, B. F. (2013). Characteristics of kenaf fibre/epoxy composites subjected to thermal degradation. *Polymer Degradation and Stability*, *98*(12), 2752-2759.

Yousif, B. F., Orupabo, C., & Azwa, Z. N. (2012). Characteristics of Kenaf Fiber Immersed in Different Solutions. *Journal of Natural Fibers*, *9*(4), 207-218.

Azwa, Z. N., Yousif, B. F., Manalo, A. C., & Karunasena, W. (*In progress*). Thermal degradation and thermo-mechanical study of bamboo fibre/polyester composites.

Azwa, Z. N., Yousif, B. F., Manalo, A. C., & Karunasena, W. (*In progress*). Physical and mechanical characteristics of bamboo fibre/polyester composites subjected to moisture and hygrothermal conditions.

Refereed Conference Proceedings

Azwa, Z. N., & Yousif, B. F. (2013, August). Thermal degradation study of kenaf fibre/epoxy composites using thermo gravimetric analysis. In *Proceedings of the 3rd Malaysian Postgraduate Conference (MPC 2013)* (pp. 256-264). Education Malaysia.

Azwa, Z. N., Yousif, B. F., Manalo, A. C., & Karunasena, W. (2014, April). Moisture absorption and hygrothermal ageing in bamboo fibre/polyester composite. Composites Australia and CRC-ACS, 7-9 April, Newcastle, Australia.

Contents

Appendix A: Acrylic Coating Technical Data Sheet
Appendix B: Preliminary Study on the Thermal Degradation of Kenaf Fibre/Epoxy Composite

List of Figures

List of Tables

List of Abbreviations

Al(OH)₃	Aluminium hydroxide
AO	Antioxidants
APP	Ammonium polyphosphate
ASTM	American Society for Testing and Materials
BPC-0	0% NaOH treated bamboo fibre/polyester composite
BPC-4	4% NaOH treated bamboo fibre/polyester composite
BPC-6	6% NaOH treated bamboo fibre/polyester composite
BPC-6C	Coated BPC-6
BPC-8	8% NaOH treated bamboo fibre/polyester composite
CO	Carbon monoxide
CO₂	Carbon dioxide
DAP	Diammonium phosphate
DMA	Dynamic mechanical analysis
DTA	Differential thermal analysis
DTG	Derivative thermo gravimetric
FR	Fire retardant
FRC	Fibre reinforced cement
FRP	Fibre reinforced polymer
FTIR	Fourier transform infrared
H₂O	Water
HALS	Hindered amine light stabilizers
HDPE	High-density polyethylene
HIPS	High impact polystyrene
HRR	Heat release rate
IFSS	Interfacial shear strength
KOH	Potassium hydroxide
KSR	Swelling rate parameter
LDI	Lysine-based diisocyanate
LLDPE	Linear low density polyethylene
LLG	Limited life geotextiles
LOI	Limited oxygen index
MAPE	Maleic anhydride
MAPP	Maleic anhydride polypropylene
Mg(OH)₂	Magnesium hydroxide
MLR	Mass loss rate
MPS	Methacryloxymethyltrimethoxy silane
MST	Moisture saturation time
MSW	Municipal solid waste
NaOH	Sodium hydroxide
NP	Neat polyester
PBS	Poly-butylene succinate
PCL	Polycaprolactone
PE	Polyethylene

PHB	Poly-hydroxybutyrate
PLA	Poly-lactic acid
PP	Polypropylene
PVC	Polyvinyl chloride
RH	Relative humidity
rHDPE	Recycled high density polyethylene
RT	Room temperature
SEA	Specific extinction area
SEM	Scanning electron microscopy
SFFT	Single fibre fragmentation test
SFTT	Single fibre tensile test
T_d	Decomposition temperature
T_g	Glass transition temperature
TGA	Thermo gravimetric analysis
THR	Total heat released
TS	Thickness swelling
TTI	Time to ignition
UPE	Unsaturated polyester
US	United States
UV	Ultraviolet
UVA	Ultraviolet light absorber
VTS	Vinyltrimethoxy silane
WF	Wood fibre
WPC	Wood/polymer composites
Wt	Weight
XPS	X-ray photoelectron spectroscopy

Chapter 1 : Introduction

1.1   Introduction

Over recent years, traditional building materials such as concrete and steel are increasingly being replaced by advanced composite materials; for example, fibre reinforced polymers (FRP) and fibre reinforced cement (FRC). It is expected that use of fibre/polymer composites will expand in the near future, due to their advantages: high strength, low weight, corrosion resistance and low maintenance costs (Chen et al. 2011; Ho et al. 2012; Saravanakumar et al. 2013) . Despite these advantages, engineers are being challenged to 'go green' in many aspects of the engineering discipline; this includes finding more environmental friendly processes and innovations in biodegradable or recyclable materials. Municipal solid waste (MSW) landfills represent the dominant option for waste disposal in many parts of the world, with 70% of MSW in Australia being directed to landfills without pre-treatment in 2002 (Laner et al. 2012). According to a recent World Bank report (WorldBank 2012), global urban MSW due to rapid urbanisation has been estimated at 1.3 billion tonnes per year and is projected to increase to 2.2 billion tonnes per year. In Australia, the Department of Sustainability, Environment, Water, Population and Communities (Randell et al. 2014) reported that total waste generated in 2010/2011 was around 48 million tonnes per year, with a total disposal tonnage of about 19.5 million tonnes per year. It was also reported that 18 million tonnes of waste generated is from the construction and demolition industry. An effort to overcome this challenge is to replace synthetic materials with natural materials, such as reinforcements in polymer composites.

Fibres such as hemp, kenaf, jute and bamboo have been studied for their mechanical properties and their potential contribution to composite materials. These natural fibre reinforced composites are finding their way into the construction industry, with wood fibre polymer composites (WPC) leading the way. The production of biocomposites in the European Union for 2012 was reported to be 357,000 tonnes, with a forecast 710,000 tonnes in 2020: 190,000 tonnes of the 2012 production was of WPC in the construction and extrusion industry (Carus et al. 2014). Natural fibre composites production consumes, on average, 40 to 60% less energy than the manufacture of glass fibres (Dittenber & GangaRao 2012). In contrast, natural fibres have some issues and disadvantages when used as reinforcements for polymeric composites (Yousif & Ku 2012). These include: degradability, fire resistance and interfacial adhesion. Therefore, emphasising these issues may improve composite quality and initiate new applications for these attractive materials.

Figure 1.1 shows the number of articles published on the degradation of FRP composites due to moisture, thermal, fire, and ultraviolet (UV) rays over the past 10 years. Although the increment is unsteady, the figure roughly indicates increased interest of researchers on this topic, with natural FRPs less explored. More importantly, the degradation and fire resistance of natural fibres are the main limitations to use in civil engineering applications. As such, there is a need to expand the research on natural fibre/polymer composites regarding their degradability under different environmental conditions.
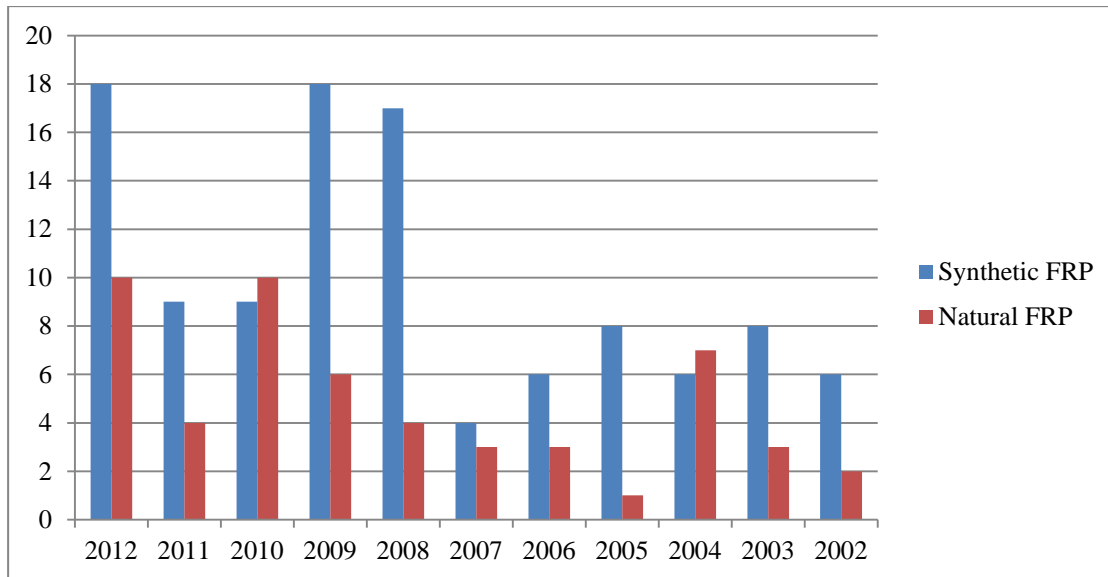
Figure 1.1: Number of journals published on the degradability of synthetic and natural FRP composites due to moisture, thermal, fire and UV exposures

Source: www.sciencedirect.com; Keywords: fibre composites, degradation.

Bamboo is one of the oldest construction materials and is commonly found in countries like India, China and Malaysia. It has potential to be developed in the natural composite industry due to its fast growing rate, high renewability rate, and its abundance in tropical and subtropical regions. Bamboo fibres are considered one of the strongest natural fibres. Along with other natural fibres such as jute, sisal, kenaf, flax and hemp, bamboo is comparable with glass fibre. It is a promising reinforcement material in composite products, due to its combinations of low density, high stiffness and strength (Manalo et al. 2013).

In this study, randomly oriented bamboo fibres were used to reinforce polyester matrices; the resultant composites were exposed to several conditions to study degradation behaviour. These conditions include: elevated heat exposure, high moisture environments and hygrothermal effects due to the combination of heat and moisture. The effects of fibre surface treatments through alkalisation and acrylic coating applications on the composites were also evaluated in terms of their mechanical and physical properties, both before and after degradation. Observations on the fibre/matrix interfaces through SEM were also conducted for all cases to better explain the behaviour of these composites.

It is expected that this study will produce a deep understanding of the degradability of bamboo fibre reinforced polyester composites in outdoor environments. This will be limited to non-load bearing structures such as panels and railings, and how alkali treatments influence these behaviours. These outcomes are anticipated to support the expansion of outdoor applications of natural fibre/polymer composites with improved performance.

1.2   Objectives

The main objective of this study is to evaluate the degradability of bamboo fibre/polyester composites subjected to thermal, moisture and hygrothermal effects.

The specific objectives shall include:
1) To study the effects of different NaOH concentrations (0, 4, 6 and 8 wt.% NaOH) on the physical and mechanical properties of bamboo fibres through morphology, diameter and density observations as well as single fibre tensile test and single fibre fragmentation test. This will lead to the development of an optimised NaOH treatment on bamboo fibres for the fabrication of bamboo fibre/polyester composites with optimum tensile properties, evaluated through tensile test and fibre/matrix adhesion observations.
2) To study the effects of incorporating randomly oriented bamboo fibres, treated and untreated, in polyester resin on its thermal and moisture degradation behaviour as well as its tensile properties after the degradation exposure.
3) To investigate the physical and tensile behaviours of treated and untreated bamboo fibre/polyester composites and neat polyester exposed to both moisture and heat, simulating hygrothermal degradation condition.
4) To assess the compatibility and effectiveness of commercial acrylic coating on the outdoor durability performance, for instance heat and moisture exposures on optimally treated bamboo fibre/polyester composites.

1.3   Project significance

The significance of the outcomes from this research is as follows:
1) The evaluation of different levels of treatment on bamboo fibres is important to understand the individual performance of the fibres and their contribution to the overall behaviour of the composite at different exposure conditions.
2) It is important to thoroughly identify the optimum alkali treatment for bamboo fibres to obtain its optimum mechanical properties as well as interfacial shear strength with neat polyester. This will assist in fabricating a composite with higher strength and stiffness, thus increasing its potential.
3) The findings from the heat exposure at different temperatures on the composites is vital to evaluate whether the fibres improve the properties of neat polyester at high temperatures, such as in hot weather conditions or fire, thus assessing the most advantageous condition.
4) The findings on the composite's moisture response are useful to predict its behaviour in high moisture conditions, such as exposure to humid environments, rain or underwater applications. Understanding the physical and tensile degradations will assist in addressing the composite's limitations.
5) Providing hygrothermal exposure to bamboo fibre/polyester composites is essential to simulate an accelerated weathering environment, with the presence of both heat and moisture. This will present information on the extent of composite degradation in extreme conditions.
6) It is also significant to assess the compatibility of bamboo fibre/polyester composites with commercially available coating products in the market. The findings will promote adaptability of the composite with easily accessible products in increasing its service life.

7) This study is fundamental to gain vital information on the material behaviour of bamboo fibre/polyester composites exposed to outdoor environments. This will promote the expansion of natural fibres in civil engineering applications and support recyclability and green-building technology.

8) Improving the degradability of natural fibres such as bamboo will contribute to the field of sustainable materials. In turn, this will make natural fibres more competitive with synthetic fibres. This will potentially result in high reductions in the cost and power consumption of manufacturing polymeric composites.

1.4 Dissertation organization

This dissertation is divided into seven chapters, as shown in the layout in Figure 1.2. Chapter One comprises a brief introduction to the research idea, highlighting the development of natural fibres as reinforcements in polymeric composites, substituting for synthetic fibres. The research objectives and significance are also explained. Chapter Two presents the literature review relating to natural FRP composites and their degradability issues. Relevant background information, as reported by other researchers, on the behaviour of various natural fibres and their composites is summarised. Focus is given to the durability of these materials subjected to potential outdoor conditions, such as moisture, heat and UV rays. Chapter Three describes in detail the methodology used throughout the study, covering the material selection, fibre alkali treatment and the composite fabrication processes, as well as the experimental programme of the physical, mechanical and degradation testing procedures. Chapter Four covers the preliminary study of the physical, morphological and mechanical behaviour of the composite and its constituents under varied NaOH concentrations. Interfacial adhesion of the fibre with the matrix is also evaluated to obtain the optimum NaOH concentration for treating bamboo fibres. In Chapters Five and Six, the thermal and moisture degradation of the fibre, resin and composites are studied, respectively. Deterioration of mechanical properties from different exposures is presented, and the condition of the fibre/matrix adhesion is observed to further explain the changing behaviour of degraded samples. Chapter Six also focuses on the effect of a hygrothermal environment on the samples. Finally, Chapter Seven concludes all the findings of this research and provides recommendations for possible future developments of natural fibre/polymer composites in outdoor applications.

```
Dissertation Layout

Chapter 1
Introduction

Chapter 2
Literature Review

Chapter 3
Methodology

Sample          Fibre           Experimental
preparation     characterization    details

Chapter 4
Alkali treatment optimisation study on bamboo fibre
and its composite

Chapter 5
Thermal degradation study on bamboo fibre and its
composite

Glass transition              Coating
temperature determination      study

Chapter 6
Moisture degradation study on bamboo fibre and its
composite

Room temperature              Hygrothermal
effect                        effect

Chapter 7
Conclusions and recommendations
```

Figure 1.2: Layout of the dissertation

Chapter 2 : Literature Review

2.1   Introduction

A comprehensive literature review covers different research areas related to natural FRP composites. These areas include: applications, mechanical properties, physical properties, weaknesses and degradation issues in natural fibres and their compatibility with synthetic resins. The comprehensive literature review has been published in an international journal, *Materials and Design*. In the next sections, a brief literature review is introduced, emphasising the most related and important issues regarding the degradation of natural FRP composites.

2.2   Natural fibre reinforced polymer composites and their degradation
2.2.1   The applications and drawbacks of natural fibre composites

The application of natural fibres as reinforcements in composite materials is constantly in development. The drawbacks of its mechanical properties are being studied to maximise the full potential as an alternative to synthetic fibres. Civil infrastructure composites have to resist loadings from tension, compression, impact, fatigue, blast and creep (Hollaway 2010). Presently, natural fibre applications are limited to interior and non-structural applications, due to their poor mechanical properties and poor moisture resistance (Dittenber & GangaRao 2012). It is used in furniture, architectural and more recently, in automotive industries (Araújo et al. 2008). Much effort is currently underway to expand its application; for instance, to the development of continuous sisal fibre reinforced composites that allow the design of thin-walled elements with high strength in tension and compression. Applications may include: permanent formworks, facades, tanks, pipes, long span roofing elements, strengthening existing structures, and structural building members (Silva et al. 2010). The application of natural fibres is also being studied in geotechnical engineering. They have been tested for use in limited life geotextiles (LLG), a reinforcing fabric only required to perform for a limited time. LLG can be applied as temporary roads over soft land, as well as for basal embankment reinforcement (Methacanon et al. 2010).

Using natural fibres as reinforcement in polymer composites has some associated disadvantages. These include: the incompatibility between fibres and polymer matrices; the tendency to form aggregates during processing; poor moisture resistance; inferior fire resistance; limited processing temperatures; lower durability; variation in quality and price; and difficulty in using established manufacturing process (Araújo et al. 2008; Dittenber & GangaRao 2012). The incompatibility between natural fibres and polymer matrices leads to low interface strength, compared to glass or carbon fibre composites. The major cause is the presence of hydroxyl and other polar groups in natural fibres, which makes them hydrophilic. This hydrophilicity results in incompatibility with the hydrophobic polymer matrix (Chen et al. 2009; Dittenber & GangaRao 2012; Shih 2007; Xie et al. 2010). Hydrophilicity of natural fibres indicates the high moisture absorption of the fibres, which is the main reason for weak adhesion to hydrophobic matrices. This causes the produced composites to fail in wet conditions through surface roughening by fibre

swelling or delamination (Araújo et al. 2008; Dittenber & GangaRao 2012). Moisture present during manufacturing also leads to poor processability and low mechanical performance of the composite (Chen et al. 2009). Additionally, the majority of natural fibres have low degradation temperatures (~200°C), which are inadequate for processing with thermoplastics with processing temperatures higher than 200°C (Araújo et al. 2008). Interfacial treatments can improve this condition, either through surface treatments, resins, additives or coatings (Dittenber & GangaRao 2012; Shih 2007).

Although it has been highlighted that natural fibres are cheaper than their synthetic counterparts, some processes related to overcome their drawbacks may incur additional costs. Surface modification is necessary and thus needs to be optimised to compete with glass fibre composites. The cost of natural fibres varies due to crop variability and the difficulty associated with storing, transportation and processing fibres. To promote price reduction, new applications using natural fibres must be developed (Dittenber & GangaRao 2012). Further, a detailed understanding of the composition of natural fibres and the different factors that affect its degradation is required.

2.2.2 Compositions of natural fibres and its effects on degradation

It is necessary to understand the nature and composition of natural fibres, to gain an in depth understanding of degradation. Natural fibres are subdivided based on their origins: from plants, animals or minerals. Figure 2.1 shows the types of natural fibres based on their origins. Animal fibres are composed of proteins taken either from hair, silk or wool (Dittenber & GangaRao 2012; John & Thomas 2008). For structural applications, bast fibres provide the best properties. For example, flax fibres are low cost, light weight and have high strength and stiffness (Dittenber & GangaRao 2012). In numerous applications, natural fibres from plants are considered reinforcements for polymeric composites. Natural fibres from plants can be extracted from the plants' stem or soft sclerenchyma (bast fibres), leaf, seed, fruit, wood or cereal straw.
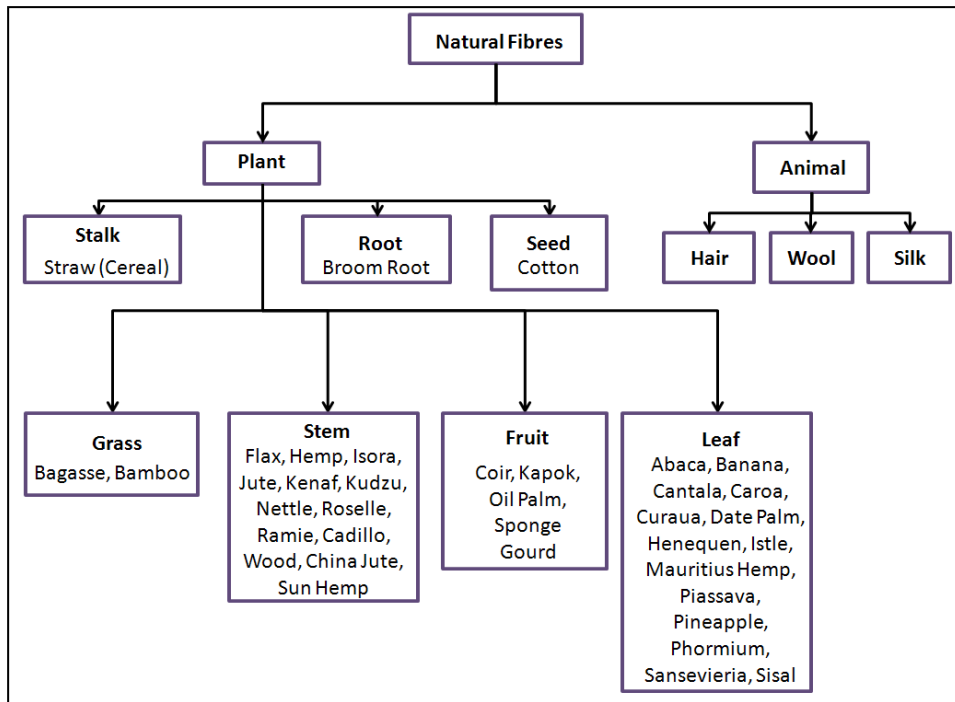
Figure 2.1: Subdivision of natural fibres based on origin, adapted from John and Thomas (2008)

Natural fibres derived from plants consist mainly of cellulose fibrils embedded in a lignin matrix. Figure 2.2 shows a biofibre structure. Each fibre has a complex layered structure, containing one primary cell wall and three secondary cell walls. The thick middle layer of the secondary cell wall determines the mechanical properties of the fibre. It consists of a series of helically wound cellular microfibrils, formed from long chain cellulose molecules. Each cell wall is made up of three main components: cellulose, hemicelluloses and lignin. Lignin-hemicelluloses acts as matrix, while microfibrils (made up of cellulose molecules) act as fibres (Dittenber & GangaRao 2012; John & Thomas 2008). Other components include pectins, oil and waxes (John & Thomas 2008; Wong et al. 2010). The presence of lumen in natural fibres ensures they are hollow structures, unlike synthetic fibres (Liu et al. 2012).
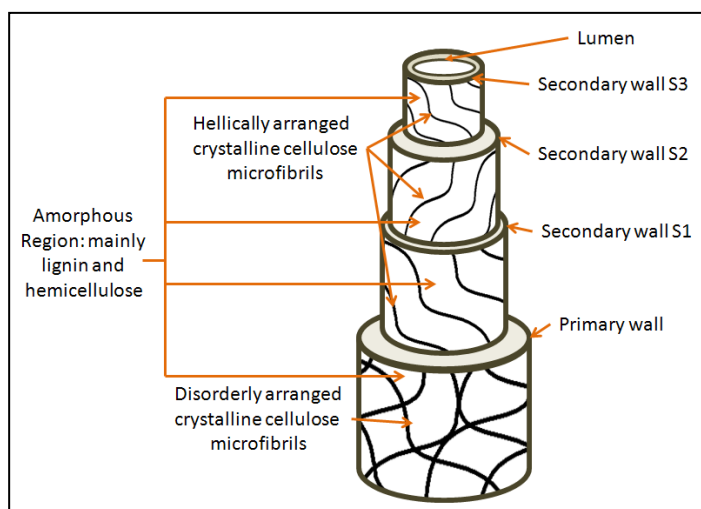
Figure 2.2: Structure of biofibre, adapted from John and Thomas (2008)

The most important structural component in many natural fibres is cellulose, a natural polymer with each repeating unit containing three hydroxyl groups. In plants, cellulose is found in the form of slender rod-like crystalline microfibrils, aligned along the length of fibre. Cellulose is resistant to hydrlolysis, strong alkali and oxidising agents, but to some extent is degradable when exposed to chemical and solution treatments. Hemicelluloses are lower molecular weight polysaccharides that function as a cementing matrix between cellulose microfibrils, forming the main structural component of the fibre cell. It is hydrophilic and can be easily hydrolysed by dilute acids and bases. Lignin is a complex hydrocarbon polymer that gives rigidity to plants and assists with water transportation. It is hydrophobic, resists acid hydrolysis and most microorganism attacks, is soluble in hot alkali, readily oxidised, and easily condensable with phenol. Pectin is a collective name for heteropolysaccarides and gives plants flexibility. Waxes consist of different types of alcohols (John & Thomas 2008; Summerscales et al. 2010). Wax and oil are substances on the fibre's surface that give protection (Wong et al. 2010). Some examples of the chemical compositions of various natural fibres are presented in Figure 2.3.
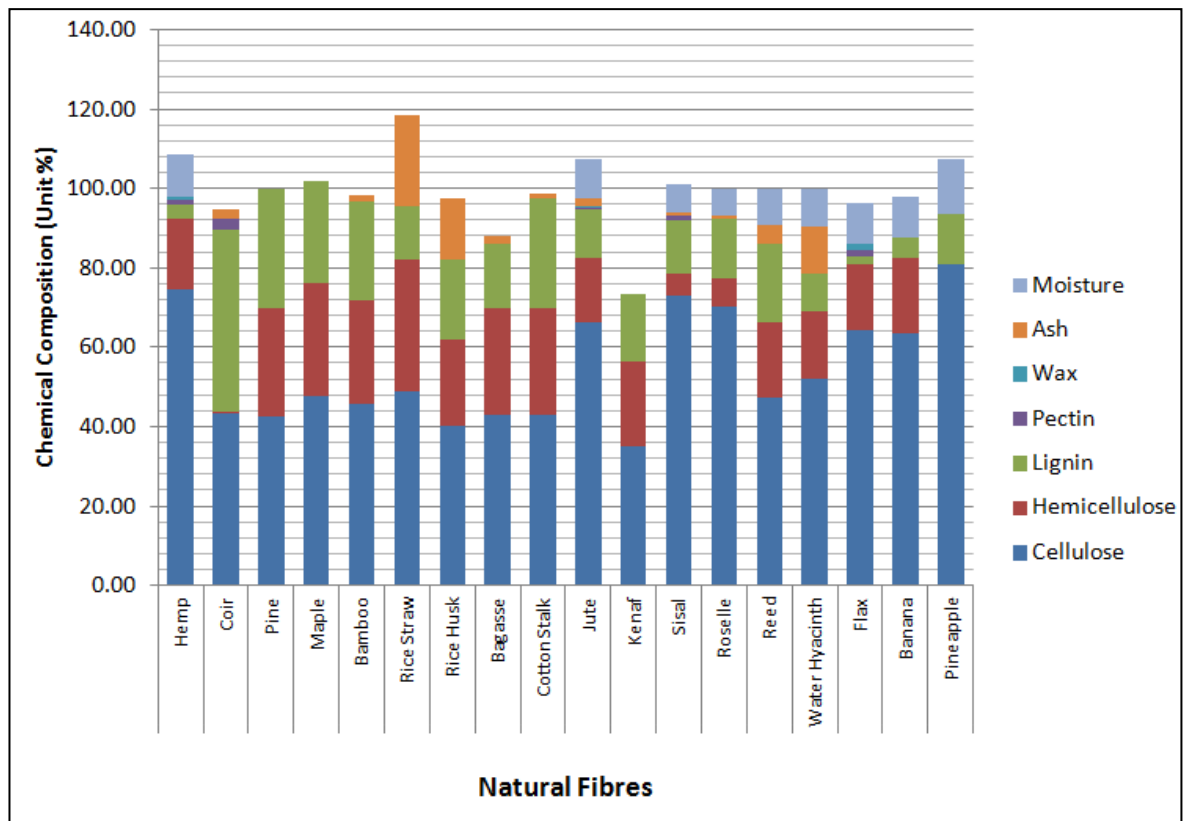
Figure 2.3: Chemical composition of various natural fibres
Sources: Dhakal et al. (2007), Khedari et al. (2005), Yao et al. (2008), Methacanon et al. (2010), Manfredi et al. (2006) and Idicula et al. (2006).

Important variables that determine the overall properties of fibres are its structure, microfibrilar angle, cell dimensions, defects and chemical composition (Dittenber & GangaRao 2012; John & Thomas 2008; Wong et al. 2010). The microfibrilar angle is the angle between the fibre axis and microfibrils with a diameter of 10 to 30 nm. Microfibrilar angles are responsible for the mechanical properties of fibres. Smaller angles lead to higher strength and stiffness, while larger angles provide higher

ductility. Generally, natural fibres with higher mechanical strength possess higher cellulose content, a higher degree of cellulose polymerisation, longer cell length and lower microfibrilar angle. Tensile strength and Young's modulus increases as cellulose content and cell length increase (John & Thomas 2008; Methacanon et al. 2010). Voids are also present in fibres, indicating a certain degree of porosity (Wong et al. 2010; Yousif & El-Tayeb 2009; Yousif et al. 2012). Higher degrees of voids are found in fibres of plants living in wet habitats. This condition promotes higher moisture absorption (Methacanon et al. 2010).

Reinforcing efficiency of natural fibres is related to the nature of cellulose and its crystallinity (John & Thomas 2008). Filaments are bonded into a bundle by lignin and are attached to stems by pectin. Lignin and pectin are weaker polymers than cellulose and must be removed by retting and scotching for effective composite reinforcement (Dittenber & GangaRao 2012).

Natural fibre reinforced composites have a higher risk of degradation when subjected to outdoor applications, compared to composites with synthetic fibres. This is attributed to the characteristics of natural fibres which are susceptible to biodegradation. Biodegradation of a composite occurs with the degradation of its individual constituents, as well as with the loss of interfacial strength between them. Figure 2.4 shows the cell wall polymers responsible for lignocellulosics' properties. Referring to Figure 2.3, we can predict the degradation characteristics of different natural fibres based on their chemical compositions. For example, the tensile strength for jute and hemp are among the highest, 400-800 N/mm^2 and 550-900 N/mm^2, respectively (Sen & Reddy 2011), which can be correlated to their high cellulose content. From a study between water hyacinth, reed, sisal and roselle (Methacanon et al. 2010), it was observed that water hyacinth and reed—fibres with higher hemicellulose contents—absorb more moisture and experience thermal degradation at a lower temperature, compared to sisal and roselle. Another study on flax, jute and sisal fibres showed that degradation of flax fibres begins at a relatively higher temperature, which the author attributes to its low lignin content (Manfredi et al. 2006).
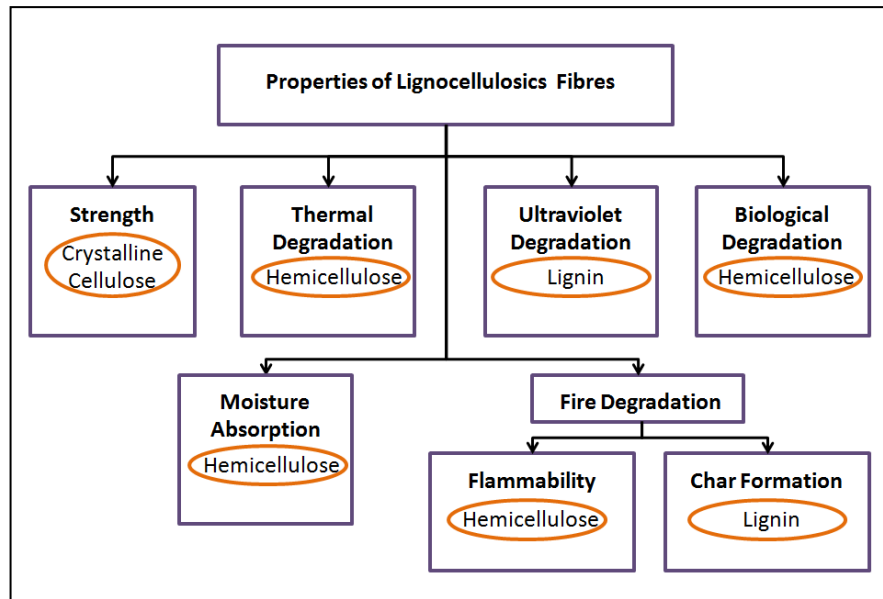
Figure 2.4: Cell wall polymers responsible for the properties of lignocellulosics
Sources: Methacanon et al. (2010), John & Thomas (2008), Beg & Pickerin. (2008), Matuana et al. (2011), Dittenber & GangaRao (2012) and Suardana et al. (2011).

Degradation of natural fibre/polymer composites in an outdoor environment is influenced by factors such as moisture, temperature, UV radiation and microorganism activities. The following sections discuss each factor in depth, except for biodegradation by microorganisms.

2.3 Moisture durability

Polymer composites can absorb moisture in humid atmospheres and/or when immersed in water, especially natural fibre/polymer composites (Shubhra et al. 2011; Yousif & Ku 2012). In turn, this affects the fibre–matrix interface, leading to poor stress transfer efficiencies. Further, moisture absorption by natural fibres affects their physical, mechanical and thermal properties (Dhakal et al. 2007). It has been reported that water absorption for biocomposites is typically 0.7–2% after 24 hours, 1–5% after a week, and up to 18–22% after several months: this behaviour was attributed to the wood fibre chemical compositions having a high hydrophilic content. Natural fibre composites fail in wet conditions through surface roughening by fibre swelling or delamination (Dittenber & GangaRao 2012). The surface morphology of composites affected by moisture absorption is different to that of dry composites in terms of voids, porosity, swelling, sorption in microcracks, and disbanding around filler (Athijayamani et al. 2009).

The fibre component responsible for moisture absorption in natural fibres is the hemicelluloses, which is the plant cell wall associated with cellulose (Methacanon et al. 2010). It consists of comparatively low molecular weight polysaccharides, built up from hexoses, pentoses and uronic acid residues. Higher content of hemicelluloses causes higher moisture sorption and biodegradation. Natural fibre morphology related to hollow cavities decreases bulk density, results in light weight, and absorbs more water. Moisture content in fibre influences the degree of crystallinity, crystalline orientation, tensile strength, swelling behaviour, and fibre porosity. Higher moisture absorption increases the ease of microbial attack (biodegradation).

Cellulose fibres are difficult to dissolve due to their high crystallinity; this enables them to retain liquids in the interfibrillar space. The degree of sorption and swelling obtained are determined by the ability of the liquid to interact with cellulosic fibres (Joseph et al. 2002).

It was observed that water absorption and desorption patterns at room temperature follows Fickian behaviour, where the water uptake process is linear in the beginning; it then slows and approaches saturation after prolonged time. Fickian diffusion refers to the spreading of water from areas of highest to lower concentrations, caused by concentration gradient (Bao et al. 2001). At higher immersion temperatures, moisture uptake behaviour is accelerated and moisture saturation time is greatly shortened. This non-Fickian behaviour has been attributed to the difference in sorption behaviour and state of water molecules existing in the composites (Dhakal et al. 2007; Joseph et al. 2002). The diffusion coefficient characterises the ability of solvent molecules to move among the polymer segments. As the temperature rises in a moist environment, microcracks on the surface and in the bulk of the material develop, leading to peeling and surface dissolution of the composite. This results in an increase in the permeability coefficient (Joseph et al. 2002). Figure 2.5 (a) and (b) show typical graphs of Fickian and non-Fickian diffusion, respectively.
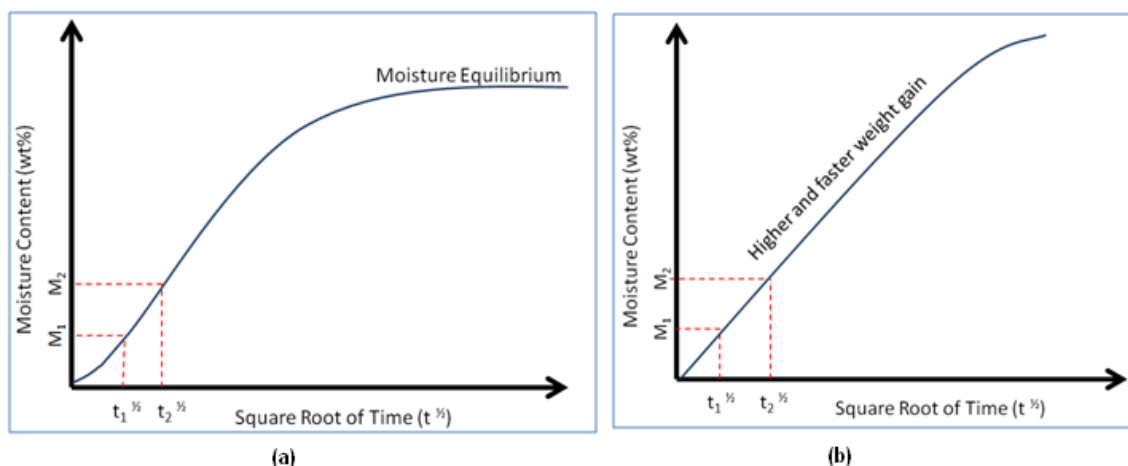
Figure 2.5: (a) Fickian diffusion at room temperature, (b) Non-Fickian diffusion at elevated temperature, adapted from Dhakal et al. (2007)

In a polymer composite, the water transport can be facilitated by three mechanisms: diffusion inside the matrix; imperfections within the matrix (microspace, pores or cracks); and capillarity along the fibre/matrix interface (Assarar et al. 2011; Beg & Pickering 2008). Moisture diffusion into a polymer depends on its molecular and microstructural aspects, which include: polarity, the extent of crystallinity of thermoplastics and the presence of residual hardeners or other water attractive species (Joseph et al. 2002; Wang et al. 2006). The diffusion process of moisture absorption was studied by Wang et al. (2006), focusing on the pattern of electrical conductivity in the composite. The composite studied started showing conductivity after it absorbed approximately 50% of maximum moisture.

Water absorbed in polymers consists of free water and bound water (Chen et al. 2009). Free water refers to water molecules that can move independently through voids, while bound water refers to dispersed water molecules bounded to the

polymers' polar groups. Figure 2.6 shows the conditions of moisture in a polymer matrix.
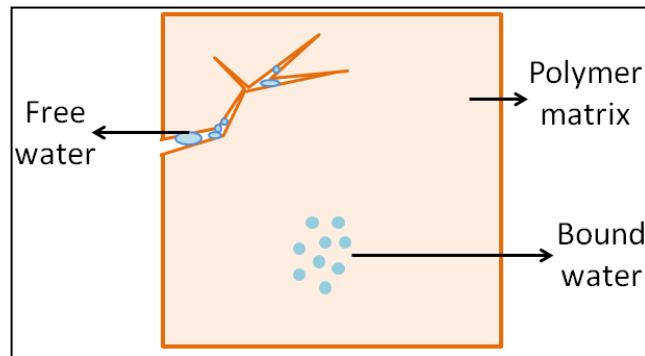
Figure 2.6: Free water and bound water in polymer matrix (Chen et al. 2009)

When a natural fibre/polymer composite is exposed to moisture, water penetrates and attaches onto hydrophilic groups of fibre, establishing intermolecular hydrogen bonding with fibres, and reducing interfacial adhesion of fibre and matrix. Degradation processes occur when swelling of cellulose fibres develops stress at interface regions, leading to microcracking mechanisms in the matrix around swollen fibres. This promotes capillarity and transport via micro cracks. Free water decreases and bound water increases as water is absorbed excessively. Water soluble substances start leaching from fibres and eventually lead to ultimate debonding between fibre and matrix, as reported with hemp fibre reinforced unsaturated polyester (hemp/UPE) composites (Dhakal et al. 2007). Debonding between fibre and matrix is initiated by the development of osmotic pressure pockets at the fibre surface, due to the leaching of water soluble substances from that surface (Joseph et al. 2002). This process is summarised in Figure 2.7. After long period, biological activities, such as fungi growth, degrade natural fibres (Chen et al. 2009). The characteristics of natural fibre composites immersed in water are influenced by the nature of the fibre and matrix materials, by the relative humidity and manufacturing technique, all of which determine factors such as porosity and volume fraction of fibres (Dhakal et al. 2007). The manner in which composite materials absorb water depends upon several factors, such as: temperature, fibre volume fraction, orientation of reinforcement, the permeability nature of fibre, area of exposed surfaces, diffusivity, reaction between water and matrix and surface protection (Joseph et al. 2002).
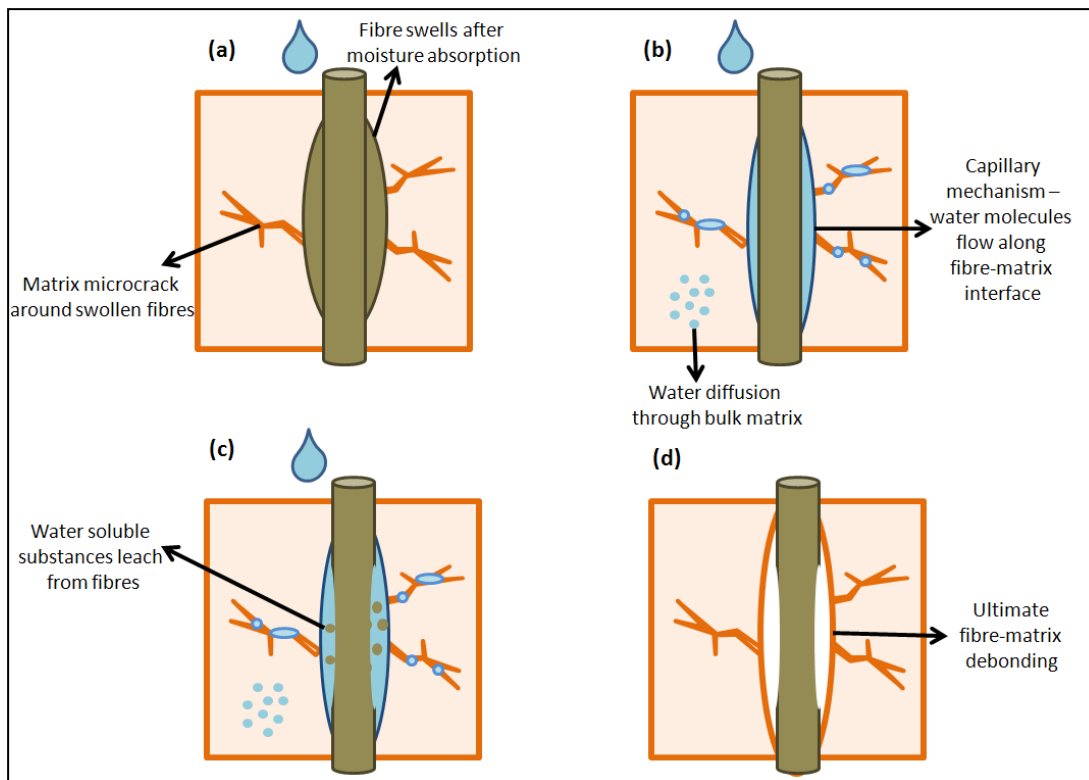
Figure 2.7: Effect of water on fibre/matrix interface (Dhakal et al. 2007)

Natural fibre/polymer composites are sensitive to moisture and with time, moisture exposure causes them to lose functionality. This aspect should be considered in producing a composite that can be used in a high humidity environment. One consideration is the selection of an appropriate fibre to ensure that it possesses the right characteristics for high moisture resistance. At high temperatures, the damage caused by moisture is known to accelerate; thus for composites exposed to this condition, added protection is vital.

2.3.1   Effect of fibre content on moisture absorption

From the literature, it has been reported that the fibre volume fraction influences the amount of moisture absorption and may enhance or worsen the matrix properties. For instance, sisal fibre/cement composites showed that drying shrinkage increases with the presence of sisal fibres, as reported by Silva et al. (2010). The drying shrinkage of a cement matrix is related to the magnitude of its porosity and to the size, shape and continuity of the capillary system in the hydrated cement paste; that is, natural fibres enhance matrix porosity. The porous nature of fibre at a microstructure level creates more moisture paths into the matrices, which leads to higher drying shrinkage. In contrast, the absorption amount increased in poly-lactic acid (PLA) and poly-butylene succinate (PBS) composites as bamboo fibre content increased; this lowered the strength of the PLA and PBS, despite PLA and PBS only being able to absorb about 1% of water. The increase in bamboo fibre content caused the absorption rate to quicken, because of the strong hydrophilicity of bamboo fibres (Lee & Wang 2006). The degradation in mechanical properties of hemp fibre/UPE composite specimens increased with an increased percentage of moisture uptake and was more significant at elevated environmental temperatures. Moreover, the diffusion coefficient values increase steadily with the increase in fibre volume

14

fraction, due to higher cellulose content, as reported with hemp fibre/UPE and sisal fibre reinforced polypropylene (sisal fibre/PP) composites (Dhakal et al. 2007; Joseph et al. 2002). With regard to the mechanical properties of composites under moisture absorption, the results on sisal and roselle fibres reinforced hybrid composites revealed that the percentage reduction in tensile and flexural strength of the composites increased with fibre content and length, when the composites were tested under wet conditions (Athijayamani et al. 2009).

In terms of the age of fibres used, its effect on the resulting composite strength was studied by Mukhopadhyay and Srikanta (2008). They found that the adhesion property of natural fibres was superior with matured fibre, due to the aged fibre having less moisture absorption, possibly because they were kept in air tight containers. Despite these fibres having better strength, composites with aged fibres show better mechanical properties under wet conditions.

Fibres are added to polymers to create a composite that is stronger and less prone to cracks. However, the addition of cellulosic fibres in a polymer composite makes it more susceptible to moisture absorption. As the volume of fibres increase, the rate of moisture absorption also increases. Therefore, for a natural fibre composite to be used outdoors, the fibre content should be limited to attaining the intended strength. This will minimise moisture absorption and increase the durability of composites.

2.3.2   Effect of surface treatment on moisture absorption

Poor adhesion between fibres and the polymer matrix generates void spaces around the fibres in natural fibre composites, which leads to a higher water uptake (Hamid et al. 2012). Fibre modification through the alkalisation process can reduce moisture absorption. Potassium hydroxide (KOH) or sodium hydroxide (NaOH) is commonly used to decrease the hydrogen bonding capacity of cellulose and eliminate open hydroxyl groups that tend to bond with water molecules. It also dissolves hemicelluloses (most hydrophilic), thus reducing the ability of fibre to absorb moisture (Dittenber & GangaRao 2012). These coupling agents build up chemical and hydrogen bonds that reduce the fibre/matrix debonding caused by moisture. This improves the fibre/matrix adhesion and consequently, the composites' moisture resistance. The decreased rate of water absorption and the extent of decrease varies, and depends on the nature of the chemical treatment (Joseph et al. 2002).

Silane treatment is used to stabilise polymer composites reinforced with natural fibres, by treating the fibres to resist against water leaching. Silicon is accumulated in the cell lumina and bordered pits of fibres, plugging these typical penetration pathways for water. Treatment in bulk is more effective than surface coating: the latter only decreases the water sorption rate, but does not reduce the amount of water absorbed as the cell walls are not filled with polymeric silane. In contrast, bulking treatment may reduce the cell wall nano-pore size and deactivate or mask the hydroxyl functionalities, thereby decreasing water sorption (Xie et al. 2010).

Maleic anhydride polypropylene (MAPP) coupling agent was introduced to a bamboo FRP. Moisture uptake by the composite due to immersion in water decreased. This was attributed to the increase in interfacial adhesion, where less water accumulates in the interfacial voids and prevents water from entering bamboo

fibre (Thwe & Liao 2002). Water absorption for PLA/bamboo fibre composite increased greatly during the first 20 hours of immersion and then levelled-off. With the addition of a bio-based coupling agent, lysine-based diisocyanate (LDI), the absorption amount and time to reach the plateau were smaller and longer than without LDI, indicating that the addition of LDI makes the absorption of water difficult. This is a result of improvement in interfacial adhesion between the polymer matrix and bamboo fibres, due to the coupling effect of LDI and the reaction of LDI with the hydroxyl groups of polymers and bamboo fibres, which causes less hydrophilicity (Lee & Wang 2006).

Moisture decreases bond strength by bonding with a fibre's hydroxyl group, lessening the bond with the matrix. Water evaporates, leaving voids in cured composites. For better bonding, fibres must be dried before the matrix is introduced. For short to medium term protection, polymer coatings can be applied to reduce moisture absorption (Dittenber & GangaRao 2012). A short jute fibre/PLA composite was coated with 0.1 mm thick polypropylene plastic adhesive tape and subjected to a hygrothermal environment, as performed by Hu et al. (2010). At the end of the tests, fewer microcracks occurred in the coated sample with lower moisture absorption rates. Temporarily, the coating effectively served as an isolating barrier of moisture diffusion, but the film was still inevitably permeable. Over time, water molecules penetrated the film and were absorbed by the PLA matrix and natural fibre, causing debonding, microcracks and delamination in the coated sample.

Fibre treatments improve moisture durability by reducing fibre hydrophilicity, improving fibre/matrix bonding and/or plugging water penetration pathways in fibre. These treatments done in bulk, are applied throughout the whole composite material and are more effective and long lasting than surface isolation through coating. A combination of these protection systems will give a better moisture resistance, as coating provides a front line defence against moisture penetration, while fibre treatments ensure long-term durability. A maintenance schedule is required to monitor coating effectiveness during a composite's service life, as with steel coating for corrosion protection.

2.3.3 Effect of degradation due to moisture on mechanical properties of composites

A study performed by Methacanon et al. (2010) showed that the maximum tensile strength and elongations for wet yarns from natural fibres are higher than dry ones. This is because moisture in fibre influences the degree of crystallinity and the crystalline orientation of fibres, resulting in higher amounts and better orientation of crystalline cellulose in fibres. Elongation is also higher, as absorbed water molecules act as a lubricant. Fibres could slide over one another during stretching, which results in extra extension and elongation. However, natural fibre reinforced composites face adverse effects when exposed to moisture. This decreases the mechanical properties, provides the necessary conditions for biodegradation, and changes their dimensions (Beg & Pickering 2008; Chen et al. 2009; Wang et al. 2006; Wang et al. 2005). Decrease in mechanical properties was reported to be due to poor stress transfer caused by degradation of the fibre–matrix interface (Beg & Pickering 2008).

The moisture absorption properties of natural fibre composites depend on the filler component. A study by Wang et al. (2006) found that high-density polyethylene (HDPE) films submersed in distilled water at room temperature experience no weight gain after one year, unlike the ones containing rice hull as reinforcements. This shows that moisture only penetrates into composites through rice hulls. The factors affecting fibre distribution will ultimately affect moisture absorption ability. This includes fibre concentration, size and shape. In contrast, Hu et al. (2010) stated that the ageing of biopolymer composites is a chemical and physical interaction process, where water molecules were adsorbed physically by both the matrix and fibres, and were absorbed chemically by polymer molecules. Irreversible weight gain after ageing observed by Hu et al. (2010) in jute fibre/PLA composites subjected to a hygrothermal environment was attributed to the chemical reaction between water and PLA that results in water molecules being permanently absorbed by PLA and transformed into hydrolytic products. This PLA hydrolysis process resulted in molecular chain breakage and caused a decrease in strength.

A study by Joseph et al. (2002) revealed that the tensile properties of sisal/PP composites decreased with increased water uptake, time of immersion and fibre loading. The plasticisation effect of water weakens the fibre/matrix bonding, resulting in interfacial failure. The behaviour was strongly dependent on chemical treatment and fibre orientation, whereby longitudinally oriented composites (anisotropic) provide maximum strength and reinforcement along the direction of fibre alignment as compared with randomly oriented composites.

The tensile strength and modulus of bamboo FRPs were considerably degraded after ageing in water at 25^0C, and further reduced with increased soaking time. The decrease in mechanical properties is due to dissolution of the polymer matrix, debonding of fibre/matrix interface, and degradation of fibres during ageing in water. The composite experienced different swelling and shrinkage of fibres, causing uncoupling at the interface. As moisture levels increase, the modulus of polymers is reduced, presumably through a plasticising process (Thwe & Liao 2002). Commercial decking boards made from approximately 1:1 of rice hull and HDPE absorbed 4.5% moisture after 2000 hour exposure to 93% relative humidity (RH) and 40^0C, under simulated extreme climatic exposure conditions. Moisture content was the major factor causing deformation: swelling and bowing of the boards (Wang et al. 2005).

Studies were done on the effect of moisture on bamboo composites. Bamboo absorbs moisture when it is exposed to humid conditions or immersed in water, due to its structure and composition. Moisture absorption depends on species and treatment conditions (Chen et al. 2009). Water absorption is the main shortcoming when it is used as reinforcement or permanent shutter form with concrete, as untreated bamboo faces dimensional variation due to water absorption. This causes micro and macro cracks in cured concrete. Bamboo as a reinforcing bar suffers dimensional change due to moisture and temperature variations, which severely influences the bond with concrete. Water-repellent treatment is necessary to ensure strength of bonding (Ghavami 2005).

The effect of moisture absorption on bamboo strip vinyl ester composites was studied by Chen et al. (2009). Ground tissue occupies a large proportion of volume in

bamboo strips. This honeycomb structure, with numerous capillary spaces, is ideal for holding water. Bamboo strips undergo anisotropic dimensional expansion as they absorb moisture. A softening effect on the strip is indicated by a consistent increase in breaking strain and a decrease in modulus of elasticity. Increase in tensile strength is due to the availability of free water molecules, providing a plasticising effect that is advantageous to cellulose fibre strength. This result is comparable to a study on Duralin fibre, wherein water uptake is seen to be advantageous for some natural fibres at 66% RH, due to fibre's plasticising effect as a result of the presence of free water (Dhakal et al. 2007).

Higher fibre volume composites immersed in water generally have greater decrement in tensile and flexural properties compared to dry samples. However, it is interesting to note that for certain natural fibres, the ultimate tensile stress of wet samples is higher than that of dry samples. This may be due to fibre swelling causing gaps between the fibre and the polymer–matrix to be filled, leading to an increase in the mechanical properties of the composites (Dhakal et al. 2007).

Based on these studies, it can be said that generally, water absorption by fibres in a natural fibre composite causes degradation to their mechanical properties. An optimum fibre/polymer content ratio is required to achieve optimum composite strength (Thwe & Liao 2002; Wong et al. 2010; Wong, et al. 2010a). This strength will deteriorate when exposed to moisture attack, influenced partly by the fibre volume, length and characteristics. To preserve the strength of a natural fibre/polymer composite, it is essential to protect it from excessive moisture exposure.

2.4   Thermal resistance

A critical technical barrier for widespread use of FRP in structural engineering applications is the material's degree of fire resistance. Additionally, there is limited information available regarding behaviour of FRP under fire. At lower temperatures of 100–200^{0}C, FRPs soften, creep and distort (a degradation of mechanical properties), causing buckling in load bearing structures. It is essential requirement for FRP strengthened concrete structures to meet the minimum strength requirements of non-strengthened concrete structures in fire. Any strength contribution from FRP is ignored in a fire situation (Hollaway 2010). At 300-500^{0}C, polymer matrices decompose, releasing heat and toxic volatiles (Hollaway 2010). Decomposition of burning polymers produces combustible and non-combustible gases, liquids, solids (usually char) and entrained solid particles (smoke). These outcomes may produce hazards such as toxic gases, loss of physical integrity, and melting and dripping, which can provide other ignition sources (Stark et al. 2010). Polyvinyl chloride (PVC) is a self-extinguishing material, but it should be avoided due to toxic generated gases. Polyolefins and HDPE burn and drip when in contact with fire resulting in an instant loss of integrity. However, the addition of fibres improves this behaviour, and the integrity of composites (García et al. 2009).

For natural fibres, flammability is in part due to differences in chemical composition. Higher cellulose content results in higher flammability, while higher lignin content results in greater char formation (Dittenber & GangaRao 2012; Suardana et al. 2011). The presence of silica or ash provides better fire resistance. In terms of the fibre

microstructure, high crystallinity and lower polymerisation improve fire resistance. Phenolic-based synthetic composites have low flammability, less smoke, low flame spread, high ignition delay, low peak heat release rate, and a high oxygen index. Char during fire exposure protects the material core, thereby increasing structural integrity. This is the best matrix for natural fibre (Dittenber & GangaRao 2012). Flax fibres have low lignin content and are considered best for thermal resistance among the natural fibres studied. During thermal decomposition of lignin, relatively weak bonds break at lower temperatures, whereas cleavage of stronger bonds in the aromatic rings takes place at higher temperatures. With lower lignin content, degradation begins at a higher temperature, but fibres do not have the oxidation resistance given by aromatic rings in the lignin (Manfredi et al. 2006).

The burning process is comprised of heating, decomposition, ignition, combustion and propagation. Flame retardation can be achieved by interfering with any of these stages, terminating the process before actual ignition occurs (Sain et al. 2004). A few methods are available to improve the fire resistance of natural fibre composites. Fire barriers that can be applied are ceramics, intumescents, silicone, phenolics, ablatives, glass mats and chemical additives. Intumescent systems (coatings/additives) are the most promising fire barrier treatments, as they foam and expand when heated, forming a cellular, charred surface that protects underlying material from heat flux/flame. The best potential for flame retarding of natural FRP is by combining char-forming cellulosic material with intumescent system (Dittenber & GangaRao 2012). It is possible to minimise combustion generation of natural FRP by increasing its polymer stability or by encouraging char formation. This will reduce visible smoke, decrease flammability and limit the volume of combustion products formed (Manfredi et al. 2006). Other methods for improving fire resistance of composites include fire retardant coating of the composites at the finishing stage; and impregnation or modification of lignocellulosic particles or fibres with fire retardants before the manufacturing process (Suardana et al. 2011).

Polymer alone, when exposed to high temperatures, behaves poorly and becomes very hazardous. Fibre is introduced to improve this condition; however, with natural fibres, the improvement is limited due to the characteristics of the fibres, which are more flammable than synthetic fibres. Many methods can be introduced to increase the durability of composites against thermal degradation. Method selection may be influenced by cost and the degree of resistance.

2.4.1   Thermal degradation of natural fibre composites

There are a few methods chosen by researchers to study the behaviour of natural fibre composites in a fire situation. This section discusses cone calorimeter and the TGA method to measure the thermal degradation of natural fibres.

2.4.1.1 Cone calorimeter

Cone calorimeter is widely used for assessing the flammability of polymer materials, by exposing samples to a specific radiant flux. It can be used to measure heat release rate (HRR), total heat released (THR), mass loss rate (MLR), time to ignition (TTI), smoke emission (specific extinction area, SEA), and average carbon monoxide (CO) and carbon dioxide (CO_2). Lower HRR indicates a smaller contribution to a fire (Stark et al. 2010; Zhang et al. 2012). Shubhra et al. (2010) had adopted a comparative study regarding loss of composites' mechanical properties during thermal ageing by heating composite samples at 50^0C for 30 days in an oven. The loss of tensile strength was measured periodically; the loss increased with heating time. The magnitude of reduction depends on the moisture content, heating medium, exposure period and fibre species. Single flame fire or flame propagation tests were performed by García et al. (2009) to study the burning speed of composites. Flame was applied for 5 seconds; the time to burn 45 mm length specimens was determined. The limiting oxygen index (LOI) test measures the minimum concentration of oxygen required to support flaming combustion of a material in a flowing mixture of oxygen and nitrogen, calculated using Equation 2-1 (Zhang et al. 2012):

$$LOI\ (\%) = [\frac{Volume\ of\ oxygen}{Volume\ of\ nitrogen} + Volume\ of\ oxygen] \times 100 \qquad \text{Equation 2-1}$$

Oxygen concentration reported is its volume percentage in a mixture of oxygen and nitrogen (Fatima & Mohanty 2011). LOI test does not predict how a material will perform in a fire, but does compare between materials, whereby higher OI suggests better fire performance. The LOI of natural fibre is higher than that of polymer, suggesting that natural fibres may be easier to extinguish in a fire than polymers, due to the higher concentration of oxygen required to sustain burning (Stark et al. 2010; Zhang et al. 2012). Smoke density in the process of burning samples was measured by the change of light intensity in a chamber. It is useful for measuring and observing the relative amounts of smoke obscuration produced by burning or decomposition of material (Fatima & Mohanty 2011).

2.4.1.2 Thermogravimetric analysis

TGA is used to study the thermal stability of natural fibres. A typical TGA curve for composite thermal degradability shows a sample subjected to heat will slowly suffer weight drop, then the weight will drop sharply over a narrow range and finally turn back to zero slope as the reactant is exhausted. The shape of the TGA curve is determined by the kinetic parameters of the pyrolysis, such as reaction order, frequency factor and activation energy, while the values obtained depend upon atmosphere, sample mass, sample shape, flow rate, heating rate and the mathematical treatment used to evaluate the data. Theoretically, when a reaction occurs in a differential thermal analysis (DTA), the change in heat content and in the sample's thermal properties is indicated by a deflection or peak. If the reaction proceeds at a rate varying with temperature (indication of activation energy), the position of the peak varies with the heating rate if other experimental conditions are fixed. This variation in peak temperature could be used to determine the energy of activation for different reaction orders (Alvarez & Vázquez 2004). In short, TGA and derivative thermo gravimetric (DTG) curves determine weight loss and identify the decomposition of material at a certain temperature, respectively (Suardana et al.

2011). A typical thermo gravimetric graph for the decomposition process of natural fibres is shown in Figure 2.8.
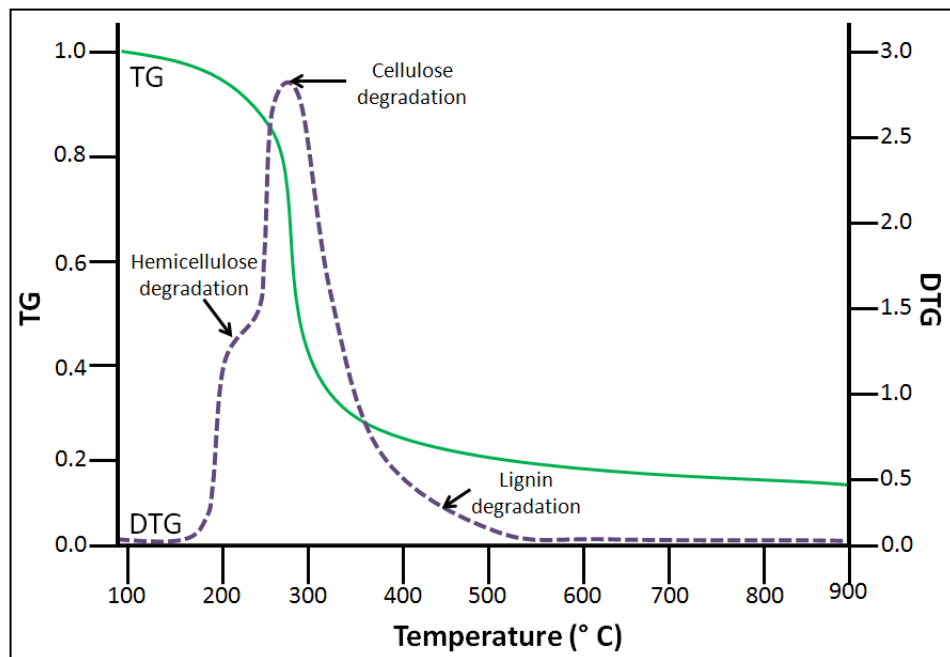
Figure 2.8: Typical thermo gravimetric decomposition process of natural fibres
Sources: Lee & Wang (2006), Suardana et al. (2011) and Fatima & Mohanty (2011).

Thermal decomposition processes of different lignocellulosic fibres have very similar TG and DTG curves, due to similar characteristics. Approximately 60% of the thermal decomposition of most natural fibres occurs within a temperature range between 215 and 310^0C, with an apparent activation energy of 160-170 kJ/mol (Yao et al. 2008). Thermal degradation behaviour can be evaluated through the decomposition temperature (T_d). For studied fibres by Methacanon et al. (2010), the T_d is at 290-490^{0}C. Based on Beg & Pickering (2008), the degradation process of natural fibres includes dehydration combined with emission of volatile components initiating at a temperature of about 260^0C, and rapid weight loss due to oxidative decomposition, corresponding to the formation of char as the temperature increases. Early decomposition shows less thermal stability (Methacanon et al. 2010). Three main stages of weight loss of natural fibres during fire, as highlighted by a few researches, are presented in

Table 2.1.

Table 2.1: Three main stages of weight loss of natural fibres

Stage 1	Stage 2	Stage 3	Reference
50-100^{0}C: Evaporation of moisture in the fibres.	200-300^{0}C: Decomposition of hemicelluloses.	400-500^{0}C: Weight loss due to lignin and cellulose degradation.	(Methacanon et al. 2010)
300^{0}C: Corresponds to the thermal decomposition of hemicellulose and the glycosidic links of cellulose.	360^{0}C: Corresponds to the thermal decomposition of α-cellulose.	200- 500^{0}C, max at 350^{0}C: Lignin peak is wider and appears superposed on the other two peaks.	(Alvarez & Vázquez 2004; Araújo et al. 2008; Manfredi et al. 2006)
250-300^{0}C: Characteristic of low molecular weight components, such as hemicelluloses.	300-400^{0}C: Corresponds to the thermal degradation of cellulose.	Near 420^{0}C: Due to lignin decomposition.	(Lee & Wang 2006)
220–315^{0}C: Pyrolysis of hemicelluloses.	315–400^{0}C: Pyrolysis of cellulose.	160–900^{0}C: Pyrolysis of lignin.	(Suardana et al. 2011)
97^{0}C: Attributed to water loss.	325^{0}C: Attributed to protein degradation.	Major thermal decomposition of the composites began at about 260^{0}C and beyond 390^{0}C the rate of decomposition was slow.	(Shubhra et al. 2011) For natural silk fibre reinforced gelatin composites.

Thermal degradation of composites can also be studied through TGA. The parameters obtained can be used during processing for determining the degree of degradation of materials when they are processed (Alvarez & Vázquez 2004). The main decomposition range of various natural fibres studied by Yao et al. (2008) overlaps with the processing temperatures of some thermoplastics. Temperature plays a significant role in the dimensional stability of natural fibre composites, where it causes direct thermal expansion or contraction, and by affecting the rate and amount of moisture adsorption that will lead to fibre swelling (Wang et al. 2005). To some extent, thermal degradation of polyethylene/cellulose composites during processing undergoes an oxidation process, which results in enhanced adhesion between polymer and cellulose fibres (Abu-Sharkh & Hamid 2004).

TGA curves were plotted by Lee and Wang (2006) to analyse the thermal degradation of PLA/bamboo fibre composites, and PBS/bamboo fibre composites and their components. The thermal degradation of biopolymers, PLA and PBS show a single stage and occurred at 376^{0}C and 405^{0}C, respectively. The thermal degradation of bamboo fibre is shown in

Table 2.1. The composites for both polymers with bamboo fibre have lower degradation temperatures than the pure polymers (Lee & Wang 2006). For a given heating rate of a biopolymer composite, the temperature at the maximum degradation rate shifts slightly to higher values, as sisal fibre content increases. This has been attributed to the decrease in starch content in the composite (Alvarez & Vázquez 2004). With increased weathering time, TGA curves are shifted to lower temperatures, showing a decrease in thermal stability for both pure polypropylene (PP) and its composites. The decrease in thermal stability of PP could be due to the reduction of PP's molecular weight. For the composites, TGA transitions were shifted to slightly lower temperatures after 1000 hour weathering. This could be the result of PP chain scission along with degradation of both the fibre and the fibre–matrix interfacial bonding (Beg & Pickering 2008).

With the addition of fire retardants (FRs) (ammonium polyphosphate and silica), the thermal decomposition steps were altered as follows (Zhang et al. 2012):

Stage 1: Decomposition is accelerated, with generation of volatile compounds (ammonia and H_2O), a phosphorus rich layer and more char residual, which could protect the polymer matrix against heat.

Stage 2: Char layer shows heat insulation properties and inhibits the heat and mass transfer between surface and melting polymer, resulting in the increase of composite fire resistance, so the second decomposition is shifted to higher temperature.

The main problem for quantitative analysis in TG experiments is the overlap of peaks (particularly in the case of composites) of DTG curves, as shown in Figure 2.9. For example, research on sisal fibre reinforced polycaprolactone/starch (PCL/S) composites by di Franco et al. (2004) shows at least four peaks were obtained: a large first peak (191-230^{0}C) represents loss of low molecular weight components; the second peak (T_{max} = 311^{0}C) may be assigned to starch, plus the contributing overlapping of the first peak of the sisal fibre (hemicellulose); the third shoulder at T_{max} = 354^{0}C is attributed to the second peak of sisal fibre (attributed to cellulose); and the fourth and main peak corresponds to the degradation of PCL. These partially overlapping decomposition curves of the biodegradable matrix and sisal fibre are attributed to the components of each compound, which are starch and cellulose derivatives from the matrix, and lignin, hemicellulose and cellulose from the fibre (Alvarez & Vázquez 2004).
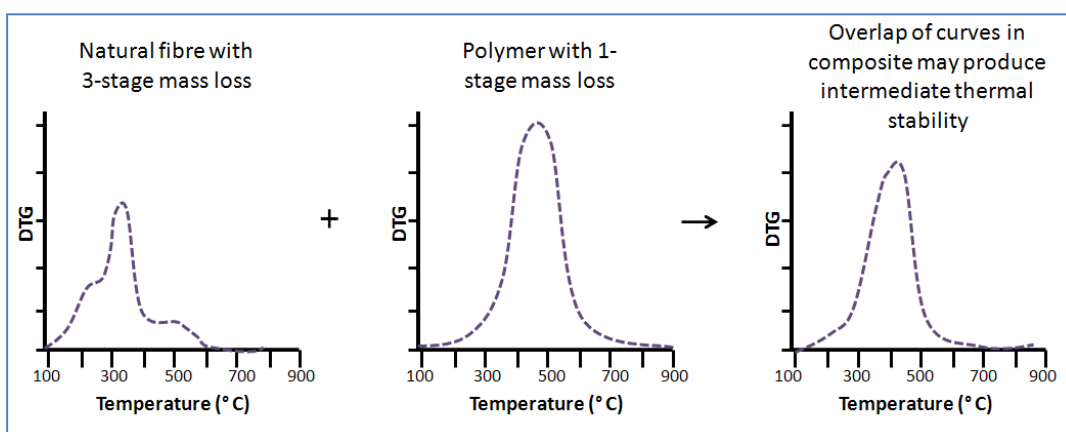
Figure 2.9: Curve overlap in TG Analysis of natural fibre/polymer composite
Sources: Suardana et al. (2011), Alvarez & Vázquez (2004) and di Franco et al. (2004).

It is important to identify the type of information required to choose the most suitable test methods. TGA is widely used by most researchers to study the thermal degradation of natural fibre composites. Early decomposition, observed by lower temperatures at the start of degradation, implies less thermal stability. This can be used to compare the thermal performance of various composites.

2.4.2   Effect of surface treatment on thermal degradation

The biocomposites studied by Lee and Wang (2006) were mixed with a bio-based coupling agent, LDI. Although lower than the pure polymers, the thermal degradation temperature was increased by increasing LDI content. The increase of molecular weight by cross-linking reactions between the matrix and bamboo fibre, or molecular chain-extension of the matrix itself, could have influenced the increase of thermal degradation temperature.

A study on jute/HDPE composites treated with a coupling agent, maleic anhydride (MAPE), shows higher temperatures in the first degradative process than in the composites without a coupling agent; in addition, the percentage of weight loss in both degradation processes was also lower than in the untreated composites. MAPE in the composites ensures better thermal stability, as compatibilised composites present more interfacial interaction due to reactions between acid groups of the maleic anhydride groups and hydrophilic groups on the fibre's surface. This larger interaction promotes greater interaction between the degradation processes of the two components, whereby degradation of one component may accelerate degradation of the other component (Araújo et al. 2008).

A study on the thermal stability of unbleached and bleached composites was undertaken by Beg & Pickering (2008). They found that unbleached fibre composites began decomposing earlier than bleached fibre composites. Residual lignin and hemicellulose contents decreased with bleaching, supporting the increase in thermal stability. However, unbleached fibre composites have greater amount of residue due to higher amounts of lignin, contributing to char formation. This insulates them against further thermal degradation.

From the studies above, it can be concluded that surface treatment improves thermal performance of natural fibre/polymer composites. It is important to note that higher lignin content in untreated fibres produces more char. The optimum degree of lignin removal can be studied further to evaluate the positive contribution of lignin in forming chars, as well as its negative impact on low temperature degradation.

2.4.3   Effects of fire retardants

The most widely used method to acquire flame retardation is incorporating FRs. Depending on the nature of the additives, they can act chemically or physically in the solid, liquid or gas phase (Sain et al. 2004), although most are particles or powders (Stark et al. 2010). To improve fire performance of natural fibre/polymer composites, FRs can be added to the plastic melt during processing (Stark et al. 2010). FRs for biocomposites should be temperature resistant to avoid decomposition during processing (Hamid et al. 2012) and should not contain any halogen. These

compounds produce toxic gases like those formed during PVC combustion (García et al. 2009). Halogen-based and phosphorus-based compounds prove effective in suppressing the flame behaviour of synthetic polymers at the expense of negative environmental effects and health concerns (Hamid et al. 2012). An anatomy-based system on its own is not fire resistant, but show synergistic effects with halogenated compounds. The use of organic FRs can produce high toxic products after thermal decomposition and combustion. Nano-composites constitute a new development in flame retardation, but is very expensive and thus not suitable in commodity products like construction elements (Stark et al. 2010). A small amount of nano-clay can significantly improve the flame retarding properties of wood fibre reinforced HDPE nano-composites (Zhang et al. 2012).

To produce safe composites, FRs should be selected from phosphorus (this contradicts Hamid et al. (2012)) and inorganic systems like borates, stannates or hydroxides (Stark et al. 2010). For environmental and health safety reasons, increasing attention on inorganic compounds such as metallic hydroxide additives are being considered as FRs (Sain et al. 2004). Stark et al. (2010) stated that the most effective additives in producing flame retardants are compounds containing bromine, chlorine or phosphorous, or two or more of these elements. Other elements that have exhibited some flame retardant effects include antimony, boron, nitrogen, silicon, dicyanodiamide, ammonium and zinc; these are often used with phosphorous or halogenated compounds (Sain et al. 2004; Stark et al. 2010).

Additive-type flame retardants improve fire performance through the following mechanisms (Stark et al. 2010):
a) Redirect decomposition and combustion reactions towards the evolution of non-combustible gases, or heavy gases that interfere with the interchange of combustion gases and air.
b) Redirect the decomposition and combustion reaction towards reducing the heat of combustion.
c) Maintain physical integrity of the material.
d) Increase the specific heat or thermal conductivity.

However, it must be noted that FR worsened the outdoor durability (García et al. 2009); thus, an optimum blend ratio should be employed to achieve a balance between the strength and fire safety of composites. Addition of FRs and other additives like antioxidants affects the interfacial adhesion, orientation and dispersion of fillers in the polymer matrix (Hamid et al. 2012). Some FRs, and their mechanism of flame retardance, are summarised in Table 2.2.

Table 2.2: Fire retardants and their mechanism of flame retardation

Fire Retardant	Description
Phosphorous compounds Example: Ammonium polyphosphate Sodium phosphate	• An intumescent material, char formers (García et al. 2009) and leads to auto-extinguishing behaviour. • Generation of solid form of phosphoric acid, inhibits access to oxygen and shields it from releasing flammable gases able to feed flames (Stark et al. 2010; Zhang et al. 2012). • Only increase char in polyolefins when there is another char-forming additive present, typically a nitrogen containing compound (phosphorous-nitrogen synergism) (Stark et al. 2010). • Ammonium polyphosphate: water soluble, not suitable for products exposed to exterior environments (Stark et al. 2010).
Bromine-based compounds Example: Decabromodiphenyl oxide	• Act in the condensed phase to redirect or terminate chemical reactions involved in combustion. Heavy-bromine gases protect the material from exposure to oxygen and heat. Bromine-based flame retardants are practically always used with an antimony synergist, often antimony trioxide (Stark et al. 2010).
Antimony- based compounds Example: Antimony trioxide	• The compounds alone do very little, but in combination with halogens form antimony trihalides. Antimony trihalides both scavenge free radicals and increase char formation (Stark et al. 2010).
Metal hydroxides Examples: Aluminium-based Magnesium-based	• An inorganic compound thus health and environmentally safe (Sain et al. 2004). • More effective as hydrated compounds (Stark et al. 2010) and provide effective flame retarding effects by releasing contained water at high temperatures, absorbing heat from the combustion zone, producing char, generating metal oxide coating that act as insulator and reducing smoke (Stark et al. 2010). • $Mg(OH)_2$ has superior endothermic flame retarding reaction and are more suitable for polyolefins, polypropylene and polyamides because it decomposes at a higher temperature (300–320 °C) thus allowing it to be processed in plastics, for which $Al(OH)_3$ (decomposition temperature: 200 °C) is not thermally stable enough (Sain et al. 2004).

<u>Boron-based compounds</u> Example: Zinc borate	• Are generally char producers. • Zinc borate compounds reduce smoke production and are mostly used as hydrates. • The heat required for dehydration also contributes to fire retardant capability (Stark et al. 2010).
<u>Melamine-based compounds</u> Example: Melamine cyanurate	• Aids in char formation. • Compounded with phosphates to achieve a phosphorous-nitrogen synergism. • Creates endothermic reactions and scavenges free radicals. Decomposition produces nitrogen and ammonia, which dilutes fuel gases (Stark et al. 2010). • Melamine cyanurate: undergoes endothermic decomposition above 320°C to melamine and cyanuric acid, acting as a heat sink in the process. Vaporised melamine acts as an inert gas source diluting the oxygen and the fuel gases present at the point of combustion (Stark et al. 2010).
<u>Silica</u>	• Recognized as inert diluents and shows some flame retardant effect. • Synergistic effect with APP, accumulate on the surface in fire and consequently forms a charred layer by combining with APP. Smoother and more compact char is formed which prevents heat transfer and transportation of degraded products between melting polymer and surface (Zhang et al. 2012).
<u>Halogenated compounds</u>	• Function primarily by a vapour phase flame inhibiting mechanism through radical reaction (Sain et al. 2004).

The addition of 9% FR in a study by García et al. (2009) showed no bubble formation during burning, and the rate of flame spread was much slower than specimens without FR. Only the external surface of the specimens was burnt, while the internal zone was not altered. A blend of sodium metasilicate and zinc borate in solid form was used as a fire retardant by Shubhra et al. (2010) in hybrid biocomposites reinforced with rice husks and sawdust. The TG curves for composites with FRs have higher temperature curves than the samples without fire retardants. This improved fire retardation was attributed to the thermal shielding and diffusion barrier effects yielded by the effective silica layer formed during the combustion process, together with the addition of flame retardant agents that slow the propagation of the burning reaction. The high silica content in rice husks may also contribute synergistically (Shubhra et al. 2010). Fibres treated with diammonium phosphate (DAP) used in biocomposites show a decrease in burning rate and weight loss rate. Exposure to heat below the decomposition temperature of cellulose ($<160^0$C) formed phosphoric acid and ammonia. Phosphoric acid can phosphorylate the primary hydroxyl group of cellulose to form a phosphorus ester that catalyses the dehydration of cellulose, promoting char formation and water at the expense of levoglucosan. The char residues increase with increased DAP treatment. The acid may also crosslink with the cellulose, changing the normal pathway of pyrolysis to yield less flammable products. Untreated fibre composites disintegrated completely and formed ash after glowing. For PP composites, the addition of DAP showed poor compatibility between DAP on the fibre surface and PP, due to absence of chemical interaction; hence, lowering the composite's mechanical properties (Suardana et al. 2011).

At higher loading of flame retardant, the mechanical properties of the composites tend to decrease. Shubhra et al. (2010) observed that biocomposites added with 0.5% AOs and 20% FRs contents gave the best dispersion of hybrid fibres in the matrix, leading to high performance in both physical and mechanical properties. A study by Ayrilmis et al. (2012) observed that water resistance of uncoupled WPCs significantly decreased with increasing FR content but improved with the addition of MAPP. At 6 wt. % MAPP, the negative effect of 12 wt. % FR suppressed the compatibility between wood fibre and polymer due to a high contamination of the wood surface by the crystalline deposits of the FR, as shown in Figure 2.10. The severity of wood surface contamination increases with increasing volumetric percentage of FRs, indicated by a decrease in particle density. It was observed that phosphate treatments provided more improvement in fire performance than the boron treatments. WPC containing 4% FR and 2% MAPP produced optimum physical and mechanical properties. The addition of ammonium polyphosphate (APP) and silica as FRs in WPC showed a decrease in tensile strength and elongation at break. This could be attributed to the poor compatibility of the added FR with polymer, the existence of the cavities formed via thermal decomposition of fillers and release of steam during the process, and larger size of silica agglomerates at higher loading levels that act as stress concentrators and mechanical failure points, initiating fracture of the specimens (Zhang et al. 2012). Despite the presence of a coupling agent, the addition of FRs shows a negative impact on the tensile and flexural properties of natural fibre/PP composites. However, these composites exhibit better performance compared to pure polypropylene. Impact properties of the composites are not greatly affected by the addition of FRs. It was found that magnesium hydroxide can effectively reduce up to 50% of these composites' flammability. Replacing part of it

with boric acid or zinc borate results in a reduction of the retarding effect of magnesium hydroxide (Sain et al. 2004).
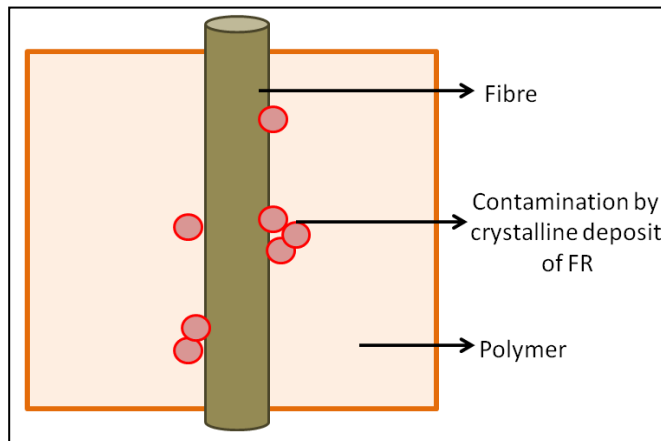
Figure 2.10: Fire retardant contamination on fibre surface (Ayrilmis et al. 2012)

At present it is impossible to compare various classes of FRs. As an example, studies on WPCs are done with different matrix materials, fire retardant contents and use a range of fire performance tests. Flame retardation is complex, whereby each fire retardant is effective via several mechanisms. For examples, Stark et al. (2010) performed a study on several FRs and observed that, although the decomposition of both magnesium hydroxide and zinc borate compounds produced water vapour, only magnesium hydroxide contributed to fire retardant capabilities. Boron-based compounds, bromine-based compounds and APP are all char producers. However, only the latter was observed to perform well. This study concluded that magnesium hydroxide and APP most improved the fire performance of WPCs, while a bromine-based fire retardant and zinc borate improved fire performance the least. It also highlighted that although all FRs had a positive effect on WPC fire performance, the addition of wood flour alone into polyethylene (PE) dramatically improved the fire performance (HRR) of PE. Figure 2.11, Figure 2.12 and Figure 2.13 show the improved fire performance of several natural fibre composites treated with different FRs using different tests. The graphs do not provide conclusive results, as the parameters used in each study differed widely.

Various FRs were used to achieve improved fire resistance of composites with a wide range of results. It was observed from the above reviews that magnesium hydroxide provided a promising positive effect on fire durability of natural fibre/polymer composites. However, the strength of the composites was jeopardised with the addition of FRs.

	Wood/Polyp ropylene Composite + 12% boric acid/borax	Wood/Polyp ropylene Composite + 12% zinc borate	Wood/Polyp ropylene Composite + 12% monoammo nium phosphate	Wood/Polyp ropylene Composite + 12% diammoniu m phosphate	Wood flour/polyet hylene composite + 10% decabromod iphenyl oxide/antim ony trioxide	Wood flour/polyet hylene composite + 10% magnesium hydroxide	Wood flour/polyet hylene composite + 10% zinc borate	Wood flour/polyet hylene composite + 10% melamine phosphate	Wood flour/polyet hylene composite + 10% ammonium polyphospha te	PP/wood– fiber composite + 20% ammonium polyphospha te	PP/wood– fiber composite + 20% ammonium polyphospha te + 10% silica
% Improvement	8.29	4.66	8.29	5.70	14.29	30.61	14.29	-2.04	-10.20	50.00	166.67

Figure 2.11: Fire performance improvement using test method: Time to Sustain Ignition
Sources: Ayrilmis et al. (2012), Stark et al. (2010) and Zhang et al. (2012).

	Wood fibre/HDPE composite + 9% aluminium hydroxide	Wood fibre/HDPE composite + 9% melamine cyanurate	5% NR latex jute composite + 1% sodium phosphate	Coconut filter fiber/PLA composites + 5% diammonium phosphate	Coconut filter fiber/PP composites + 5% diammonium phosphate	Jute fiber/PP composites + 5% diammonium phosphate	Sawdust/PP composite + 25% magnesium hydroxide	Sawdust/PP composite + 20% magnesium hydroxide + 5% boric acid	Sawdust/PP composite + 20% magnesium hydroxide + 5% zinc borate	Ricr husk/PP composite + 25% magnesium hydroxide
■ % Improvement	23.61	-6.25	52.48	48.28	44.44	30.77	51.61	29.03	9.68	48.00

Figure 2.12: Fire performance improvement using test method: Flame Propagation Test
Sources: García et al. (2009), Fatima and Mohanty (2011), Suardana et al. (2011) and Sain et al. (2004).

32
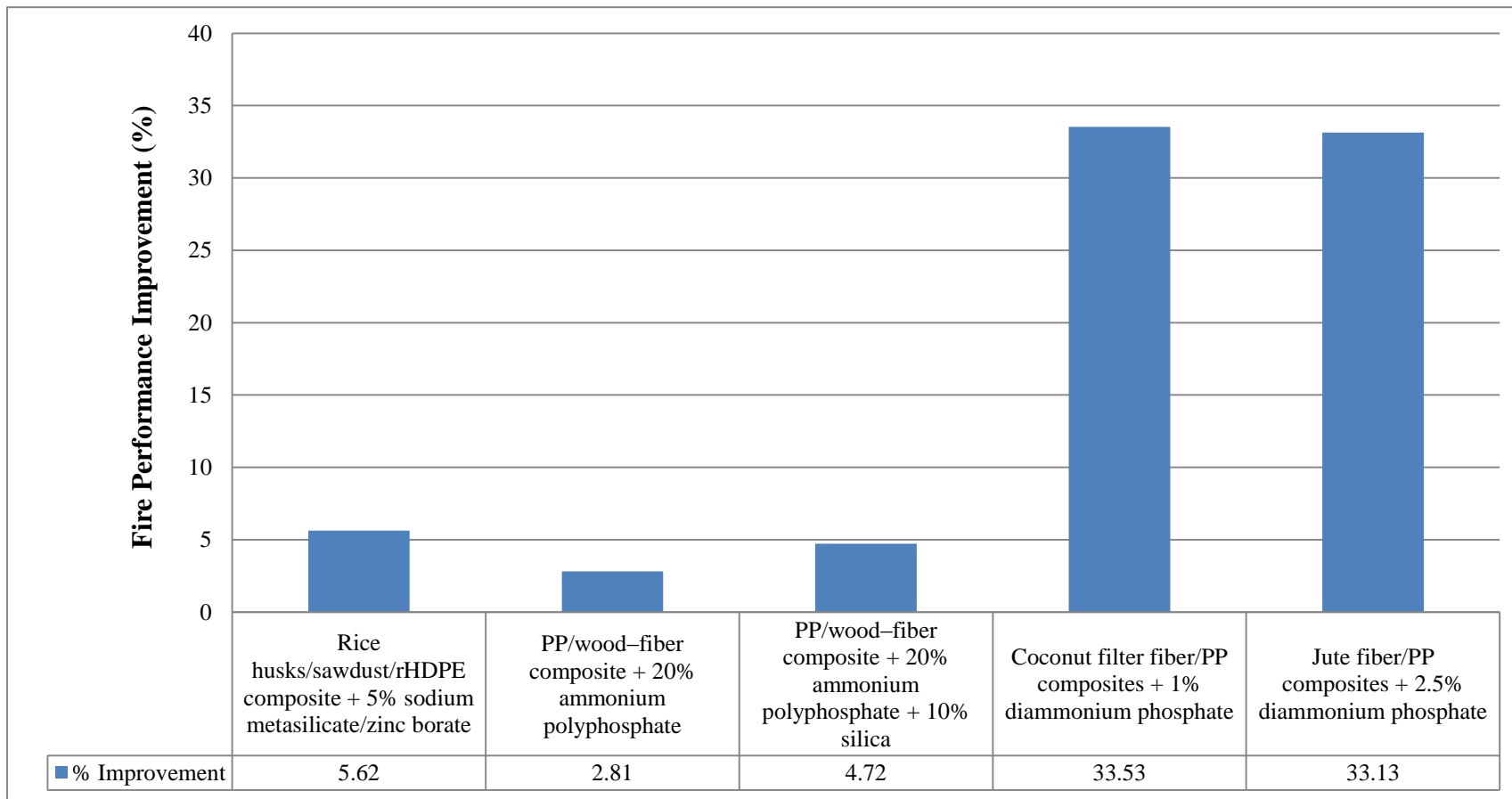
Figure 2.13: Fire performance improvement using test method: Thermo gravimetric Analysis
Sources: Hamid et al. (2012), Zhang et al. (2012) and Suardana et al. (2011).

2.5   Effects of weathering on degradation

Natural fibre composites exposed to direct sunlight are subjected to radiation that breaks the covalent bonds in organic polymers, causing yellowing, colour fading, weight loss, surface roughening, mechanical property deterioration and embrittlement, with greater reduction in wetter conditions (Dittenber & GangaRao 2012; Hollaway 2010). The important durability properties for outdoor application of construction products include: fungal resistance, UV resistance, moisture resistance and dimensional stability (Matuana et al. 2011; Wang et al. 2005). After weathering periods, the loss of tensile strength of composites occurs due to fibre and matrix degradation (Shubhra et al. 2010).

Photodegradation causes changes in all scales of polymer dimension, including the monomer unit (oxidation), the chain (cross-linking or chain scission), the morphology (breakdown of tie molecules and crystal), and on the macroscopic scale (Matuana et al. 2011). The UV radiation absorbed by polymers modifies the chemical structure, providing molecular chain scission and/or chain cross-linking. Degradation processes by weathering—including photo-radiation, thermal degradation, photo-oxidation and hydrolysis—change the chemical, physical and mechanical properties of materials (Beg & Pickering 2008; Wang et al. 2005). Photodegradation of polymers due to photo-oxidation is promoted by UV irradiation. Oxygen is used up before it can diffuse to the interior, thus degradation is concentrated near the surface. This occurs even in polymers with high UV levels in the interior. The photo-oxidation process also occurs in amorphous regions because of their higher permeability to oxygen (Beg & Pickering 2008). Oxidation gradients cause density gradients that result in stresses. When these combine with chain scission (reduction in molecular weight), leading to shorter polymer chains, they will initiate and propagate cracks. Cracks on surfaces lead to light diffusion (a whitening effect in appearance) and deterioration of mechanical properties (Fabiyi et al. 2008; Matuana et al. 2011). The presence of catalyst residues, hydroperoxide groups and carbonyl groups can also be introduced during polymer manufacturing, processing and storage. These species absorb UV light above 290 nm and may initiate photochemical reactions (Matuana et al. 2011). A schematic diagram of natural fibre/polymer composite degradation due to UV exposure is presented in Figure 2.14.
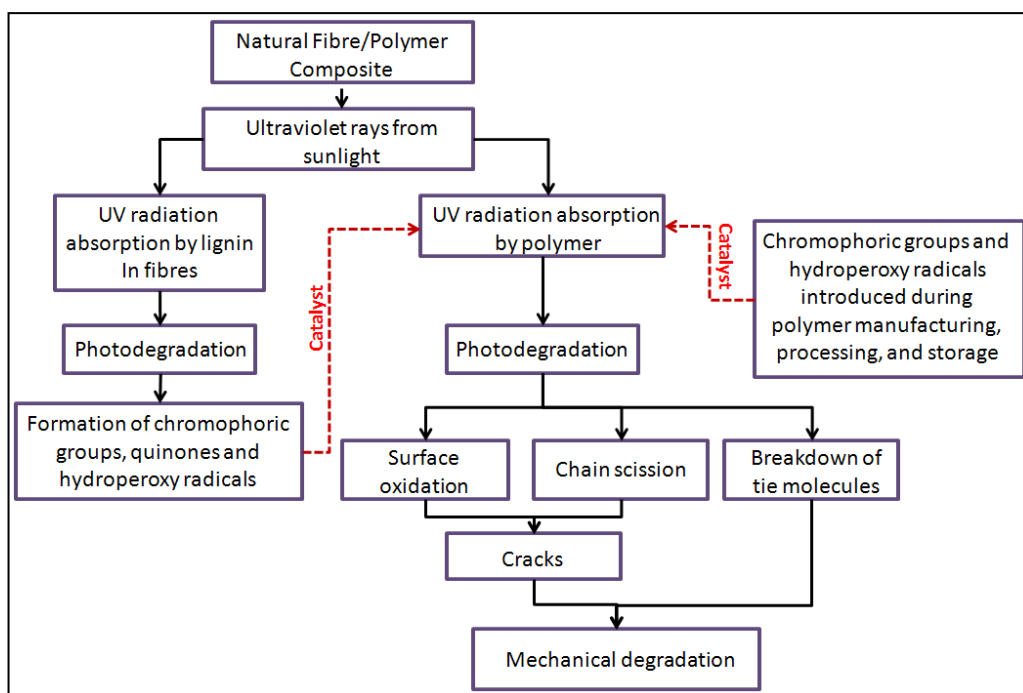
Figure 2.14: UV Degradation of natural fibre/polymer composite and its components

For lignocellulosic fibres, ageing or degradation occurs due to UV radiation absorption by lignin, formation of quinoid structures, Norrish reactions, and reactions of photo yellowing that occur in lignin. UV degradation leads to the formation of chromophoric groups, such as carboxylic acids, quinones and hydroperoxy radicals, which are responsible for the characteristic yellow colour associated with ageing paper (Beg & Pickering 2008). Visible light has energy lower than 292.9 kJ/mol; this is not sufficient to break the major chemical bonds in the fibre components. Thus, photodegradation of fibre results primarily from the UV aspect of sunlight. The degrees of photodegradation of fibre components largely depend on their ability to absorb UV light. Photodegradation, or weathering of major components of natural fibres/polymer composites, results from the combined effects of light, water, oxygen and heat. All main polymeric components of fibres (cellulose, hemicellulose, lignin and extractives) suffer from photodegradation. Most natural fibre chromophores are located in lignin, which accounts for 80–95% of light absorption. This ensures a significant contribution to discolouration (Matuana et al. 2011).

Many weathering studies are performed on WPC, as it is already being used in North America for non-structural and semi-structural outdoor applications, such as decking, siding, railings, fences, window, roof tiles and door frames. It is preferable to solid wood due to the presence of a hydrophobic polymer phase in WPCs, which improves resistance to water absorption and biological decay, increasing durability and lowering maintenance requirements. WPCs have better thermal and acoustic isolation than aluminium, and a lower price than neat plastics, with an appearance rather similar to wood. However, their outdoor applicability is hindered by poor weathering properties. After weathering, WPCs show fading and swelling (Butylina et al. 2012; García et al. 2009; Matuana et al. 2011; Stark & Matuana 2004).

The mechanical properties of natural fibre composites undergo changes after UV irradiation. These can be attributed to composite surface oxidation, matrix crystallinity changes and interfacial degradation (Campos et al. 2011). Photodegradation of natural fibre/polymer composites involves several factors, such as fibre content, coupling agents, manufacturing methods and weathering conditions. Oxidation rates of composites increase with fibre content and decrease when compatibilisers are present, due to better dispersion of fibres in polymer matrix (Matuana et al. 2011). At low sisal content (<20%), the sisal fibre acts as a nucleating site, increasing crystallinity. However, when the sisal content is above 20%, crystallinity decreases as the fibre begins to hinder the molecular motion of polypropylene (Stark & Matuana 2004). Composites experience more lightening and mechanical property loss when exposed to UV radiation with a water spray cycle, compared to a UV radiation cycle alone (Beg & Pickering 2008; Matuana et al. 2011). In terms of manufacturing methods, injection moulded composites degrade more slowly than extruded ones due to the formation of a hydrophobic HDPE-rich surface layer on injection moulded composites (Matuana et al. 2011). PP-based WPCs experienced quicker photodegradation in terms of lightness and wood loss compared to HDPE-based WPCs (Fabiyi et al. 2008; Matuana et al. 2011).

Upon UV exposure, WPCs underwent two competing redox reactions:
  a) Formation of paraquinone chromophoric structures generated by the oxidation of lignin, resulting in yellowing.
  b) The reduction of the paraquinone structures to hydroquinones, leading to photobleaching.

During the first 250 hours of exposure, yellowing of composite preceded the photobleaching mechanism that became dominant with increased exposure time (Matuana et al. 2011).

Increases in the carbonyl groups for WPC suggest that surface oxidation increased upon weathering. However, with longer exposure time, carbonyl (both carboxylic acids and esters) and vinyl concentrations began to decrease, most probably due to the decrease of wood and plastic concentrations in the outer surface; the concentration of talc increased. Wood components preferentially degraded during WPC weathering. This reveals that more attention needs to be focused on stabilising the wood component rather than the polymer matrix (Fabiyi et al. 2008).

Study of the weathering effect on natural fibre composites should include the combined action of UV radiation, heat and moisture. This could be accomplished through natural or artificial ageing (Wang et al. 2005). The effects of degradation due to natural or artificial ageing could be evaluated through the quantification of chemical degradation and/or by analysis of physical properties such as mechanical behaviour and visual appearance (Beninia et al. 2011).

2.5.1 Natural weathering

The natural ageing process is influenced by natural elements, weathering, or environmental action in which the material is subjected to conditions of use (Beninia et al. 2011). The long-term behaviour of materials due to environmental exposure is evaluated by real time observations over several years. However, research

programmes lasting 10 years or more are rare for organisational and economic reasons (Beg & Pickering 2008).

Weathering studies on jute/phenolic composites with 2 years of exposure showed resin cracking, bulging, fibrillation and black spots, with decreased tensile strength of over 50% (Dittenber & GangaRao 2012). A 9-month natural weathering study was conducted on palm fibre/PP composites. The composites showed little drop in strength compared to pure PP, which showed a large drop in strength after 3 months of exposure. The drop increased and the PP lost more than 50% of its strength after nine months of exposure. A minor increase in strength was observed at long exposure times in natural weathering, possibly due to enhanced interfacial adhesion by degradation as a result of carbonyl groups forming in PP; this is more compatible with the cellulose fibre surface (Abu-Sharkh & Hamid 2004). The tensile strength of a neat PP sample after 3 months exposure to UV radiation decreased 92.57% whereas for 10% sisal fibre loading is 58%, for 20% sisal fibre loading is 37% and for 30% sisal fibre loading is 23% as studied by Joseph et al. (2002). Degradation of PP is due to photo-oxidation promoted by UV irradiation. Oxygen is used up in the reaction before it can diffuse to the interior, so degradation is concentrated near the surface. Surface cracks of composites can be caused by thermal stresses during outdoor exposure due to day–night variations in temperature, or due to the tensile residual stresses that develop at the surface of some polymers during weathering. Crack propagation can be controlled to some extent by the addition of fibres to PP, where with increases in fibre loading, the extent of retention in tensile properties increases (Joseph et al. 2002).

Natural weathering studies may prove impractical due to the amount of time required; accelerated weathering tests are preferred. However, the results from accelerated weathering tests have no exact correlation to what happens in real conditions, due to regularity of cycles, duration, intensity and exposure conditions (Beninia et al. 2011). It is difficult to transfer artificial weathering to life expectancies under natural weathering conditions, as rates of fibre degradation in nature depend on various external factors such as intensity of radiation, temperature, humidity and air pollution (Methacanon et al. 2010). Different weathering regimes lead to different weathering patterns, as discovered by Fabiyi et al. (2008). The degree of WPC degradation in a 2-year natural test was not as severe as that in a 2000-hour accelerated test, but was more severe than that observed in a 400-hour test. It can be seen from the study done by Abu-Sharkh and Hamid (2004) that higher stability was displayed by compatibilised samples in artificial weathering compared to natural weathering. This can be attributed to the UV source in the accelerated weatherometer not reproducing the light spectrum produced by solar radiation. Moreover, it is possible that the maleated polypropylene used as a compatibiliser is susceptible to degradation by radiation frequencies that are more abundant in solar radiation.

2.5.2 Accelerated weathering

The accelerated ageing process occurs in ageing chambers that simulate a natural environment and the damaging effects of long-term outdoor exposure, by exposing test samples to UV radiation, moisture and heat in a controlled manner. The advantages include faster testing than natural exposure and reproducability (Abu-

Sharkh & Hamid 2004; Matuana et al. 2011). It is a more convenient alternative for assessing long-term behaviour. However, some variables must be considered such as exposure time, UV exposure as radiant energy over a specific wavelength range, and water exposure as a number of cycles, or in time. For the best comparison between studies, it is recommended that performance after weathering be reported after a specific radiant exposure, commonly termed the 'time integral of irradiance' (Beg & Pickering 2008).

FRPs exposed to accelerated weathering affect the polymeric matrix and the components within the matrix, including: pigments, processing additives and reinforcements (Wang et al. 2005). Visual observation of samples subjected to accelerated weathering tests show colour fading and partial shrinkage, resulting in sample bending. In addition, deposition of white chalky material was observed on the surface. During the weathering process, lignin and water soluble products leach from the samples, apparently due to colour fading (Beg & Pickering 2008; Beninia et al. 2011; Methacanon et al. 2010).

During the course of accelerated weathering of polymer composites, two mechanisms compete: chain scission and cross-linking. Chain scission lowers molecular weight, whereas cross-linking raises molecular weight by increasing the bonding between polymer chains. Chain scission is directly indicated by accumulation of the carboxylic acids and vinyl groups, as well as increases in crystallinity. The shorter chains produced during chain scission are more mobile and are readily crystallised, which increases crystallisation and embrittlement. In contrast, cross-linking does not affect polymer crystallinity. While chain scission occurs in the amorphous phase of the polymer and is controlled by the diffusion of oxygen in this region, UV-induced cross-linking occurs in imperfect crystalline regions (Stark & Matuana 2004). The reduction in molecular size dominates in short-time exposures to weathering, favouring crystallisation. In contrast, after extended periods, the presence of many extraneous groups in the molecules of highly degraded polymers makes crystallisation more difficult (Butylina et al. 2012). This phenomenon can be correlated with the SEM results of Hu et al. (2010), whereby fibre breakage mainly occurred in short-term aged tensile samples, while fibre debonding and pull-out occurred in long-term aged tensile samples.

Study on accelerated weathering of WPC by Stark and Matuana (2004) showed that while neat HDPE may undergo cross-linking in the initial stages of accelerated weathering, wood fibre (WF) may physically hinder the ability of HDPE to cross-link, resulting in the potential for HDPE chain scission to dominate in the initial weathering stage up to 1000 hours before decreasing. At this point, chain scission begins to affect the tie molecules, resulting in a net decrease in crystallinity.

Fibre tensile strength decreases with increased exposure time (Methacanon et al. 2010), while little change is observed for pure PP (Beg & Pickering 2008). Tensile strength and modulus for the composites were found to decrease due to embrittlement of the matrix, and degradation of fibre and fibre/matrix interfacial bonding, evidenced by increased fibre pull out (Beg & Pickering 2008). Increases in strength observed at long exposure times in natural weathering are not present in accelerated weathering. It seems that the fast rate of degradation in accelerated weathering tests might offset any enhancement in interfacial adhesion caused by

degradation (Abu-Sharkh & Hamid 2004). Due to the short period of exposure, Beninia et al. (2011) observed no changes in the ultimate tensile of a high impact polystyrene (HIPS) matrix. However, there was a small increase in tensile modulus that might have been caused by onset of a cross-linking process that occurs with some thermoplastics subjected to certain processes of degradation. Degradation processes from accelerated weathering are influenced by fibre volume and chemical treatment. The effects of weathering exposure was found by Beninia et al. (2011) in composites compared to pure HIPS, indicating that fibres decrease the degradation resistance of material. Through SEM analysis, exposure did not cause degradation of the fibre/matrix interface.

Most researchers acknowledge that accelerated weathering tests cannot be directly correlated to the natural weathering process. If time is not an issue, then it is more accurate to analyse data from natural weathering tests, which gives the actual site conditions. Accelerated weathering tests provide basic understanding of the degradation mechanism of composites subjected to predetermined exposure cycles.

2.5.3   Effect of moisture on weathering of composites

Weathering in the presence of water enhances the rate of degradation of WPC, as wood cell walls swell when penetrated by water, facilitating light penetration further into the wood and providing sites for more degradation. Swelling of wood particles creates microcracks in the matrix, and washes away loose wood particles, loose cellulose, and degraded lignin at the wood surface (Beg & Pickering 2008; Matuana et al. 2011). Pure polypropylene has no significant change in weight while unbleached and bleached fibre composites showed an increase in weight after accelerated weathering. The overall increase in weight of the composites show that water absorption is dominant compared to leaching of lignin and water soluble products from the samples. Reductions in hardness for composites observed could also be due to plasticisation by water. The degree of crystallinity of PP in composites was also found to decrease with weathering, attributed to the swelling of composites by absorbed water (Beg & Pickering 2008).

As a result of the wetting and drying cycle, WPCs were differentially contracted between the surface and interior sections. Together with polymer chain scission, which results in highly crystallised polymer zones that crack, crazing was observed for both natural and accelerated weathering. Three stages of degradation were identified (Fabiyi et al. 2008):
  a) The surface layer was eroded, creating several cavities on the surface of composites.
  b) The frequency and size of the cavities increased upon extended exposure time.
  c) Small cracks developed on the weathered surface of WPC.

A study on the weathering effects of rice hull composite decking boards was conducted, and the dimensional stability was studied by Wang et al. (2005). Dimensional changes of the composites were attributed to three components:
  a) The recoverable swelling and shrinking of the rice hull component under humidity changes.
  b) Thermal expansion/contraction effects.

c) Irrecoverable swelling due to relaxation of the compressive stresses induced during the extrusion process.

Moisture adsorption was the major factor in dimensional instability. Moisture adsorption/desorption was influenced by temperature, whereby high temperatures facilitated high and quick moisture adsorption; while low temperatures trapped the already adsorbed moisture. The decking boards were found to achieve constant dimensions relatively quicker than moisture equilibrium when ambient conditions were changed (Wang et al. 2005). In reality, moisture sorption of natural fibre composites in-service is slow and seldom reaches an equilibrium condition in a moist environment. The surface of the composites may be saturated with water while the core layers may have significantly less moisture (Xie et al. 2010).

Hemp fibre/poly-hydroxybutyrate (PHB) films composites exposed to accelerated weathering suffer a decrease in molecular weight via chain scission from UV photo-oxidation and ester hydrolysis from exposure to moisture. Cracking of composites is caused by incompatibility between the coefficients of polymer matrix and fibre thermal expansion and, in the presence of moisture fibre swelling is dominated by free water bonding with readily available hydroxyl groups in the cellulosic fibres. Hoop stresses, generated by fibre swelling, exceed the tensile capacity of the PHB surrounding the fibre. Hence, it was observed that mass changes in the composites depend more on the fibre/matrix interface and on the fibre moisture content than on the mass stability of the PHB matrix itself. With increased crystallinity and embrittlement from photo-oxidation, degradation of composites was accelerated (Michel & Billington 2012).

Water worsens the weathering effects on natural fibre/polymer composites. Therefore, in outdoor applications where a composite will be exposed to direct sunlight and rain, it can be expected to undergo severe deterioration.

2.5.4 Discolouration and chemistry changes of composites due to weathering

A significant feature of WPC is its aesthetic value which becomes compromised by weathering through severe discolouration. Wood exposed to weathering initially becomes yellow and brown due to the photo-oxidation of lignin, and then gray due to leaching of the degraded product of lignin. This discolouration and yellowing results from a loss of lignin's methoxyl content, photo-dissociation of carbon-carbon bonds and formation of carbonyl-based chromophoric groups. Faster fading of composites was observed with the combination of fibre bleaching by UV radiation and water spray, which accelerates oxidation reactions, facilitates light penetration into the composites, and removes water soluble wood extractives (Matuana et al. 2011; Michel & Billington 2012). Research has shown that, for both natural and accelerated weathering, longer exposure times increase the degree of colour change and lightness, carbonyl concentrations and wood loss on weathered WPC surfaces (Assarar et al. 2011).

Colour measurement of composites is analysed as per ASTM D2244, and is conducted in a spectrocolorimeter, adapted to colour-data software. It is determined by calculating the discolouration (ΔE) of the weathered samples in terms of lightness

(L*) and chromaticity (a* and b*) of unweathered and weathered specimens. The equation is given as:

$$\Delta E = \sqrt{(\Delta L^{*2} + \Delta a^{*2} + \Delta b^{*2})} \qquad\qquad \text{Equation 2-2}$$

Where ΔL^*, Δa^* and Δb^* are the difference of initial and final values of the colour coordinates L^*, a^* and b^*. L^* ranges from 0 (black) to 100 (white) while a^* (red-green) and b^* (yellow-blue) (Matuana et al. 2011; Michel & Billington 2012) are interpreted as: +a expresses redness, -a expresses greenness, +b expresses yellowness and –b expresses blueness (Fabiyi et al. 2008; García et al. 2009). This is represented in Figure 2.15. The relationships between chemical (wood lignin content and carbonyl concentrations) and colour changes (L) were established by Fabiyi et al. (2008), where strong correlations between lightness and wood lignin degradation, lightness and carboxylic acid concentration, and lightness and esterification were observed. It was concluded that delignification and oxidation lead to increased lightness.
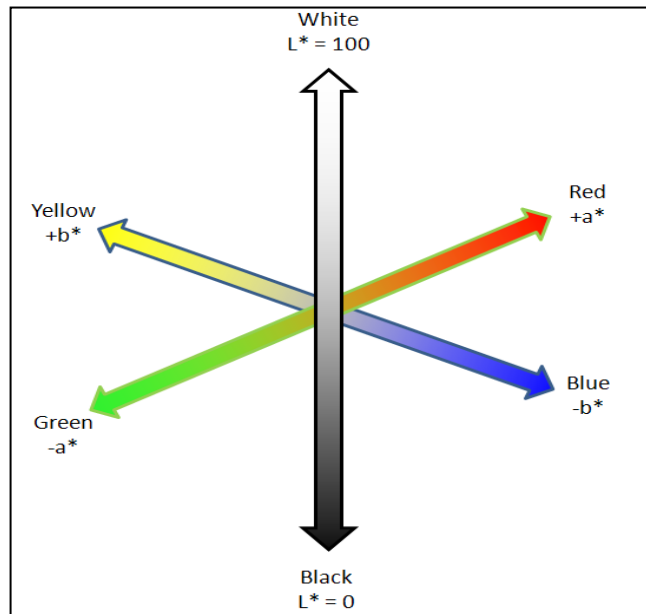
Figure 2.15: L*a*b* colour space adapted from HunterLab (2008)

A study by Butylina et al. (2012) proved that higher wood fibre content led to more significant changes in colour. The decrease of yellowness (Δb) with exposure time can be linked to the reduction of paraquinones (chromophoric structures) to hydroquinones, which results in photobleaching and a more serious degradation of the surface layer. As fibre content exceeds 40%, encapsulation of wood fibres with polymer becomes impossible. Degradation was found to be limited to 0.5 mm depth; below this, the intensities of different bands were similar to those of the non-weathered composites.

Changes in surface chemistry can be studied using spectroscopic analysis but they cannot distinguish between the surface oxidation of polymer and that of the fibre (Butylina et al. 2012). X-ray photoelectron spectroscopy (XPS) was used to verify the occurrence of surface oxidation by studying the concentration of carbon to oxygen atoms through Equation 2-3 (Stark & Matuana 2004):

$$C_{ox/unox} = C_{oxidized}/C_{unoxidized} = [C2+C3+C4]/C1 \qquad\qquad \text{Equation 2-3}$$

Fourier transform infrared (FTIR) spectroscopy monitors the development of degradation products, such as carbonyl groups and vinyl groups, and determines changes in polymer crystallinity (Stark & Matuana 2004). The addition of WF to the HDPE matrix increases the concentration of carbon–oxygen bonds (C2,C3,C4) in the samples. This is as expected: cellulose, hemicelluloses, and lignin of wood have a larger percentage of oxidised carbon in their chemical structure than manufactured neat HDPE. Hydroxyl groups are the main carbon–oxygen functional groups in wood. Concentration of vinyl groups was larger for neat HDPE than for WPCs, indicating it is important for the degradation of the polymer only, not the wood (Stark & Matuana 2004).

A study performed by Matuana et al. (2011) on coextruded and uncapped WPCs suggested that discolouration of WPCs upon UV weathering is a combination of both chemical and physical changes. Photo-oxidation of wood components is responsible for the chemical changes and determines the initial colour change. Coextrusion prevents surface erosion and removal of degraded wood components (it maintains adhesion between fibres and matrix); thus, the composites become dark and yellow but fade once the cap layer is damaged, due to removal of loose wood components by water spray. The cap layer absorbed some UV light and reduced the availability of oxygen at the interface of coextruded composites, thus decreasing the photodegradation rate.

UV rays are responsible for colour changes in both synthetic and natural FRPs. These colour changes can indicate chemical changes on the surface of the composites, which reflects the degree of deterioration. In a non-load bearing natural FRP, the importance of its physical appearance may exceed its mechanical strength. As such, the method selected to block the damaging effects of UV rays must not hide its aesthetic surface.

2.5.5 Effect of surface treatment and additives on weathering of composites

For a high degree of UV resistance, UV stabilisers are incorporated into polymer during manufacturing (Hollaway 2010). Coated polyurethane results in little surface deterioration and together with fibre modification (bleaching, alkalisation and silanes) will help slow weathering effects (Dittenber & GangaRao 2012). However, chemically treated composites show a relatively greater extent of decrease in tensile strength with increases of exposure time, compared to untreated composites. This proves that treated composites undergo severe degradation compared to untreated composites; MAPP treated composites experience the worst degradation (Joseph et al. 2002). It is also important to note that metallic-based additives and plasticisers may introduce chromophores into the composites, which will lead to the generation of phenyl and carbonyl groups during degradation (Fabiyi et al. 2008; Michel & Billington 2012).

To provide colour stability against UV radiation, additives and fibre modifications can be incorporated during composite fabrication, as listed in Table 2.3. Oxidative degradation is the most common reason for failure of biocomposites after mechanical failure. Biocomposites are much more sensitive to oxidative degradation compared to pure plastics. In addition, their induction time, durability and lifetime is dependent on

the antioxidants (AO) and their amounts (Hamid et al. 2012). Samples with 0.5 wt.% of antioxidants and 20 wt.% of FRs were observed by Hamid et al. (2012) to have the most reasonable strength and elasticity of recycled high density polyethylene (rHDPE), reinforced with a high loading hybrid of rice husks and sawdust. The AOs were consumed by protecting the polymer from oxidation and ended up as stable peroxide, an oxidised antioxidant, or as other stable structures. Although samples with AOs had higher water absorption rates compared to samples with no antioxidant content added, they had a better reinforcing effect, as higher results of tensile, flexural and impact strengths were obtained.

Table 2.3: Composite treatment for colour stability

Treatment	Description
Photostabilisers	Classified into two types according to their action mode: 1. UV Light Absorber (UVA): Absorbs some UV radiation. Act by shielding the material from ultraviolet light (García et al. 2009). 2. HALS (hindered amine light stabilisers). Act by scavenging the radical intermediates formed in the photo-oxidation process (García et al. 2009). High effectiveness in the initial stage due to their fast diffusion to the surface but alternatively, low effectiveness with increased exposure time due to their loss by surface evaporation (Matuana et al. 2011).
Pigments/Colourant	Pigments are added as photo-blockers at material surface for cost effective production because weathering primarily occurs in this region. Composites containing darker colour pigments had better colour stability (Butylina et al. 2012). Blocks the penetration of UV radiation as well as masking the bleaching of fibres (Matuana et al. 2011).
Colour Dye	Colouring fibres with an oil-based stain significantly improved the colour stability of composites upon weathering while water-based dye does not improve the colour stability (Matuana et al. 2011).
Coating	Opaque pigmented coatings block UV/visible light. Non-photostabilised UV, curable acrylic clear films fails to protect wood against discolouration. Photodegradation of the interfacial layer led to flaking and peeling of the coating (Matuana et al. 2011). Disadvantages: difficulty in coating plastic composite due to the low surface energy of plastic, solvent evaporation and often causes environmental concerns, drying stage of coating requires additional time (Matuana et al. 2011).
Lamination	Lamination is achieved by melt fusion or an adhesive layer. Delamination often occurs with the bending of the laminated composites. Disadvantage: the difficulty to use lamination technology to manufacture a fully encapsulated structure in plastic composites

	rather than a planar layered structure (Matuana et al. 2011).
Coextrusion	Coextrusion provides a protective surface by producing a multilayered product with different properties at outer and inner layers. By coextruding a hydrophobic clear cap layer onto WPCs, discolouration due to water effect can be retarded (Matuana et al. 2011).

Composites exposed to moisture and UV radiation have more effect on lignocellulosic fibres than on the fibre/matrix interfacial region. Bleached fibres have less amounts of lignin from the removal treatment process, which leads to higher mechanical interaction with the matrix. Mercerised fibres have higher amounts of lignin than bleached fibres; thus, they are more susceptible to UV radiation and moisture (Beninia et al. 2011). Bleached fibre composites were found to have higher tensile strength, failure strain and impact strength than unbleached fibre composites, due to the removal of relatively weaker and more brittle non-cellulosic compounds, which allow better fibre/matrix bonding. The crystallinity of PP in bleached fibre composites was better than unbleached fibre composites, due to the removal of lignin and hemicelluloses. This allows better packing of cellulose microfibrils, providing a better substrate for crystal growth (Beg & Pickering 2008; Campos et al. 2011). After UV exposure, composites with bleached fibres showed greater decreases in tensile properties in comparison with untreated composites, due to the change in the morphology upon UV irradiation. However, the lower level of surface damage in irradiated composites compared to neat polycaprolactone (PCL) suggests some protection of PCL. This indicates possible interaction of PCL with cellulose from sisal fibres, as demonstrated by the Fourier transform infrared (FTIR) spectrum with increased carbonyl groups in the PCL. Strong fibre/matrix interaction and carboxyl/hydroxyl group interaction contributed to retention of crystallinity, elasticity modulus, morphology and the structure of composites after UV irradiation (Campos et al. 2011).

Irgastab and Tinuvin-783 were used to stabilise pure PP, compatibilise and uncompatibilise composites for thermal and UV degradation during processing and weathering. This enhanced stability was imparted by the presence of fibres in the composites, and enhanced interfacial adhesion resulting from oxidation of the polymer matrix, which is the source of retained mechanical strength. The study concluded that compatibilised samples were generally less stable than uncompatibilised ones, as a result of the lower stability of the maleated polypropylene. As for comparison with pure PP, the presence of natural antioxidants, for example lignin, in composites is known to provide stabilisation to natural fibres. The dark colour and the surface layer of fibres also act as a protective layer that prevents UV radiation from penetrating the sample and causing degradation in the bulk (Abu-Sharkh & Hamid 2004).

A stabiliser composed of a blend of HALS, UV filters and antioxidants was produced by García et al. (2009). The blend gave better results compared to using HALS alone. No cracking or fractures occurred in the aged WPCs. However, colour change in the stabilised composites was much lower than that of neat composites and most industrial samples. Oil palm fibres modified with vinyltrimethoxy silane (VTS) in an

alcohol–wax mixture (60:40) and soaked in water at different temperatures showed a reduced water uptake at all temperatures. With this, the resulting polymer composites were relatively dry in moist environment, thereby reducing the risk of environmental damage such as deformation and fungal decay (Xie et al. 2010). Coir or oil palm fibre composites modified with methacryloxymethyltrimethoxy silane (MPS) were subjected to one year of weathering. The mass loss due to fungal decay and the moisture content of modified composites was less compared to unmodified composites. The tensile and flexural strength of the modified composites were slightly reduced (by up to 8%), which is distinctly less than over 30% for the untreated composites (Xie et al. 2010). However, despite the incorporation of these chemical additives, natural fibre composites still underwent photo-degradation (Fabiyi et al. 2008).

From the reviewed studies, one could conclude there are a few chemical treatments available to improve UV resistance and weathering durability of natural fibre composites. However, there is a lack of published literature in this subject matter. More research needs to be conducted to compare the effects of various chemical treatments in providing UV protection on a standardised weathering cycle. Additionally, it must be noted that treated natural fibre/polymer composites suffer more mechanical degradation than untreated ones.

2.6   Chapter summary

The degradability of polymer composites based on natural fibres was reviewed in this chapter. This includes degradation due to moisture, thermal effects, fire, and UV rays. The fundamental points can be summarised as follows:

1) Natural fibres are susceptible to biodegradation: thus, composites based on them have a higher risk of degradation when subjected to outdoor applications, compared to composites with synthetic fibres. Different cell wall polymers of lignocellulosics fibres have different influences on their properties and degradability. For instance, cellulose is responsible for fibre strength, hemicelluloses for thermal, biological and moisture degradation, while lignin is responsible for UV degradation and char formation.

2) Fibre content is the major factor affecting water absorption of composites, as it enhances matrix porosity by creating more moisture path into the matrices. Poor adhesion between fibre particles and polymer matrix generates void spaces around the fibre particles. Higher fibre volume composites immersed in water generally have greater decrement in tensile and flexural properties compared to dry samples. Moisture absorption can be reduced through fibre modifications, such as alkalisation and addition of coupling agents.

3) A polymer matrix decomposes at 300–500°C. Flame retardants are used to improve thermal durability. The best potential for flame retardant of natural FRP involves the combination of a char-forming cellulosic material with an intumescent system. FRs from inorganic compounds, such as metallic hydroxide additives are preferred for environmental and health safety reasons, with magnesium hydroxide showing very good results.

4) Weathering causes degradation of polymer composites through photo-radiation, thermal degradation, photo-oxidation and hydrolysis. These processes result in changes in their chemical, physical and mechanical properties. Water enhances rates of degradation through swelling of fibres,

leading to further light penetration. Weathered chemically treated composites show a relatively greater extent of decrease in tensile strength, which proves that treated composites undergo more degradation compared to untreated composites.

2.7 Future Developments

From the highlighted degradation characteristics of natural fibre composites, improvement plans can be further researched to increase their durability for outdoor applications. The outcome of such research is expected to assist the future developments and wider acceptance of natural fibre composites as reliable civil engineering materials. Some issues that need to be considered for future studies on the degradability of natural fibre composites include:

1) Natural fibres are prone to moisture attack, so it is expected that the moisture durability of a natural fibre composite will decrease with increased fibre content. Thus, the amount of fibre in a composite shall be limited to its optimum fibre/matrix ratio to achieve maximum strength capacity and limit moisture susceptibility. Fibre treatments are essential to enhance strength and moisture durability of composites by promoting improved fibre/matrix interface. Water resistant coating can be applied on the composite surface to avoid contact between moisture and fibre.

2) Low lignin content in a natural fibre leads to better thermal performance of its composite. However, lignin is a source of char that can provide protection to the inner layers of composites during a fire. With the removal of lignin through fibre treatment, char-forming FRs can be added to provide improved thermal resistance of the composite. However, FRs worsened outdoor durability; as such, an optimum blend ratio shall be employed to achieve a balance between composite strength and fire safety.

3) Generally, chemically treated composites possess higher strength, higher moisture durability and better thermal performance, but poorer UV resistance. Various additives can be added to a natural FRP to stabilise it against the damaging effects of UV rays. However, more research is required to compare the effect of these additives on a more standardised weathering cycle. Coloured coating may not be an option if the natural element is to be preserved.

Chapter 3 : Methodology

3.1   Introduction

An overview of the experiments and the scope of the study are introduced in Figure 3.1. The first stage details research on NaOH optimisation of alkali treatment of bamboo fibre and its composites with neat polyester. Alkali treatment was introduced to the fibres at 0, 4, 6 and 8% NaOH. The effect of this treatment on the physical, morphological and tensile characteristics of the individual fibre was observed for further understanding of contributions to the composites' properties. Next, the effects of this fibre treatment on the composites were studied through single fibre fragmentation test (SFFT) and tensile test to determine the interfacial shear strength and initial tensile properties of the composites, respectively. The optimum NaOH concentration for the mechanical strength of bamboo fibre/polyester composites was identified and has been used for composite fabrication in stage two.

The second stage involves two types of degradation study; thermal and moisture degradation of bamboo fibre/polyester composites and their constituents. An acrylic coating was introduced to the optimally treated composites for added durability of the sample. The thermal degradation study consists of TGA, DMA and thermo-mechanical tests, while the moisture degradation study focuses on water immersion of samples at room temperature and at elevated temperatures. The effects of these degradation conditions on the physical, morphological and tensile properties of the composite samples were compared with neat polyester and also to the initial properties of undegraded samples. Through this research scope, it is believed that the present study will prove to be helpful in understanding the performance bamboo fibre/polyester composites under outdoor degradation conditions.
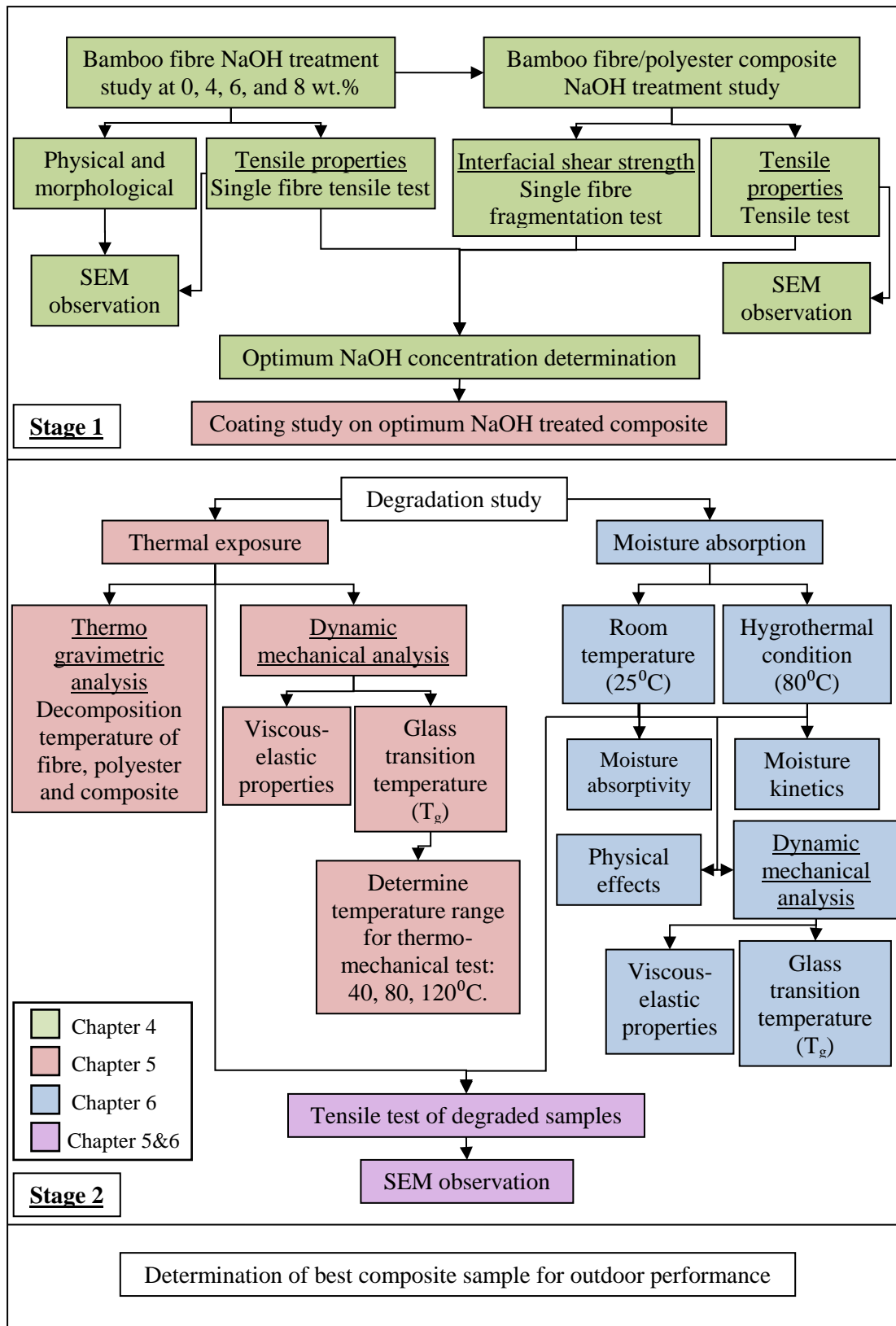
Figure 3.1: Flowchart of research scope

3.2   Material selection and preparation

The preparation of the samples used in this research consists of cleaning and treating fibres, composite fabrication and curing, cutting composite samples to required dimensions, coating samples with acrylic coating, as well as neat polyester fabrication and curing.

3.2.1   Fibre preparation and treatment

Untreated bamboo fibres—extracted through a steam explosion process—were obtained from an industrial partner in Hong Kong. Before treatment, the fibres were washed thoroughly with tap water to remove any debris, dirt and undesired substances and then dried at an atmospheric temperature (25^0C). In the chemical treatment, alkali solutions were prepared by diluting sodium hydroxide (NaOH) pallets in water, whereby the amounts of NaOH were varied to achieve 4%, 6% and 8% by weight of NaOH solutions. Bamboo fibres were immersed in the NaOH solutions for 24 hours at room temperature. After the chemical treatment process, the fibres were washed under running tap water until all traces of excess alkali were completely removed. Finally, the treated and untreated fibres were oven dried at 50^0C for 24 hours.

3.2.2   Neat polyester sample preparation

The resin used in the current work is neat polyester (NP) (AROPOL 1472/25P) supplied by Nuplex Composites Australia. The catalyst (Butanox M-50) was added for room temperature curing at a quantity of 1.5% by weight of the polyester resin. The liquid polyester was poured into a dogbone shaped mould, as per Figure 3.2, in reference to ASTM D638 (ASTM 2010b) and left to cure at room temperature for 24 hours. These specimens were then removed from the mould and placed in the oven for 5 hours at 80^oC for post-curing. The dimension of the specimens is shown in Figure 3.3.

Figure 3.2: Preparation of neat polyester specimens
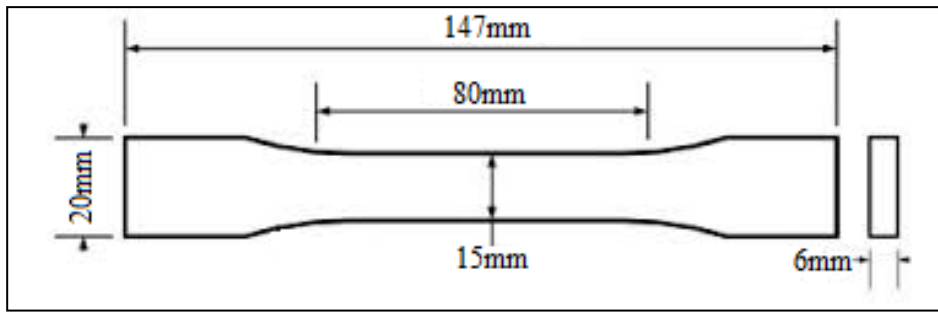
Figure 3.3: Neat polyester specimen dimension

3.2.3 Composite laminates preparation

The bamboo fibres were prepared as per Section 3.2.1, producing 0%, 4%, 6% and 8% NaOH treated fibres. The bamboo fibre/polyester composites were prepared using vacuum bagging process, which produced composite laminates with a dimension of 400 mm x 400 mm, at a fibre volume fraction of approximately 20% by weight. This percentage of fibre volume fraction was found to be most suitable for composite fabrication using the vacuum bagging method. In this process, the bamboo fibres were arranged randomly, but in an evenly distributed manner on an infusion table with six layers of wax (TR-108 Mold Release) applied. A transparent glass was placed on top of the fibres to provide a resultant smooth composite surface with a levelled thickness throughout the panel. A vacuum bag was laid on top of the set-up and was sealed along its parameter using adhesive clay. This set-up is presented in Figure 3.4, with the inlet on the right-hand side clamped tightly, while the outlet on the left-hand side is fixed to the vacuum machine.
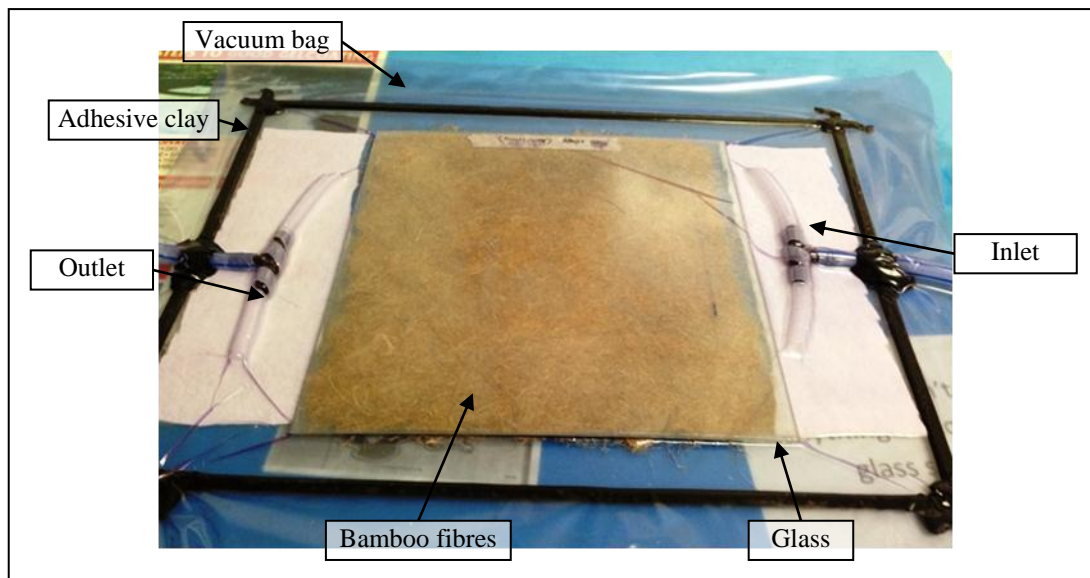
Figure 3.4: Vacuum bagging process for composite preparation

Air was removed from the set-up by applying a vacuum of 92 bars. Once it was confirmed the set-up was completely sealed, the neat polyester resin was infused through the fibres until the fibres were completely soaked by the resin. The pressure in the set-up was maintained from 24 hours at room temperature until the panels were cured. The panels were then removed from the mould and were oven cured at

80°C for 5 hours. Finally, the panels were cut into tensile specimen dimensions of 300 mm x 25 mm x 5 mm as shown in Figure 3.5.
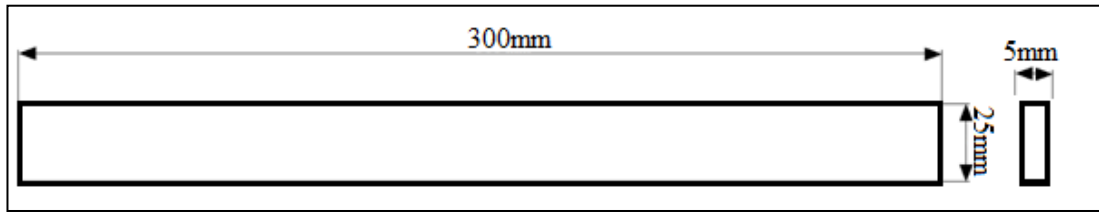
Figure 3.5: Bamboo fibre/polyester composite specimen dimension

3.2.4 Coating of composite sample

Coating of composite samples treated at 6% NaOH provided additional protection from outdoor degradation. A commercial water-based acrylic clear electrometric coating was supplied by UltraLast Ecoating System Australia was used. This is designed to provide durable protection against UV rays, microorganisms, moisture, rotting, abrasion and chemical exposure. The coating was applied as per technical data sheet (Appendix A) directions, using synthetic applicator pads. To ensure effective adhesion of coating on the porous surface of the composite, two layers of Ultralast Bond were applied and lightly sanded after drying. Finally, two layers of the acrylic coating were added to the composite surface, with each layer thoroughly dried and tack-free before the next coat was applied (after 1 hour). The coated samples were left to cure for 12 hours at room temperature with a final film thickness of approximately 10 µm. Figure 3.6 shows an SEM of the surface of a 6% NaOH treated bamboo fibre/polyester composite, coated with acrylic coating. The layer of coating was observed to provide full encapsulation on the composite, covering both the fibres and polyester resin.
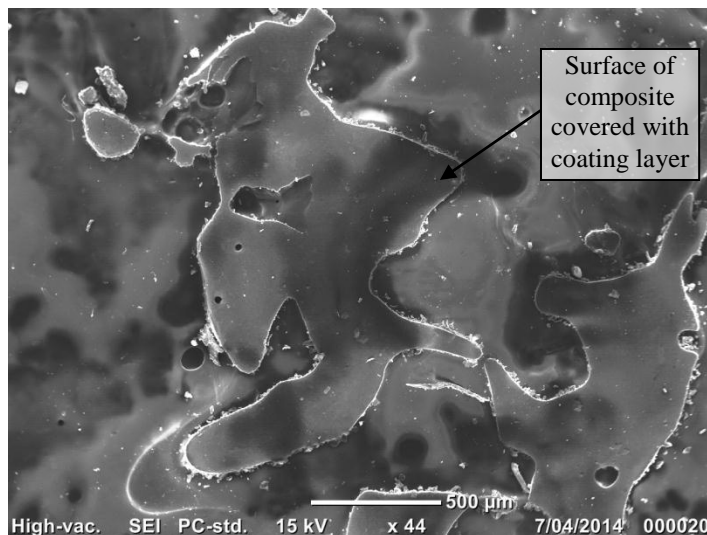
Figure 3.6: SEM of acrylic coating on bamboo fibre/polyester composite

Overall, the samples used in this research (based on the experimental program) are presented in Table 3.1.

Table 3.1: Type of samples

Sample	Description
BPC-0	Untreated bamboo fibre/polyester composite
BPC-4	4 wt.% NaOH treated bamboo fibre/polyester composite
BPC-6	6 wt.% NaOH treated bamboo fibre/polyester composite
BPC-8	8 wt.% NaOH treated bamboo fibre/polyester composite
BPC-6C	Coated BPC-6
NP	Neat polyester

3.3   Fibre characterization

Before tests were conducted on the bamboo fibre/polyester composites, some physical and mechanical properties of the fibres were identified to understand the behaviour of the fibres individually without resin influence. Experiments and observations on the morphology, diameter, density, tensile strength and stiffness of the fibres were conducted, focusing on the effect of NaOH treatment and its concentration on the changes of these properties.

3.3.1   Morphology study

Optical microscopy (Motic-SMZ 168) was used to study the surface of the fibres, before and after treatment. Ten fibres from each set (untreated, 4%, 6%, and 8% NaOH treated) were selected and evaluated. The diameters of the fibres were measured to identify the average dimension of the bamboo fibres. For high magnification observation of the microstructure of the fibres, SEM was performed using Jeol JCM-6000 with a balance scale range of $\pm$ 0.1μg. The fibres were attached to a carbon adhesive disc, placed on aluminium mounts. The samples were later coated with gold prior to conduction, and the surface modifications resulting from the alkali treatment were examined. Fibre breakages resulting from the fibre tensile test were also observed using SEM to understand the mechanism of failures.

3.3.2   Density measurement

A multipycnometer (Quantachrome MVP-D160-E) was used to measure the volume of the dried fibres. Fibres were chopped to approximately 1 mm in length and weighed prior to volume measurement, using 0.1 mg precision weighing scale (Sartorius CP225D). A known volume of helium gas in the pycnometer's reference cell was released into the sample cell containing the fibres. The remaining pressure of the helium gas in the reference cell was used to determine the volume of the fibres (Truong et al. 2009). Three repetitions were performed for each set and the densities calculated.

3.3.3   Single Fibre Tensile Test

In the single fibre tensile test (SFTT) sample preparation, two ends of each fibre

were adhered into sandpaper grips using adhesive glue with a gauge length of 10 mm: the test set-up is presented in Figure 3.7. Principally, the technique is to elongate the single fibre under tensile load until it fails or breaks. The tensile test was performed using a dynamic mechanical analysis machine (DMA Q800), whereby the fibres were subjected to tensile loading at a rate of 1 N/min until complete breakage, according to ASTM D3379 (ASTM 1989). The TA Instrument Explorer software recorded the load and extension and then the stress and strain of the fibres were calculated based on the diameter at the fracture point obtained by stereo zoom microscope (Motic-SMZ 168). A minimum of 10 fibres from each set were tested and the average values have been reported.
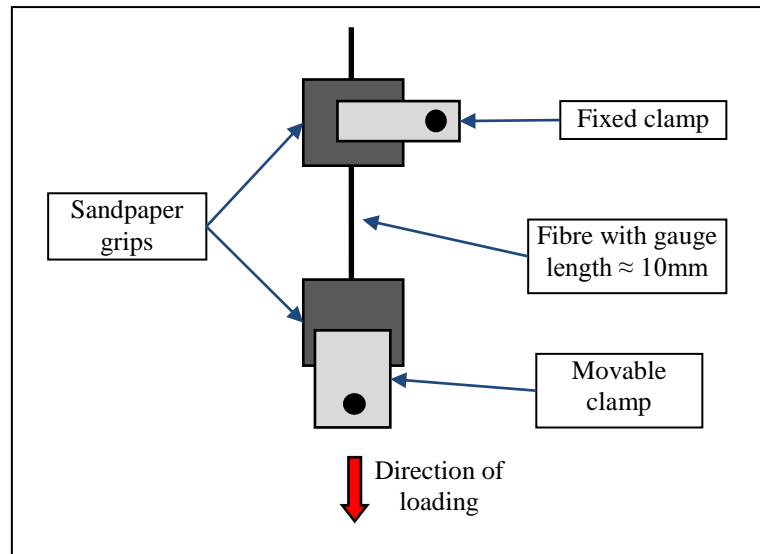
Figure 3.7: Test set-up for Single Fibre Tensile Test

3.4 Mechanical properties of composite

The strength of mechanical interlocking between the untreated and treated fibres with polyester resin was studied using single fibre fragmentation test (SFFT). This allows for some basic understanding of the behaviour of bamboo fibres with the influence of polyester resin. The initial mechanical properties of bamboo fibre/polyester composites and neat polyester, as well as after moisture and thermal degradation, were evaluated based on the tensile strength and Young's modulus of the samples. Comparison was made of the strength between degraded and undegraded samples, describing the durability of materials for outdoor applications. The fractured surfaces of the tensile damaged samples were later observed using SEM to evaluate the effect of morphological changes on the strength of the composites.

3.4.1 Single Fibre Fragmentation Test

Single fibre fragmentation test (SFFT) was performed to determine the interfacial shear strength between reinforcing fibres and a polymer resin in a composite system. The current study is based on the Kelly and Tyson (1965) technique. This basically subjects the specimen to an increasing tensile load, which is transferred to the fibre through the fibre/matrix interface. Each test specimen for SFTT consists of a single fibre embedded in unsaturated polyester resin with a gauge

length of 12 mm, as shown in Figure 3.8. The specimens were prepared in a dogbone shaped mould. Using a small syringe, all air bubbles were removed. The prepared specimens were cured for 24 hours at atmospheric conditions. Next, the samples were removed from the mould and cured again in an oven with a temperature of 50⁰C for 24 hours. Four sets of SFTT samples were fabricated according to the percentage of NaOH treatment: 0%, 4%, 6% and 8%.

The specimens were mounted on the grips of the tensile machine using two steel pieces with suitable grooves for specimen ends, avoiding any compression load that may lead to micro-cracks on the specimen. The test was carried out using a 5 kN capacity load cell (Hounsfield H5K-S) at a cross head speed of 1.3 mm/min. The interfacial shear strength (τ_{IFSS}) was computed using the following equation (Saravanakumar et al. 2013; Wong et al. 2010):

$$\tau_{IFSS} = \frac{F_{deb}}{d_f \pi L_e}$$ Equation 3-1

Where F_{deb} is debonding force, d_f is the fibre diameter and L_e is the fibre embedment length. The interfacial shear strength for each set was taken from the average values of six specimens.
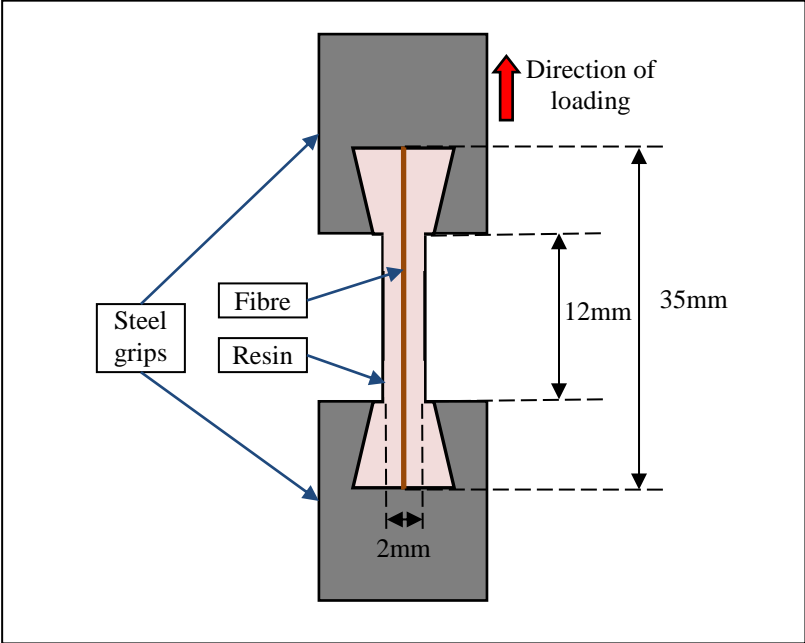
Figure 3.8: Test set-up for Single Fibre Fragmentation Test

3.4.2 Tensile test

Experimental investigation on the tensile properties of composite samples and neat polyester resin, before and after degradation, was conducted as per ASTM D638 (ASTM 2010b), using a universal testing machine, MTS Alliance RT/10, equipped with a 10 kN load cell and MTS Laser Extensometer LX300 to measure the elongation of the specimen. This is shown in Figure 3.9. All tests were conducted with five replicates for each sample type at a cross head speed of 1.3 mm/min. Both

ends of neat polyester and coated composite (BPC-6C) samples were roughened using sand paper to prevent slippage at the grip during testing. This was not required for the other bamboo fibre/polyester composites, as the relatively rougher surface was sufficiently gripped by the machine. The stress-strain curves were plotted by TestWorks software until failure was detected. The average values of the tensile strength and elastic modulus were reported.
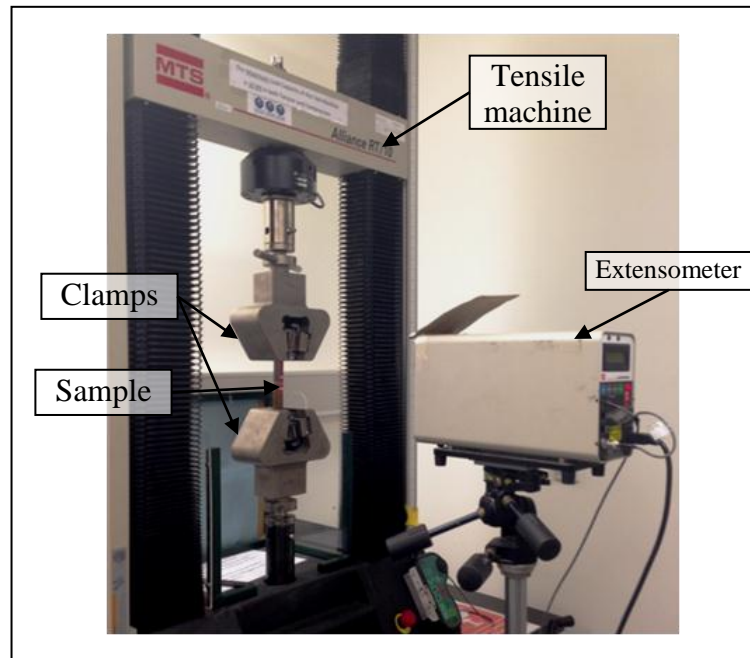
Figure 3.9: Tensile test setup with laser extensometer

3.4.3   Morphology observation of fractured surface

The fractured surface morphologies of the tensile tested samples were further investigated using scanning electron microscopy (SEM), Jeol JCM-6000, with a balance scale range of $\pm$ 0.1μg. The specimens were cut to approximately 10x10x10 mm and attached to carbon adhesive discs, placed on aluminium mounts. To eliminate charge effect, 10 nm of gold coating was used to coat the specimens prior to SEM conduction. The morphologies were observed, including fibre/matrix interaction, as well as fibre and resin conditions.

3.5   Thermal decomposition experiments

To study the thermal resistance of bamboo fibre/polyester composites and their constituents, three types of tests were used: thermo gravimetric analysis (TGA), dynamic mechanical analysis (DMA) and thermo-mechanical test. TGA was performed on untreated and treated bamboo fibres, neat polyester and the composites to identify the decomposition temperature and charring capability of these materials. The visco-elastic properties of neat polyester and bamboo fibre/polyester composites were analysed using DMA, with the glass transition temperature (T_g) obtained from the loss modulus curves. Finally, the static tensile properties of the samples exposed to increased temperature in the plastic region up to T_g were studied using thermo-

mechanical test, whereby tensile tests were conducted in a controlled environment at 40^0C, 80^0C and 120^0C.

3.5.1   Thermo gravimetric analysis

Thermo gravimetric analysis (TGA) was used to study the thermal degradation of untreated and treated bamboo fibres, as well as their composites and neat polyester resin. This study was performed to determine changes in weight, in relation to temperature, in a controlled atmosphere. For the bamboo fibres, the samples were chopped into short strands with an initial weight of approximately 5 mg, while the composites and neat polyester were cut into small cubes weighing approximately 20 mg, as shown in Figure 3.10. The TGA equipment (TA Instrument TGA Q500) was programmed for heating from room temperature to 600^0C, with a heating rate of 10^0C/min. For the TGA environment, Monteiro et al. (2012) noted that both atmosphere and nitrogen environments could be used to test cellulosic fibres. Partial overlapping of this peak with the exothermic peak was noted as corresponding to the oxygen reaction with the cellulose. As a consequence, the main TGA peak is shifted to lower temperatures in oxidative atmospheres, compared to inert atmospheres. Moreover, nitrogen is used during TGA testing for natural fibres as performed by most researchers (Araújo et al. 2008; Aziz & Ansell 2004; Lee & Wang 2006; Manfredi et al. 2006; Shih 2007; Suardana et al. 2011; Yao et al. 2008). Based on this information, the current work was tested in a nitrogen environment. TGA and DTG curves were obtained from the runs and were used to determine the percentage of weight loss and the decomposition temperatures with the number of degradation steps, respectively. The percentage of residues left after the TGA runs represent the materials' char production.
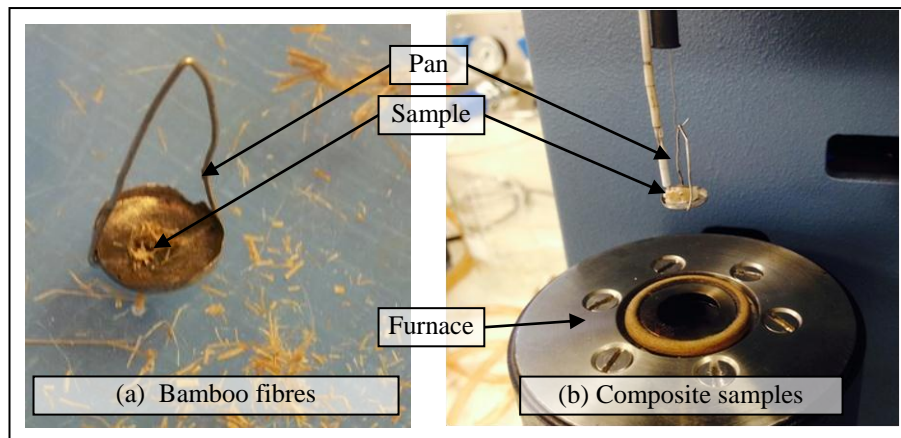
Figure 3.10: Thermo gravimetric analysis test set-up

3.5.2   Dynamic mechanical analysis

TA instrument DMA Q800 was used to evaluate the dynamic mechanical properties of the composite materials and the neat polyester. Rectangular samples with the dimension of 60x 15x5 mm were used in the test; the set-up is presented in Figure 3.11. The equipment was operated in a dual cantilever mode (oscillation amplitude: 15 μm) at 1 Hz frequency, from room temperature to 180^0C, at a heating rate of 3^0C/min. The data, which includes storage modulus, loss modulus and tan δ, were recorded by the TA Instrument Explorer software and were plotted against temperature. The glass transition temperatures (T_g) were obtained from the peak of the loss modulus curves.
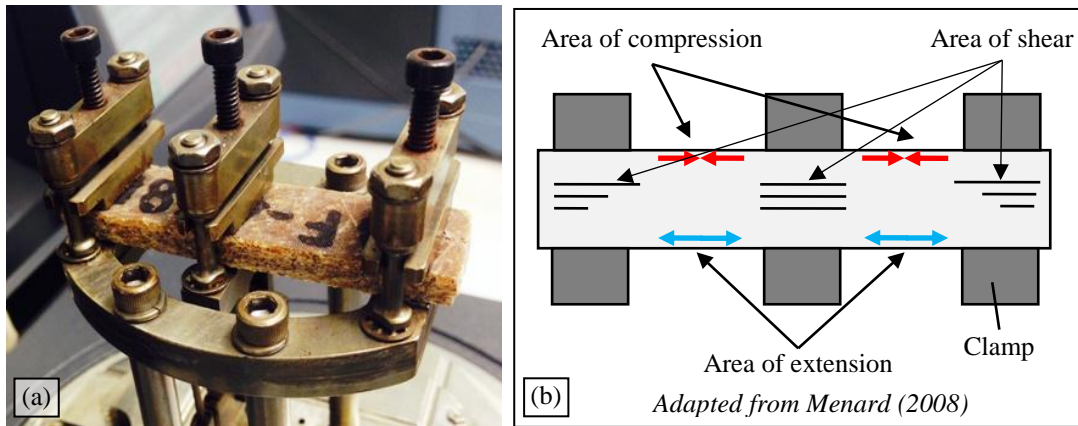
Figure 3.11: Dynamic mechanical analysis test setup

3.5.3 Thermo-mechanical test

Untreated (BPC-0), treated (BPC-6) and coated composites (BPC-6C), as well as neat polyester (NP) samples, were exposed to three temperature settings: 40^0C, 80^0C and 120^0C, to study the effect of elevated temperatures on the mechanical properties of these materials. An INSTRON 3119 Environmental Chamber was incorporated onto the MTS tensile machine; the test set-up is shown in Figure 3.12. Five specimens for each sample were placed in the environmental chamber at the specified temperature setting for 1 hour prior to tensile testing. The initial weight and thickness of the specimens were taken using 0.1 mg precision weighing scale (Sartorius CP225D) and 0.01 mm precision vernier calliper (Kincrome), respectively. After 1 hour of heat exposure, changes in weight and thickness were recorded. The specimens were immediately mounted on the tensile machine as described in Section 3.4.2, but this time within the environmental chamber. The tensile load was applied in a controlled environment at constant temperature, simulating fire exposure (without flame effect) on the samples during in-service conditions. The displacement was also measured using an MTS Laser Extensometer, which was placed outside the chamber, recording the data through the chamber's glass window. The stress-strain curves were plotted until failure was detected.
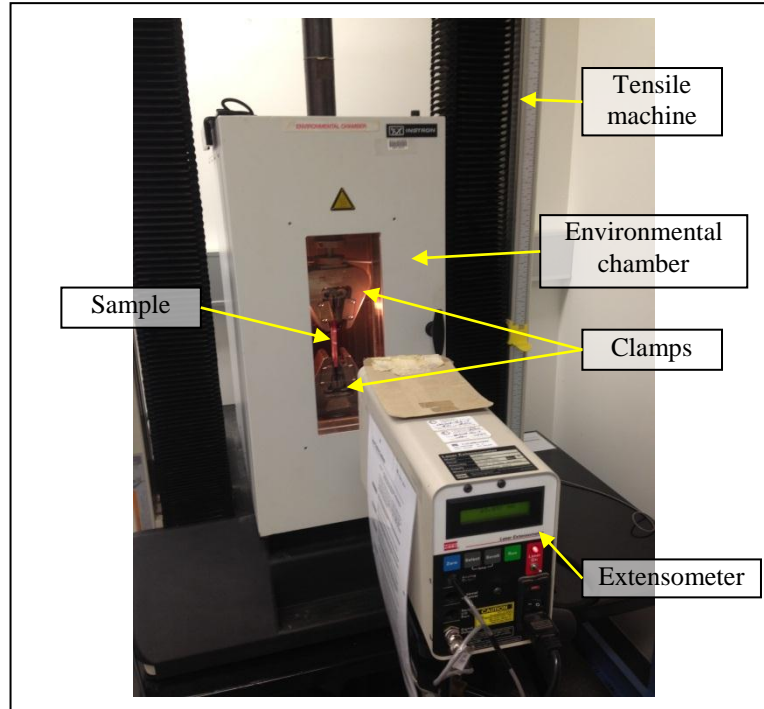
Figure 3.12: Equipment setup for thermo-mechanical test

Changes in weight and thickness due to the temperature exposure were calculated based on Equation 3-2 and Equation 3-3:

$$W(\%) = \frac{W_f - W_o}{W_o} \times 100$$
Equation 3-2

Where W_o and W_f denote the initial weight and the final weight of the sample, respectively.

$$T(\%) = \frac{T_f - T_o}{T_o} \times 100$$
Equation 3-3

Where T_o and T_f denote the initial thickness and the final thickness of the sample, respectively.

Results of the tensile strength, elastic modulus, and changes in weight are presented as an average of five specimens. The fractured surfaces were visually inspected and the morphologies studied using SEM.

3.6 Moisture degradation experiments

The effect of moisture on the physical and mechanical properties of bamboo fibre/polyester composites and their constituents is generally investigated by immersing these materials in water. The moisture absorptivity, moisture kinetics, thickness swelling, volume expansion and tensile properties of the moisture degraded neat polyester and composite samples were later calculated. Two sets of conditions were evaluated in this study: moisture degradation at room temperature (25^0C), and hygrothermal degradation at 80^0C.

59

3.6.1 Fibre moisture absorption study

Untreated and treated fibres were subjected to three conditions: immersion in distilled water, immersion in rain water, and exposure to room humidity to study the moisture absorptivity of the bamboo fibres. Before and after immersion, all fibres were oven dried at 50^0C for 24 hours, and the dry weight was measured using a high precision scale ± 0.1 µg (Sartorius CP225D). The fibres were then exposed to the three sets of conditions at room temperature (25^0C) for 24 hours. Fibres that had been immersed in distilled water and rain water were placed in air tight containers to avoid any effect of water evaporation. The fibres were reweighed after surface moisture was removed. The percentage of moisture content was determined by the weight gain relative to the dry weight of the fibres and computed as follows:

$$M(\%) = \frac{W_f - W_o}{W_o} \times 100 \hspace{3cm} \text{Equation 3-4}$$

Where W_o and W_f denote the dry weight of the sample and the final weight, respectively.

3.6.2 Moisture absorption of composites at room temperature

For the composite and neat polyester samples, two types of specimens with different dimensions were prepared. The physical study for moisture absorption was conducted on small pieces of square samples, measuring 15x15x5 mm. For the tensile test, the same sized samples were prepared as per Figure 3.5.

For the first test condition, all samples were immersed in water at room temperature; that is, 25^0C. For the physical study specimens, the initial weight and exact dimensions were recorded using 0.1 mg precision weighing scale (Sartorius CP225D) and 0.01 mm precision vernier calliper (Kincrome), respectively. At regular intervals, the specimens were removed from water and immediately wiped with filter paper to remove surface water. Within 30 seconds, the sample was weighed to avoid errors due to evaporation. The change in dimension was also measured. The samples were reimmersed in water to permit the continuation of sorption until saturation limit was reached. In this case, it took approximately 60 days of test duration. The test was carried out according to ASTM D570 (ASTM 2010a). The final physical appearances of the specimens were observed and the morphologies were evaluated using SEM.

The weight, thickness, surface area and volume gain relative to dry condition were reported in terms of percentage against time, using the following equations:

$$W(\%) = \frac{W_f - W_o}{W_o} \times 100 \hspace{3cm} \text{Equation 3-5}$$

$$T(\%) = \frac{T_f - T_o}{T_o} \times 100 \hspace{3cm} \text{Equation 3-6}$$

$$A(\%) = \frac{A_f - A_o}{A} \times 100 \hspace{3cm} \text{Equation 3-7}$$

$$V(\%) = \frac{V_f - V_o}{V_o} \times 100 \hspace{3cm} \text{Equation 3-8}$$

Where W, T, A, and V represent weight, thickness, area and volume. The subscripts 'o' and 'f' refer to the initial and final values, respectively. From these results, moisture absorptivity, moisture absorption kinetics, thickness swelling rate and volumetric strain were calculated and discussed.

As saturation was achieved after 60 days, the samples for tensile test were left to soak in water for the same duration. To minimise moisture loss, the specimens were removed from the conditioning chamber immediately before the tests. Tensile testing was conducted as described in Section 3.4.2. The tensile ruptured surfaces were later observed under SEM to study the degraded samples' morphologies.

3.6.3 Moisture absorption in hygrtohermal condition

Considering that outdoor materials placed under direct sunlight in summer can be exposed to elevated temperatures of up to 80^0C, possibly along with high humidity, the second test condition involves both heat and moisture exposure. This hygrothermal condition was conducted on the physical study samples and the tensile test samples, whereby specimens were subjected to immersion in water, and placed in a laboratory oven at 80^0C. The same test procedures were conducted for these specimens as for the first condition. The hygrothermal test was terminated after signs of physical deterioration were observed on the specimens; in this case, they occurred after two days of test duration. All results obtained for both conditions were compared to data for undegraded samples.

DMA was also performed on moisture saturated samples. DMA specimens were soaked in water at room temperature for 60 days to ensure moisture equilibrium was reached. The same procedure as described in Section 3.5.2 was conducted, exposing the samples to increased temperatures up to 170^0C. The change in visco-elastic properties and T_g due to hygrothermal effect were reported.

Chapter 4 : Alkali Treatment Optimization on Bamboo Fibre/Polyester Composites

4.1   Introduction

To understand the contribution of bamboo fibres in a composite system, the characteristics of the fibre should be comprehensively evaluated. One major issue regarding the use of natural fibres in the polymer composite industry is the incompatibility between hydrophilic fibres and hydrophobic polymer resin. This renders weak interfacial adhesion that leads to ineffective load transfer from the matrix resin to the reinforcing fibres. One of the most recent and effective techniques to improve interfacial adhesion between natural fibres and polymer matrices is alkali treatment, which involves the immersion of fibres in NaOH solution.

While several studies have shown the potential of using bamboo fibres as reinforcement in natural composites, limited work has been conducted to comprehensively study the influence of NaOH on the structural, physical and tensile characteristics of bamboo fibre. Such study is essential to understand these important characteristics of bamboo fibres. This will lead to mechanical improvement, producing composites with enhanced properties and eventually, expanding the use of bamboo fibres in the polymer composite industry. This chapter aims to evaluate the effect of alkali treatment on the structural, physical and tensile characteristics of bamboo fibres, as well as the interfacial and tensile properties of the corresponding bamboo fibre/polyester composites. The morphological changes of the fibres and the effects on the interfacial adhesion of the fibre/matrix interface have been studied using SEM to understand the composites' mechanical behaviour. SFTTs and SFFTs were used to study the tensile and interfacial behaviours of the fibres, respectively.

4.2   Influence of fibre treatment on the structural properties of fibres

Changes in the structure of bamboo fibres from the effect of alkali treatment are discussed in this section. Figure 4.1 shows the lateral views from optical micrographs and SEM of untreated and treated bamboo fibres. For untreated bamboo fibres, the optical micrograph shows an almost smooth fibre surface. The SEM indicates that the fibre surface is mostly covered with cell wall, and only some fibrils are visible. Through alkalisation, the surfaces of all treated bamboo fibres are rougher than the raw fibres. It was further observed that different concentrations of NaOH provided different levels of modification on the fibres surface. At 4% NaOH treatment, some cell walls can still be observed, but most have been removed from the fibre surface and more microfibrils have been exposed. The fibre surface is further roughened at 6% NaOH treatment, and some voids were observed from the optical micrograph. This was confirmed by the SEM, wherein voids in the matrix of the fibre are present. At 8% NaOH treatment, more matrices were removed, exposing the fibrils to alkali attack. It can be observed that the surface of the fibrils experienced some surface disintegration.

Optical Micrograph	Scanning Electron Micrograph
(a)	0 wt.% NaOH

| (b) | 4 wt.% NaOH |

| (c) | 6 wt.% NaOH |

| (d) | 8 wt.% NaOH |
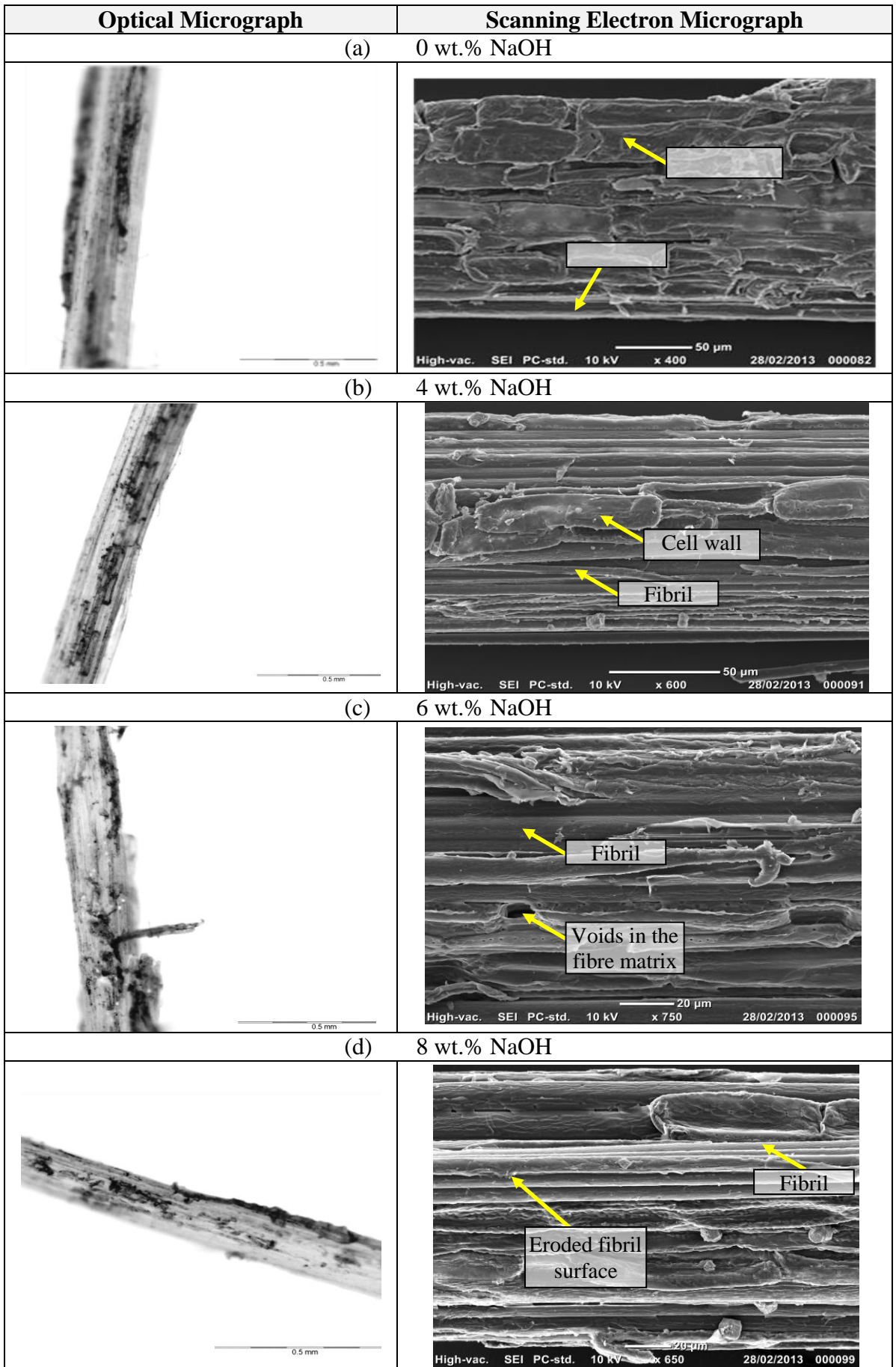
Figure 4.1: Morphology of treated and untreated bamboo fibres

To further explain these mechanisms, it is important to understand the arrangement of bamboo's structural components. The structure of bamboo from macro to nano-level is represented in Figure 4.2. Bamboo fibre itself is a composite, with two main components: parenchyma tissues made up of lignin-hemicellulose matrix, and sclerenchyma tissues consisting of vascular bundles made up of many phloem fibres (Tong et al. 2005). The chemical composition of bamboo fibres is 45.70% cellulose, 25.90% hemicelluloses, 24.95% lignin and 1.65% ash (Yao et al. 2008). However, through the steam explosion process, Shao et al. (2008) suggested that xylan, which is the major hemicelluloses of bamboo cell walls, was largely removed during treatment. The strength of natural fibres is thought to be influenced by their cellulosic components (John & Thomas 2008; Methacanon et al. 2010). As such, this suggests that nearly 50% of the composition of a bamboo fibre's composition contributes to its strength.
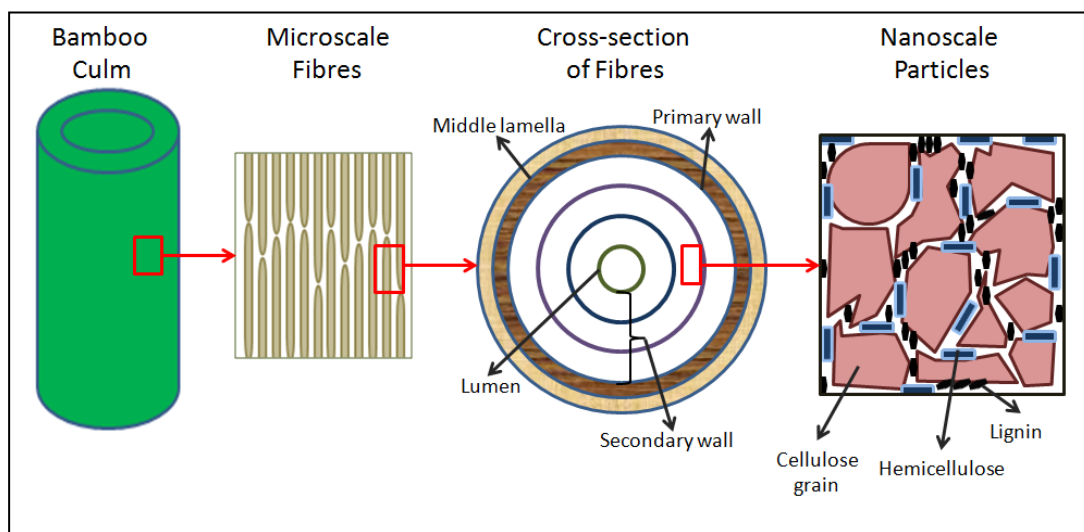
Figure 4.2: Structure of bamboo from macro to nano level, adapted from Zou et al. (2009)

Raw bamboo fibres are protected by the outer layer, which is the cell wall. This can be observed in Figure 4.1(a), whereby a thick layer covers most of the fibre's perimeter, providing a smooth surface profile. However, some exposed fibril is also visible, which implies that some areas on the fibre surface are affected by the steam explosion process. As NaOH is introduced in the fibre treatment, these cell walls were removed, exposing more fibrils; in Figure 4.2 this refers to the cellulose grains. At 6% NaOH, the alkali may have been strong enough to erode the hemicelluloses-lignin matrix, explaining the presence of voids in Figure 4.1(b). This has also been reported by Wong et al. (2010), whereby hemicelluloses, lignin, waxes, oil and surface impurities of bamboo fibres are soluble in NaOH aqueous solution, causing the cell wall to open up as these substances were dissolved. As the NaOH concentration is further increased to 8%, more hemicellulose-lignin matrix was removed from the fibre, exposing more fibrils. These fibrils are also more vulnerable to alkali attack, which may explain the rougher fibril surface observed in Figure 4.1(d). Once the cellulosic component of the fibre is affected by alkali, the strength of the fibre may be compromised. Most studies limit the concentration of NaOH to 10 wt.% for alkali treatment of natural fibres as higher concentrations worsen the fibre's mechanical properties (Wong et al. 2010).

Studying the morphology of natural fibres is important for predicting interactions with polymer resins in a composite system (Spinacé et al. 2009). The smooth surface texture of untreated bamboo fibres provides poor friction and weak interlocking with polymer, possibly resulting in a composite with low strength. In comparison to other natural fibres, similar findings were also observed with changes in fibre morphology due to increased NaOH treatment. Hemp and kenaf fibres treated at 6% NaOH were observed through SEM to be roughened with obvious removal of wax, oil and other surface impurities in comparison to raw fibres (Aziz & Ansell 2004). Sydenstricker et al. (2003) confirmed that at 5 and 10% NaOH , sisal fibres suffer serious physical effects, with a rougher surface compared to fibres treated at 1 and 2% NaOH, whereby fibre integrity is still preserved. Surface impurities on Borassus fruit fibre was observed to be completely removed at 15% NaOH treatment, but with an increased pore presence. The authors highlighted that if these pores exceeded the desired amount, the mechanical properties of the fibres might be reduced (Boopathi et al. 2012). However, some natural fibres exhibit a different reaction towards NaOH treatment. Raffia fibres become smoother and cleaner as the concentration of the solution is increased from 0 to 10% NaOH (Elenga et al. 2013). Untreated coir fibre contains globular protrusions and cuticles on their surfaces, which were removed at 7% NaOH, making the fibre smoother (Nam et al. 2011). Thus, it is noteworthy to highlight that different natural fibres undergo different morphological changes from alkalisation. It is important to understand how NaOH treatment and its various concentrations alter the fibre surface to predict its consequent interlocking with the polymer resin.

4.3 Influence of fibre treatment on the physical properties of fibres

From the morphology study in Section 4.2, it is expected that that the alkali treatment may have an effect on the physical and mechanical properties of bamboo fibres. The physical observations discussed in this section include the visual appearance, as well as the changes in fibre diameter and density.

4.3.1 Visual inspection

Figure 4.3 shows the colour changes experienced by bamboo fibres. Treated fibres are darker compared to untreated ones. They are more brownish as oppose to the paler raw fibres; thus it is possible to visually differentiate between raw and treated fibres. However, there was no obvious difference in appearance between the 4%, 6% and 8% NaOH treated fibres. Other researchers had also observed some changes in colour due to exposing fibres to treatments. The lignin component of a natural fibre is said to be responsible for its colour changes (Mohanty et al. 2000). Elenga et al. (2013) had measured the changes in colour of Raffia textilis fibre using a spectrocolorimeter. They found that alkalisation increased the yellowness and redness, and reduced the lightness of the fibres. This can also be visually observed on the bamboo fibres studied. Elenga et al. (2013) also agreed that the lightness did not vary significantly with the NaOH concentration. Khan and Ahmad (1996) also reported a reduction in lightness of jute fibres by 10 to 20% due to alkalisation, which resulted from lignin removal. However, some natural fibres experienced increased lightness after treatment. Rout et al. (2001) had reported that by bleaching coir fibres, the fibre changed colour from dark brown to silvery white, which they

attributed to the removal of lignin. Sisal fibres were also reported by Sydenstricker et al. (2003) to become lighter in colour and rougher at treatments higher than 5% NaOH.

Figure 4.3: Changes in appearance of bamboo fibres due to alkalisation

4.3.2 Diameter distribution

The diameter of the bamboo fibre's cellulose fibril was measured using SEM, and is shown in Figure 4.4. The diameter is approximately 11.3 µm. In a nano-scale study conducted by Zou et al. (2009), the authors observed that the diameter of the microfibrils, or the building blocks of bamboo fibres, is about 5 to 20 µm. This concurs with the measurement performed in this study.
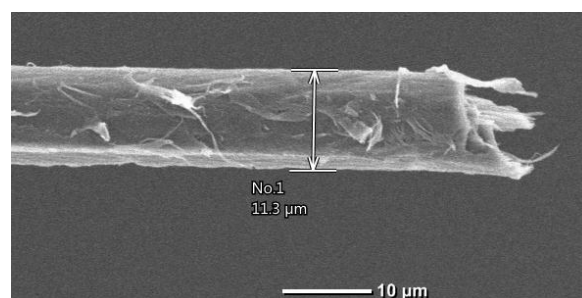
Figure 4.4: Diameter of a bamboo fibre microfibril

The average diameter, measured from 40 fibres for each treatment concentration, is shown in Figure 4.5. The average diameter decreases as the fibres undergo alkalisation up to 6% NaOH. This corresponds to the SEMs in Figure 4.1, which shows the removal of the fibre cell walls, as well as other surface impurities, thus reducing the diameter of alkalised fibres. However, at 8% NaOH, the average diameter was observed to increase. This can be attributed to the partial separation of fibrils with the removal of hemicellulose and lignin, which acts as matrix binding these fibrils together. Overall, the average diameter of the bamboo fibres used in this

study was 161.52 μm, with a range from 89 to 317 μm, measured from 160 fibres. This measurement is within the range of 88 to 330 μm presented by Ratna Prasad and Mohana Rao (2011) for bamboo fibres.
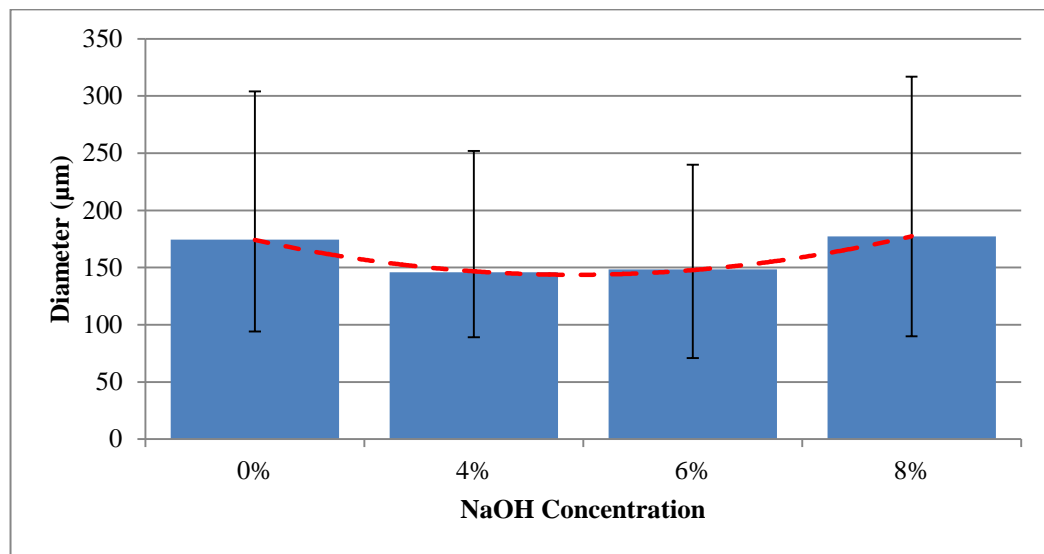
Figure 4.5: Average of fibre diameter for treated and untreated fibres

Figure 4.6 shows the distributions of fibre diameters at different levels of treatment. The frequency distribution for all fibre conditions is Gaussian. Fibres treated with 4 and 6% NaOH (Figure 4.6 (b) and (c)) present a narrower range of distribution due to the removal of the cell walls and surface impurities, while alkalisation at 8% NaOH (Figure 4.6 (d)) presents a wider distribution, similar to the untreated fibres. This is probably due to weakening of the interaction between fibrils in the fibre bundle, leading to partial fibrillation (Spinacé et al. 2009). This phenomenon can be demonstrated in Figure 4.7, whereby erosion of the cell wall and partial removal of the fibre matrix leads to separation of the individual fibrils, dispersing further from one another.
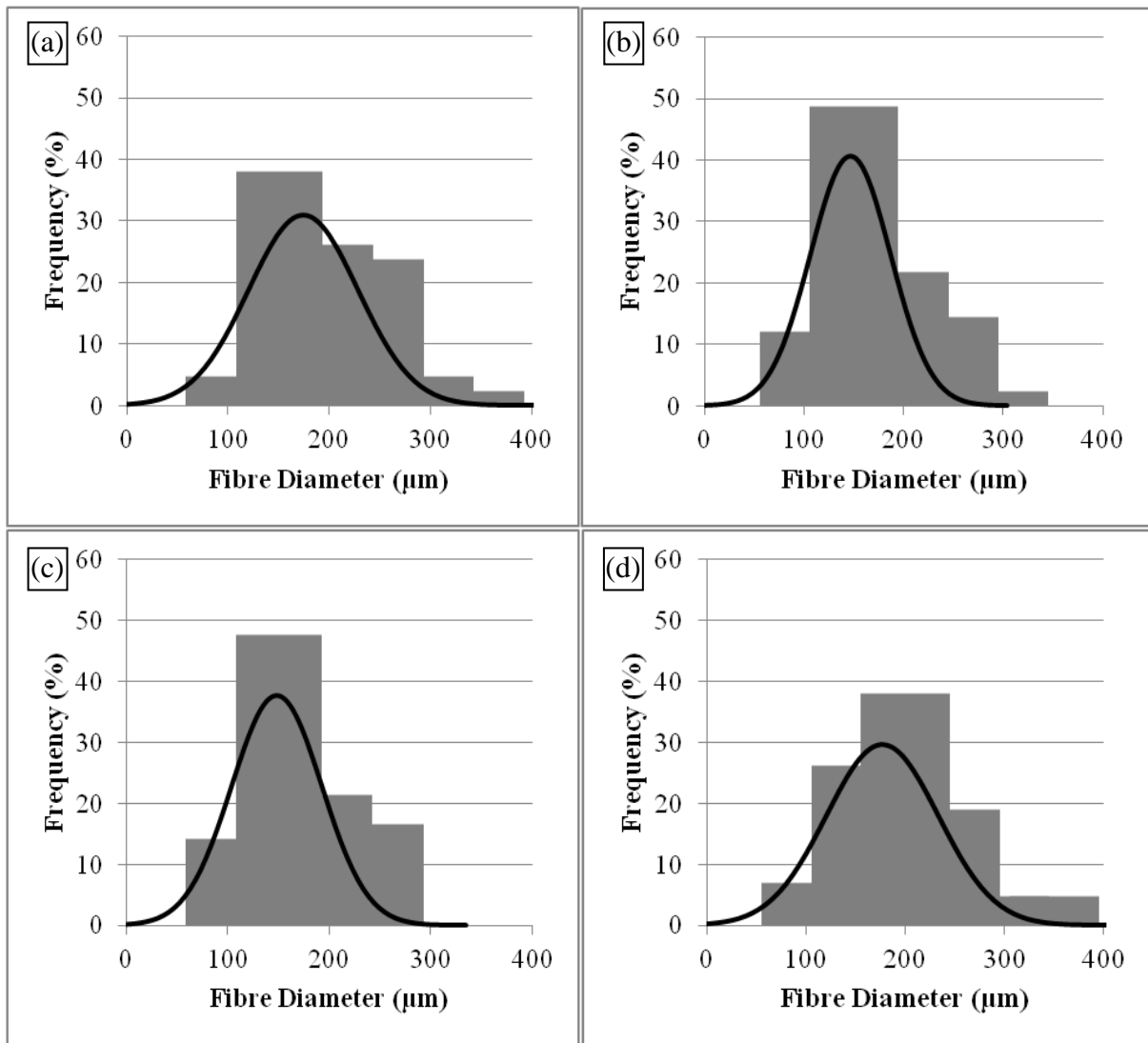
Figure 4.6: Distributions of fibre diameters: (a) 0%, (b) 4%, (c) 6% and (d) 8% NaOH
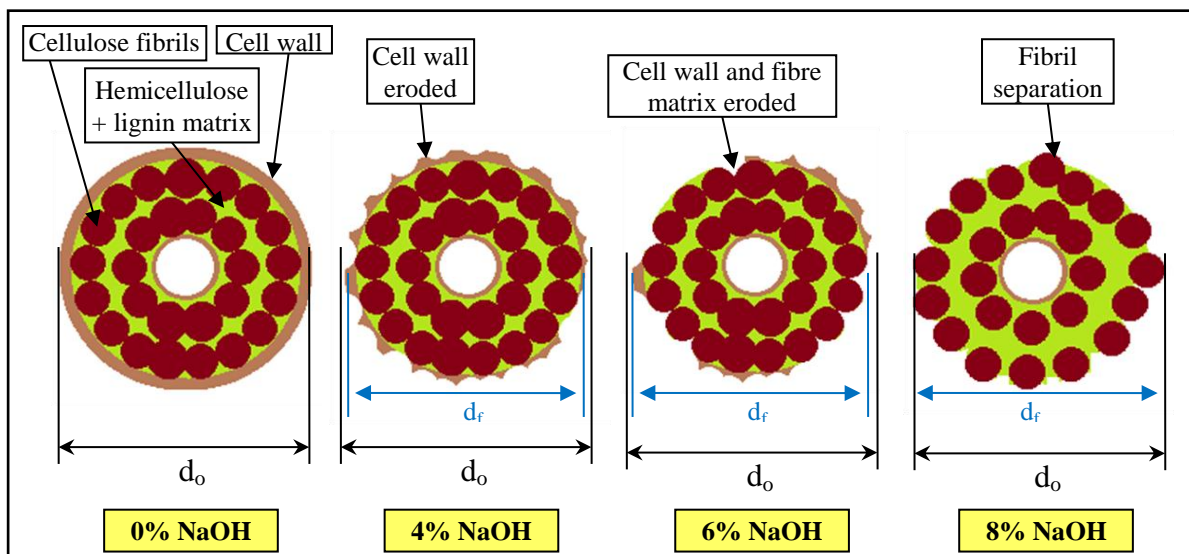
Figure 4.7: Schematic diagram of diameter change of a bamboo fibre due to alkalisation

Note: d_o = initial diameter, d_f = final diameter

4.3.3   Changes in density

As the concentration of treatment is increased, the density of the fibres decreases slightly, as shown in Figure 4.8. Without treatment, raw bamboo fibres have a density of 1.47 g/cm^3, which reduces to 1.39 g/cm^3 at 8% NaOH treatment. This can be attributed to the extraction of the fibre's soluble components such as hemicelluloses, lignin and other impurities, as well as corrosion of the cell wall. From the morphology observations, the number of voids on treated fibres is higher than on untreated fibres; this can contribute to the lower density of treated fibres.

Helium pycnometer measures the absolute density of a fibre, which does not account for the lumen and pores. Therefore, it only measures the solid matter of the fibres (Mwaikambo 2009). Different natural fibres react differently to alkalisation in terms of densities, as presented by Mwaikambo (2009), whereby some fibres experienced a reduction in density, some experienced an increase, while others exhibited no changes. The decrease in density due to alkalisation was also observed on sisal fibres (Rong et al. 2001; Sydenstricker et al. 2003) and bamboo fibres (Wong et al. 2010). However, some fibres underwent increase in density, such as reported on Borassus fruit fibres (Boopathi et al. 2012), and hemp and kenaf (Aziz & Ansell 2004); due to cell wall densification of these fibres.

	0% NaOH	4% NaOH	6% NaOH	8% NaOH
□ Density	1.47	1.43	1.41	1.39
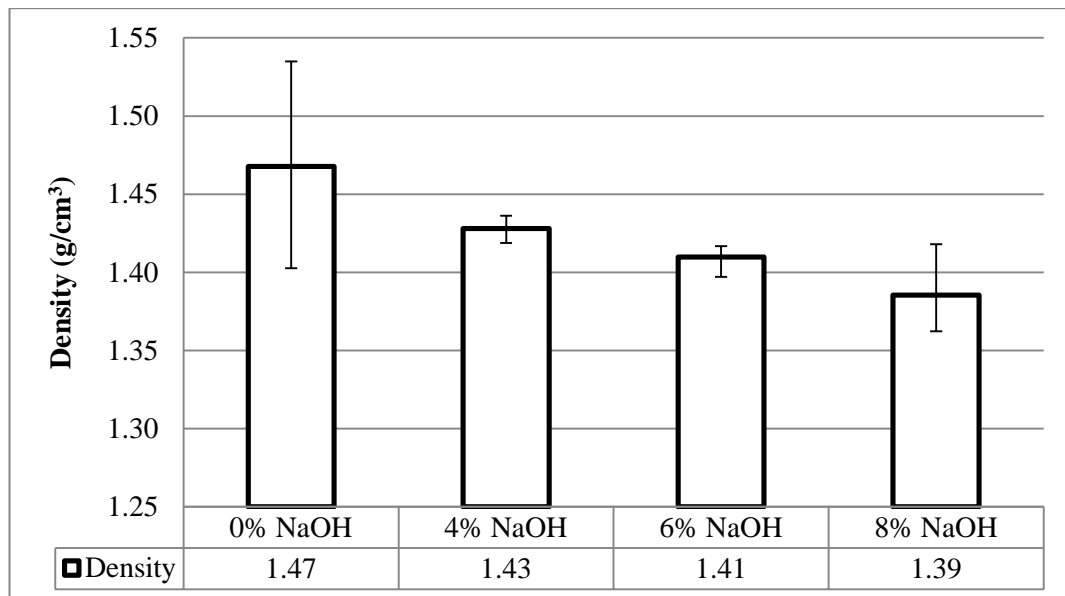
Figure 4.8: Density of bamboo fibres at different concentration of alkali treatment

4.4   Tensile properties of fibres

The single fibre tensile test performed on bamboo fibres yields typical stress-strain curves, as presented in Figure 4.9. Initially, the curves show increased strain at very low stress which can be neglected as it may be caused by the clamps adjusting to the full length of the fibres. Once this has been established, it can be observed that all fibres behave in a brittle manner whereby a sudden halt in linear stress increment was achieved at maximum load.   Generally, the highest maximum stress was obtained by 6% NaOH treated fibres, followed by 4, 0 and 8% NaOH treated fibres. A minimum of ten fibres for each fibre sample was tested. The tensile properties of

the fibres were extracted from the stress-strain curves and the average values obtained.
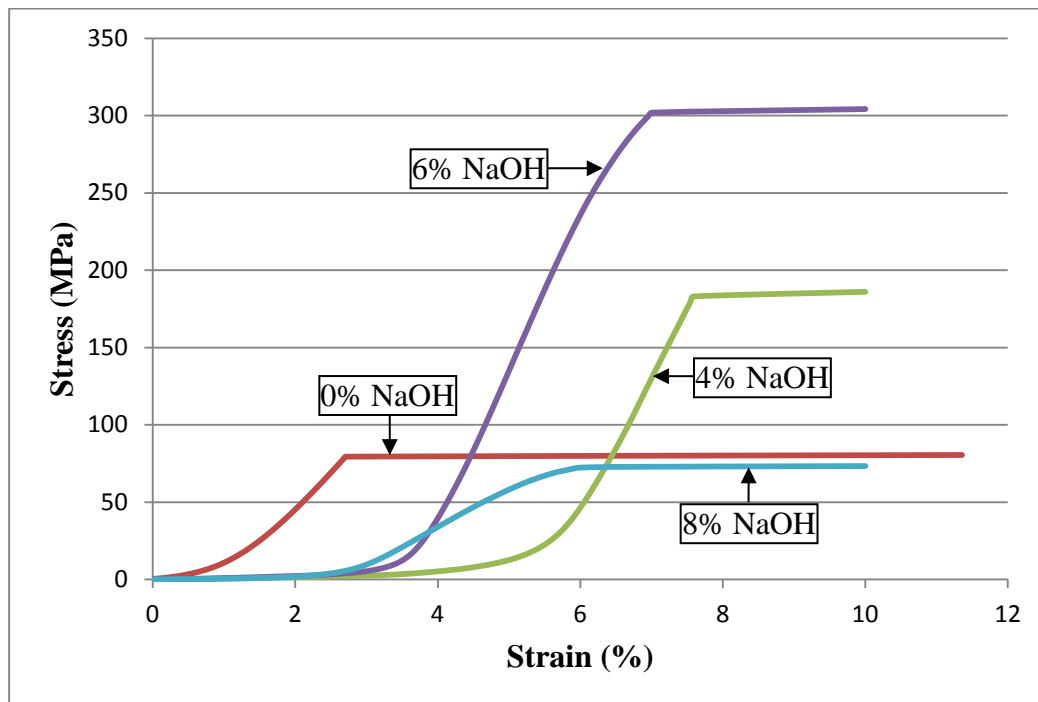
Figure 4.9: Stress-strain curves of bamboo fibres at different concentration of NaOH treatment

Figure 4.10 shows the average tensile strength, while Figure 4.11 shows the average modulus of elasticity of untreated and treated bamboo fibres. The tensile strength and elastic modulus of bamboo fibres are higher for treated fibres up to 6% NaOH, decreasing at 8% NaOH. The increase in tensile strength and elastic modulus is highest at 6% NaOH treatment, with 181% and 47% improvement, respectively. Through the SEM observations, the partial removal of weaker components of the fibre can be clearly seen as the concentration of alkali is increased. This shows that with the absence of these components, the cellulosic fibrils, which provide the strength to the fibre, were able to align themselves in the direction of loading thus decreasing its microfribil angle. This maximises their load-carrying ability and reduces the chances for higher elongation.

The increased tensile strength due to fibre treatments were also observed on Agave fibres (Bessadok et al. 2008) and Borassus fruit fibres (Boopathi et al. 2012). Further, Boopathi et al. (2012) indicated that alkalisation causes the fibre matrix to partially dissolve and allows better alignment of fibrils. This may contribute to the increase in tensile strength. Kalia et al. (2009) had highlighted that alkalisation affects the chemical composition of natural fibres, the degree of polymerisation and molecular orientation of the cellulose crystallites, due to the removal of cementing substances like lignin and hemicellulose, with long-lasting effects on the strength and stiffness of the fibres. The improvement in strength among NaOH treated bamboo fibres (1, 3 and 5% by weight) was also reported by Wong et al. (2010), who predicted that higher concentrations of caustic soda caused a decrease in microfibril angle, whereby natural fibres with low microfibril angles exhibited high strength. However, at higher concentrations of NaOH, which in this case is at 8% concentration, fibres are

weakened by higher matrix removal and damage on cellulosic fibrils (Boopathi et al. 2012). This was observed through SEM, as shown in Figure 4.1, whereby some damage can be observed on the fibril surface of the 8% NaOH treated fibre. This reduced the tensile strength even further, by up to 24% more than the untreated fibres. The stiffness was also observed to decrease by 29%.
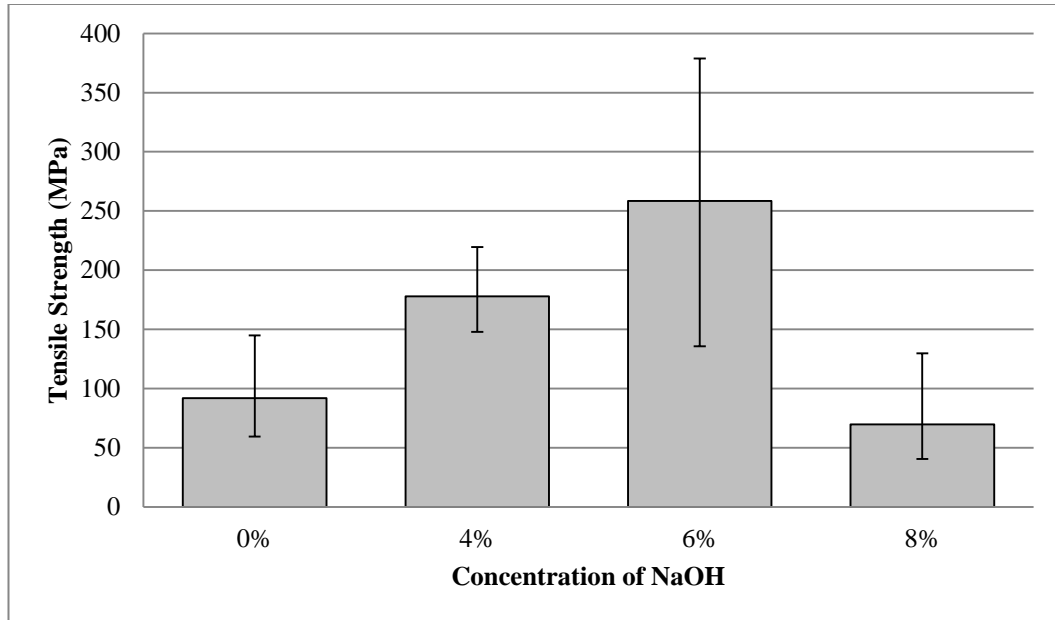
Figure 4.10: Tensile strength of bamboo fibres at different NaOH concentration
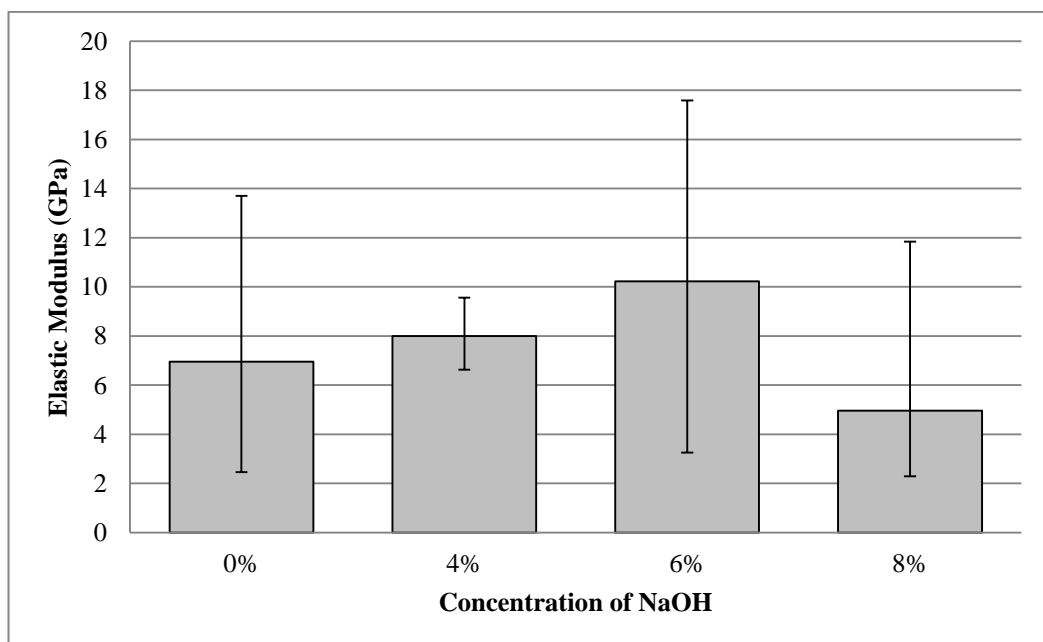
Figure 4.11: Elastic modulus of bamboo fibres at different NaOH concentration

The increased in stiffness of the treated fibres, as highlighted by the values of the elastic modulus, was also observed by some researchers. The authors attributed this to the densification of the fibre cell walls, caused by the high removal of hemicellulose through alkalisation and also by the formation of new hydrogen bonds between the cellulose fibril chains (Obi Reddy et al. 2013; Sawpan et al. 2011). However, based on the density measurement of the bamboo fibres, alkalisation

caused the density of treated fibres to decrease when voids were present. The improved stiffness of natural fibres was mentioned by Kalia et al. (2009) as attributable to the crystalline region (cellulosic) of the fibre. Therefore, in this case, the possible improvement in fibril alignment that causes increased fibre tensile strength may also contribute to improvements in stiffness. With better alignment, less deformation can be expected as the fibres are being stretched in the tensile direction.

4.5   Morphology of fractured fibres

Figure 4.12 to Figure 4.15 show comparisons between the fractured surfaces of untreated and treated fibres obtained through SEM. In Figure 4.12, it can be seen that the untreated fibre experienced a brittle-like failure, where the fracture occurs all the way through the cross-section of the fibre. Presence of the fibre matrix may contribute to this, as it ensures cohesion between fibrils. It can be noted that brittle materials have low values of elastic modulus. The failure of 4 and 6% NaOH treated fibres can result from individual fibril breakages, as presented in Figure 4.13 and Figure 4.14. With partial removal of the fibre matrix, the tensile load is mainly transferred along the fibrils, with less influence from neighbouring fibrils, making it less brittle than the untreated fibre. The stiffness decreases for 8% NaOH treated fibres, due to damage on the fibrils. It was observed that the fractured surfaces for 8% NaOH treated fibres are similar to the untreated fibres. The absence of cell wall with some mid-splitting of fibrils can be seen clearly in Figure 4.15, which may contribute to the decrease in the modulus of elasticity.
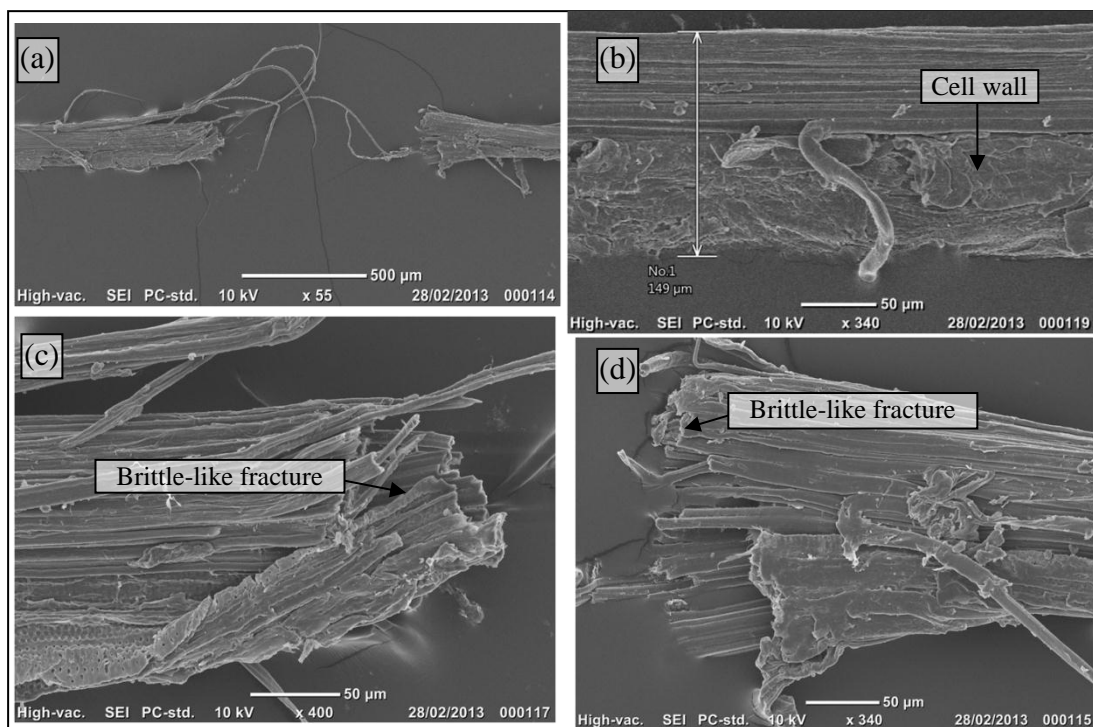
Figure 4.12: SEM of fractured untreated fibres due to single fibre tensile test
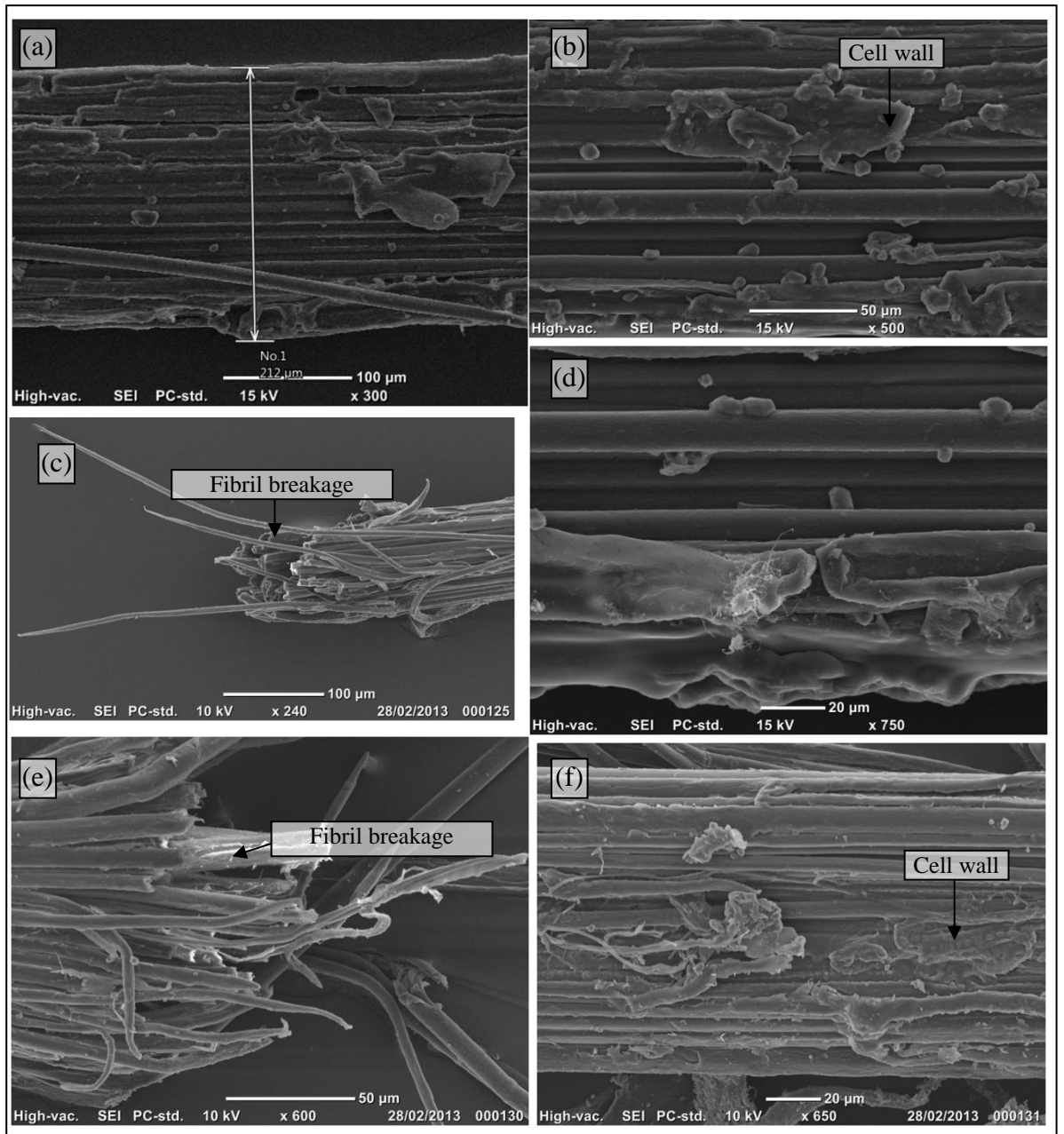
Figure 4.13: SEM of fractured 4% NaOH treated fibres due to single fibre tensile test
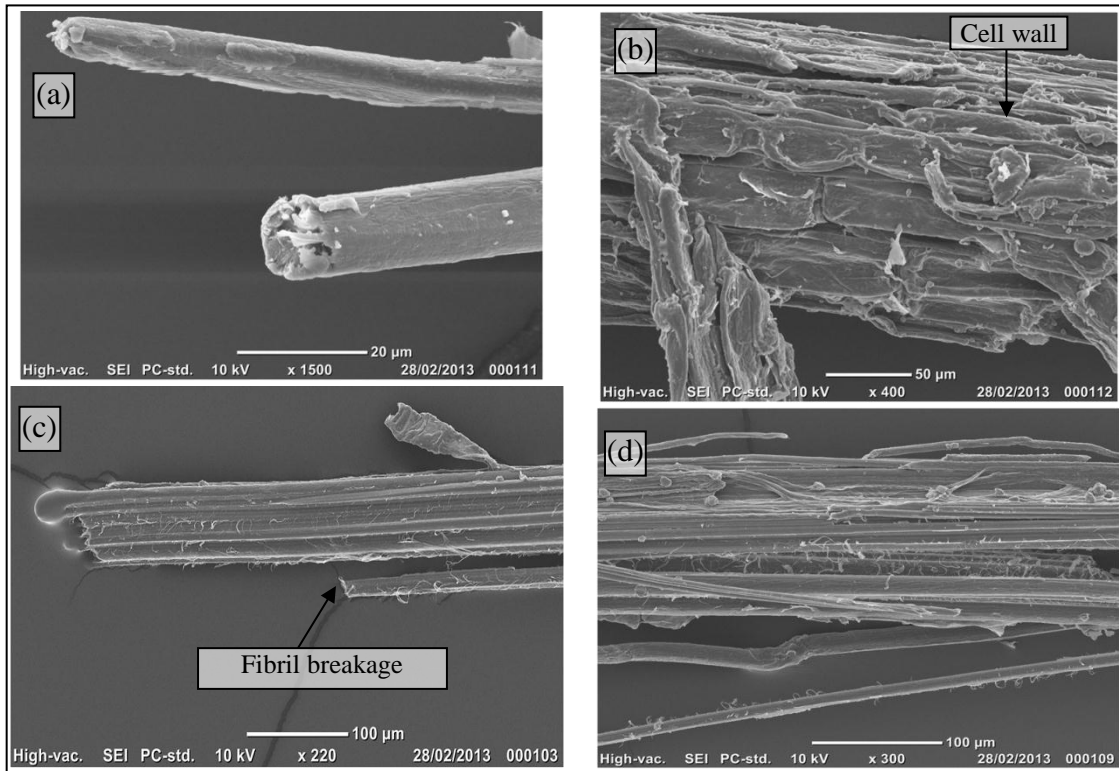
Figure 4.14: SEM of fractured 6% NaOH treated fibres due to single fibre tensile test
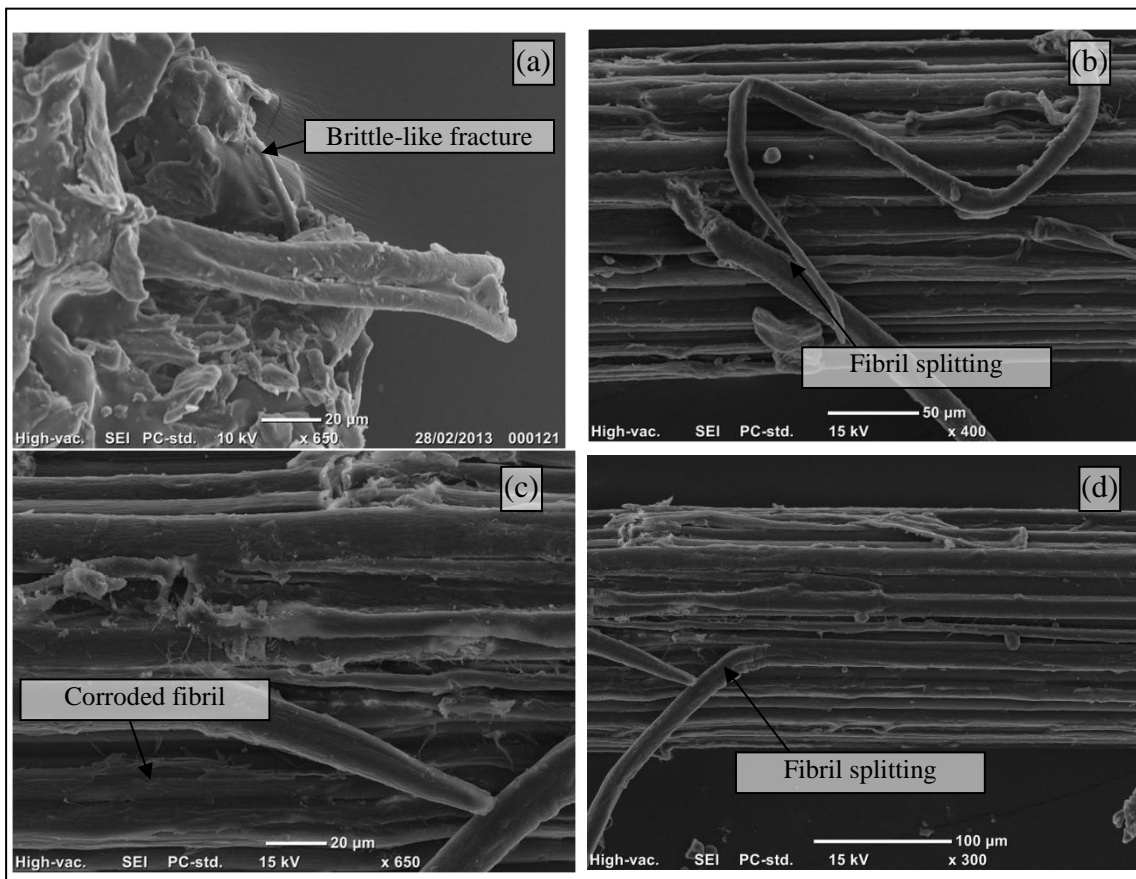
Figure 4.15: SEM of fractured 8% NaOH treated fibres due to single fibre tensile test

74

4.6   Comparison of bamboo fibre properties to other natural fibres

The characteristics of untreated bamboo fibres studied in this thesis are presented in Table 4.1, along with other natural fibres. The bamboo fibres are physically comparable to hemp fibres but with lower tensile properties. This corresponds to the amount of cellulosic component present in the fibres, which plays a major role in the fibres' tensile strength (John & Thomas 2008). The percentages of cellulose in hemp, jute, bamboo and coir fibres are 74.40%, 66.25%, 45.70%, and 43.44%, respectively (Dhakal et al. 2007; Khedari et al. 2005; Yao et al. 2008). Generally, the tensile properties of fibres increase with increasing amounts of cellulose.

Table 4.1: Comparison of several characteristics of untreated bamboo fibres along with other natural fibres

Properties	Hemp	Coir	Jute	Bamboo
Diameter (μm)	80-300 (Ratna Prasad & Mohana Rao 2011)	100-460 (Ratna Prasad & Mohana Rao 2011)	54 (Defoirdt et al. 2010)	94-304
Density (g/cm3)	1.45 (Ratna Prasad & Mohana Rao 2011)	1.29 (Defoirdt et al. 2010)	1.39 (Defoirdt et al. 2010)	1.40-1.53
Tensile strength (MPa)	227-700 (Ratna Prasad & Mohana Rao 2011)	120-304 (Defoirdt et al. 2010)	307-1000 (Defoirdt et al. 2010)	60-145
Elastic modulus (GPa)	9-20 (Ratna Prasad & Mohana Rao 2011)	4-6 (Defoirdt et al. 2010)	13-54 (Defoirdt et al. 2010)	3-14

4.7   Interfacial properties of bamboo fibre/polyester composite

The typical load-displacement curves obtained from the SFFT for bamboo fibres treated at different concentrations of NaOH reinforced polyester composite is presented in Figure 4.16. It can be observed that upon loading, the force increased at a similar rate for all NaOH concentration, with 0 and 4% NaOH treated fibres experiencing higher displacement at the test's beginning. This may indicate that the fibre/matrix interface for 0 and 4% NaOH treated fibres have weaker bonding with the polyester, which may lead to higher sliding of the fibre throughout the hole, compared to the 6 and 8% NaOH treated fibres. The fibre/matrix interface provides the platform for load transfer from the polyester to the bamboo fibres. Across this interface, in an equilibrium state, a frictional shear force acts equally in the opposite direction of the applied force (Wong et al. 2010). Upon reaching the peak load, debonding occurs, causing the load to drop drastically, indicating the release of stored energy.
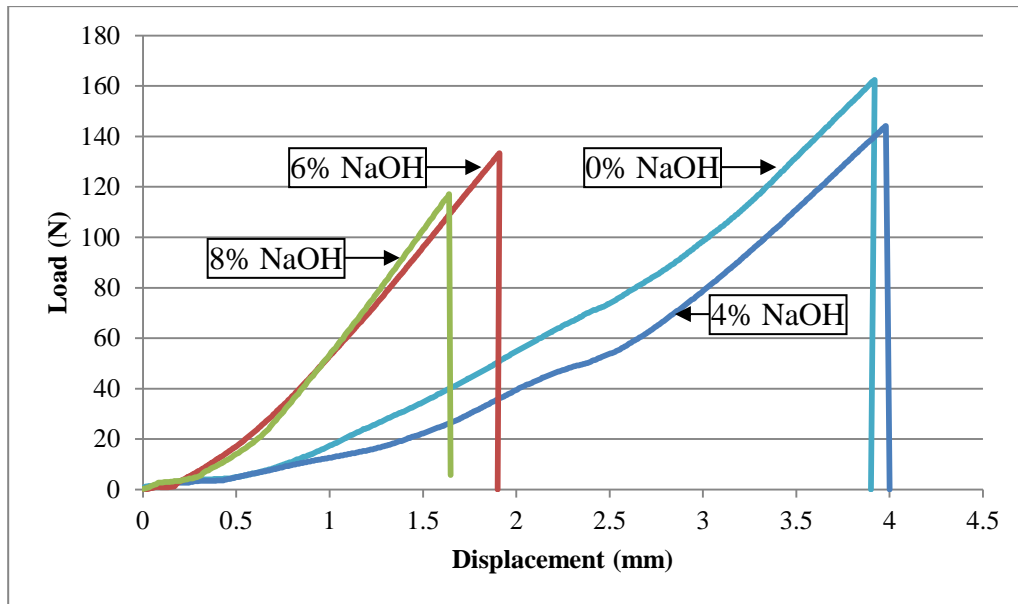
Figure 4.16: Load-displacement curves of SFFT at different concentration of NaOH

The mean interfacial shear strengths (IFSSs)—calculated from Equation 3-1 for treated and untreated bamboo fibre/polyester composites, with F_{deb} values taken from maximum loads in Figure 4.16—are presented in Figure 4.17. The IFSS for 0, 4, 6 and 8% NaOH treated bamboo fibres, at an embedment length of 12 mm are 23, 25, 28 and 22 MPa, respectively. The trend shows an increment in IFSS as the concentration of treatment is increased up to 6% NaOH, with an optimum improvement of 22%. At higher concentration of 8% NaOH, a reduction of IFSS was observed. The raw, untreated fibres have a low IFSS value which reflects its hydrophilic nature that may be incompatible with the hydrophobic polyester (Akil et al. 2011; Wambua et al. 2003). The incompatibility weakens the bonding strength with the matrix; together with the smoother fibre surface (as observed in Figure 4.12(b)), as well as the presence of surface impurities, this renders poor interlocking between the two components of the composite. With the rougher fibre surface and the removal of surface impurities achieved through alkalisation, the IFSSs increased for 4 and 6% NaOH treated fibres indicating an improvement in the mechanical interlocking between the fibres and the matrix. The rougher surface and the presence of voids on the treated fibres also provide a higher surface area for contact and adhesion which increases the frictional shear force. 6% NaOH treated fibres have a higher IFSS value than the 4% NaOH treated fibres and less early displacement as observed in Figure 4.16. This may suggest that the fibre achieves its optimum surface condition for fibre/matrix adhesion, and together with its improved tensile strength, shows the best mechanical performance at 6% NaOH treatment. This improvement in interfacial strength values was also observed on untreated and NaOH treated coir fibres, with a poly(butylene succinate) matrix, where the authors observed an increased in roughness of the fibre surface after alkalisation (Nam et al. 2011).
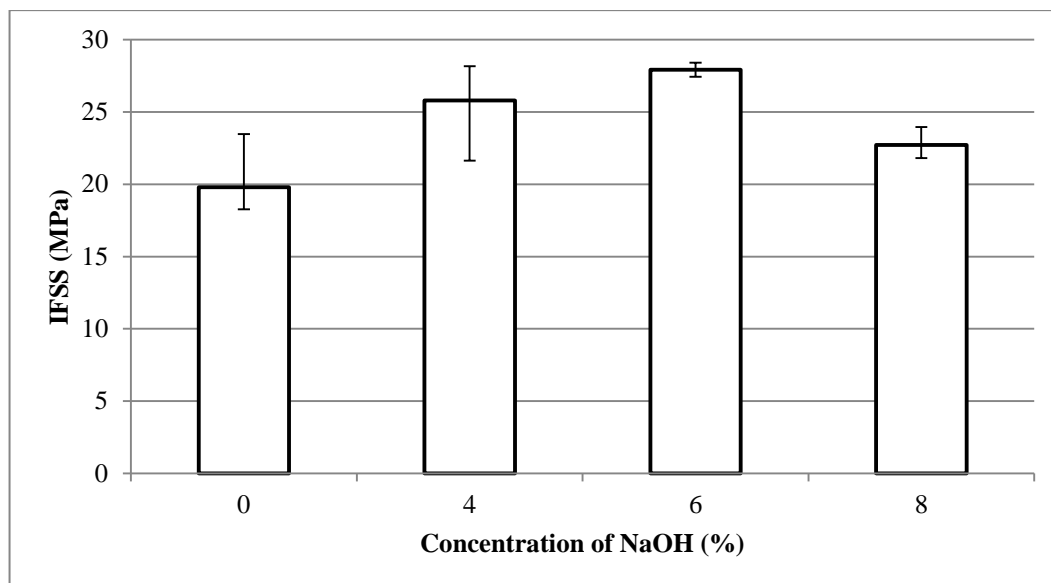
Figure 4.17: Effect on alkalization on the interfacial shear strength of bamboo-polyester

However, there is a limit to the concentration of NaOH in bamboo fibre treatment. The IFSS for 8% NaoH treated fibres was observed to be slightly higher than the untreated fibres. As observed in Figure 4.15 (d), these fibres have a considerably rougher surface due to exposure of the individual fibrils as a result of complete cell wall removal, compared to untreated fibres. In Figure 4.16, the displacement due to tensile loading for 8% NaOH treated fibres was similar to the 6% NaOH treated fibres. This may suggest that the interfacial adhesion between the matrix and fibre is better than with untreated fibres. However, as observed in Figure 4.1 and Figure 4.15 (c and d), the corroded fibril and fibril splitting suggest that at 8% NaOH, the concentration of the caustic soda may be too corrosive for bamboo fibres, resulting in damage to the fibres. This was also proven on the tensile test performed, whereby the tensile strength of the fibre was reduced. It can be assumed that although there was better interfacial adhesion between fibre and matrix for 8% NaOH treated fibres, the damaged fibres may have contributed to the failure of the composite, affecting its IFSS value. The behaviour of the fibre/matrix adhesion can be simplified, as demonstrated in Figure 4.18, whereby better fibre/matrix interlocking is expected as the fibre surface is roughened by alkali treatment.
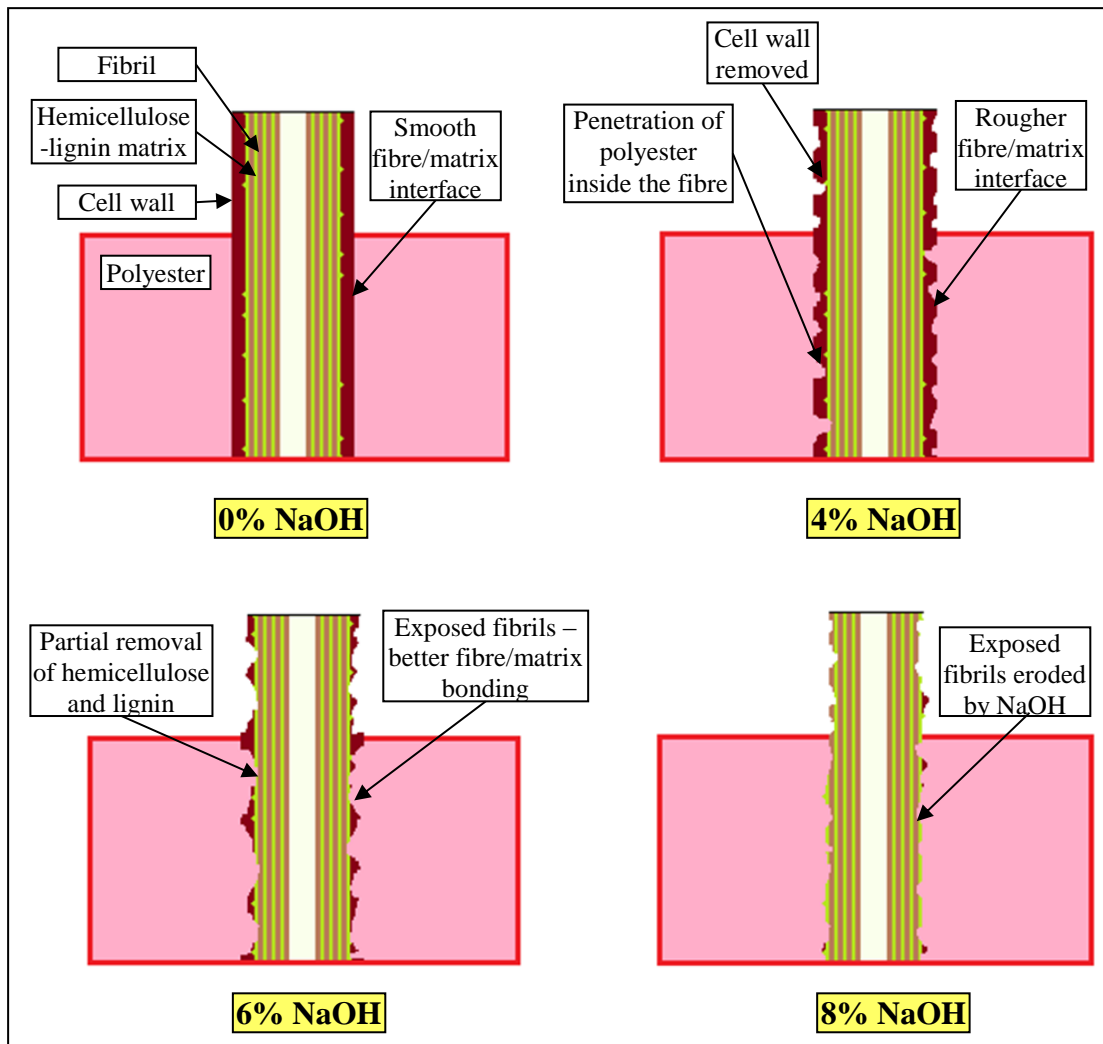
Figure 4.18: Schematic diagram of fibre/matrix interface at different NaOH concentrations

4.8   Tensile properties of bamboo fibre/polyester composite

Tensile tests were conducted on the untreated (BPC-0) and treated composites (BPC-4, BPC-6, and BPC-8), as well as the neat polyester (NP) to obtain the initial mechanical strength values. These values are established as benchmark for comparison with the strength of the degraded samples that will be discussed in the following chapters. The samples were tested with tensile loading until failure, and the stress-strain diagrams were plotted. The elastic moduli were experimentally determined from the slopes of the linear portion of the stress-strain curves. The theoretical values of the elastic moduli were also calculated for comparison.

4.8.1   Stress-strain diagram

Figure 4.19 to Figure 4.22 represent the stress-strain curves of the bamboo fibre/polyester composites, with different concentrations of NaOH treatment. The stress-strain curves for NP are presented in Figure 4.23. Each set of tests was conducted on five specimens and only the best curves were utilised to determine the tensile strength and elastic modulus.
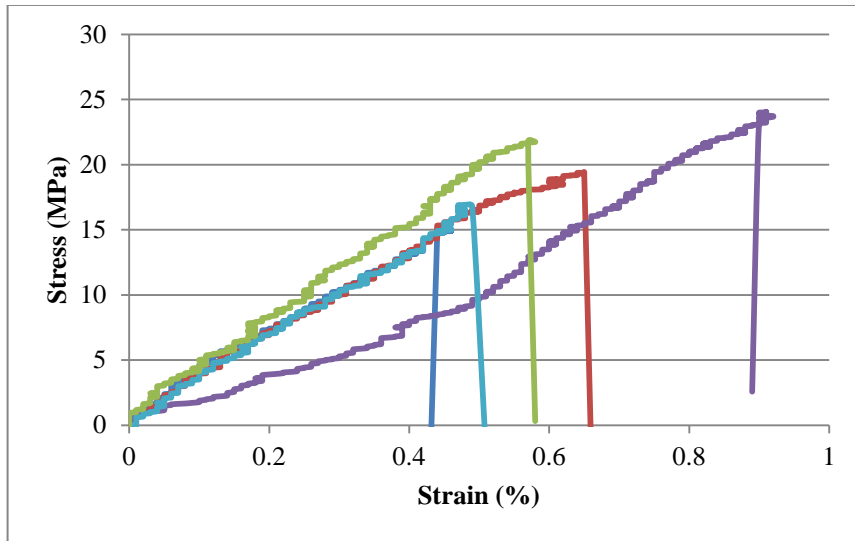
Figure 4.19: Stress-strain curves for composites with 0wt.% NaOH treatment
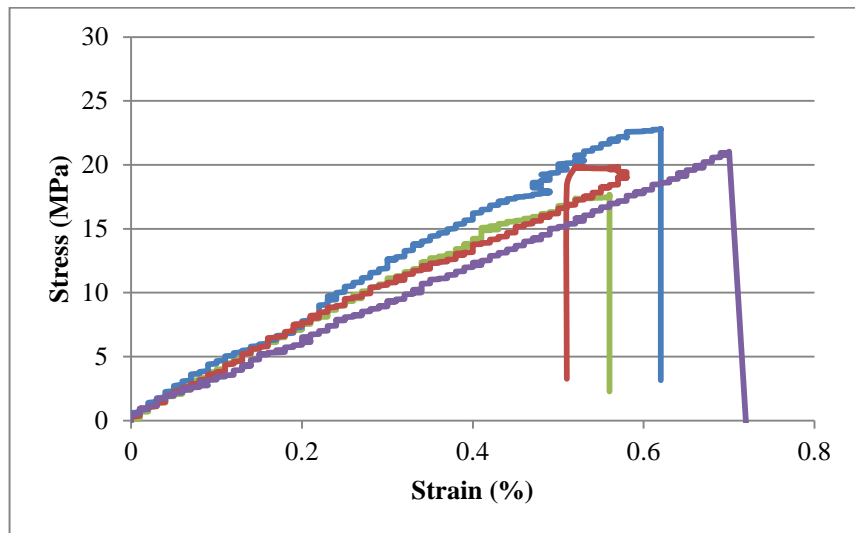
Figure 4.20: Stress-strain curves for composites with 4wt.% NaOH treatment
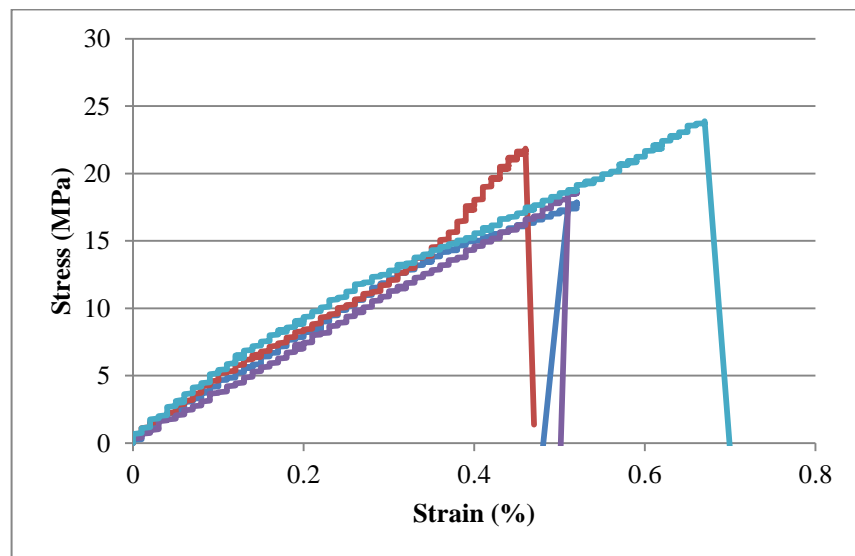
Figure 4.21: Stress-strain curves for composites with 6wt.% NaOH treatment
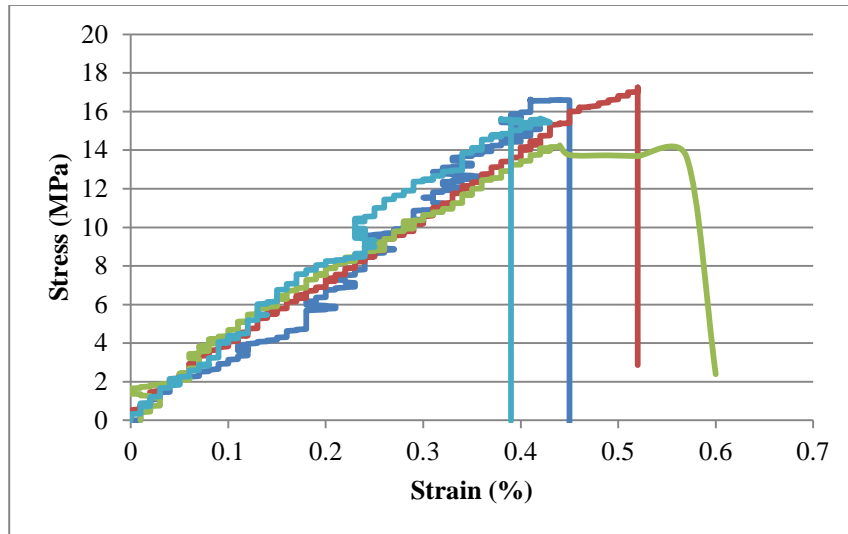
Figure 4.22: Stress-strain curves for composites with 8wt.% NaOH treatment
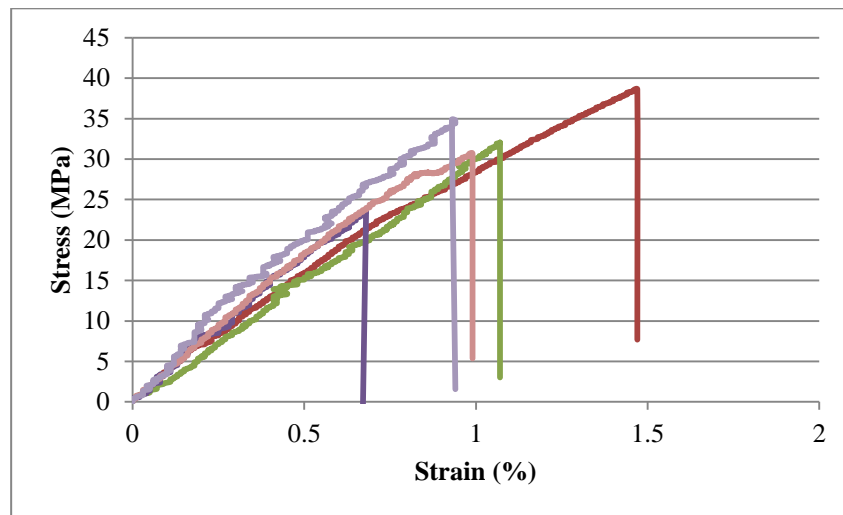
Figure 4.23: Stress-strain curves for neat polyester

The results for tensile strength are summarised in Figure 4.24. It is observed that NP has the highest tensile strength at 33.79 MPa. This agrees with the values provided by the manufacturer: 30.9 MPa. With the addition of bamboo fibres, a decrease of approximately 10 MPa was observed on the bamboo fibre/polyester composites. It was highlighted by Manalo et al. (2013) that only the fibres oriented perpendicular to the load provided reinforcement in a composite laminate fabricated with randomly oriented fibres. The maximum tensile strength achieved by samples BPC-0, BPC-4 and BPC-6 are very comparable, with only a slight increase in the average values for the treated samples. A mere 6% increase in strength was observed for BPC-6. However, there was an obvious drop in tensile strength at higher NaOH concentration as demonstrated by the BPC-8 sample, with an 18% reduction observed.

The improvement in tensile strength of the fibres as well as the interfacial properties between the bamboo fibres and polyester matrix for fibres treated at 4 and 6% NaOH may have contributed to the slight increase in average tensile strength of their corresponding composites. BPC-6 had the highest tensile strength value. Generally,

80

the mechanical performance—such as the tensile properties of a fibre/polymer composite—depend on the strength and modulus of the reinforcement, strength and toughness of the matrix, and the effectiveness of the interfacial stress transfer between the fibres and the matrix (Rong et al. 2001). Other researchers have also reported the effect of alkali treatment on the improvement of natural fibre/polymer composites' mechanical properties. Nam et al. (2011) had observed an increase in tensile strength of coir/poly(butylene succinate) composites treated at 5% NaOH. The increased strength was observed for all fibre mass content and is also higher than for NP. It is interesting to note that these fibres were arranged uniformly. Rong et al. (2001) attributed the increased strength of sisal fibres and better wetting of the fibres by the epoxy resin as the reason for better strength of sisal/epoxy composites treated with 2% NaOH. The decrease in strength for BPC-8 is due to the degradation experienced by the fibre, caused by the high level of NaOH corrosiveness. The weakened fibre fails to sustain the load transferred from the matrix, causing early failure of the composite.

	BPC-0	BPC-4	BPC-6	BPC-8	NP
■ TS	18.97	19.45	20.03	15.55	33.79
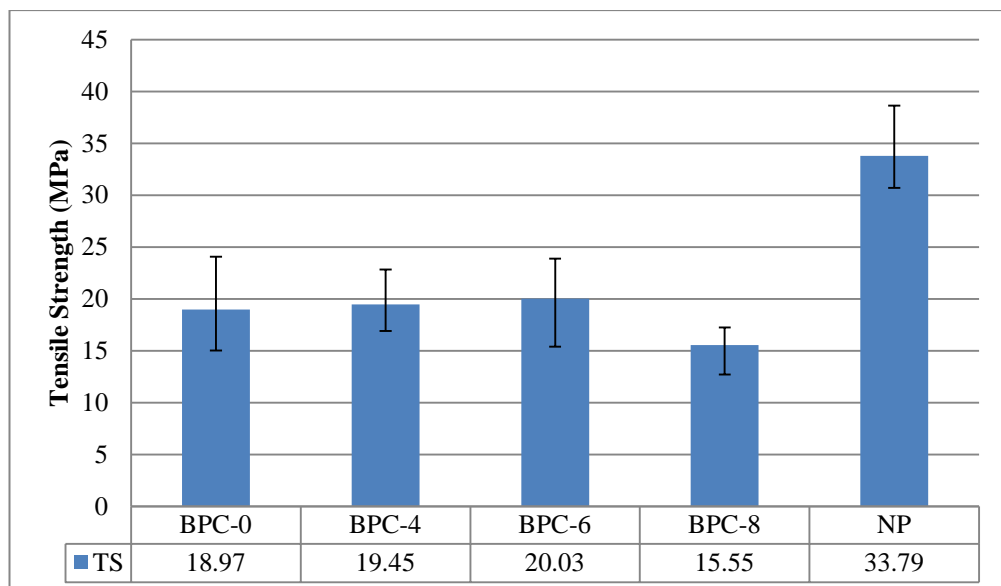
Figure 4.24: Tensile strength of specimens at different concentration of NaOH treatment

The elastic modulus for all samples are summarised in Figure 4.25. The elastic modulus for the NP resin, as provided by the supplier, is 3.1 GPa. This is comparable to the value obtained from this experiment, which is approximately 3.3 GPa. With the addition of untreated bamboo fibres, the stiffness of the composite was observed to decrease slightly to 3.18 GPa. However, this behaviour improved with alkali treatment, as exhibited by all treated composites. BPC-6 achieved the highest modulus of elasticity, 14% higher than the NP, while BPC-8 experienced a slightly lower average stiffness, but a higher standard deviation. The influence of the damaged fibres with better fibre/matrix adhesion may vary the effect on stiffness, depending on fibre distribution. Many authors agree that the efficiency of the interfacial adhesion may contribute to higher elastic modulus. The Young's modulus of bamboo fibre/poly (lactic acid) composite was reported by Lee and Wang (2006) to increase rapidly from 2666 to 2964 MPa, with the addition of a bio-based coupling agent. Aziz and Ansell (2004) indicated that the flexural moduli of a composite depends on the type of chemical bonds between the fibre surface and resin matrix.

Their study on hemp/polyester and kenaf/polyester composites showed that treatment of fibres by alkalisation helped to improve the mechanical interlocking and chemical bonding between the resin and fibre, resulting in superior mechanical properties, with better performance by composites with long fibres rather than short fibres.
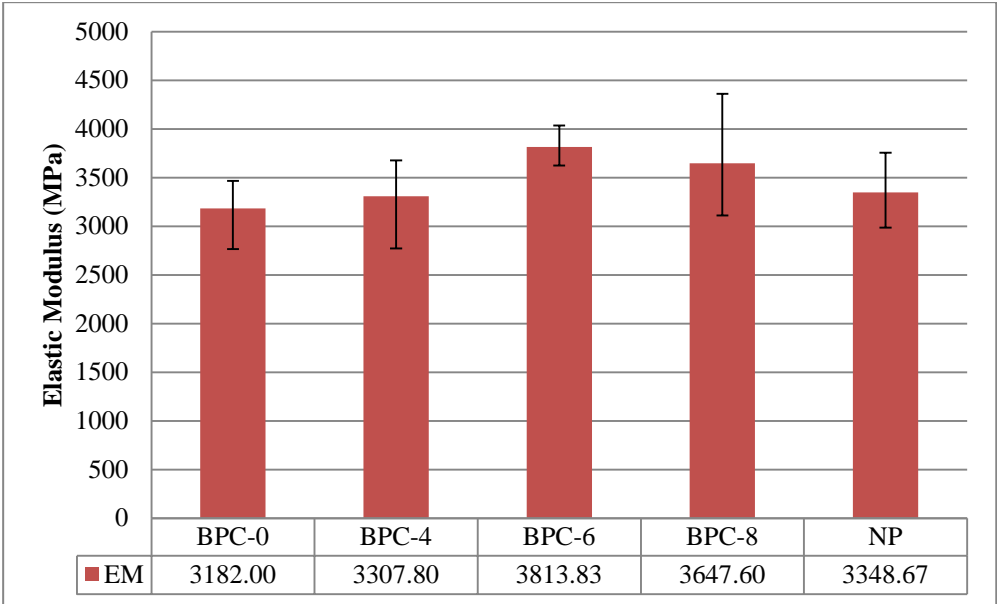
Figure 4.25 Elastic modulus of specimens at different concentration of NaOH treatment.

	BPC-0	BPC-4	BPC-6	BPC-8	NP
■EM	3182.00	3307.80	3813.83	3647.60	3348.67

4.8.2 Theoretical values of elastic modulus

The elastic modulus of a composite, E_c, can be theoretically calculated using the Rule of Mixture, whereby the elastic modulus of each composite component contributes to the final product, based on its volume fraction. This is formulated as follows:

$$E_c = E_f V_f + E_m V_m \qquad \text{Equation 4-1}$$

Where E_f is the elastic modulus of the fibre, V_f is the volume fraction of the fibre, E_m is the elastic modulus of the matrix and V_m is the volume fraction of the matrix. A Krenchel factor, n_θ, is introduced into the modified Rule of Mixture equation to account for the orientation of the fibres distributed throughout the composite (Aziz & Ansell 2004; Krenchel 1964; Wong et al. 2010a). This alters the original equation as follows:

$$E_c = n_\theta E_f V_f + E_m V_m \qquad \text{Equation 4-2}$$

For a unidirectional fibre/polymer composite, $n_\theta = 1$, indicating that the fibre stiffness is entirely used by the composite. However, for a randomly oriented fibre/polymer composite, $n_\theta = 0.25$. This means that the mechanical properties of the composite will depend more on the matrix, with only a quarter of the fibres' stiffness is influential. Table 4.2 represents the theoretical values for the modulus of elasticity of bamboo fibre/polyester composites used in this study, taking the volume fraction of fibres as 20%.

Table 4.2: Theoretical modulus of elasticity of bamboo fibre/polyester composites

n_θ	BPC-0	BPC-4	BPC-6	BPC-8
1.00	4.07 GPa	4.28 GPa	4.73 GPa	3.67 GPa
0.25	3.03 GPa	3.08 GPa	3.19 GPa	2.93 GPa
$E_{experimental}$	3.18 GPa	3.31 GPa	3.81 GPa	3.65 GPa

The theoretical elastic modulus calculated for the randomly oriented fibre composite with 0% treatment is comparable to the experimental value obtained, with only a 4.7% difference between the two values. As the treatment concentration is increased, the gap difference between the theoretical and experimental values is enlarged. One possible explanation for this is that the equation of the Rule of Mixture did not consider the improvement of the interfacial adhesion between the fibres and the matrix as the result of the alkali treatment. The enhancement of the fibre stiffness due to treatment is reflected in the equation. Fibres treated at 8% NaOH exhibited the lowest stiffness, theoretically producing a composite with the lowest modulus of elasticity. However, the experimental value obtained for BPC-8 is higher than BPC-0 and BPC-4, indicating that the improved fibre/matrix adhesion plays an influential role on the improved stiffness of the composite.

It is often observed that the addition of fibres as reinforcement in a polymer matrix increase the strength and modulus of the composite, as fibres have much higher strength and stiffness values than the matrices (Ku et al. 2011).Theoretically, if the potential of the bamboo fibres were fully used, whereby all fibres were aligned uniformly in the direction of the applied tensile load, the elastic modulus would be much higher than the NP resin, improving the mechanical properties of the polyester. This improvement is shown in Table 4.2 for n_θ value equals to 1 for a unidirectional fibre orientation. However, due to the nature of the fibres extracted through the steam explosion process which are relatively shorter than the length of the composite, it is impossible to fabricate a continuous uniformly oriented fibre composite. A study by Wong et al. (2010a) showed that even when short bamboo fibres were arranged in a unidirectional manner, only a maximum 25% increase in the tensile strength of polyester composites was achieved. The authors also highlighted that only the longitudinal fibres contribute to energy dissipation and crack retardation in the composite system.

4.9   Morphology of fractured composites

The visual observations of the fractured surfaces of the tensile tested samples are presented in Figure 4.26. The NP shows a rough surface profile, with some samples experiencing multiple fracture points. Once the failure load was reached, failure occurred abruptly with pieces of the damaged samples prone to fling away from the tensile machine, demonstrating the material's brittleness. With the addition of bamboo fibres, the composites did not fail in this manner. The samples were mainly intact, with one fracture point within the gauge length. The presence of bamboo fibres helped to suppress the abrupt separation of any fractured polyester particles. Cracking sounds were audible even before the maximum load was reached, indicating that the failure occurred gradually. At close inspection, it is interesting to note that the exposed fibres at the failure surface for treated composites had more resin particles attached to them compared to the untreated composite. This suggests better fibre/matrix adhesion for the treated composites, and a more thorough examination was performed using SEM.

Sample	Fractured Surface
NP	(a) 15mm — Rough surface showing brittle fracture
BPC-0	(b) 25mm — More fibre pull-outs observed
BPC-4	(c) 25mm
BPC-6	(d) 25mm — Resins adhered to fibres
BPC-8	(e) 25mm — Flatter surface-fibres broken at fractured plane
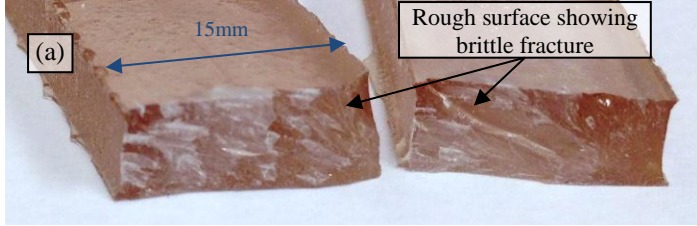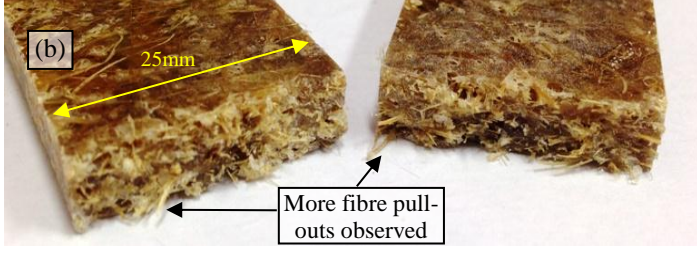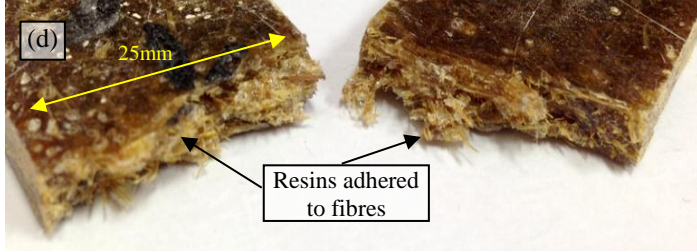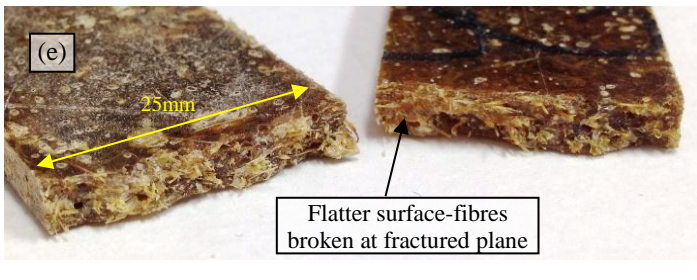
Figure 4.26: Fractured surface of neat polyester and bamboo fibre/polyester composites

Micrographs of the samples' fractured surfaces are presented in Figure 4.27. Defragmentation of polyester particles was observed throughout the NP surface. The failed surface is uneven and rough due to the brittle nature of the failure condition. For the untreated composites, holes on the matrix surface were observed, left by debonded fibres pulled-out during tensile loading. Higher magnification at the fibre/matrix interface shows the fibre and matrix are separated by voids, proving that bonding between the two materials was poor. Therefore, with low interlocking strength for BPC-0, the fibres can easily slip through the polyester resin, leading to failure of composites through fibre pull-outs. For 4% NaOH treated fibres, a similar morphology to BPC-0 on the fibre/matrix adhesion was observed, as some areas showed poor resin bonding. However, resin particles were found to adhere along the fibres, as observed in Figure 4.27 (e). The treatment provided a better fibre surface than the raw fibres for matrix adhesion, but may still be insufficient. Some surface impurities could still be present on the fibres; consequently, this has only slightly improved the strength of the composite for BPC-4. Polyester resin showed better adhesion to 6% NaOH treated fibres as some parts of the resin were still bonded to the fibre, although the surrounding matrix was fractured and removed. Resin particles were also found to adhere to the fibres, even in between the fibrils. The improved fibre/matrix interlocking was further confirmed by the mode of failure shown in Figure 4.27 (g), whereby the breakage of a fibre bundle may imply that the fibres were damaged first before debonding could take place. As for BPC-8, the condition of the fibres was poor due to its vulnerability to high alkali strength. Fibril damage and erosion were evident. However, the fibre/matrix adhesion was very good as no gaps were observed between the fibre and matrix, and the apparent chunk of resin still adhered to a fibril. This supports the SFFT graph (Figure 4.16) where the displacement reading for 8% NaOH treated fibres was comparable to the 6% NaOH treated fibres due to good fibre/matrix interlocking. Therefore, the lower tensile strength for BPC-8 is influenced by the damaged fibres. It is interesting to note that the stiffness of BPC-8 is higher than NP, BPC-0 and BPC-4. This may imply that the elastic modulus is highly influenced by the fibre/matrix adhesion, rather than the individual components of the composite.

Sample	SEM
NP	

Sample	SEM
BPC-0	
BPC-4	
BPC-6	
BPC-8	
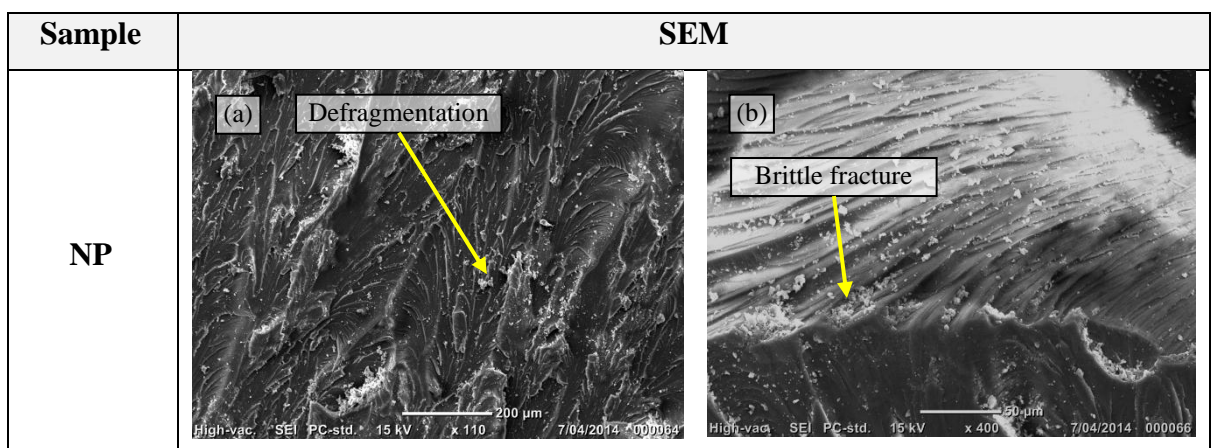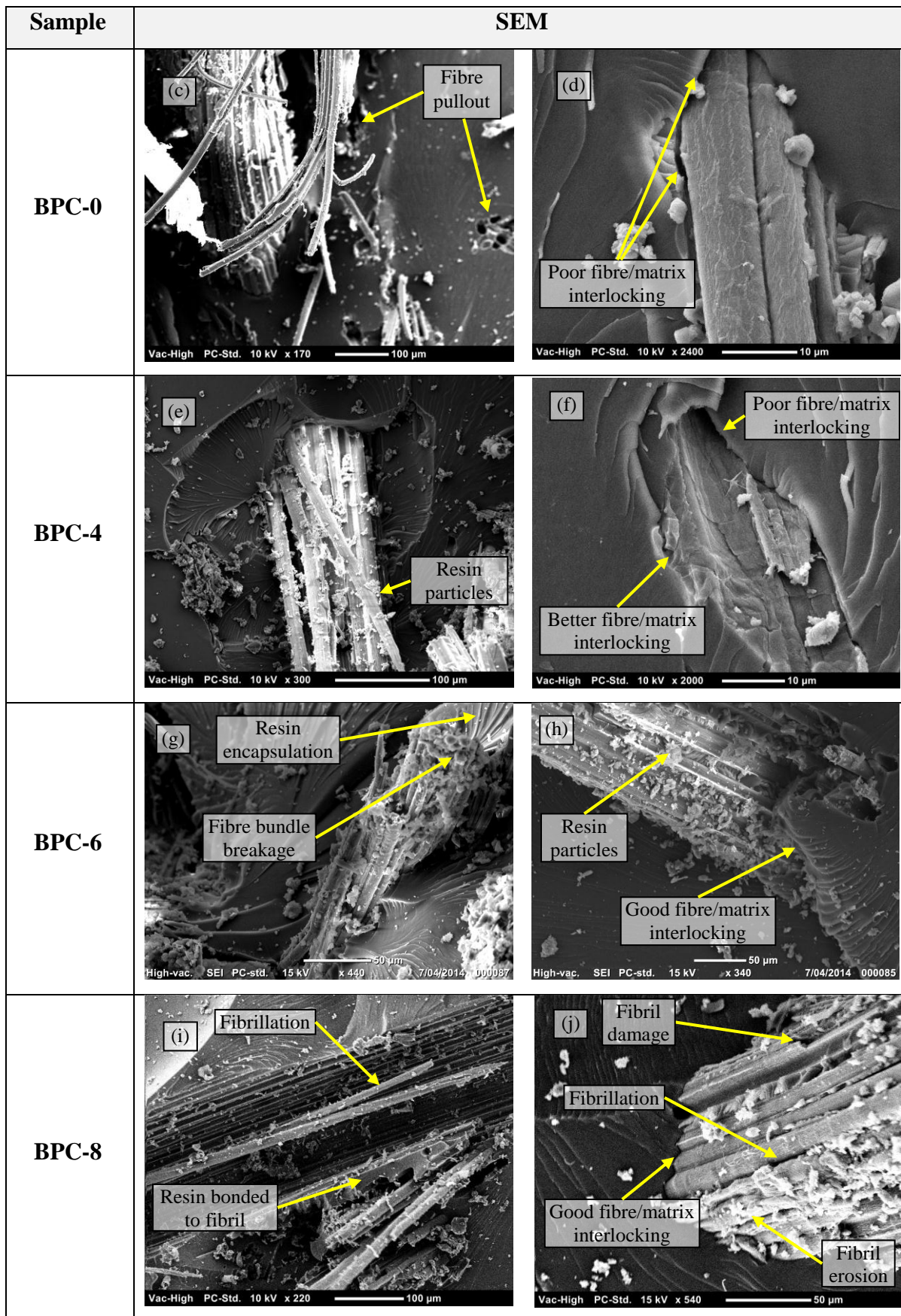
Figure 4.27: Morphologies of neat polyester and bamboo fibre/polyester composites

86

The morphologies of tensile fractured surfaces of other natural fibre polymer composites treated with NaOH were reported to have similar properties with the bamboo fibre/polyester composite in this study. Alkalised banana fibre/polypropylene composites were reported by Annie Paul et al. (2008) to have significant improvement in the fibre/matrix adhesion, as shown by the absence of holes and debonding of the fibres that were apparent in untreated fibres. Instead, fibre breakage rather than pull-out was detected, indicating better interfacial strength. Pulled-out coir fibres, along with cracks at the broken fibre ends in 5% alkali treated coir/polyester composites observed by Rout et al. (2001) suggested that failure occurred at the fibre due to strong adhesion between the fibre and matrix. Another study on coir fibres by Nam et al. (2011) showed that the gaps present on untreated fibres with poly(butylenes-succinate) resin were unobservable on the alkali/treated composites. A larger quantity of residual epoxy resin was observed by Rong et al. (2001) on the surface of alkali treated sisal/epoxy composites and even at the gaps between the ultimate cells, proving the penetration of epoxy into alkali treated sisal fibre bundles. Overall, these authors agree that the SEM observations indicate that the increased strength of these composites was influenced by the improvement in fibre/matrix adhesion, due to alkalisation on the fibres.

4.10   Chapter summary

Bamboo fibres were treated with sodium hydroxide at a concentration of 4%, 6% and 8% by weight. The characteristics of the fibres were observed and studied to determine the changes resulting from the alkalisation process. These changes were correlated with the morphology of the fibres, as observed through SEM. The results have shown that:

1) The fibre matrix was partially removed through alkalisation. The amount of removal is higher as the concentration of treatment is increased, causing rougher fibre surfaces with voids observed between the microfibrils. However, there is an optimum NaOH concentration for natural fibre treatment, whereby at a concentration higher than the optimum level, degradation of the cellulosic component of the fibre may occur which will affect the bamboo fibre strength. This was observed on the 8% NaOH treated fibre, whereby deterioration of the fibril surface was observed.

2) Alkalisation on bamboo fibres resulted in changes in appearance and texture. Treated fibres are darker than untreated fibres. The change in colour may suggest that lignin was removed from the fibre, which alters its composition. In addition, hemicelluloses and other surface impurities also partially removed may contribute to the presence of voids within the fibre. This causes slight reductions in the diameter and density of treated fibres.

3) The tensile properties of bamboo fibres improved at 6% NaOH treatment, with an increment of 181% and 47% in tensile strength and elastic modulus, respectively. In contrast, the tensile strength and stiffness decreased at 8% NaOH treatment, due to the damaged fibrils, with 24% and 29% reductions observed in tensile strength and stiffness compared to untreated fibres.

4) The interfacial properties of bamboo fibres with a polyester matrix improved with alkali treatment. This correlates well with the fact that the alkalisation roughens and removes surface impurities for a better interfacial bonding between the composite's two components. Optimum interfacial shear strength was observed for 6% NaOH treated fibres, at 22% improvement. However, the

damaged fibrils at 8% NaOH treatment hinder the effect of improved bonding, causing a reduction in the composite's IFSS.

5) The tensile strength of the composite is lower than the NP, due to the random orientation of the fibres, which hinders full use of the fibres' strength. Fibre treatment caused a slight enhancement of about 6% for 6% NaOH treated fibres on the tensile strength of the composite, but reduced the strength as much as 18% at 8% NaOH due, to fibre damage.

6) The elastic modulus of the composite is optimised at 6% NaOH treatment, which is 14% higher than the NP resin. Apart from the increase in fibre stiffness due to alkalisation, the improved interfacial adhesion plays a major role in providing higher elastic modulus of the treated composites.

7) The SEM observations confirmed that fibre/matrix interlocking was improved with increased NaOH concentration. Untreated fibres were surrounded by voids at the interface with some fibre pull-outs observed. BPC-6 and BPC-8 showed good fibre/matrix adhesion, even though the 8% NaOH treated fibres suffered some fibril damage.

Chapter 5 : Thermal Degradation Study on Bamboo Fibre/Polyester Composites

5.1   Introduction

One of the limitations of natural fibres is their tendency to degrade at lower temperatures compared to synthetic fibres. This behaviour is expected to influence the durability of polymer composites reinforced by natural fibres when exposed to heat. The majority of natural fibres have low degradation temperatures, which are inadequate for processing with thermoplastics, which have processing temperatures higher than 200^0C (Araújo et al. 2008). Even for synthetic FRPs, at a temperature of 100^0C, a load bearing structure will experience failure (Hollaway 2010).

Temperature plays an influential role in the thermal stability of natural fibre composites where it causes direct thermal expansion or contraction and affects the rate and volume of moisture absorption that leads to fibre swelling (Wang et al. 2005). The degradation process of natural fibres includes dehydration combined with emission of volatile components initiating at a temperature of about 260^0C, and rapid weight loss due to oxidative decomposition, corresponding to the formation of char as the temperature increases (Beg & Pickering 2008). As the fibres degrade, organoleptic properties such as smell and colour undergo changes, while the mechanical properties are compromised. This is caused by changes in mass and crystallinity, and a reduction in the degree of polymerisation, due to chain breakage by cellulose glycosidic union decomposition, releasing carbon dioxide and water (Alvarez & Vázquez 2004). Higher cellulose content in a natural fibre results in higher flammability, while higher lignin content results in greater char formation with a lower degradation temperature (Dittenber & GangaRao 2012; Manfredi et al. 2006; Suardana et al. 2011). However, it is important to highlight that hemicellulose and cellulose in lignocellulosic fibres are considerably degraded by heat before the lignin is affected (Mohanty et al. 2000).

In this chapter, TGA is used to evaluate the thermal decomposition behaviour of bamboo fibres, neat polyester and their composites. The effects of alkalisation treatment on the thermal degradation process are also analysed. Additional protection, such as additives and coating were introduced in the composite system to evaluate whether these methods had any effect on the composite's durability. DMA was performed on the composites to study the effect of temperature on the mechanical properties of the samples, and also to identify the samples' T_g. The composites were also exposed to different temperatures (40, 80 and 120^0C) for one hour before being subjected to tensile loading. The influence of heat on the tensile properties of the composites was analysed. The fractured surface and physical changes experienced by the composites were also observed. It is expected that from this study, the limit of heat exposure on bamboo fibre/polyester composite can be further understood to better define its application as a non-load bearing structure.

5.2 Influence of temperature on the decomposition behaviour of bamboo fibres

Raw and treated bamboo fibres were subjected to a temperature range of 25 to 600^0C to study the decomposition behaviour. The results of the TGA runs are summarised in Table 5.1.

Table 5.1: Thermal decomposition of bamboo fibres from TGA

Alkali Treatment (wt.%)	0%	4%	6%	8%
1st Temperature Peak (^{0}C)	291.83	237.96	-	-
2nd Temperature Peak (^{0}C)	351.47	313.95	321.91	303.71
Final Weight after Decomposition (%)	15.90	25.96	27.53	35.69

From the DTG curves in Figure 5.1, it can be observed there are two temperature peaks for untreated fibres: the first at 291^0C, corresponding to the decomposition of hemicelluloses; the second at 351^0C, corresponding to the decomposition of cellulose. The lignin peak is wider and is usually superposed on the other two peaks (Araújo et al. 2008; Manfredi et al. 2006; Shih 2007; Suardana et al. 2011). The 4% NaOH treated fibres had a slight first peak at 237^0C (indicated by the arrow in Figure 5.1), while at a higher treatment concentration of 6% and 8% NaOH, the first peak is no longer present. This may indicate some traces of hemicelluloses remain at 4% NaOH treatment, but are removed at higher concentrations. The initial peaks on the DTA curves observed at temperatures below 100^0C represent the evaporation of moisture from the fibres, proving the hydophilicity of natural fibres. The fibres are observed as stable at the temperature range of 120^0C to 180^0C. Although there is no apparent weight loss in this region, Mwaikambo (2009) highlighted that gradual degradation—which includes depolymerisation, hydrolysis, oxidation, dehydration and decarboxylation—may also occur in this temperature range.
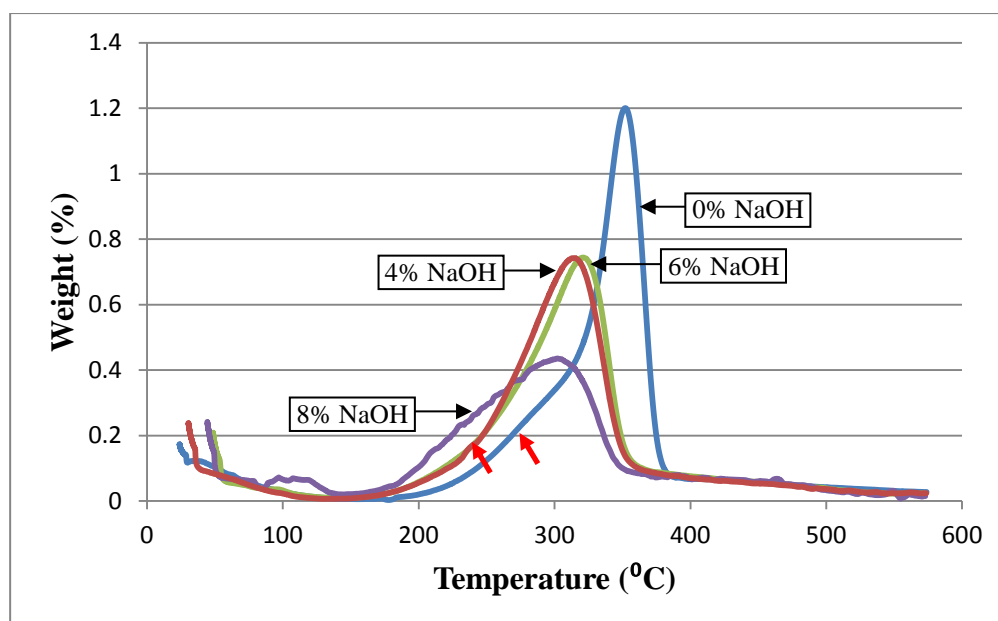
Figure 5.1: DTG curves of raw and treated bamboo fibres

As the concentration of NaOH treatment increased, the temperature of the second peak decreased, with 8% NaOH treatment resulting in the earliest decomposition at 303^0C, a decrement of 13.4% of thermal stability compared to the untreated fibre. It was reported by Mwaikambo (2009) that at a concentration of NaOH higher than 0.32%, the converted cellulose structure is rendered less stable to thermal degradation. As such, care must be taken in selecting the level of alkali treatment to take this effect into consideration. With optimum strength achieved at 6% NaOH treatment in this study, the adverse effect on thermal stability was observed. The reduction in thermal stability of alkalised fibres may also be attributed to the removal of lignin through alkalisation. Suardana et al. (2011) highlighted that lignin decomposition occurs at temperatures between 160 and 900^0C, while Lee and Wang (2006) stated that lignin decomposes at about 420^0C. Without the higher-temperature-lignin peak superposing the cellulose peak, lower decomposition temperatures were observed, representing only the degradation of cellulose.

The TGA curves are presented in Figure 5.2, whereby the percentage of sample weights at the end of the run represents the remaining solids after thermal decomposition. The results show that char formation increases with increased concentration of treatment. Bamboo fibre treated with 8% NaOH produced 125% more char than untreated fibres. In natural fibres, lignin is the component responsible for charring by which higher lignin content generally produces more char (Dittenber & GangaRao 2012; Suardana et al. 2011). However, in this study, fibres treated at higher NaOH concentration (presumably with lesser lignin) produced higher residues at the end of the TGA run. This behaviour was also observed on other natural fibres treated with NaOH, which includes kenaf fibres (see Appendix B) and Raffia textilis fibres (Elenga et al. 2013). As suggested by Elenga et al. (2013), further studies should be conducted on the residues and gas emitted during heating for better understanding of this behaviour. With the removal of lignin, other substances may have a more influential role on the final product of the degraded treated fibres.
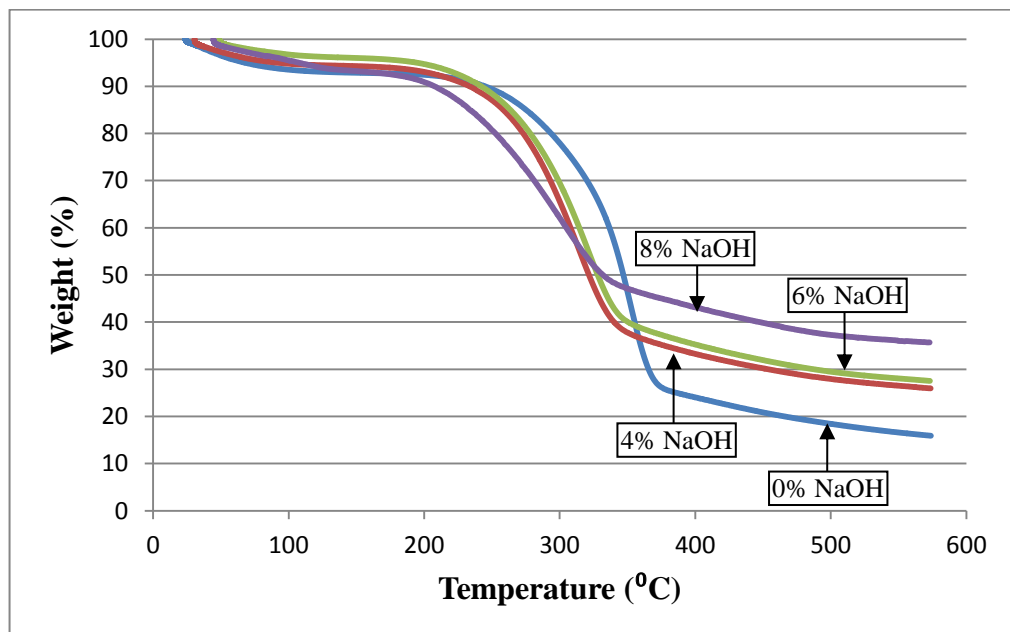
Figure 5.2: TGA curves of raw and treated bamboo fibres

5.3 Influence of temperature on the decomposition behaviour of bamboo fibre/polyester composites

The bamboo/polyester composites at different alkali treatment concentrations, as well as the neat polyester resin were subjected to thermal decomposition from a temperature range of 25^0C to 600^0C. The results of the TGA runs are summarised in Table 5.2: Thermal decomposition of bamboo fibre/polyester composites and neat polyester from Table 5.2.

Table 5.2: Thermal decomposition of bamboo fibre/polyester composites and neat polyester from TGA

Alkali Treatment (wt.%)	NP	BPC-0	BPC-4	BPC-6	BPC-8
1st Temperature Peak (°C)	387.89	359.65	358.22	358.30	336.62
2nd Temperature Peak (°C)	-	394.71	388.69	391.76	387.10
Final Weight (%)	5.18	11.62	10.29	9.77	10.98

As observed in Figure 5.3, all bamboo fibre/polyester composites have two temperature peaks, while the NP has only one obvious peak. These two peaks on the DTA curves of the composites represent the decomposition temperature of the bamboo fibres, which is the smaller first peak, and the NP denoted by the second larger peak. Since the NP sample consists of only one material, it is expected that only one peak would be present. The untreated bamboo fibre composite had the highest decomposition temperature among the composite samples, at 359.65^0C. The decomposition temperatures slightly decreased for BPC-4 and BPC-6, but drop further at about 6.4% for BPC-8. For the NP resin, the decomposition temperature is at 387.89^0C, and this is also reflected in the second peak of the composites for BPC-4 and BPC-8. However, the decomposition temperature for polyester in BPC-0 and BPC-6 is slightly higher, with the untreated composite having the better thermal resistance.
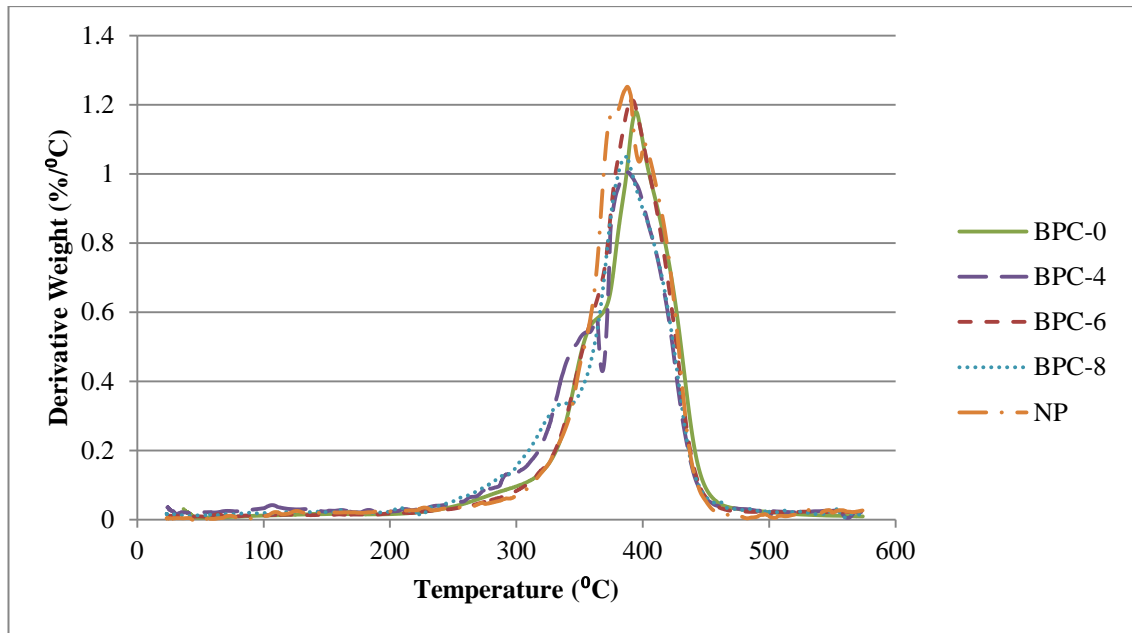
Figure 5.3: DTA curves of bamboo fibre/polyester composites and neat polyester

To evaluate these results with the results obtained from the DTA curves on the individual bamboo fibres, Figure 5.4 was charted to summarise the relationship between the thermal decomposition of the bamboo fibres and the bamboo fibre/polyester composites. The composites start to decompose at a higher temperature than the cellulose of the individual bamboo fibres. This may be due to overlapping between the peaks of the fibres and polyester, which shifts the degradation to a higher temperature. This may also indicate that the polyester matrix is more influential on the thermal resistance of the composites than the fibres, which may be due to the higher volume fraction of the polyester. This was confirmed by Lu and Oza (2013): as the amount of fibre volume fraction increases in the composites, there is a decrease in the composites' thermal stability, due to the much lower thermal stability of natural fibres than polymer resins. Although there is a drop in the decomposition temperature of the bamboo fibres as the concentration of treatment is increased from 0% to 6% NaOH, this effect is not reflected in the composites, as the decomposition temperatures for BPC-0, BPC-4, and BPC-6 are relatively the same. However, an obvious effect was observed for BPC-8, as the thermal stability of its bamboo fibres suffered the highest reduction. Basically, the second peaks of the composites are not significantly influenced by the condition of the fibres. For a composite material in engineering applications, the first peak in a DTA curve, which is the first sign of thermal degradation, is more important than the second peak (Monteiro et al. 2012).
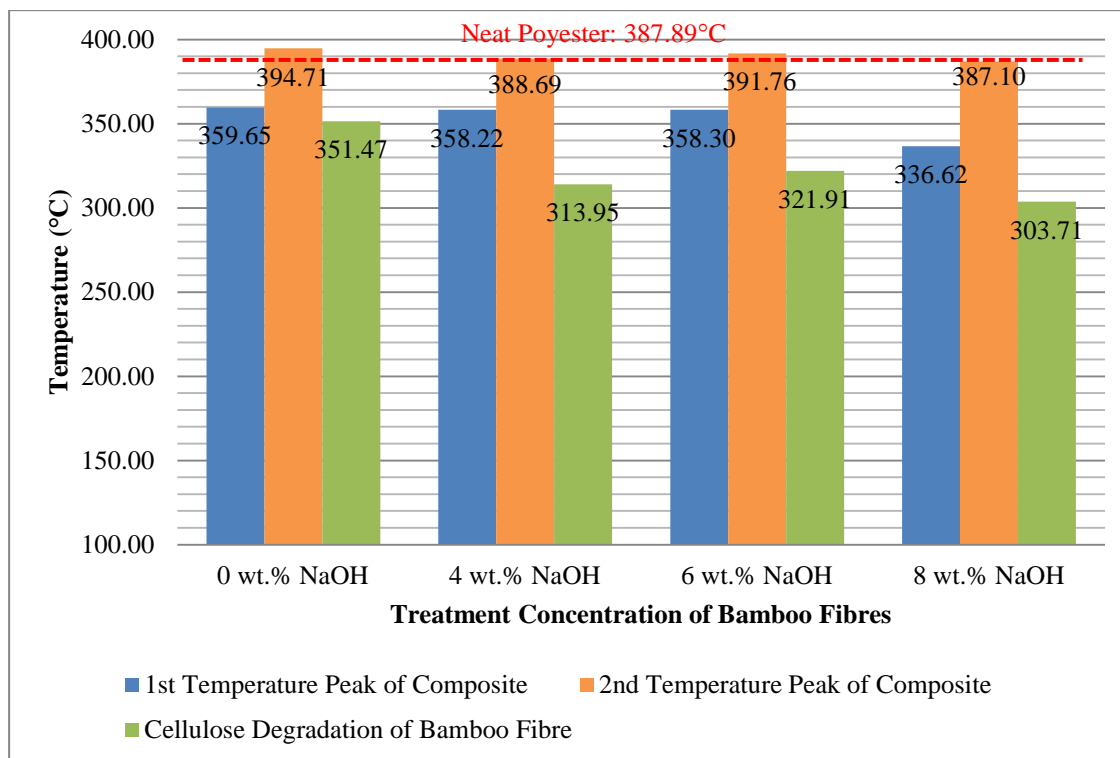
Figure 5.4: Temperature peaks from DTA curves of bamboo fibres and bamboo-polyester composites

Based on Laoubi et al. (2014), the thermal decomposition process of all unsaturated polyesters may occur between 130^0C and 400^0C. This occurs by scission of highly strained portions of the polystyrene cross-links, with the formation of free radicals that then undergo further decomposition. This results in the release of low molecular weight volatiles, which include carbon monoxide, carbon dioxide, methane, ethylene, propylene, butadiene, naphthalene, benzene and toluene. Note that adding fibres reduces thermal performance compared to NP. This was also observed by Milanese et al. (2012) on sisal/phenolic composites through TGA, whereby the composite showed greater stability than the sisal fibre itself, but possessed lower stability than the neat resin. The author concluded that the thermal stability of phenolic matrix decreases with the addition of vegetable fibres; which in their case, a 20^0C reduction was observed on the composite's thermal stability compared with the neat resin. In terms of the effect of fibre treatment on the thermal stability of natural fibre composites, several researchers have obtained varying results. Beg & Pickering (2008) found that unbleached WF/polypropylene composites started to decompose earlier than bleached fibre composites, while Lu and Oza (2013) observed that hemp fibre/polyethylene composites treated with NaOH had better thermal stability than untreated composites, but lower stability than silane treated composites. This behaviour was mostly attributed to the removal of the less thermally stable components of fibres, such as hemicellulose and pectin, which renders less heat for decomposition of treated fibres (Kabir et al. 2011; Norul Izani et al. 2013). Interestingly, Beckermann and Pickering (2008) reported no difference in thermal stability between untreated and alkali treated hemp fibre/polypropylene composites, but the authors counter this by indicating that the poor thermal stability of hemicelluloses and pectins in a composite was negated by the inclusion of MAPP coupling agent. From the results in this study, the thermal stability of bamboo fibre/polyester composites may not be dependent on the presence of hemicellulose of

94

the fibres alone. As mentioned in Section 5.2, the compromised thermal stability of the cellulose after alkalisation may influence this behaviour but only at higher concentrations, as demonstrated by sample BPC-8. Otherwise, the effect of treatment may not have a significant impact on the composites compared to the fibres alone.

From the TGA curves in Figure 5.5, the percentage of sample residues at the end of the run can be obtained, and represent the amount of char produced. As expected, NP has the lowest residue, as it mostly decomposes from thermal exposure. With the addition of bamboo fibres, an increase of approximately 90% of char production was observed. Untreated composites show the highest amount of char at 11.62%, followed by BPC-8, BPC-4, and BPC-6 at 10.98%, 10.29% and 9.77%, respectively. However, the differences in the final weight percentages between the composites are very small and may be negligible.
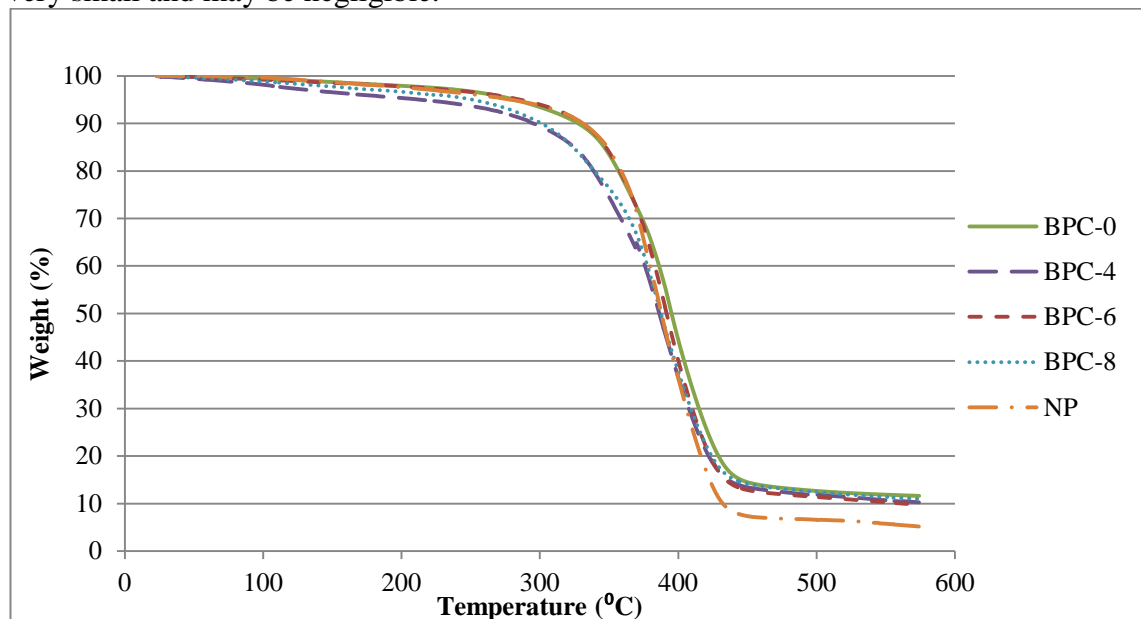
Figure 5.5: TGA curves of bamboo fibre/polyester composites and neat polyester

Comparison between the char production of the composites and their individual constituents, that is, the bamboo fibres and polyester matrix, is presented in Figure 5.6 in the form of percentage of final weight after decomposition as recommended by Dhakal et al. (2007), Shih (2007) and Shukor et al. (2014). Although the individual bamboo fibres produced char at different amounts, based on the concentration of alkali treatment, the composites' final residues were not significantly affected by the alkalisation process. It was observed that, as the concentration of NaOH increases, the bamboo fibres left higher residues but the composites, both treated and untreated, produced a fairly similar amount of char. Generally, the final percentages of composite residue were closer to NPs, compared to bamboo fibres. This can indicate that NP is more influential, due to its higher volume fraction. Thus, at low fibre volume fraction, which in this case is approximately 20%, it can be noted that the absence of hemicellulose and lignin may not have an obvious effect on the charring capability of bamboo fibre/polyester composites.
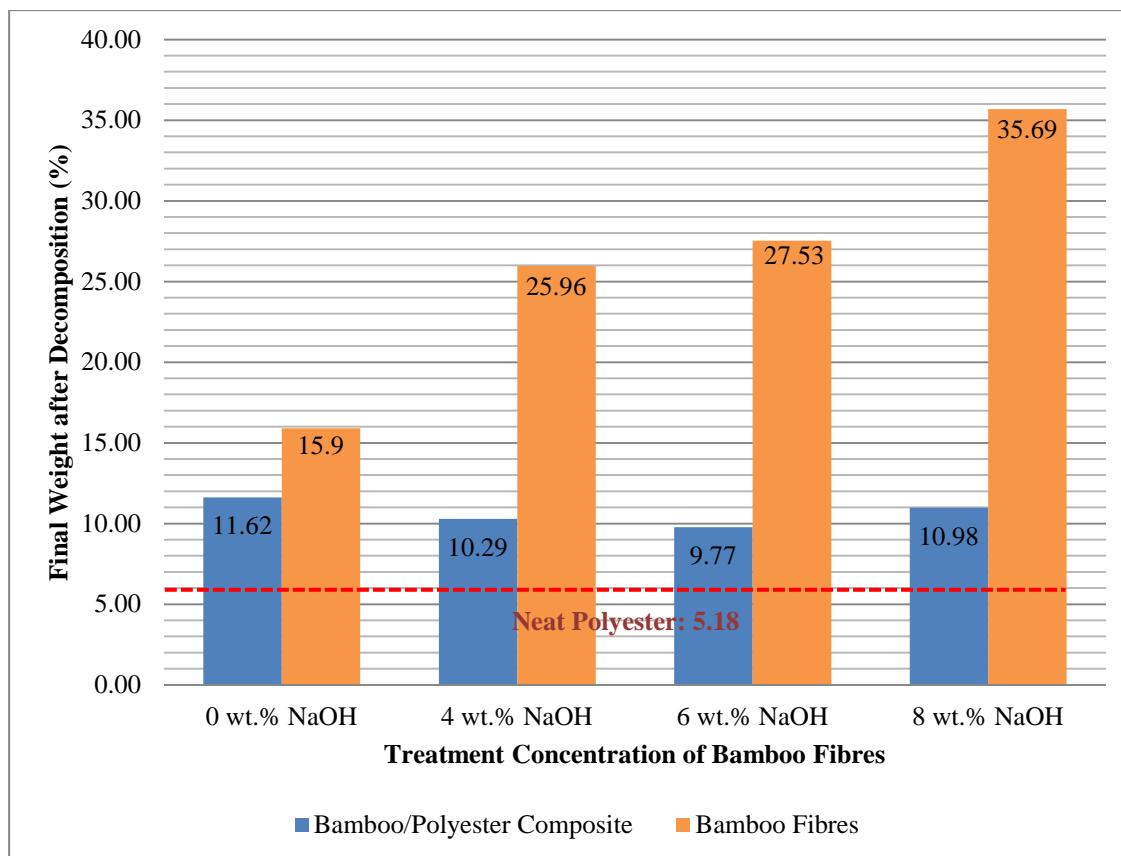
Figure 5.6: Final weight after decomposition of bamboo fibres and bamboo fibre/polyester composites

Shih (2007) highlighted the importance of char in a polymer composite, as it directly correlates to the potency of flame retardation for polymers. The increase in char formation may lead to lower production of combustible gases, decrease the exothermicity of the pyrolysis reaction, and hinder the thermal conductivity of burning materials. Basically, adding reinforcements to polymers improves their charring capability. This was discovered by Dhakal et al. (2007) in hemp/polyester composites, whereby NP yields approximately 2.53% char, which increased to 10.84%, 12.81% and 19.56% with the addition of untreated hemp, NaOH treated hemp and glass hybridised hemp, respectively. Higher charring was observed for treated composites, while adding glass fibres improved charring, due to high heat resistance. However, some researchers have observed deterioration in char formation for alkali treated fibre/polymer composites. Shukor et al. (2014) noted a decrement in formation of carbonaceous char for kenaf fibre/PLA biocomposites as the treatment was increased from 3% to 9% NaOH. The authors concluded that alkalisation increases thermal stability but reduces the residual char content, due to lignin removal. This was also mentioned in Section 5.2, whereby several researchers believed that lignin was responsible for charring.

5.4   Additional protection study for improved durability

As natural fibres/polymer composites have several limitations, which are emphasised when subjected to degradation by the environment of their intended applications, additional protective materials or substances can be introduced to the composites. Incorporating additives such as antioxidants, thermal stabilisers and flame retardants

in a composite system is the simplest form of protection. Nano-composites form a newer technology that enhance thermal and mechanical durability; barrier coatings are post-fabrication protections representing an engineering solution (Pochiraju et al. 2012). In this section, the application of both fire retardant additives and coatings are studied to help improve the durability of bamboo fibre/polyester composites.

5.4.1 Thermal decomposition of bamboo fibre/polyester composites with additives

Initially, two types of additives were proposed for incorporation into the bamboo fibre/polyester composite. Magnesium hydroxide ($MgOH_2$) is used as a thermal stabiliser, while Uvinul 3030 is used as a UV light absorber. Before these two additives can be employed together in the composite system, the optimum level of concentration for each substance needs to be identified to produce the best thermal protection. Based on the literature review, $MgOH_2$ performs well as a thermal stabiliser. For this kind of additive, the mechanical properties of the composite are less jeopardised at lower concentrations (Shukor et al. 2014; Zhang et al. 2012). As for Uvinul 3030, the manufacturer recommends the concentration level be in the range of 0.2 to 10% depending on substrate and performance requirements of the final application. Most literature limits the addition of UV stabilisers or antioxidants to below 1% (Abu-Sharkh & Hamid 2004; García et al. 2009). From these findings, Table 5.3 was tabulated to separately obtain the optimum concentration of both additives.

Table 5.3: Concentration of thermal stabilizer and UV absorber for optimization study

Sample	MH1	MH2	MH3	UV1	UV2	UV3
Magnesium Hydroxide (wt.%)	4	6	8	0	0	0
UV Stabilizers (wt.%)	0	0	0	0.4	0.6	0.8

Using mechanical stirring, these additives were mixed together, based on Table 5.3 with liquid polyester for one hour and poured into moulds. However, this technique was unsuccessful with apparent settlement of the additives causing layers of unequal substance distribution throughout the thickness of the polyester resin, as shown in Figure 5.7. While Tibiletti et al. (2011) found this technique successful, most authors have used compounding techniques with extruders to ensure homogeneity of all the composite components. However, in this study, additive incorporation into the composites was unachievable due to lack of equipment. Moreover, since the additives failed to blend together with the polyester resin, it was impossible to distribute them evenly throughout the composites, especially between the bamboo fibres, using the vacuum infusion process.
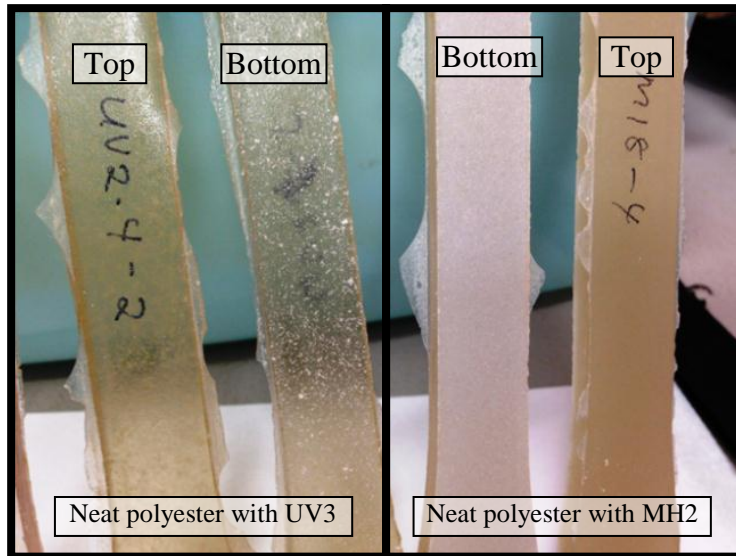
Figure 5.7: Settlement of additives in neat polyester

Even if the additives were able to be dispersed evenly throughout the composite, the expected effect, such as improved thermal stability, may not be achieved. The additives are not homogeneously blended together with the NP, and are basically a separate unit residing within the NP. To study this, small samples of bamboo fibre/polyester composite, with 12, 16 and 20wt.% $MgOH_2$ were fabricated for thermal analysis through TGA. The concentrations were increased to ensure that any effect on thermal resistance could be easily detected. The DTA curves are presented in Figure 5.8.
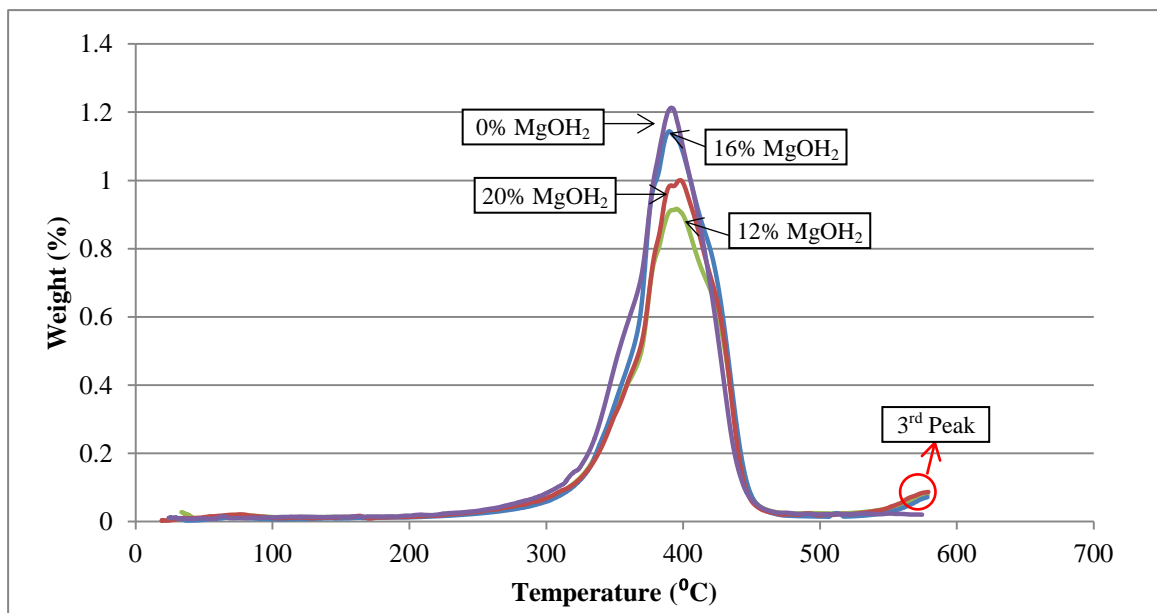
Figure 5.8: DTA curves of bamboo fibre/polyester composites with MgOH2 additive

Since bamboo fibres treated with 6% NaOH showed better mechanical properties, the additives were added to sample BPC-6, and the resulting DTA curves were compared to BPC-6. As observed in Figure 5.8, all three samples with additives have

98

a third peak at 580^0C, which seems to ascend at the end of the TGA run. This proves that the $MgOH_2$ decomposes separately from the polyester, and may require higher temperatures to fully decompose. The polyester for all four samples decomposed at a relatively similar temperature, approximately 392^0C. No improvement in thermal stability was achieved by the additives, due to the insufficient compounding technique.

Other researchers have successfully increased the thermal resistance of natural fibre/polymer composites by compounding additives with the polymer. Hamid et al. (2012) has found that by adding a fire retardant made up of sodium metasilicate and zinc borate has increased the second peak of the DTA curve of a biocomposite reinforced with rice husks and sawdust from 445^0C to 470^0C. However, the increased concentration of the fire retardant did not provide further improvement. This was also achieved by Tibiletti et al. (2011) on unsaturated polyesters filled with metallic oxides fillers. Both studies showed a higher formation of char with the presence of the additives. In this current study, the amount of residues was higher with the addition of $MgOH_2$, but this may correspond to the $MgOH_2$ not fully decomposing at the end of the TGA run. Therefore, another option must be considered to substitute the use of additives to provide additional protection for the composite.

5.4.2 Thermal decomposition of bamboo fibre/polyester composites with coating

Additives may at times be difficult to incorporate into a composite. If this occurs, consideration should be given to using an inherently low heat release polymer or other protective methods, such as polymer nano-composites and integrated barrier systems. Barrier coating is a reactive mode of protection that is easy to apply but may also be easily defective, leaving the composite vulnerable to damage stimuli such as UV, heat and abrasion (Adhikary et al. 2008). However, it is widely used in maintenance works on structures, due to its easy application.

This study used a non-hazardous water-based acrylic clear electrometric coating system for outdoor protection. It is not an intumescent coating but contains Tinuvin for UV resistance. The manufacturer also claims it has good water proofing properties, heat and fire resistance, is non-toxic and odourless, as well as colourless to maintain the aesthetic advantage of bamboo fibres. The coating was applied to BPC-6 samples; it shows good mechanical properties, as discussed in Chapter Four. Thus in this section, the thermal degradation and mechanical properties of BPC-6 coated with a commercially available coating system used for domestic and industrial applications is evaluated. There is a lack of literature relating to the effect of this type of coating on natural fibre composites.

A coated sample of BPC-6 was subjected to thermal decomposition using TGA. The sample is labelled as BPC-6C, and the DTA curve obtained is compared to the uncoated sample and presented in Figure 5.9. It can be observed that sample BPC-6C has a slight peak between 80^0C and 200^0C, which is absent for the uncoated sample, indicated by the arrow in the Figure 5.9. This implies that the coating is decomposed at temperatures higher than 100^0C. As the coating is designed for outdoor environments, it is understandable it can only withstand high temperatures up to

80^0C. However, this shows it may not be fire resistant, as claimed by the manufacturer. Both BPC-6 and BPC-6C experience a temperature peak at approximately 358^0C, as the bamboo fibres are decomposed. The main peak, however, is shifted from 391.76^0C to 401.40^0C with the presence of coating. A possible explanation for this is that the coating's decomposition may have caused charring, which provides some insulation to withstand another 10^0C of temperature increment. This can be observed in Figure 5.10, as indicated by the arrow on the TGA curves.
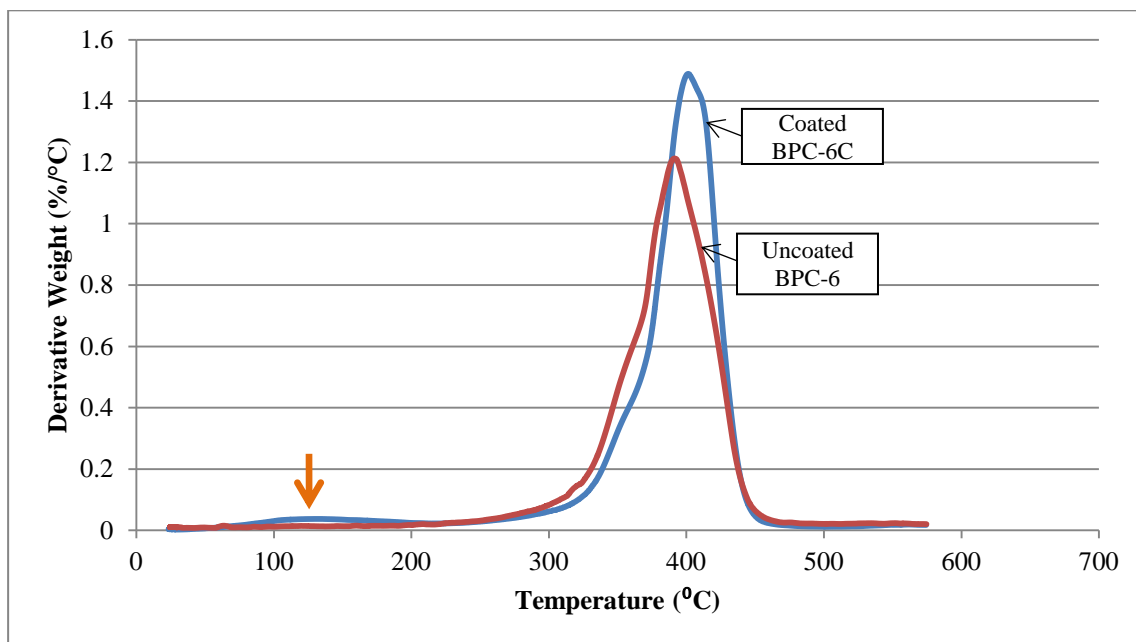
Figure 5.9: DTA curves of 6% NaOH treated bamboo fibre/polyester composites with and without coating

The weight percentage for BPC-6C starts to decrease more than the uncoated sample starting from 100^0C to 340^0C, representing the coating decomposition. Subsequently, the weight percentage becomes higher than the uncoated sample, which may signify the formation of char from the decomposed coating. However, it is interesting to note that at temperatures higher than 410^0C, a higher decrement in residues was observed for BPC-6C. This may indicate that the char is unstable beyond this point. The chemical composition of the coating may have influenced the final char formation of the composite, with 5.45% residue left by BPC-6C and 9.74% residue left by the uncoated sample. This may be possible as the char itself can be affected by the conditions prevailing during heating. Tibiletti et al. (2011) found that the final residues of unsaturated polyester resins differ in different TGA atmospheres. Under air atmosphere, the char formed becomes unstable at 600^0C and degrades to 0.1% residue, while under nitrogen atmosphere, there was 1.4% residue left at 800^0C. In terms of the acrylic coating degradation, Yew et al. (2013) studied the thermal decomposition of acrylic films with different fillers. The acrylic films were observed to start losing weight at a temperature range of approximately 100^0C to 280^0C. From 280^0C to 330^0C, about 60% of weight loss was observed, leaving 35% of residue which was stable until 800^0C. Another 15% of weight loss was observed at 800^0C. This corresponds well with the TGA curve of BPC-6C whereby the residues at 330^0C as mentioned by Yew et al. (2013) may have caused a shift in the main peak of the curve.

100
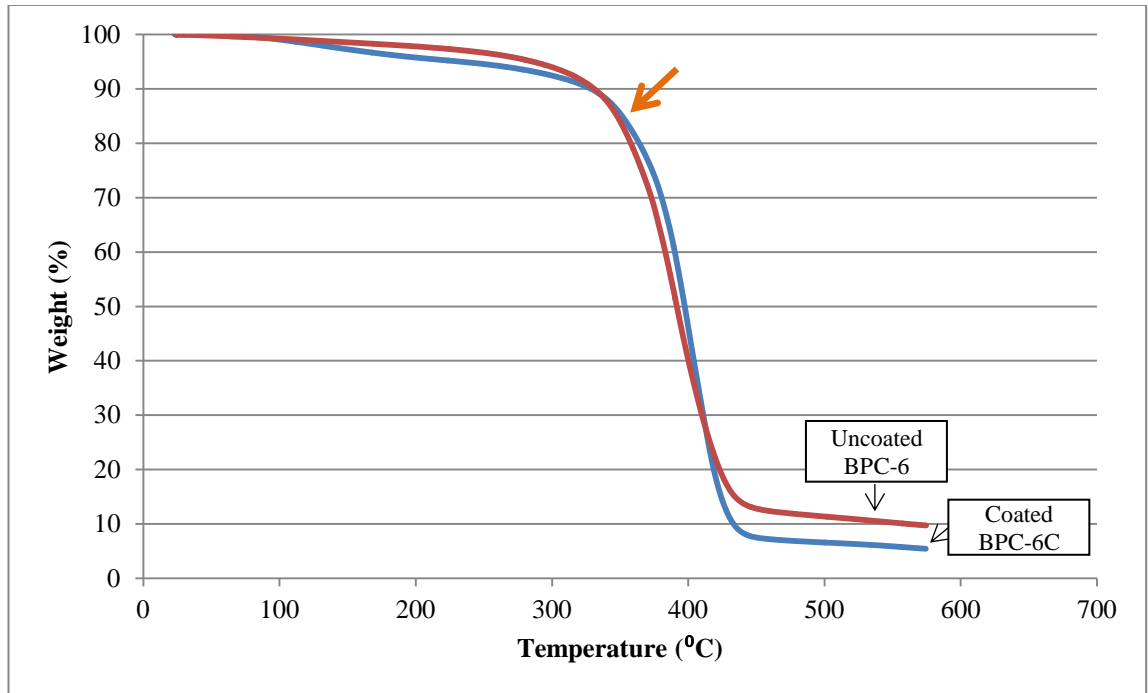
Figure 5.10: TGA curves of 6% NaOH treated bamboo fibre/polyester composites with and without coating

Generally, it is expected that the coating will only provide thermal protection on the mechanical strength of the composite up to 80^0C, as it will be degraded at higher temperatures.

5.4.3 Tensile properties of bamboo fibre/polyester composites with coating

A tensile test was performed on sample BPC-6C to establish its initial tensile properties before being subjected to any form of degradation. The stress-strain curve is presented in Figure 5.11.
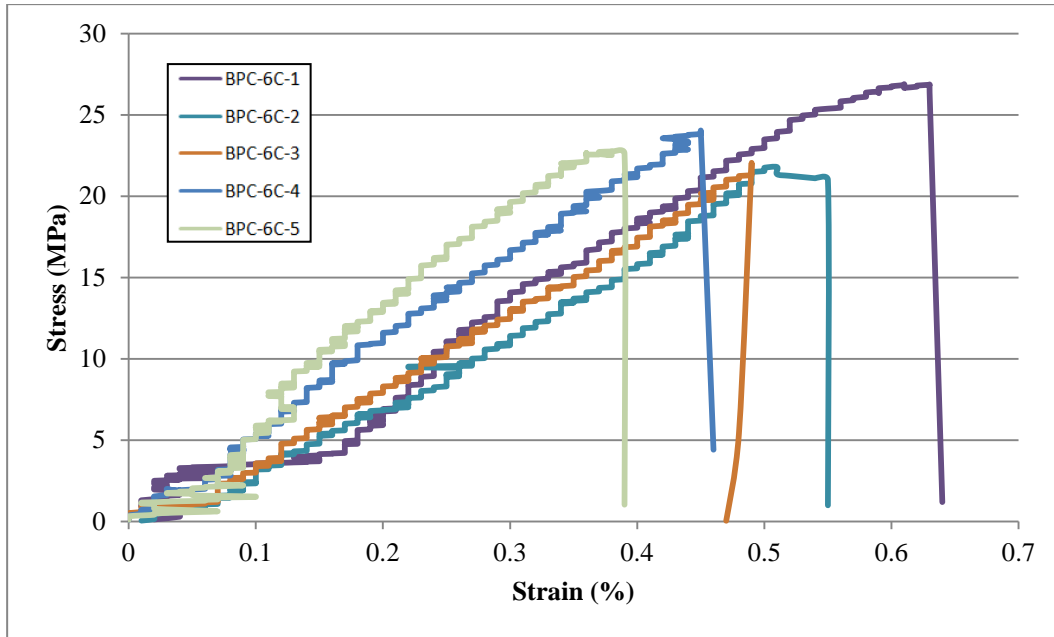
Figure 5.11: Stress-strain curves of coated 6% NaOH treated bamboo fibre/polyester composite

The average tensile strength and elastic modulus were calculated and compared to the other samples, and are presented in Figure 5.12 and Figure 5.13, respectively.
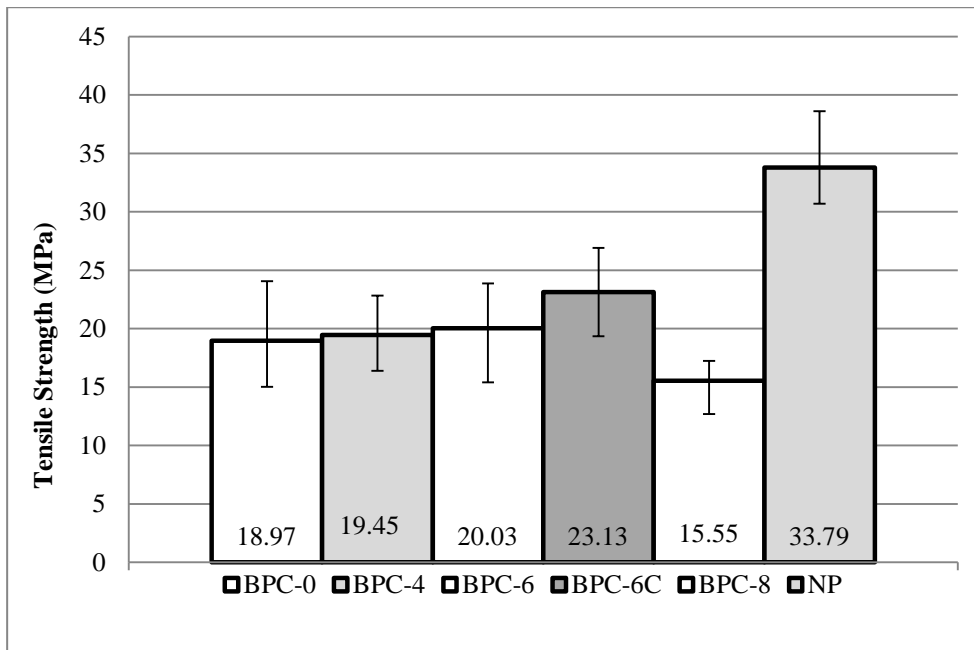
Figure 5.12: Tensile strength of coated composite in comparison with other samples
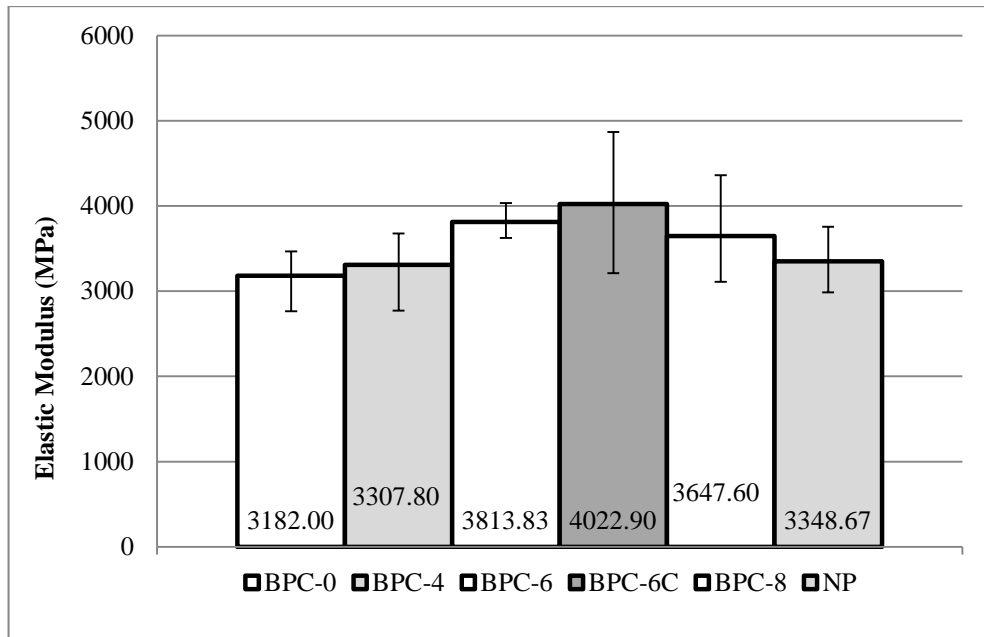
Figure 5.13: Elastic modulus of coated composite in comparison with other samples

With the application of coating on the composite, a slight increase in tensile properties was observed. The tensile strength increased from 20.03 MPa to 23.13 MPa, which is 13% higher than 6% NaOH treated composites, but is still much lower than the strength of the NP. The elastic modulus was also improved for the coated sample, reaching 4 GPa which is the highest among all the samples tested and is 5% higher than BPC-6. Although the increment in mechanical properties is not very significant, it can be noted that the coating may have provided some form of binding force on the surface of the composite, causing additional resistance to the tensile load applied. The binding strength of acrylic coating on several types of surfaces has been studied. Yew et al. (2013) found that the adhesion strength of acrylic coating with commercial calcium carbonate fillers on steel surface is 1.26 MPa. Aboudzadeh et al. (2007) found that with silane-treatment, the adhesion strength of acrylic coating can reach up to 2 MPa on a polypropylene surface. However, neither study provided any correlation between the improved adhesion strength and the tensile properties of the coated material.

As shown in Figure 5.14, it was observed that the coating experienced some peeling near the fractured surface of the composite. It is apparent that the coating was not rigid, and was mentioned by the manufacturer to remain flexible after curing. Upon tensile loading, the coating may experience stretching and finally split as the composite fails. Prior to this, some force may be required to overcome the adhesive strength between the coating and the surface of the composite, which will result in coating debonding, as demonstrated in Figure 5.14. A close-up view through SEM, as presented in Figure 5.15, shows that the coating still adhered to the composite surface, but tearing was apparent as a result of excessive stretching in the tensile direction. Thus, it can be concluded that the additional 3 MPa of tensile strength achieved by BPC-6C may have been contributed by the adhesion strength of the coating.
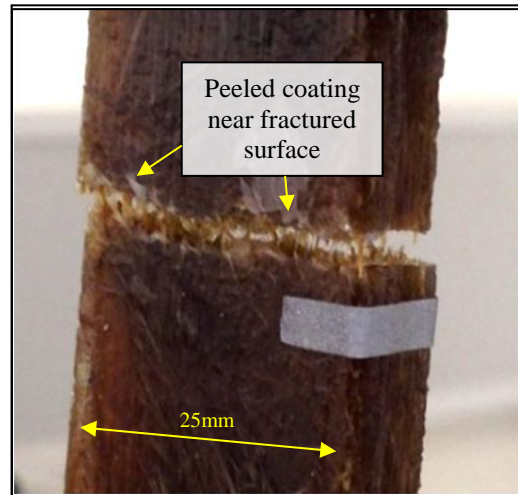
Figure 5.14: Fractured BPC-6C composite after tensile test
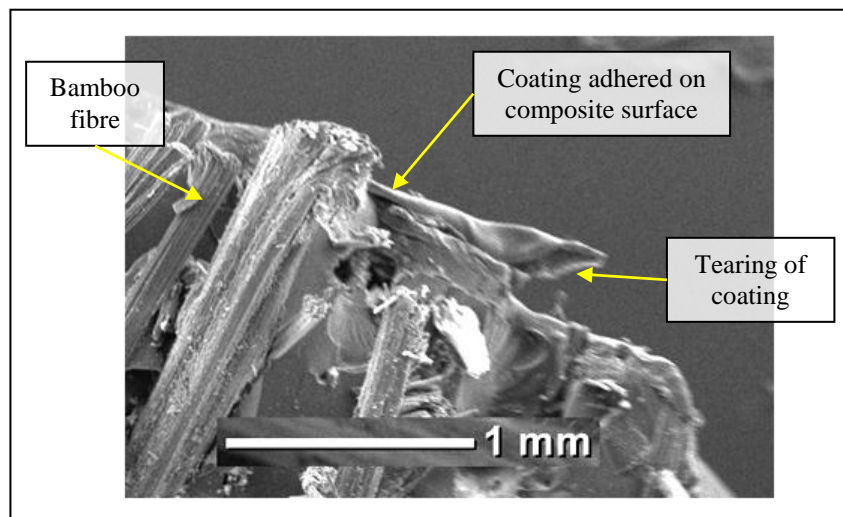
Figure 5.15: SEM of fractured BPC-6C sample

5.5 Dynamic mechanical properties of bamboo fibre/polyester composite

The visco-elastic properties of the samples over a range of temperatures were studied using DMA. In this section, the stiffness and damping of the samples subjected to oscillatory force are measured and reported as modulus and tan delta.

5.5.1 Effect of bamboo fibre reinforcement on the storage modulus with temperature

The storage modulus, E' measures the elastic behaviour of the sample and expresses the maximum energy stored in a material during one cycle of oscillation. It is conceptually similar to Young's modulus, which gauges the stiffness of a material subjected to static loading. However, the values of these two moduli will not be the same as storage modulus refers to the stiffness of the material under dynamic force. The storage modulus of the composites and NP is presented in Figure 5.16.
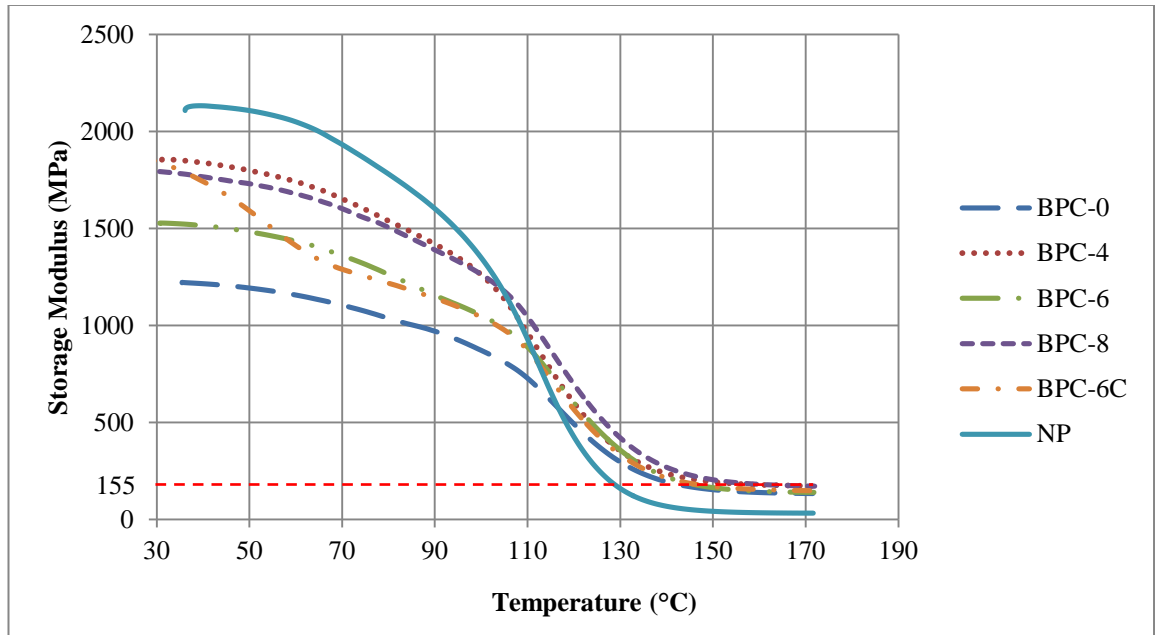
Figure 5.16: Storage modulus of bamboo fibre/polyester composites and neat polyester

From the storage modulus curves, it can be observed that all samples underwent a drop in stiffness as the temperature increased from 30^0C to 170^0C, whereby the polyester experienced a transition from plastic to rubbery state. At temperatures lower than 100^0C (i.e., the plastic region), the E' value for NP is higher than the samples with bamboo fibre reinforcement. Among the bamboo fibre composites, the untreated sample had the lowest stiffness, followed by BPC-6, BPC-8 and BPC-4, while the coating only provided improved stiffness up to 60^0C. As the temperature increases, the stiffness of NP dropped sharply, reduced to lower than the rest of the composite samples. This indicates that the addition of bamboo fibres is advantageous on the resin's stiffness at higher temperatures, as it allows a more gradual fall in the E' value. The composites, both treated and untreated, show a relatively similar behaviour at higher temperatures, as the curves converge at about 140-170 MPa.

It is interesting to see that with the addition of fibres, the stiffness of the composite decreases in the plastic region. As the test set-up was in the form of a dual cantilever test, a reference was made to the same randomly oriented bamboo fibre/polyester composite subjected to flexural loading conducted by Manalo et al. (2013). The authors stated that the addition of the randomly oriented bamboo fibres had no positive impact on the flexural strength and stiffness of the polyester resin, which indicated that the fibres did not provide effective reinforcement to the NP in bending mode. Thus, similar circumstances may also be experienced by the composites in this study. However, it must be noted that moduli from dual cantilever fixtures may have 10% to 30% difference than the same material measured in three-point bending, due to shearing strain induced by clamping, making the sample more difficult to deform (Menard 2008). In contrast, alkali treatment on the fibres caused an improvement to the stiffness of the composite, which may be attributed to better interfacial adhesion between the fibres and matrix. With the application of acrylic coating, a higher E' value was achieved by the composite treated with 6% NaOH up to 60^0C. At this point, the coating is no longer effective, as it may have been thermally degraded. At

the end of the experiment, the coating was observed to soften by adhering to the clamps, indicating it underwent degradation.

Several studies have shown varying results in terms of the storage modulus of polymers at room temperature containing natural fibres. Some indicated that the addition of fibres improved stiffness, while others observed decreases at higher fibre volume fractions. Shanmugam and Thiruchitrambalam (2013) reported that by adding alkali treated Palmyra Palm Leaf Stalk fibres and jute fibres to unsaturated polyester in a unidirectional continuous manner, the E' value was higher for all temperature ranges. Romanzini et al. (2013) highlighted that by increasing the fibre content, the ability of the resin to allow mechanical constraints with recoverable visco-elastic deformation was enhanced, causing improved stiffness. However, with adding higher volumes of keratin bio-fibres in a poly(methyl methacrylate) matrix, Martínez-Hernández et al. (2007) observed a gradual decrease in the E' value. Another study by Shih (2007) showed that untreated waste water bamboo husk fibre/epoxy composites had a lower storage modulus than neat epoxy at room temperature. With the addition of coupling agents, the E' value exceeded the neat epoxy's, which the author attributed to better fibre/matrix compatibility. Interestingly, all researchers agree that at higher temperatures, where the polymers enter into a rubbery state and soften, the presence of fibres improved the stiffness of the composites. This is because with the presence of fibres, the molecular movement of the softened polymers gets restricted (Shinoj et al. 2011).

5.5.2 Effect of bamboo fibre reinforcement on the loss modulus with temperature

The loss modulus, E" measures the viscous response of the sample and is proportional to the amount of energy dissipated as heat by the sample. The loss modulus of the composites and NP for a frequency of 1 Hz is presented in Figure 5.17.
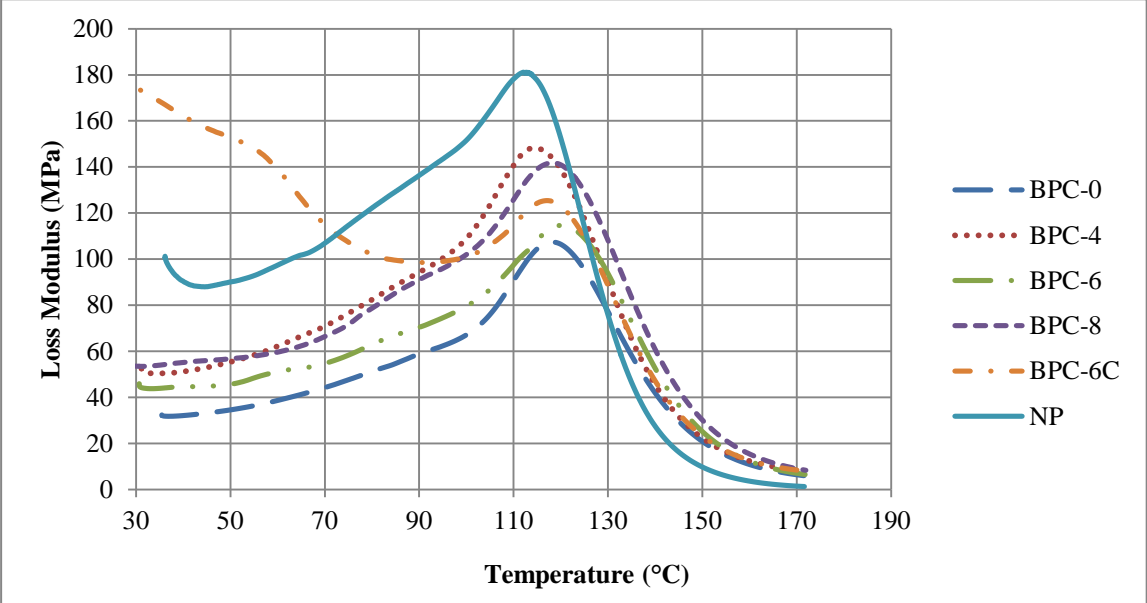
Figure 5.17: Loss modulus of bamboo fibre/polyester composites and neat polyester

It can be observed that the value of loss modulus increased and then decreased after reaching a maximum with the increase in temperature for all samples, except BPC-6C. The coated sample has a high initial E" value; this keeps decreasing until 90^0C. From this point, the curve follows the same pattern as the other uncoated samples. These two phases represent the loss modulus for the coating and the composite, respectively. Similar to the storage modulus values, the loss modulus for NP is highest in the plastic region and becomes lowest in the rubbery region. The loss modulus for all samples decreases sharply at a temperature approximately above 110^0C, indicating a sharp decrease in the viscosity in this region. The decrement of loss modulus was less abrupt with the addition of bamboo fibres. The lowest E" value was observed for untreated composites, which increased with alkali treatment. It can also be noted that curves shift slightly to the right for all composites, compared to NP. The shift of the E" peeks to higher temperatures with the incorporation of fibres is associated with decreased mobility of the matrix chains and associated stress field surrounding the particles in the presence of fibres (Shinoj et al. 2011).

The increased E" values for NP and the composites in the plastic region imply that the viscosity of the samples increased with temperature. With the addition of fibres, the loss modulus showed a decrement, suggesting lower energy dissipation in the composite. This agrees with Shinoj et al. (2011), who reported that the addition of oil palm fibres to polyethylene resin caused a decrease in E" value, but with a higher volume fraction (40%), the value increased closer to that of resin. Romanzini et al. (2013) determined adding glass/ramie fibres to polyester resin increased the loss modulus peak height. The author attributed this to the inhibition of the relaxation process within the composite, due to enhancement of the number of chain segments and in the free volume upon fibre addition. The impact was much less without the glass fibres, indicating that stiffer reinforcement caused higher heat build up in the composite. The improved fibre/matrix adhesion through alkalisation was found to increase the loss modulus of the composites, and this was also observed by Shinoj et al. (2011). The maximum heat dissipation occurred at the temperature where maximum loss modulus was reached. This temperature is the T_g of the composite system. The loss modulus curves for all samples decreased for higher temperatures, as a result of the free movement of polymer chains (Martínez-Hernández et al. 2007).

5.5.3 Effect of bamboo fibre reinforcement on the damping with temperature

Tan δ is determined by the ratio of loss modulus and storage modulus and is used to describe the damping behaviour of a material. Damping shows how well a material performs at absorbing and dissipating energy under cyclic loading (Lu & Oza 2013). Higher value of tan δ represents higher damping coefficient, which indicates greater efficiency of a material in accomplishing energy absorption and dispersal. The damping parameter of the composites and NP for a frequency of 1 Hz is presented in Figure 5.18. From the tan δ curves, it is clear that NP experienced higher damping than the composites, with a significant maximum value at 132^0C. With the addition of fibres, the maximum tan δ was reduced from 0.48 to 0.26 (a 45.8% reduction) for all composites, regardless of treatment. Consequently, it can be said that fibre alkalisation had no influence on the damping effect of the composites. These maximum values were achieved at roughly the same temperature, 130 ± 2^0C. The

coated sample had two peaks, whereby the first peak represents the maximum damping of the coating at 60^{0}C.
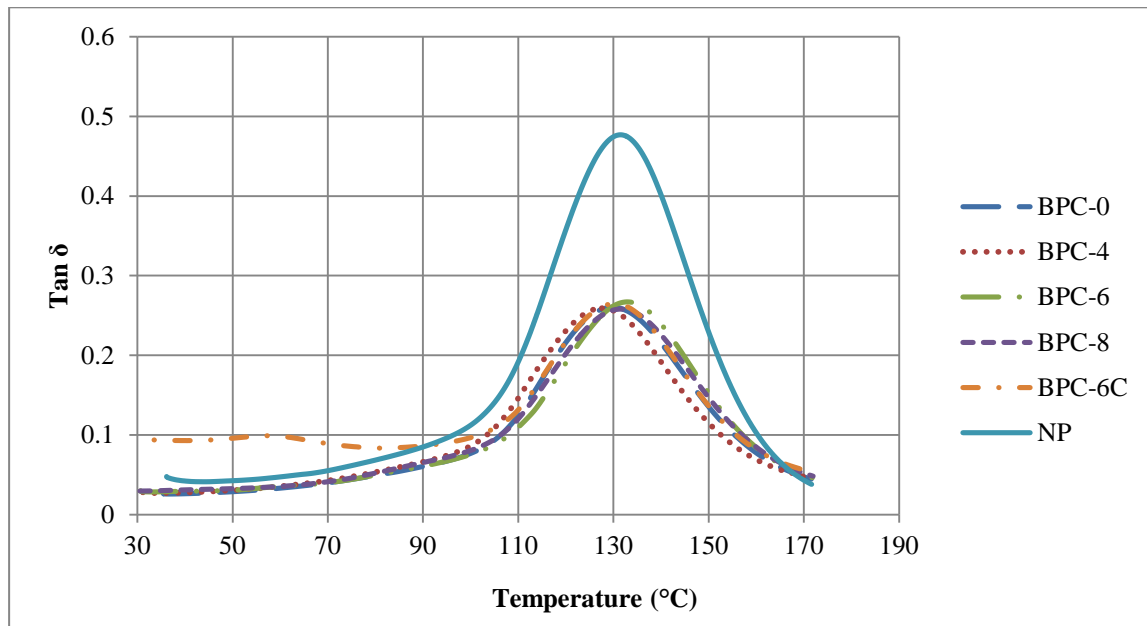
Figure 5.18: Tan δ of bamboo fibre/polyester composites and neat polyester

Reduction in damping by adding fibres has also been reported by Jacob et al. (2006) and Aziz and Ansell (2004). The lower tan δ value has been attributed to less dissipation of vibration energy due to lower matrix by volume in the composites and also by fibre agglomeration at higher fibre loading (Jacob et al. 2006). Shanmugam and Thiruchitrambalam (2013) stated that lower tan δ is a sign of good fibre/matrix adhesion, as the damping is reduced by the restricted mobility of the polymer molecules upon addition of stiff fibres. Shinoj et al. (2011) reported that the addition of fibres beyond 10% did not cause a proportional reduction in tan δ. The author concluded that for all fibre loadings, the vibration energy was dissipated to the same degree, whereby all composites possessed the same order of damping. This suggests that improved stress transfer within the composite had no effect on damping behaviour. This can also be associated with the alkali treated bamboo fibre/polyester composites. Treated and untreated composites may experience the same level of vibration energy dissipation. This was also observed by Aziz and Ansell (2004) on the tan δ peaks of untreated and treated hemp/polyester composites, which are very close in magnitude, while Shinoj et al. (2011) found no difference in tan δ between treated and untreated oil palm fibre/polyethylene composites.

5.5.4   Glass transition temperature of bamboo fibre/polyester composites

The T_g is a specific temperature at which a polymer undergoes transition from a plastic or solid phase to a rubbery or semi-solid phase. The dynamic T_g can be defined as the temperature at which (Geethamma et al. 2005):
   a)   the maximum peak of tan δ occurs or
   b)   the maximum peak of E'' occurs or
   c)   the mid-slope of E' vs. temperature curve or
   d)   the region where E' increases with increasing frequency at a constant temperature.

The T_g for NP and treated and untreated bamboo fibre/polyester composites was extracted through methods (a) and (b) mentioned above. These are presented in Table 5.4.

Table 5.4: T_g of neat polyester and bamboo fibre/polyester composites

Sample	Max peak of tan δ curve	T_g from of tan δ curve (^{0}C)	Max peak of E" curve	T_g from E" curve (^{0}C)
BPC-0	0.26	129.85	107.41	118.17
BPC-4	0.26	127.57	148.32	114.36
BPC-6	0.26	132.79	114.67	120.20
BPC-8	0.26	131.60	141.84	118.25
NP	0.48	131.59	181.14	112.08

As presented in Table 5.4, the T_g values obtained from the tan δ curves are higher than the ones obtained from the E" curves. It was mentioned by Akay (1993) that the T_g value from tan δ curve is heavily overestimated, while the T_g from E" curve is more realistic. Based on this, the T_g obtained from the later are used in this study. It can be observed that the T_g of NP increases slightly with the addition of fibres. As discussed previously, this may be caused by a lower molecular mobility of matrix chains with the presence of fibre reinforcements. The T_g of the composites differ slightly based on the alkali treatment with BPC-6 having the highest T_g followed by BPC-8, BPC-0 and BPC-4. However, the differences are very minor and may be insignificant when considering the effect of alkalisation on the composites' T_g. As for the coated samples, it was observed that the coating had no effect on the T_g of the composite, reacting separately at a much lower temperatures when subjected to heat. Therefore, the T_g for BPC-6C is considered similar to BPC-6. Table 5.5 presents the T_g values for other polymer matrices and their composites from natural fibres, as determined through DMA by other researchers.

Table 5.5: T_g values for various polymers and polymer composites obtained through DMA

Material	T_g	Remark	Reference
Unsaturated polyester resin	84^0C		(Tibiletti et al. 2011)
High density polyethylene (HDPE)	-123.6^0C		(Lu & Oza 2013)
Untreated hemp/HDPE composites	-121.6^0C	No change with NaOH treatment.	
Silane treated hemp/HDPE composites	-117.1^0C		
Neat polyester resin	114.82^0C		(Hossain et al. 2009)
Polypropylene resin	10^0C		(Wielage et al. 2003)
Epoxy resin	58^0C		(Shih 2007)
Waste water bamboo husk fibre/epoxy composites	$65-75^0$C		
Neat polyester resin	61.98^0C		(Shanmugam & Thiruchitrambalam 2013)
Palmyra Palm Leaf Stalk /polyester composites	74.56^0C	Improved with jute fibres hybridization.	
Jute fibre/polyester composites	79.62^0C		
Polylactide resin	65^0C		(Goriparthi et al. 2012)
Untreated polylactide/jute composites	71^0C		
Alkali treated polylactide/jute composites	74^0C		
Silane treated polylactide/jute composites	88^0C		
Polyester resin	94^0C	Improved with higher fibre volume fraction. Improved with glass fibres hybridization.	(Romanzini et al. 2013)
Ramie/polyester composite	98^0C at 10% volume fraction		
Linear low density polyethylene (LLDPE)	-145^0C		(Shinoj et al. 2011)
Oil palm fibre/ (LLDPE) composites	-128^0C		

From the listed studies on polyester resin, it seems that different batches of polyester resin may have different T_g values. A compilation of the literature shows that the T_g for NP may vary from 60^0C to 115^0C. This was also highlighted by Lorenz (2011), who stated that commercial polyester resin may exhibit T_g between 30 to 185^0C. Thus, it is important to note that for better comparison of a polymer's properties, and its composite, the same batch of resin must be used.

With the establishment of T_g values for NP and bamboo fibre/polyester composites, we can expect that at approximately 120^0C, the mechanical properties of these samples may suffer severe loss, due to softening of the polyester. This behaviour is further discussed in the following section.

5.6 Thermo-mechanical properties of bamboo fibre/polyester composites

Tensile tests were performed on NP and on untreated (BPC-0), treated (BPC-6) and coated (BPC-6C) bamboo fibre/polyester composites after the samples were exposed to three temperature settings: 40^0C, 80^0C and 120^0C for one hour. As the T_g of the samples are approximately 120^0C, the tests were limited to 120^0C; the samples will be in semi-liquid phase at higher temperatures.

5.6.1 Effect of temperature on the weight loss of bamboo fibre/polyester composites

Prior to tensile testing, the weights of the samples, before and after heat exposure, were measured to evaluate any physical degradation that may have been affected by heat. The weight reduction of the samples after one hour of exposure at 40^0C, 80^0C and 120^0C are presented in Figure 5.19. The weight loss experienced by all samples is minimal, less than 1% from the initial weight. However, weight loss increases with increasing temperature, thus it is expected that a more significant reduction will occur at elevated temperatures. It was observed that NP had the least weight loss compared to the composites; at higher temperatures, the difference in the weight loss between NP and the composites is larger. This indicates that the weight of natural fibres is more easily affected by heat compared to resin. The untreated samples may have a lesser average weight loss than the treated and coated composites, but the higher standard deviation shows a more varied response. The coating on the composite surface has a slight impact, showing less weight reduction than the treated composite.
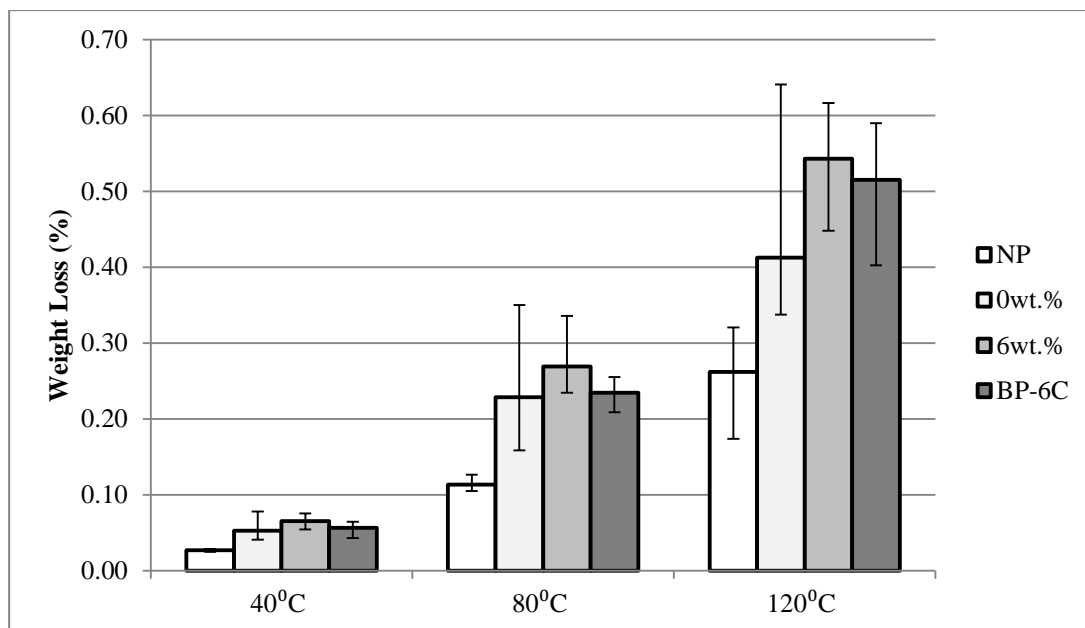
Figure 5.19: Weight loss at different temperature

At this temperature range, the weight reduction of the bamboo fibres is mostly due to evaporation of moisture, while the NP may be releasing gaseous products, such as carbon dioxide and carbon monoxide, as well as water vapour (Wang et al. 2011). A DTA on hemp fibres was carried out by Aziz and Ansell (2004) and showed a broad endotherm observed in the temperature range of 50–175^{0}C, in both the treated and untreated hemp fibres, indicating water molecules in the fibres. Due to the hydrophilic nature of bamboo fibres, it is expected that the composites will contain higher residual moisture than the NP. As the temperature increases, the evaporation of this moisture causes higher weight loss in the composites, as observed in the bar graph. With poorer fibre/matrix adhesion and higher hemicellulose content of untreated composites, it has been reported that these composites absorb higher moisture content than treated composites (Dittenber & GangaRao 2012). This moisture may have been absorbed by the fibres before or after fabrication. However, the results show that individual BPC-0 samples may have varied levels of moisture content, due to the high standard deviation obtained for all temperature settings. With the application of coating, a lesser amount of weight loss was observed. This may be due to the additional layer on the composite surface that hinders the release of vapours from within the composite to the atmosphere. Although this weight loss due to moisture evaporation is small, the voids caused by the evaporated moisture might affect the mechanical strength of the composites (Monteiro et al. 2012).

5.6.2 Stress-strain diagram at different temperature

The stress-strain curves for all temperatures are compiled in Figure 5.20 while the curves for each temperature setting are extracted and shown in Figure 5.21, Figure 5.22 and Figure 5.23.
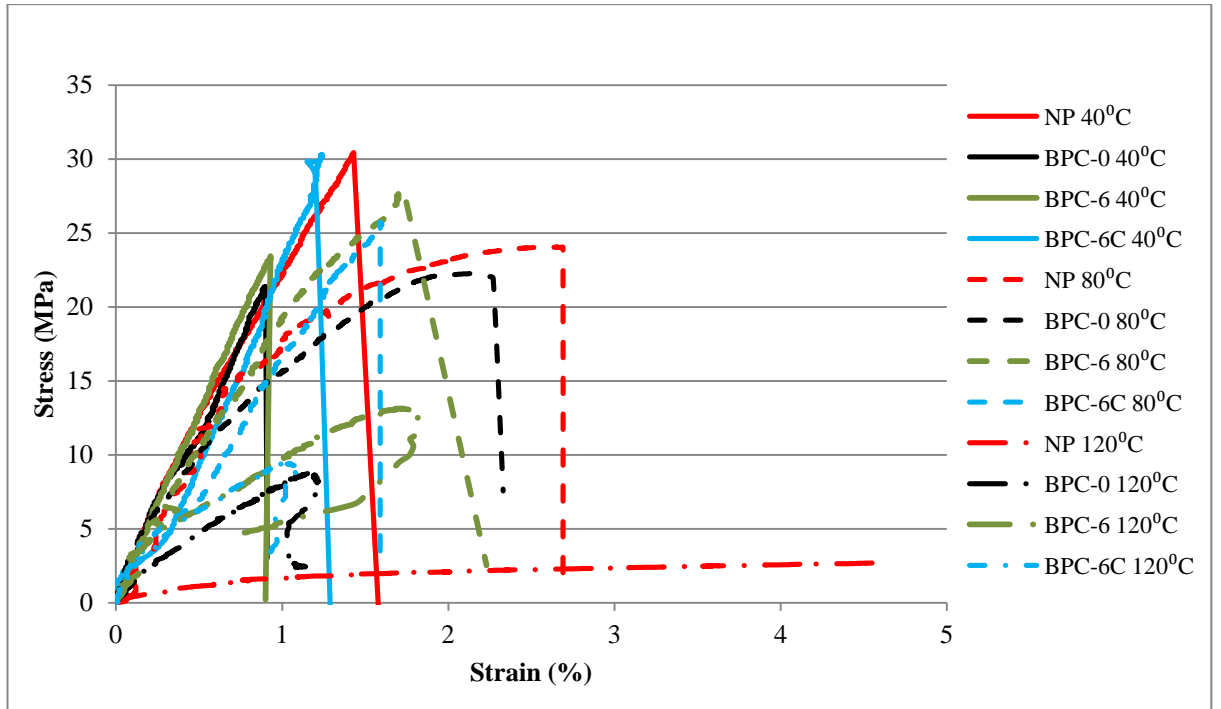
Figure 5.20: Stress-strain curves at different temperature
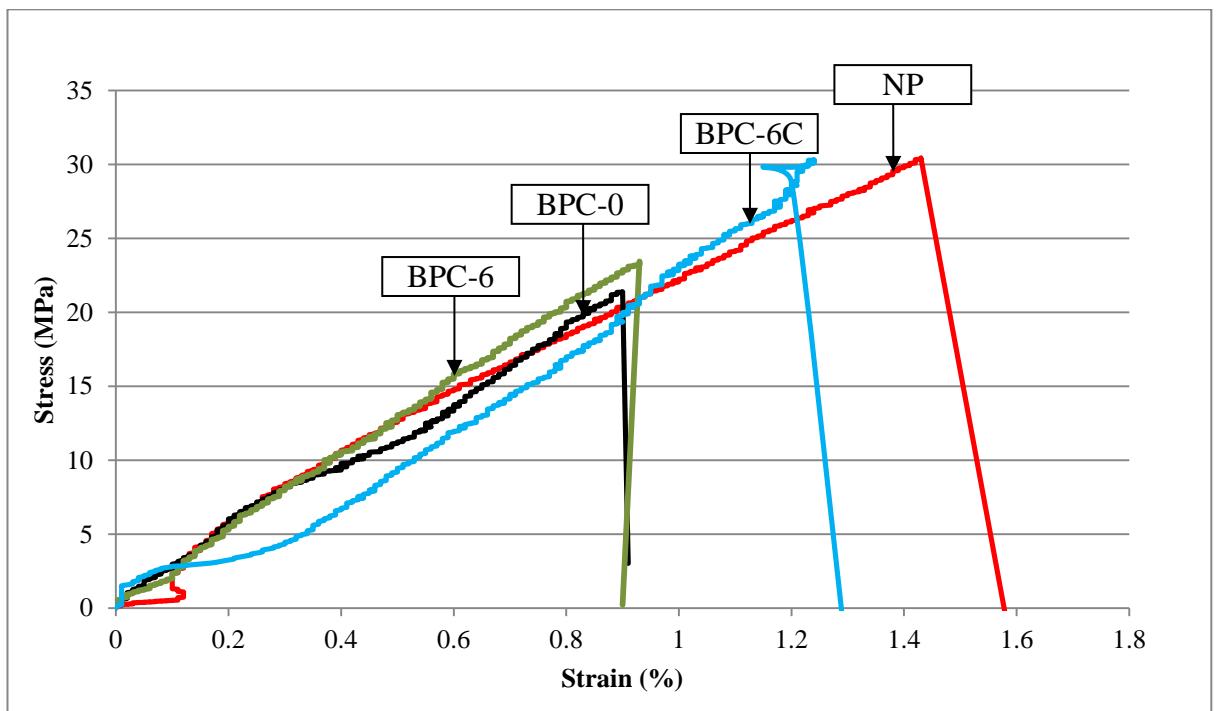
Figure 5.21: Stress-strain curves at 40°C
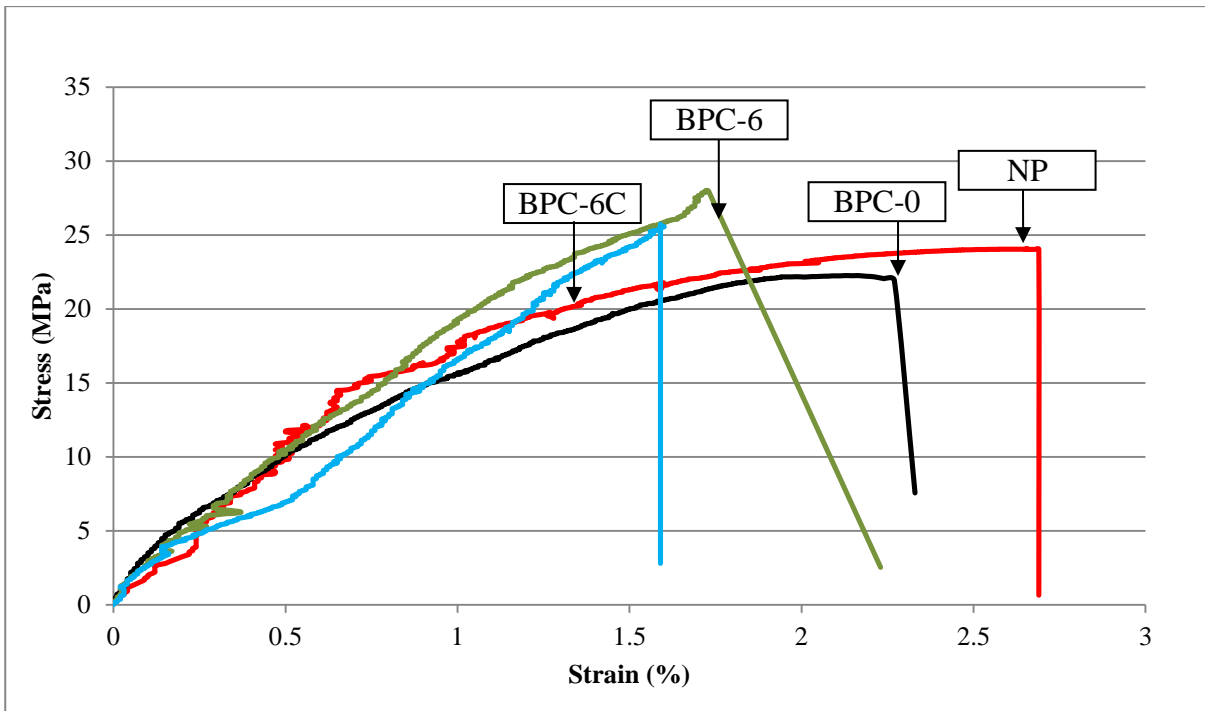
Figure 5.22: Stress-strain curves at 80⁰C
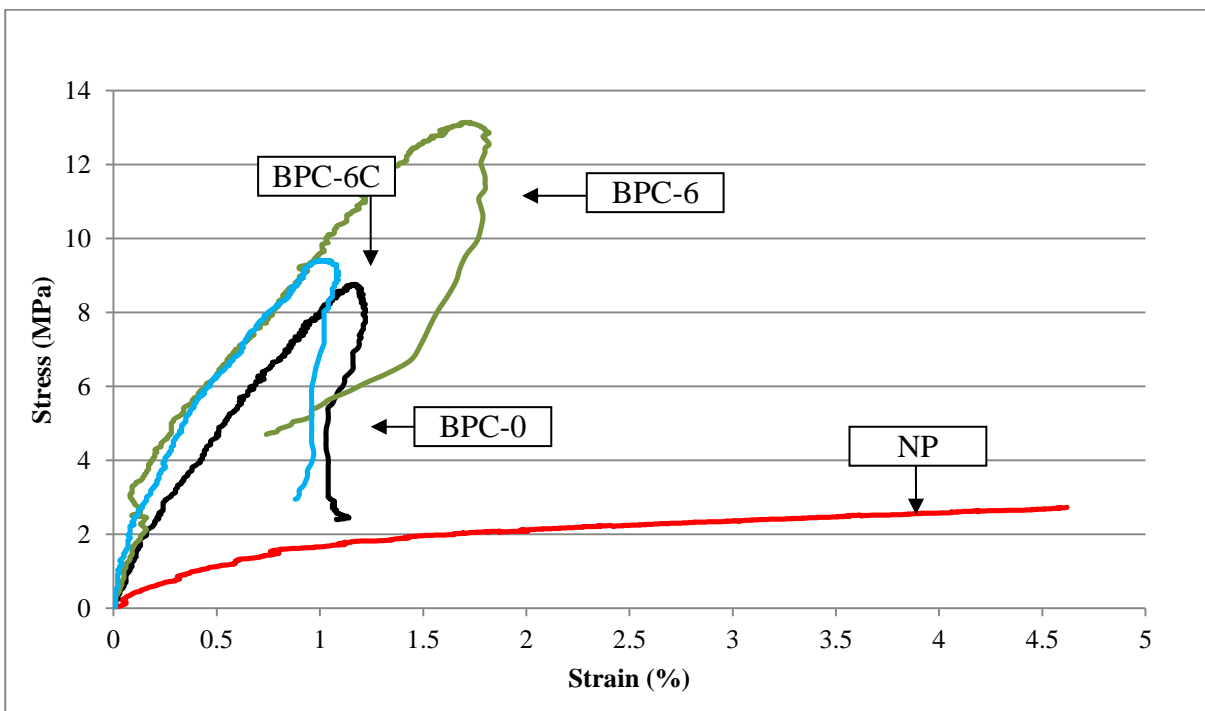
Figure 5.23: Stress-strain curves at 120⁰C

It can be observed that as the temperature increases, the shape of the stress-strain curves changes for all samples. The curves at 40^0C are similar to the stress-strain diagram obtained at room temperature. This was discussed in Section 4.8.1, whereby the slope increases linearly and drops abruptly at maximum stress. At 80^0C, the slope gradually becomes less steep; this is especially obvious for BPC-0 and NP. The maximum stresses were maintained for a few seconds before failure. As the temperature reaches 120^0C, the maximum stress achieved by NP was less than 3 MPa, with a very high percentage of strain. However, the composites managed to show higher resistance than the NP, and failed more gradually without any breakage sound.

From these graphs, the behaviour and failure mode of the neat resin and its composites upon tensile loading with increased temperatures can be evaluated. At room temperature or at higher outdoor temperatures, which may reach 40 to 50^0C, the samples are expected to be stiffer and deformation is proportionate to the load applied. The abrupt drop in the stress-strain curves indicates the samples failed in a brittle mode. At 80^0C, which is the midpoint between the solid phase of the polyester and its T_g, a transitional behaviour can be expected. The decrease in slope steepness suggests that the samples undergo a reduction in stiffness, while the plateau on the curves before the drop shows a semi-ductile failure. This behaviour suggests that even at 80^0C, the polyester may have started to soften. As the T_g is reached, the polyester resin became very ductile, while the addition of fibres provided some stiffness and hindered the mobility of the polymer's molecular chains. The gradual failure indicates that only the fibres resist the tensile load as the polyester softens. The tensile force causes gradual separation between the fibre and the matrix, deteriorating the fibre/matrix adhesion.

The tensile strength and modulus of elasticity of the samples were obtained from an average of five test specimens each. These are compared to the initial tensile properties at room temperature as presented in Figure 5.24 and Figure 5.25, respectively.

	RT	40⁰C	80⁰C	120⁰C
■Untreated Composite	18.97	20.58	22.20	9.25
□Treated Composite	20.03	21.50	24.70	12.36
■Coated Composite	23.13	24.77	24.57	10.05
□Neat Polyester	33.79	31.16	23.83	2.87
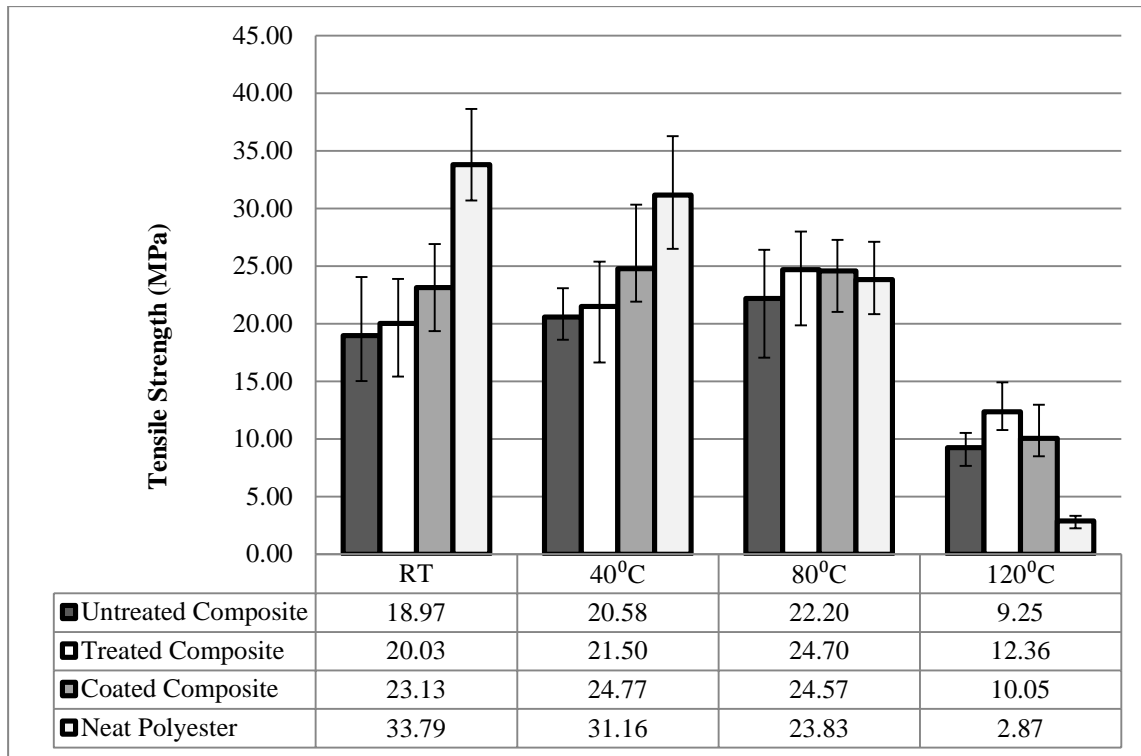
Figure 5.24: Tensile strength of composites at different temperatures

	RT	40⁰C	80⁰C	120⁰C
■Untreated Composite	3182.00	2573.75	1233.33	621.83
□Treated Composite	3813.83	2520.00	1620.50	713.80
■Coated Composite	4022.90	2838.67	1715.33	874.00
□Neat Polyester	3348.67	1812.00	1372.17	234.60
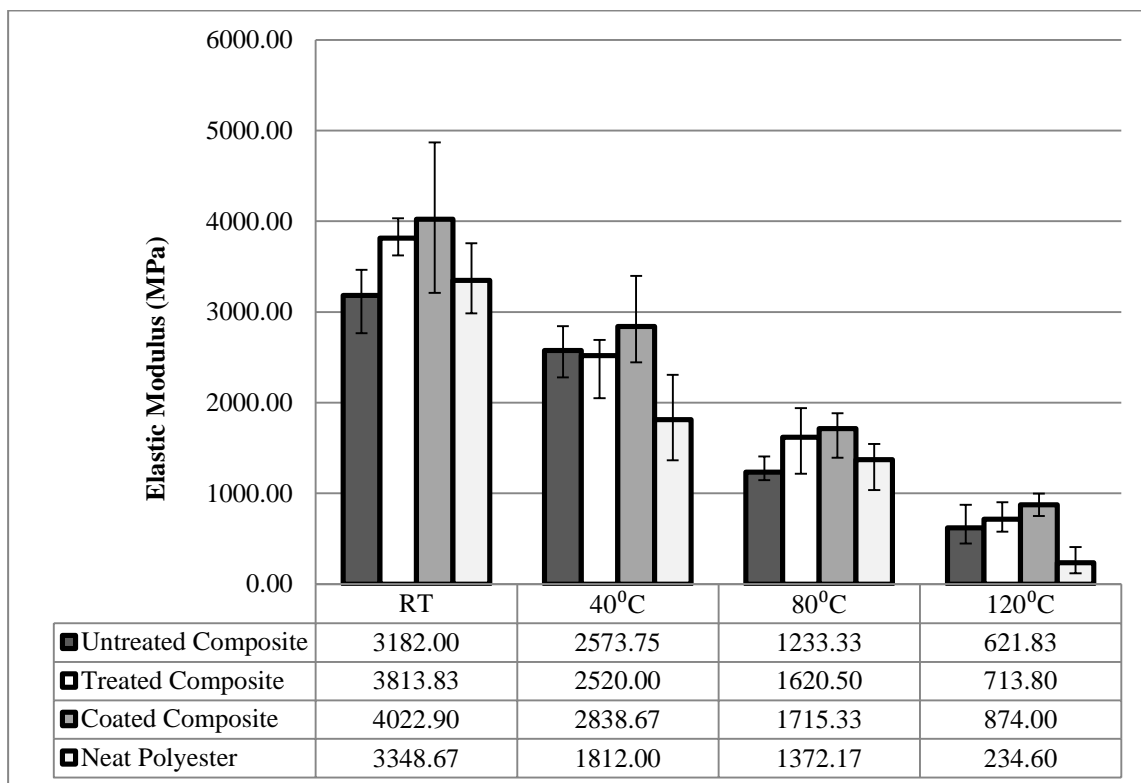
Figure 5.25: Elastic modulus of composites at different temperatures

116

The tensile strength of NP is observed to deteriorate as the temperature is increased from room temperature (25^0C) to 120^0C. The strength slightly decreases from 33.79 MPa to 31.16 and 23.83 MPa at 40 and 80^0C, but was significantly reduced to 2.87 MPa at 120^0C. This is a 91.51% reduction from the initial strength. With the addition of bamboo fibres, the strength of the composites was lower than the NP up to 40^0C. At 80^0C, the tensile strengths of all four samples were about equal, indicating that the NP suffered more strength reduction than the composites. However, at 120^0C, the strength of all the composites was higher than the NP. Among the composite samples, the untreated composites had the lowest strength at all temperature settings, while the coated samples had better strength than the treated samples up to 40^0C. It is interesting to note the slight increase in strength for the composites as the temperature reached 80^0C, dropping significantly at 120^0C, whereby BPC-6 experienced a 23% increment in strength at 80^0C and a 38% reduction at 120^0C. As for the elastic modulus, all samples experienced reduction in stiffness with increased temperatures. The coated samples exhibited the highest modulus of elasticity in all cases, while the NP suffered the highest reduction at 120^0C. With alkali treatment, generally better stiffness was observed on the treated composites compared to the untreated ones. The reduction of elastic modulus at 120^0C was 93%, 80%, 81% and 78% for NP, untreated composites, 6% NaOH treated composites and coated composites, respectively.

It is expected that the tensile properties of NP will decrease with increased temperatures, as it transitions from a solid to rubbery phase. The energy supplied by the heat causes higher mobility of the molecular chains, resulting in lower strength and stiffness of the polyester. The addition of the bamboo fibres improved its strength at higher temperatures, as the reinforcements hinder this process and also provide additional resistance to the load applied. Thus, it can be highlighted that the tensile properties of the fibres are likely more resistant to heat than the polyester. Placet (2009) reported from his findings that hemp fibre loses rigidity; therefore, the degradation of its mechanical properties occurred at a temperature above 150^0C. This was determined by observing the increase in visco-elasticity of hemp fibres for the temperature range of 20^0C to 200^0C, which could be attributed to the succession and partial stacking of in-situ glass transitions of the hemicelluloses and lignins. The same may be applied to bamboo fibres, as the tensile strength of the composites deteriorated at 120^0C. Baley et al. (2005) observed a deterioration in the mechanical properties of dried flax fibres, due to high temperatures with evidence of damage present in the dried fibres.

The small improvement in tensile strength of the composites at 40^0C and 80^0C is comparable to the study done by Laoubi et al. (2014) on E-glass fibre/polyester composites whereby a slight increase of tensile strength was observed at 100^0C, gradually decreasing beyond this temperature. The authors inferred that this behaviour may be caused by evolution of the linkage state of the resin. Post-cure or further cross-linking occurs at elevated temperatures, about $100–150^0$C in most thermosets, prior to the decomposition processes that occurs at a higher temperature range of $250–400^0$C (Gibson 2007). Another probable reason is better fibre/matrix interlocking due to the softening of the matrix. With the more flexible molecular chains, the polyester may be able to penetrate the fibres further and reduce the voids within the composite. In addition, the softening of the polymer will allow the fibres to be rearranged in the direction of the applied load. As discussed by Manalo et al.

(2013), only fibres arranged in the direction of the loading will contribute to the tensile strength of a composite. Therefore, as the fibres are able to move throughout the loading process, more fibres will participate in the load resistance of the composite. The improved mechanical properties of alkali treated BPC-6 samples, compared to BPC-0 is due to the better interfacial adhesion of the fibre and matrix; this advantage remained unchanged even at higher temperatures. Lu and Oza (2013) stated that a higher exposure of cellulose molecules in the treated fibres results in an increased number of free hydroxyl (-OH) groups for intermolecular and intramolecular bonding at the fibre/matrix interface. This causes compact packing of the molecular chains, which leads to higher stiffness compared to the untreated composite. The application of coating on the treated composites was effective up until 40^0C, whereby (as mentioned earlier), the coating was degraded at 80^0C, exposing the composites without additional protection.

However, the confinement provided by the coating resulted in higher elastic modulus of coated samples, compared to the uncoated ones throughout the temperature rise. The presence of the coated layer may have provided some restriction to the deformation of the composite. All composites suffer reduction in elastic modulus at higher temperature. Based on Essabir et al. (2013), this could be due to the evaporation of water molecules adhering to the fibres which makes the fibres stiffer, and ultimately contributes to the decrease in modulus of the composite. Unlike the storage modulus discussed in Section 5.5.1, the elastic modulus of the NP is generally lower than the composites at all temperatures. This suggests that the bamboo fibres are more effective for tensile loading reinforcements. Similar behaviour was also observed by Manalo et al. (2013) on the same randomly oriented bamboo fibre/polyester composites. The author concluded that this type of composite performed better than NP for static tensile loading, which was not achieved on flexural, compression and shear tests.

5.6.3 Visual observation of fractured surface

The pictures of fractured surface of the tensile tested specimens at different temperatures are shown in Figure 5.26. The softening process of the NP is clearly observed. The rough surface at 40^0C is a result of the NP shattering at maximum load. The brittle failure mode causes uneven separation at the centre of the samples. At 80^0C, the surface roughness was less obvious, with half of the fractured surface showing a smoother profile. Thus, this behaviour proves that the NP experienced a semi-ductile failure, implying that the transition process had initiated. A clear, smooth and evenly fractured surface was observed at 120^0C. This indicates that the sample was broken as a result of polymer melting. No cracks or forced rupture was evident, suggesting that the sample was easily separated in half and that less energy was required.

Samples	40ºC	80ºC	120ºC
NP	Rough surface 15mm	Rougher surface / Smoother surface	Smooth surface
BPC-0	25mm / Fibre/matrix debonding	Fibre/matrix debonding in tensile direction	Multiple cracks
BPC-6	25mm / Fibre/matrix breakage	Fibre/matrix debonding in tensile direction	Multiple cracks
BPC-6C	25mm / Peeled coating	Unseparated coating	Multiple cracks
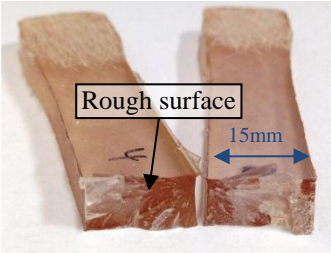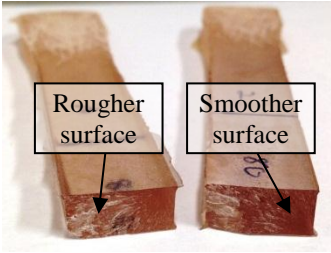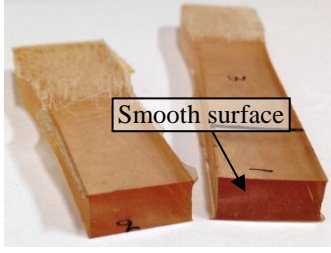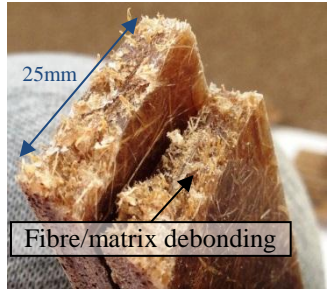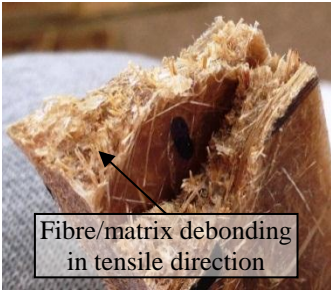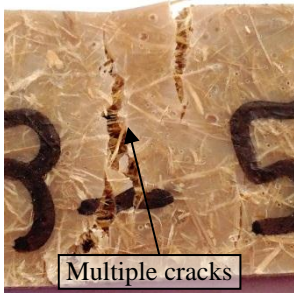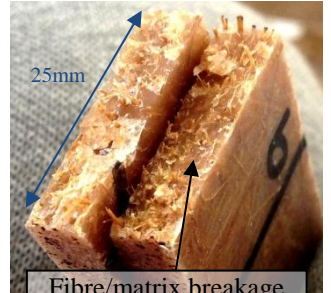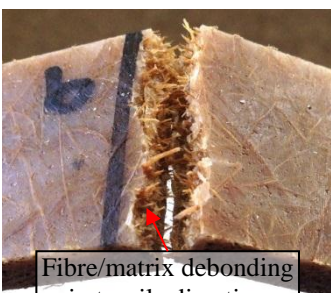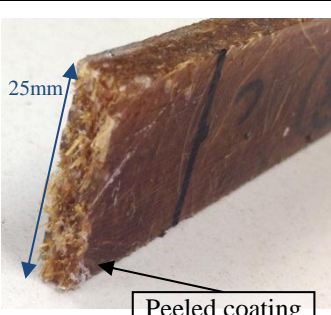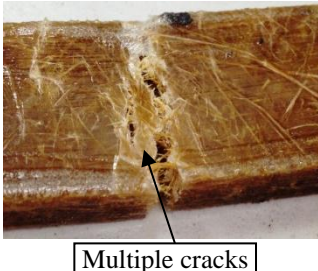
Figure 5.26: Fractured surface of tensile failure samples

With the addition of bamboo fibres, the fractured surfaces of treated and untreated composites were mostly quite similar. No composite samples broke in half at 120^0C. The tensile machine automatically stopped, due to the high deformation detected causing the experiment to end. Multiple cracks were apparent in all samples. This explains the gradual drop in stress on the stress-strain curves, whereby as crack propagation is hindered by the fibres, another crack propagates at a different point on the sample. The samples did not break into halves as experienced at lower temperatures, due to the fibres remaining unbroken at the end of the test. This may

also suggest that the fibres are still able to carry higher loads, as long as the fibre/matrix adhesion remains intact.

It was observed that the untreated composite had more fibre exposure on its fractured surface at 40^0C than the treated composite. Fibre/matrix debonding was more apparent for BPC-0, while BPC-6 had short fibres protruding out perpendicularly from the fractured surface. The poor fibre/matrix adhesion of the untreated composite allowed the fibres to slip out from the polyester, while a better grip on the fibre for BPC-6 had caused fibres to break instead. At 80^0C, it was evident that both treated and untreated composites had more fibres exposed at a 90^0 angle from the fractured surface. This proves that the softening of the matrix had allowed the fibres to be pulled in the direction of the tensile loading, rearranging themselves for better stress transfer. The higher the numbers of fibres oriented in the direction of applied load, the better the mechanical properties of the composite, as observed in Section 5.6.2. As for the coated sample, the peeled coating near the fractured area was similar to the one observed at room temperature in Figure 5.14. The adhesion strength of the coating was still effective at this temperature, resulting in higher strength of the coated sample, compared to the uncoated sample. An unseparated, softened coating layer was observed at both 80^0C and 120^0C for BPC-6C. Although the protective properties of the coating were no longer applicable, the presence of this layer may have caused higher elastic modulus for the coated samples, by providing some restriction in deformation. By observing the fractured surfaces, the behaviour of the NP and composites at different temperature increases was further understood and explained.

5.7   Morphology of thermally exposed composites

The fractured surface morphologies of the tensile loaded samples at 40^0C, 80^0C and 120^0C exposures were observed through SEM. For NP, the fractured surface is different at all temperature settings. At 40^0C, the morphology is similar to the SEM obtained for the undegraded NP discussed in Chapter Four. Defragmentation was apparent, indicating that the neat resin was fractured in a brittle manner. Polymer melting was observed at 80^0C, as well as some defragmentation. This relates to the transitional phase of the NP, which experienced semi-ductile behaviour. Exposure to heat initiated some melting and softening within the resin, evident in the smoother texture of the fractured surface. A higher degree of polymer melt can be detected at 120^0C, with some erosion on the resin particles. A major difference in texture at this temperature, compared to the other samples, is the presence of unidirectional lines across the surface. This may suggest that the increased mobility of the molecular chains had caused them to be easily rearranged in the direction of applied load. With less molecular entanglement, the mechanical properties of NP decreased dramatically.
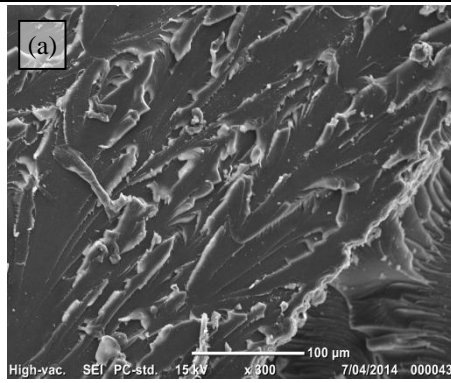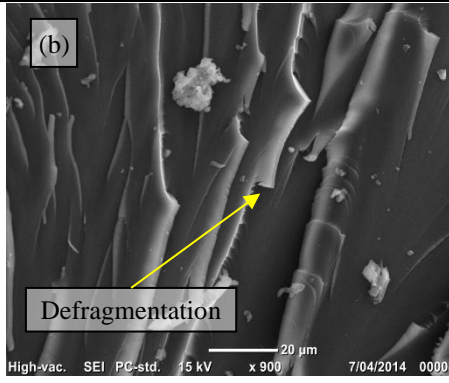
Samples	Temp.	SEM	
NP	40ºC	(a) High-vac. SEI PC-std. 15 kV x 300 100 µm 7/04/2014 000043	(b) Defragmentation High-vac. SEI PC-std. 15 kV x 900 20 µm 7/04/2014 000044
	80ºC	(c) Defragmentation High-vac. SEI PC-std. 15 kV x 80 200 µm 7/04/2014 000070	(d) Polymer melt High-vac. SEI PC-std. 15 kV x 340 50 µm 7/04/2014 000071
	120ºC	(e) Polymer melt / Particle lost High-vac. SEI PC-std. 15 kV x 500 50 µm 7/04/2014 000026	(f) Polymer softening High-vac. SEI PC-std. 15 kV x 900 20 µm 7/04/2014 000027
BPC-0	40ºC	(g) Fibre pullout High-vac. SEI PC-std. 15 kV x 220 100 µm 7/04/2014 000050	(h) Good fibre/matrix interlocking High-vac. SEI PC-std. 15 kV x 1300 20 µm 7/04/2014 000051

	80ºC	(i) Fibre pullout — High-vac. SEI PC-std. 15 kV x 270 100 µm 7/04/2014 000072	(j) Good fibre/matrix interlocking — High-vac. SEI PC-std. 15 kV x 340 50 µm 7/04/2014 000073
	120ºC	(k) Fibre damage — High-vac. SEI PC-std. 15 kV x 440 50 µm 7/04/2014 000037	(l) Fibre pullout / Fibril cracking and splitting — High-vac. SEI PC-std. 15 kV x 500 50 µm 7/04/2014 000038
BPC-6	**40ºC**	(m) Good fibre/matrix interlocking / Fibre bundle breakage — High-vac. SEI PC-std. 15 kV x 850 20 µm 7/04/2014 000048	(n) Resin binding — High-vac. SEI PC-std. 15 kV x 1500 20 µm 7/04/2014 000045
	80ºC	(o) Fibre pullout — High-vac. SEI PC-std. 15 kV x 20 1 mm 7/04/2014 000077	(p) Resin penetration between fibrils — High-vac. SEI PC-std. 15 kV x 550 50 µm 7/04/2014 000079
	120ºC	(q) Eroded fibrils — High-vac. SEI PC-std. 15 kV x 130 200 µm 7/04/2014 000022	(r) Poor fibre/matrix interlocking — High-vac. SEI PC-std. 15 kV x 750 20 µm 7/04/2014 000023

Figure 5.27: Micrographs of fractured surfaces of thermal degraded samples

For the bamboo fibre/polyester composites, untreated, treated and coated samples all experienced a slight increase in tensile strength at 40^0C and 80^0C, which was predicted to be caused by improved fibre/matrix adhesion, as discussed in Section 5.6.2. This theory was proven through the SEM observations, as all composite samples showed no voids at the fibre/matrix interfaces, unlike those experienced at room temperature conditions. The softened polyester resin was seen to encapsulate the bamboo fibres (Figure 5.27 (n) and Figure 5.27 (v)), and further penetrate between individual fibrils (Figure 5.27 (p) and Figure 5.27 (u)), increasing the contact area between the fibres and the matrix. With this, load transfer is more effective, leaving the final strength of the composite to the actual strength of the fibres. As treated fibres have higher tensile strength than untreated fibres, the improvement in strength of treated composites was higher than in untreated composites. Fibre pull-out is evident on all samples at 40^0C and 80^0C, which may indicate that softened resin could not provide a firm grip on the fibres, allowing them to slip during the loading process. However, it can be noted that for the treated fibres, breakages of fibre bundles can be observed on some part of the composites, implying good fibre/matrix interlocking, which caused failure to occur on the fibres instead.

However at 120^0C, poor fibre/matrix adhesion was obvious for all composite samples, with the presence of voids clearly seen at the fibre/matrix interfaces. This may be attributed to resin shrinkage, as heat causes the polyester to lose some of its mass in the form of moisture evaporation and gaseous release. Laoubi et al. (2014) had reported that for heating temperatures lower or equal to 100^0C, there was no apparent damage on the morphology of glass fibre/polyester composites. However, at 200^0C and higher, cracking at the fibre/matrix interface was observed and was accentuated by the increase in temperature. The authors suggest that at temperature higher than 100^0C, the polyester resin starts to release gaseous products that may remain trapped in the composites. This causes pressure build up that leads to increases in temperature and generates fibre/matrix debonding. Fibre damage was also observed at this stage, with individual fibrils showing a high degree of surface erosion (Figure 5.27 (q)) and some fibril splitting (Figure 5.27 (l)), which may weaken the fibres. An observation by Ezekiel et al. (2011) on the SEM of heated coir fibres revealed that coir fibres experienced microcracks and open micropores when heated at 150^0C for 20 minutes. Microfibril collapse was apparent when heated at 200^0C for 30 minutes. Cooled molten liquid was also reported to pour out from these micropores, which may possibly be hemicelluloses or other low molecular weight components. These consequences, coupled with increases in polyester softening that provides poor load transfer, cause the mechanical strength of composites to reduce to half of their initial strength. Since the elastic modulus of the NP and the composites gradually decrease with temperature, the improved fibre/matrix adhesion may not have any effect on the stiffness of the composites. This shows that the softening of the matrix is responsible for the decrease in stiffness and increased in ductility of the composites at high temperatures.

5.8   Chapter summary

The degradation of bamboo fibre/polyester composites subjected to thermal exposure was discussed in this chapter. The thermal decomposition behaviour and thermo-mechanical properties of the composites and constituents were studied to determine the effect of temperature increases on the degradation process. Protective methods, such as the addition of additives and application of barrier coatings were also evaluated, to provide a compatible means for improved durability. The studies have shown that:

1) The thermal decomposition of treated fibres was observed to occur at a lower temperature, compared to untreated fibres, with a decrease of 14% of decomposition temperature for 8% NaOH treated fibres, due to the reduction in thermal stability of the cellulosic component of the fibre. Although alkalisation improves the mechanical strength of bamboo fibres, it must be noted that the thermal stability may be compromised. Treated fibres were observed to have more char than untreated fibres with 8% NaOH treated fibres producing 125% more char than untreated ones.

2) The NP starts to decompose later than the bamboo fibre/polyester composites at 388^0C, and had the least char formation at the end of the TGA run with only 5.18% residue. With bamboo fibre reinforcements in the NP matrix, the effect of alkalisation on the fibres did not have much influence on the decomposition temperature of the composites. Both treated and untreated composites degrade at roughly the same temperature, with approximately 7.7% decrement in thermal stability compared to NP. The char production for

all treated composites was also similar to the untreated composite, with 90% increment in charring compared to NP. This behaviour showed that the NP had a higher influence on the thermal resistance of the composites, due to its higher volume fraction.

3) Due to unavailability of compounding equipment, the use of additives was unsuccessful and did not provide satisfactory protection to the composite. However, the coating showed a slight potential for improved tensile and thermal properties, especially below 80^0C, as it is engineered for extreme outdoor conditions. The coated samples achieved 13% higher strength and 5% higher stiffness than uncoated samples, possibly due to the binding force provided by the coating layer.

4) The DMA showed that the storage modulus and loss modulus of NP were higher than the composites below the T_g, but were lower than the composites at higher temperatures. This indicates that the addition of fibres is more advantageous at higher temperatures, as it restricts the molecular movements of the softened resin. However, all samples in the rubbery region had low mechanical properties, evident on the storage and elastic modulus, which was below 180 MPa and 10 MPa, respectively at the end of the experiment (170^0C). The untreated composites had the lowest modulus values due to poor fibre/matrix adhesion. The damping behaviour showed a 45.8% maximum reduction with the addition of fibres, but alkali treatment did not provide any further improvement.

5) The T_g for polyester resin is 112^0C, which was extracted from the loss modulus curve. With the addition of the fibres, a minor increase in Tg value was observed, with the highest at 120^0C obtained by 6% NaOH treated composite.

6) From the static tensile test at 40^0C, 80^0C and 120^0C, it was observed that NP had higher initial tensile strength than the composites, which reduced drastically starting at 80^0C onwards. The composites exhibited improved strength up to 80^0C, which may be due to reorientation of fibres in the direction of the applied load, as observed on the fractured surfaces. The composites also showed better mechanical performance than the NP at 120^0C. The tensile strength reduction of NP is 29% at 80^0C and 92% at 120^0C, while for the 6% NaOH treated composite, a 23% increment was observed at 80^0C, and a reduction of 38% observed at 120^0C.

7) The elastic modulus for all samples was reduced as temperature increases, due to softening of the matrix. Coated samples exhibited the highest stiffness at all temperature settings, which may be enhanced by the coating layer's restrictions to deformation. The reduction of elastic modulus at 120^0C was 93%, 80%, 81% and 78% for neat polyester, untreated composite, 6% NaOH treated composite and coated composite, respectively.

8) From the SEM observations, softening of NP was evident, and this was advantageous to the improvement of fibre/matrix adhesion. The softened resin further bonded with the fibres at 40^0C and 80^0C for all composite samples, resulting in improved tensile strength. However, at 120^0C, poor fibre/matrix interlocking could be observed in the presence of voids for all samples, as the elevated temperature caused resin shrinkage and mass loss in both fibre and polyester. This, with polyester softening, degraded the composite strength to half their initial values.

Chapter 6 : Moisture Degradation Study on Bamboo Fibre/Polyester Composites

6.1   Introduction

The moisture absorbency of natural fibres has a great effect on the durability of polymer composites. The plant cells responsible for moisture attraction in natural fibres are the hemicelluloses (Methacanon et al. 2010). This makes them hydrophilic and causes incompatibility with the hydrophobic polymer matrix (Araújo et al. 2008; Chen et al. 2009; Dittenber & GangaRao 2012; Shih 2007). The incompatibility leads to poor fibre/matrix adhesion with voids between the fibres and the matrix; this may generate high moisture absorption in the composite. The moisture absorbed into a composite system will cause the hydrophilic fibres to swell. This ultimately leads to delamination of the fibres (Assarar et al. 2011; Joseph et al. 2002). Once this occurs, the stress transfer from the matrix to the fibres will be disrupted, reducing the mechanical strength of the composite material.

The tensile strength and modulus of bamboo/polymer composites were reported to reduce considerably after ageing in water, and worsened with increased soaking time (Thwe & Liao 2002). At elevated temperatures, the rate and total moisture absorbed by natural fibre composites were higher than at room temperatures (Dhakal et al. 2007). Due to these limitations, researchers are studying ways to improve the moisture resistance of natural fibre/polymer composites to improve their durability, and expand their applications.

In this chapter, investigation was carried out to study the moisture absorption behaviour of treated and untreated bamboo fibre/polyester composites at room and elevated temperatures. The effects of water immersion for duration of two months on the composites were examined. Hygrothermal environment was also introduced to the composite which involves both moisture and heat, in this case at a temperature of 80^0C. Comparison was also made with neat polyester to observe the effect of bamboo fibres on the properties of the polyester. The physical changes experienced by the moisture degraded samples were analysed in terms of the gain in weight and thickness swelling until equilibrium moisture content was achieved. The moisture kinetic properties were also evaluated to understand how the moisture interacted with the composites. Another important aspect of the study concerned observing the tensile properties of the moisture degraded composites, with and without thermal influence. The fractured surface and the morphology of the composites were examined to support the findings of the tensile test performed. It is important to analyse the behaviour of natural fibre/polymer composites subjected to moisture attack to find ways to improve durability for outdoor applications.

6.2   Moisture absorption of treated and untreated bamboo fibres

To study the moisture absorption behaviour of bamboo fibres, as well as the effect of NaOH treatment on moisture resistivity, 0%, 4%, 6% and 8% NaOH treated bamboo fibres were immersed in distilled water and rain water for 24 hours. The fibres were also exposed to room humidity for 24 hours. As presented in Figure 6.1, distilled water is more easily absorbed by fibres compared to rainwater, due to the absence of

debris, chemical contaminants and other mineral contents present in rainwater (Huston et al. 2012). When left exposed to room environment, the fibres absorb moisture from the air, indicating they are hydrophilic. In all cases investigated, the results show that higher concentrations of NaOH treatment will cause higher rates of absorption. Bamboo fibres treated at 8% NaOH exhibit 40% absorption of distilled water in 24 hours, which is 14% more than untreated fibres. This is supported by the morphology observations using optical microscopy, wherein more voids are present on bamboo fibres treated with a higher concentration of NaOH compared to fibres treated with a lower NaOH concentration. These voids became present due to the removal of hemicellulose and lignin. This result may indicate that voids play a more influential role in absorbing moisture than hemicellulose, the fibre component responsible for moisture absorption in natural fibres (Beg & Pickering 2008; Methacanon et al. 2010). Although untreated bamboo fibres have more hemicelluose than treated fibres, their ability to absorb moisture is lower than the treated fibres. Methacanon et al. (2010) noted that a higher degree of voids found in fibres of plants living in wet habitats resulted in higher moisture absorption of fibres. These voids or cavities are responsible for the decrease in bulk density, resulting in lighter weight, and absorbing more water.

	0% NaOH	4% NaOH	6% NaOH	8% NaOH
Distilled Water	25.30	24.93	30.31	39.50
Rain Water	21.25	22.89	26.94	37.10
Air Humidity	0.85	0.94	1.04	1.08
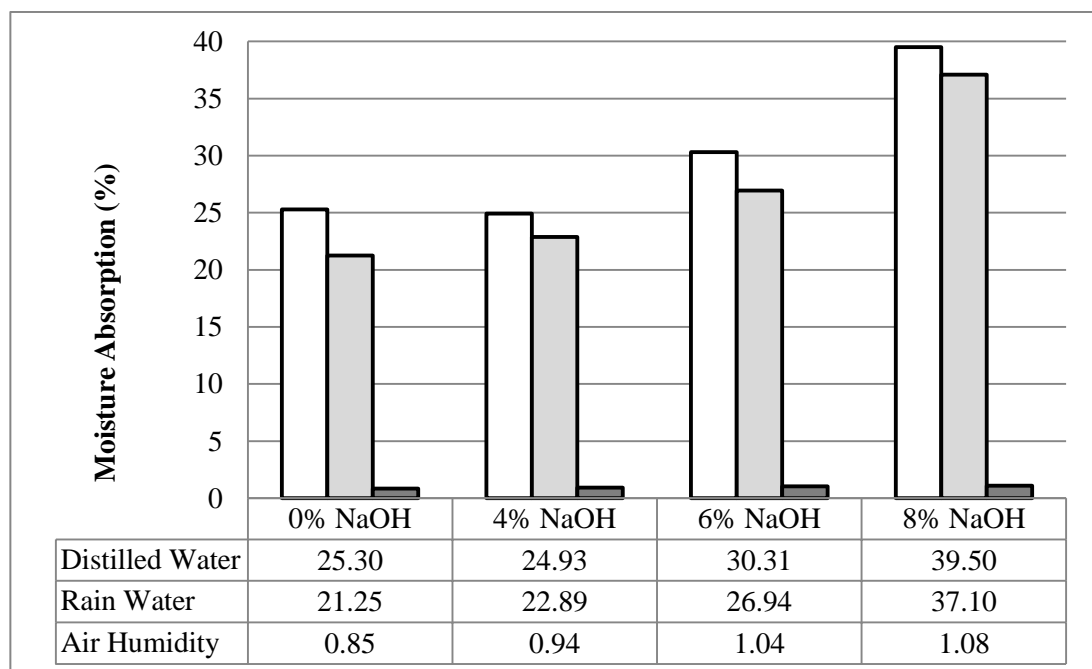
Figure 6.1: Moisture absorption behaviour of bamboo fibres at different concentration of alkali treatment

Similar observations were obtained by Boopathi et al. (2012) on treated and untreated Borassus fruit fibre, whereby increased moisture content was reported for alkali treated fibres. The raw fibres had a 6.83 wt. % of moisture content, which increased to 8.04, 8.17 and 8.13 wt. % with 5, 10 and 15% alkali treatment, respectively. However, some researchers reported contrasting results regarding the effect of treatment on the fibres' moisture absorption capability. Curaua fibres exhibited lower moisture content after treatment with aqueous sodium hypochlorite solution, but the water absorption process is similar for both treated and untreated fibres (Spinacé et al. 2009). The authors highlighted that, although hemicellulose is mainly responsible for the moisture absorption of natural fibres, accessible cellulose,

amorphous cellulose and lignin all contribute to this process as well. The cell wall of the curaua fibres swells with water until saturation; at this point, moisture accommodates void spaces as free water and does not swell the fibre further. This statement is consistent with the results obtained in this study, whereby higher voids in treated fibres cause higher moisture gains, despite the decrease in hemicellulose content. Moisture in natural fibres acts as a barrier for effective interlocking between the polymer matrix and the fibre surface, thus it is deemed necessary to remove moisture prior to composite fabrication. However, total elimination of water (even through oven drying) before incorporation into a polymer composite is not possible due to the hydrophilic nature of natural fibres (Monteiro et al. 2012). Bamboo fibres were reported by Hejazi et al. (2012) to have high moisture absorption, about 40 to 45%.

6.3 Moisture absorption behaviour of bamboo fibre/polyester composite

The amount of moisture absorbed by the composites and the NP was measured by the gain in weight after immersion in water. The behaviour was observed in two temperature settings: one at room temperature (25°C); and another at 80°C, which introduces the influence of heat in the moisture absorptivity of the samples. Hygrothermal condition is presented by the simultaneous exposure of both moisture and heat.

6.3.1 Moisture absorption behaviour at room temperature

The bamboo/polyester composites and NP were fully immersed in water and monitored for 60 days at room temperature. The moisture absorption curves were plotted against the square root of time and are presented in Figure 6.2. Generally, with the addition of bamboo fibres, the moisture absorption of the specimens increased. This can be observed as the NP has a weight gain less than 1% at the end of the immersion period, while all the polyesters with bamboo fibres had at least more than 4% weight gain. As bamboo fibres are hydrophilic (Dittenber & GangaRao 2012), they are expected to absorb more moisture.

BPC-0 demonstrates the highest water absorption among the composite specimens, with an approximately 10% weight gain achieved. As the fibres were treated with NaOH, the hydrophilic components of the fibres, such as hemicelluloses and lignin, were dissolved (Wong et al. 2010). This may contribute to improved moisture resistance of the fibres. The interfacial adhesion between the matrix and bamboo fibres was enhanced by the alkali treatment, as discussed in Section 4.7, reducing the voids and pores within the composite. With the reduction in voids within the specimens, less moisture was accommodated by the composite, which led to less weight gain in the specimen. It can be noted that BPC-6 may have the optimum fibre/matrix interlocking, as the composite have the lowest weight gain, 60% less than BPC-0, making it less prone to moisture attack. BPC-4 has slightly more weight gain than BPC-6, which may indicate that the concentration of NaOH at 4% was less efficient at removing the hemicellulose and lignin content, resulting in more moisture absorption. Due to this, the interfacial adhesion between 4% NaOH treated fibres with the polyester may also be less effective than fibres treated at 6% NaOH; thus, higher void contents may be present. At higher NaOH concentration, which in this

case is at 8% NaOH, a reduction in moisture resistivity was observed. As observed in the SEMs provided in Chapter Four, 8% NaOH causes damage to the fibres, whereby the cellulose fibrils of the fibres were degraded. The alkali attack on the fibrils may have increased the void contents within the fibrils itself, making it vulnerable to moisture absorption.
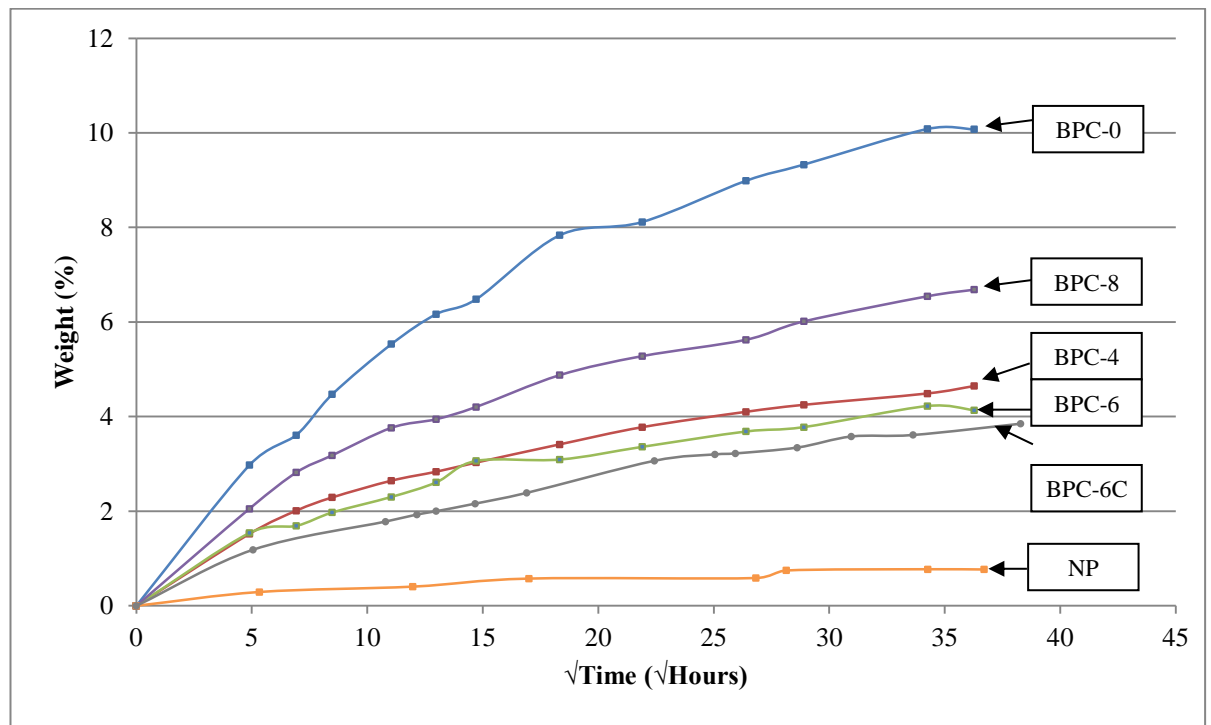
Figure 6.2: Moisture absorption behaviour at room temperature

With the presence of coating, a slight reduction on moisture absorption was observed in the 6% NaOH treated samples, with about 0.3% difference of total weight gain between the coated and uncoated samples at the end of the experiment. This result was quite consistent throughout the duration of the study, which indicates that the acrylic coating provides some improvement on the composite's moisture durability. The additional outer layer may have slowed down the movement of water from penetrating the surface of the samples.

In comparison with other natural fibre/polymer composites, a few studies reported similar moisture uptake behaviour. Hemp fibre/polyester composites experienced microcracks on the resin due to swelling of fibres after immersion in water, which activated capillary action and water transport within the composites, as observed by Dhakal et al. (2007). The rate of weight gain and equilibrium moisture content increased as the fibre volume fraction of the composites increased. It was highlighted that the water acts by damaging the fibre/matrix interface, leading to higher moisture absorption. With the addition of the coupling agent MAPP on recycled thermoplastics reinforced with Pinus radiata sawdust, the water absorption was significantly reduced due to the improved compatibility between the polymer and the wood particles, with the polymer covering more wood surface. The reduction in free hydroxyl groups in the wood cellulose, as well as improved crystallinity, were also highlighted by the authors to be possible contributors (Adhikary et al. 2008). Through alkalisation and bleach treatment of coir fibre/polyester composites, an

approximately 3% and 2% difference in water absorption, respectively was obtained, compared to the untreated composites as studied by Rout et al. (2001). This was also attributed to the masking of fibres with polyester resin in the composites, with a stronger adhesion resulting in greater hydrophobicity and lesser water absorption. Thus, the results obtained from this study concur with other natural fibre/polymer composites, highlighting the hydrophilicity of these types of composites, and how surface modification or treatment reduces this behaviour through improved fibre/matrix interface.

6.3.2   Moisture absorption behaviour at 80$^{\mathbf{o}}$C

With the introduction of heat at 80^{0}C, a different behaviour was observed in all specimens. From Figure 6.3, it can be seen that the NP initially experienced a slight loss in weight which may be due to the release of gaseous products like carbon monoxide and carbon dioxide (Wang et al. 2011). However, after more than 4 hours, NP starts to gain weight but reaches equilibrium at moisture content less than 1%. By the end of the study at 48 hours, the composite samples were physically degraded, showing signs of shrinkage and with some fibres exposure. The colour was also observed to have lightened, indicating that the heat altered the fibre pigments. This effect was not observed on samples degraded at room temperature, as shown in Figure 6.4. Beg & Pickering (2008) reported similar transformation on hygrothermally degraded wood polymer composites, whereby colour fading was observed on the surface texture. The NP was also found to experience change in colour, from pinkish to yellowish after immersion in water at 80^{0}C, which was not observed at room temperature immersion. Figure 6.5 demonstrates the difference in colour of NP after moisture degradation at both conditions. This effect may have some influence on the discolouration of the composites. For the coated samples, the coating material was still found to encapsulate the samples, but with poor surface bonding. Air bubbles were obviously trapped under the coating layer. The physical appearances of the hygrothermally degraded composites are presented in Figure 6.6.
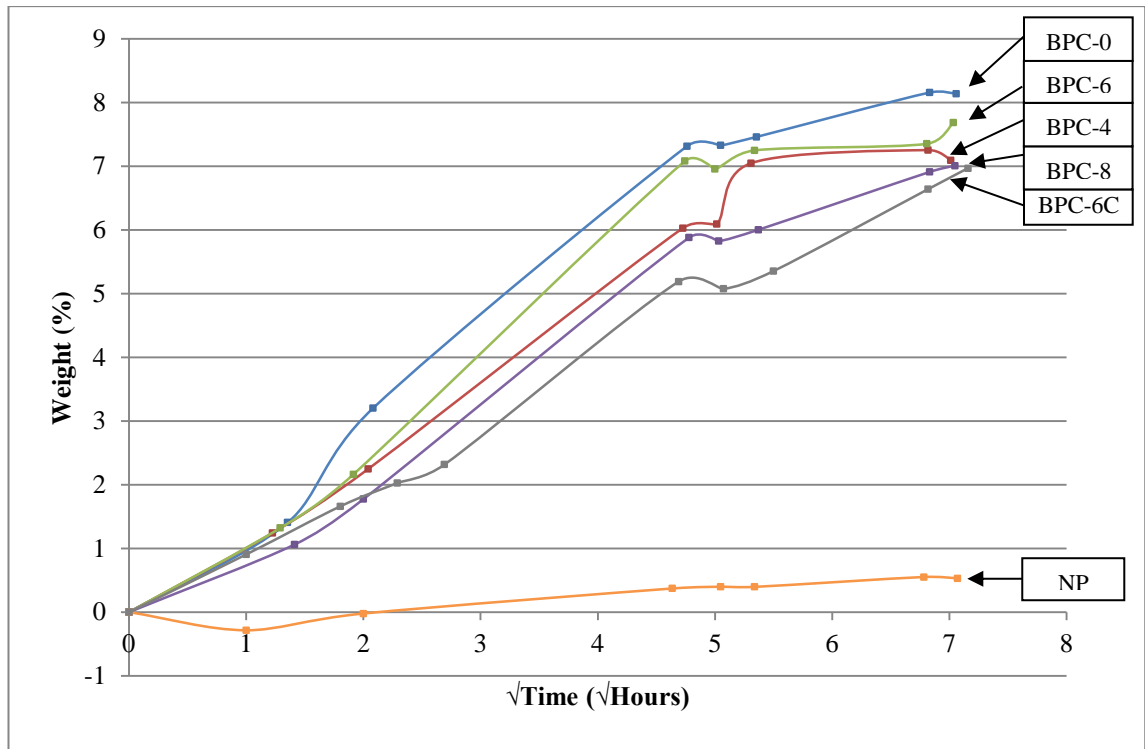
Figure 6.3: Moisture absorption behaviour at 80°C

The rate of moisture absorption of all composites was observed to be higher than at room temperature, whereby at only 2 days, an average of 7.5% weight gain was observed. This is higher than the weight gain of treated composites after 60 days at room temperature. This shows that with the presence of heat, water has more energy to be transported within the composites. Further, with the apparent degradation of the samples, micro voids may be present within the samples, accommodating higher moisture content. These voids are more likely developed by the loss of materials, either from the resin or the fibres, causeing the water transport mechanisms to become more active (Dhakal et al. 2007). Bamboo fibre swells as it absorbs moisture and shrinks once it is dried. This process may cause internal micro cracks, which can lead to fibre/matrix debonding.

Fibre treatment did not play a significant role in improving the moisture resistance of the composites, although it was observed that overall, BPC-0 experienced a slightly higher weight gain than the other composites. All BPC samples achieved approximately the same moisture content at the end of the immersion, with 8.14%, 7.09%, 7.69%, and 7.01% weight gain for BPC-0, BPC-4, BPC-6 and BPC-8, respectively. Therefore, this may indicate that the effect of the improved fibre/matrix adhesion was less significant as compared to the consequences of the heat exposure. Even with the presence of coating, the moisture resistance of the samples could not be said to have improved. While initially BPC-6C did show a relatively lower moisture uptake, a 6.97% weight gain was recorded at the end of the experiment, indicating that the coating may have been damaged and did not provide much assistance in resisting the moisture attack.
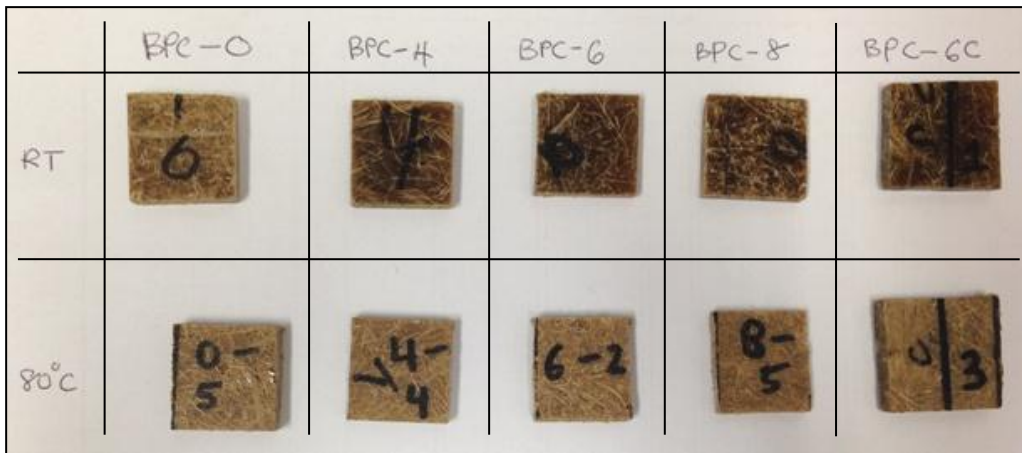
Figure 6.4: Composite samples after moisture degradation

| Neat polyester after immersion at room temperature | Neat polyester after immersion at 80^{0}C |
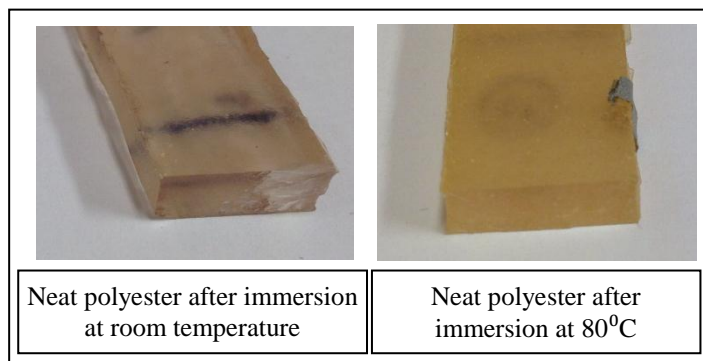
Figure 6.5: Neat polyester discolouration after water immersion
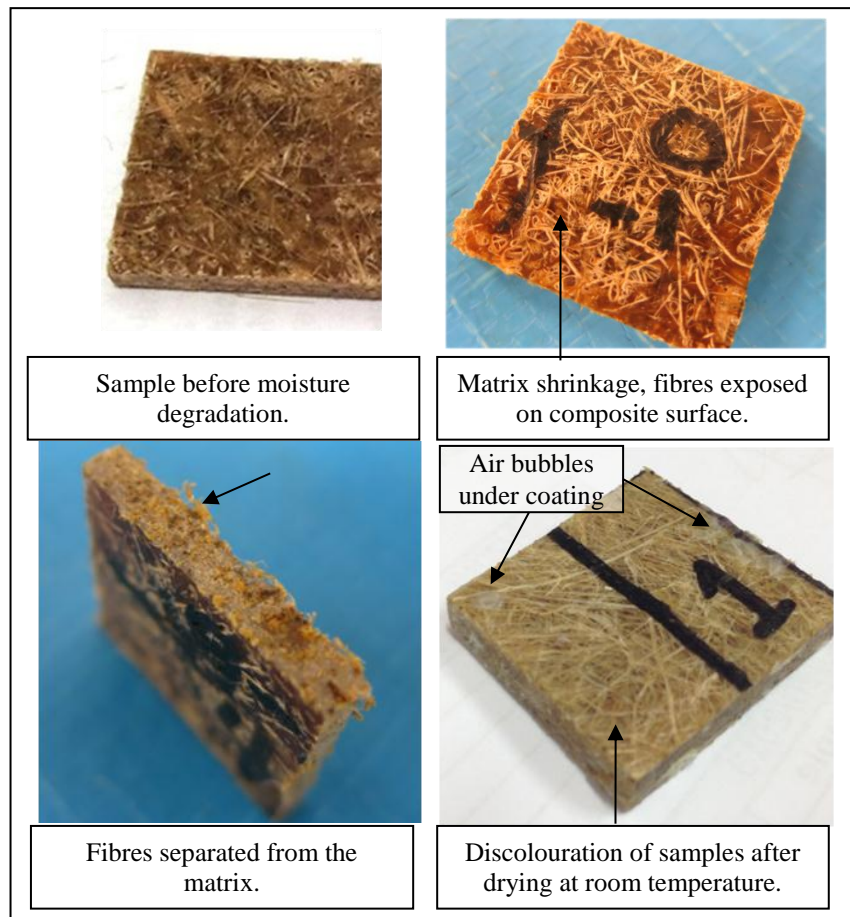
Figure 6.6: Physical deterioration of bamboo/polyester
composites immersed in water at 80°C

From the study conducted by Dhakal et al. (2007), hemp fibre/polyester composites at boiling condition was observed to reach moisture saturation time (MST) faster than at room temperature. This was attributed to the different diffusivity of water into the composites, which accelerated interfacial cracks. It was interesting to note that the authors obtained a clear indication of moisture equilibrium at durations longer than 25 hours. In this study, although it was not as clear, a drop in the rate of weight gain was also observed after 25 hours, which shows that water uptake becomes less rapid. In contrast, some studies reported that at elevated temperatures, moisture equilibrium was not achieved. A much extended immersion was performed by Thwe and Liao (2003) on bamboo fibre/polypropylene composites at 75°C for 3 months. They found that the sorption rate at initial stages was significantly higher compared to those aged at room temperature. However, a saturated moisture level was not achieved at the end of that period, although rate of sorption was reduced, starting from 400 hours. The authors attributed this to the continuous internal degradation with soaking time, which displayed pseudo-Fickian behaviour. It was also interesting to note that the effect of MAPP was observed to reduce the weight gain above 100 hours; prior to this, the sorption was comparable to samples without MAPP. In relation to this study, it may be possible that alkali treatment on fibres could influence the moisture resistance of the composites at longer soaking durations. The continued slower moisture uptake after the initial higher rate of weight gain implies a two-stage diffusion model (Bao et al. 2001). A similar coating study was conducted

by Hu et al. (2010) on jute fibre/PLA composites coated with polypropylene plastic adhesive tape. The test condition was less critical compared to this study, as the specimens were exposed to saturated water vapour at 70°C, instead of water immersion. It was found that the coated sample had lower rates of sorption than that of the uncoated sample. Through the microstructure evolution process, the coating material was found to effectively serve as an isolating barrier of moisture diffusion, although permeability of the film inevitably existed. In time, water molecules penetrated the film and were absorbed through the composites, causing debonding, microcracks and delamination. This is relatable to the acrylic coating used in this study, whereby a longer soaking duration decreased the effectiveness of the barrier system.

6.4 Moisture absorption kinetics of bamboo fibre/polyester composite

The slopes of the first part of the weight gain versus square root of time curves (Figure 6.2 and Figure 6.3) were evaluated for the diffusion properties of the specimens as described by Fick's laws (Carter & Kibler 1978). The diffusion coefficient, D, shows the ability of water molecules to penetrate through the composite specimens and under conditions of non-steady state diffusion, was described using the following formula:

$$D = \pi \left(\frac{kh}{4M_m} \right)^2 \qquad \text{Equation 6-1}$$

Where k is the initial slope of the moisture content curve vs. $t^{1/2}$, M_m is the maximum weight gain and h is the thickness of the composites. Another factor to describe the kinetics of water absorption behaviour is the thermodynamic solubility or absorption coefficient, S, which describes the amount of water absorbed per unit mass of the composite at equilibrium (Adhikary et al. 2008) and is defined as:

$$S = W_m / W_p \qquad \text{Equation 6-2}$$

Where W_m is the total weight of solvent at equilibrium swelling and W_p is the mass of sample. The product of the diffusion coefficient and solubility gives the permeability coefficient, P, which reflects the net effect of absorption and diffusion (Adhikary et al. 2008) and can be computed by the relation:

$$P = D \times S \qquad \text{Equation 6-3}$$

From Equations 6-1, 6-2 and 6-3, the diffusion coefficient, D, the composite thermodynamic solubility, S, and the permeability, P, were calculated and are presented in Table 6.1. The diffusion coefficient at room temperature is lowest for BPC-6, which may indicate that the water molecules may not easily penetrate the composites due to the enhanced interfacial adhesion between the fibres and the matrix, as well as the reduction in void content compared to the untreated composite. However, it was calculated that BPC-4 had a slightly higher D value than BPC-0, but is within the experimental error and thus may not be significant. The D values obtained from this work are comparable to other natural fibre/polymer composites achieved by other researchers. Zabihzadeh et al. (2011) reported diffusion coefficient values of 1.37 to 7.86×10^{-6} mm^2/s for rapeseed stem/polypropylene composites, while Adhikary et al. (2008) published diffusion coefficients of 2.76×10^{-6} to 9.45×10^{-6} mm^2/s for recycled thermoplastics reinforced with Pinus radiata sawdust.

The amount of water absorbed per unit mass, S, is lowest for NP, which reflects that the absorption of water in the composites mainly depends on the bamboo fibres. BPC-0 and BPC-8 have higher solubility compared to BPC-4 and BPC-6. The permeability coefficient, P, correlates well with the moisture absorption curves, with BPC-0 having the highest value, followed by BPC-8, BPC-4 and BPC-6. In general, BPC-6 seems to perform best at room temperature, while BPC-0 has the lowest moisture resistance. With the application of coating, the moisture kinetics properties of BPC-6 showed improvement in all three cases. This suggests that the coating material provided some moisture barrier on the composite sample.

At 80°C, the diffusion coefficient and permeability coefficient values increased for all composite samples. As the temperature is increased, the composites are more easily penetrable by the moisture molecules. This may be attributed to the increase in voids in the composite system, as well as fibre damage caused by the heat. Additionally, the deterioration of the fibre/matrix interface, as discussed previously, may also contribute to this behaviour. All these factors provide extra pathways for moisture transportation and more space for water to be accommodated inside the composites. However, there was no notable trend for the composites' thermodynamic solubility at increased temperature. Comparable S values were reported by George et al. (1998) on pineapple-leaf fibre/polyethylene composites, but with a clearer increase in sorption at higher temperatures, especially for NaOH treated fibres rather than untreated fibres. Overall, this study on bamboo fibre composites shows that fibre treatment through alkalisation helps to reduce the diffusion, solubility and permeability coefficients of the composites both at room temperature and at 80°C.

Table 6.1: Hygroscopic properties of bamboo/polyester composites

Sample	Max. Water Absorption (%)		D (mm^2/s)				S (g/g)		P (mm^2/s)			
	RT	80°C	RT		80°C		RT	80°C	RT		80°C	
NP	0.77	0.44	a	a	a	a	0.0077	0.0023	a	a	a	A
BPC-0	10.08	8.16	5.25	10^{-6}	6.04	10^{-5}	0.1013	0.0814	5.32	10^{-7}	4.92	10^{-6}
BPC-4	4.49	7.09	5.47	10^{-6}	5.59	10^{-5}	0.0634	0.0690	3.47	10^{-7}	3.86	10^{-6}
BPC-6	4.22	7.69	3.58	10^{-6}	4.81	10^{-5}	0.0634	0.0744	2.27	10^{-7}	3.58	10^{-6}
BPC-8	6.55	7.01	3.68	10^{-6}	3.24	10^{-5}	0.1085	0.0696	3.99	10^{-7}	2.25	10^{-6}
BPC-6C	3.85	6.97	2.98	10^{-6}	3.40	10^{-5}	0.0385	0.0696	1.15	10^{-7}	2.36	10^{-6}

[a] **Unable to calculate because slope of moisture absorption curves could not be determined precisely.**

The diffusion of moisture within a polymer composite is significantly affected by the fibre type and content as, discussed by Akil et al. (2014). Jute composites were found to have higher diffusion coefficients compared to hybrid jute/glass composites. That study utilised a high fibre/matrix ratio (70:30) and resulted in a much higher D value than the one obtained in this study and by other researchers.Wang et al. (2006) had also produced very similar results, as the fibre volume is increased from 40 to 65%. This suggests that the water molecule can easily penetrate a natural fibre composite with escalated effect at higher volume fraction. It was highlighted by Akil et al. (2014) that the diffusion coefficient is dependent on the materials, manufacturing methods and test conditions; thus, a direct comparison with other studies can be complicated. Moisture diffusion in a polymer resin is an energy-activated process and temperature plays a strong role in the diffusion coefficient (Mallick 2008), as

observed in this study. Other researchers have also reported higher diffusion coefficients at higher temperatures. Pineapple-leaf fibre/polyethylene composite (George et al. 1998) and hemp fibre/polyester composite (Dhakal et al. 2007) both experienced increases in the diffusion coefficient as the temperature increased. A dramatic increase for hemp composites was apparent as the moisture was heated to its boiling point. The moisture uptake behaviour deviated from Fickian law, which was attributed to the development of microcracks within the samples, as well as material lost, most likely in the form of resin particles. Treatment through NaOH on the pineapple-leaf fibres showed lower diffusion at 28, 50 and 70°C, compared to untreated fibres. This agrees with the current study, which indicates that improved fibre/matrix interface through alkalisation helps to slow down water penetration through the composites.

6.5 Physical effects of moisture absorption

The physical changes experienced by bamboo fibre/polyester composites due to moisture absorption are discussed in this section. This includes the thickness swelling and volume expansion of the samples immersed in water at room temperature and at 80°C.

6.5.1 Thickness swelling behaviour

The thickness swelling (TS) is an important property of a composite that represents the dimensional stability performance and is especially critical in outdoor applications. The TS of samples immersed in water is experimentally determined by the gain in thickness measured after some duration of soaking. The data were plotted in Figure 6.7 and Figure 6.8 for room temperature and 80°C, respectively. The behaviour follows a similar trend to the water absorption curves, increasing with immersion time until an equilibrium condition is reached. At room temperature, it is interesting to see that the untreated composites experienced similar swelling behaviour with BPC-6, better than both BPC-4 and BPC-8. This does not correspond to the water absorption behaviour discussed earlier, where untreated composites suffered highest weight gain among all composite samples. The final percentage of thickness gain for BPC-4 and BPC-8 is comparable, but the initial rate of swelling for BPC-8 is higher as it reached equilibrium relatively faster than the other samples. However, the differences in the final thickness gain of these uncoated composite samples are quite close in percentage, the maximum difference being approximately 1%. Higher swelling by BPC-8 among the treated samples correlates with the high absorption of moisture it experienced. Since higher fibrillation for 8% NaOH treated fibres is expected, water accommodating within these pores may cause BPC-8 to expand faster. The nature of untreated composites containing hemicellulose, lignin, and wax influences moisture absorptivity but apparently, water residing within these components caused lower swelling. The coating provided an obvious restraint to swelling, as observed on the initial curve of BPC-6C. While the rest of the samples achieved thickness equilibrium by 450 hours, the coated sample still experienced swelling although at a slow rate, with 40% less final thickness than BPC-6. The encapsulation of the acrylic coating on the sample may restrict the changes in its dimension, but in time, it can be seen that the coating became less effective. As with moisture gain, NP endured the lowest swelling, with less than 1% thickness

equilibrium reached by 300 hours. This reflects the major influence of the fibres on swelling behaviour of the composite, rather than the polyester matrix.
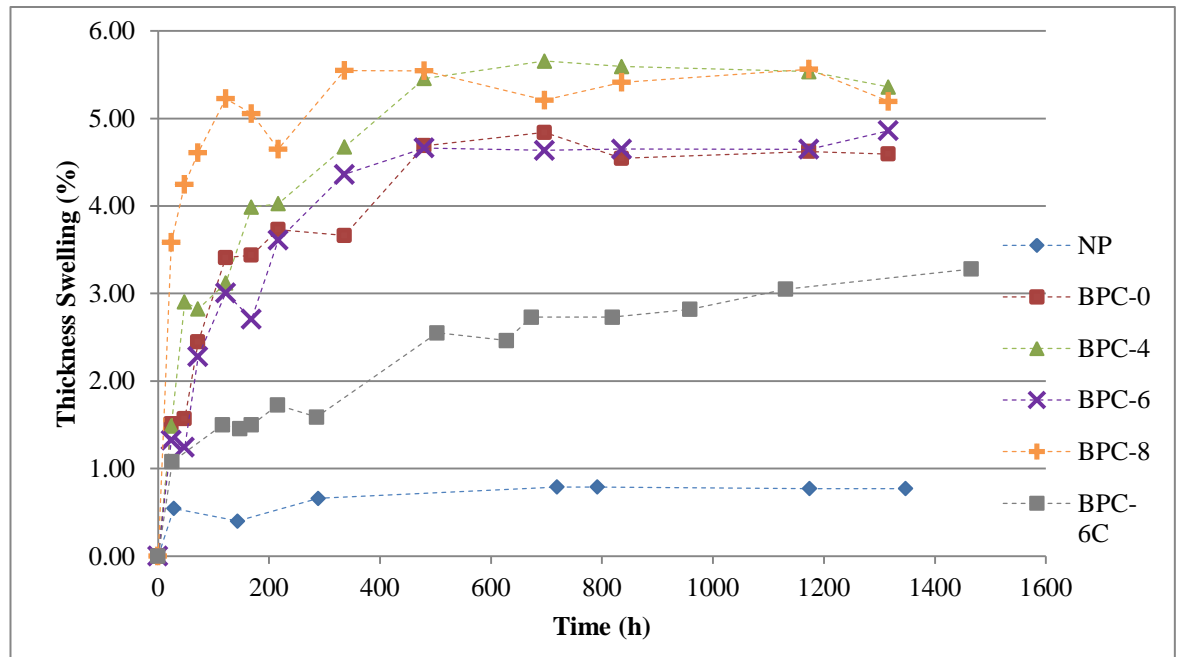
Figure 6.7: Experimental thickness swelling due to moisture absorption at room temperature

At 80°C, possible maximum swelling was reached for all composite samples at about 30 hours of immersion. The percentages of thickness gain were comparable to the ones obtained at room temperature, which may suggest that the dimension of the samples reached maximum expansion at approximately 5.5%. However, BPC-8 experienced a more definite gain in thickness at 80°C than at room temperature, as its swelling reached 7.5%. For the coated sample, the restraint provided at room temperature was less obvious, as it behaved similar to the uncoated samples. It even showed a rise in swelling towards the end of the study, which may be due to the damage in coating material caused by the heat exposure. For the NP, the behaviour was similar to room temperature immersion, with a slightly lower maximum swelling.
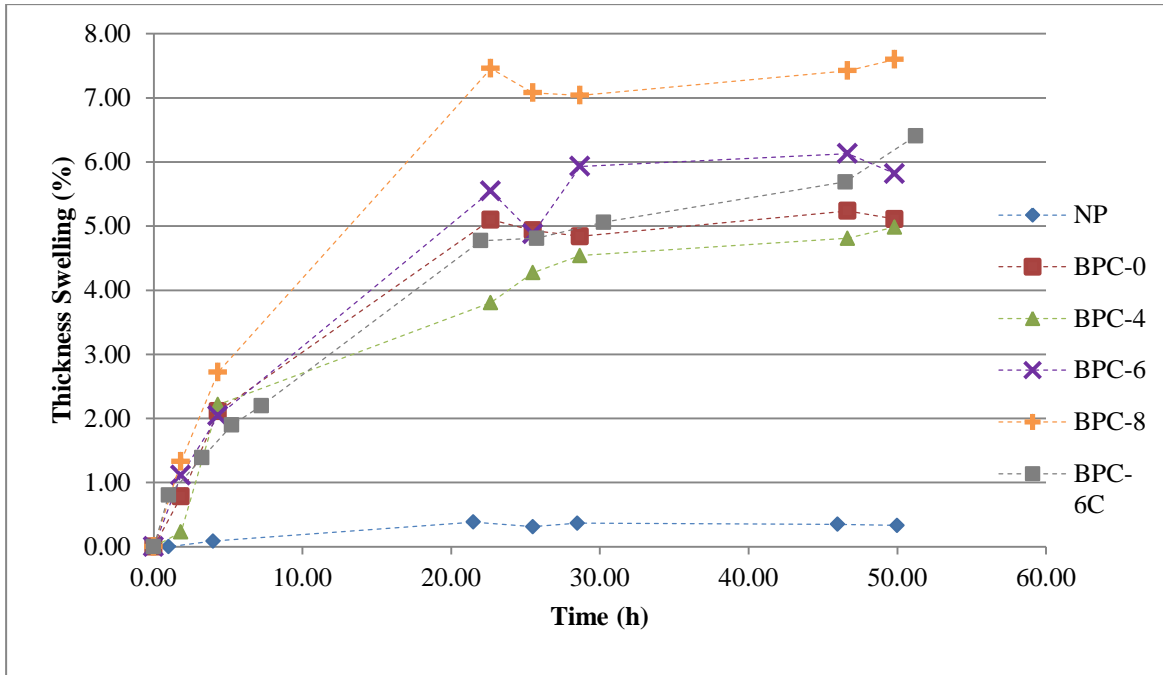
Figure 6.8: Experimental thickness swelling due to moisture absorption at 80°C

A drawback caused by TS is the reduction in the fibre/matrix adhesion of a polymer composite, leading to deterioration of its mechanical properties (Zabihzadeh et al. 2011). Apart from periodically measuring the thickness gain of moisture exposed samples, the swelling behaviour can also be predicted theoretically through a model proposed by Shi and Gardner (2006); this is represented by the following equation:

$$TS(t) = \left[\frac{h_{max}}{h_o + (h_{max} - h_o)e^{-K_{SR}t}} - 1 \right] x100 \qquad \text{Equation 6-4}$$

Where TS(t), h_o, and h_{max} are the thickness swelling, initial, and equilibrium composite thickness, respectively. K_{SR} is the intrinsic relative swelling rate parameter, which depends on how fast the composites swell and reach the ultimate TS at equilibrium. By using non-linear regression curve fitting (Brown 2001), the theoretical curves were plotted based on the experimental data and Equation 6-4, and through this method, the values of K_{SR} were obtained. These curves were compared to the experimental plots and are presented in Figure 6.9 and Figure 6.10. The theoretical curves are presented with the abbreviation Th. It was found that the experimental data fitted fairly well with the swelling model for both conditions at room temperature, and at 80°C for all uncoated bamboo fibre/polyester composites. The predicted initial swelling rate for NP at room temperature was slightly lower than the experimental result, but at 80°C, an almost perfect fit was observed. With the presence of the coating layer, the experimental swelling behaviour deviated from the model at both temperatures due to the external protection provided by the coating, which reacts separately from the composite. The initial swelling rate at room temperature was also lower than the actual data, as observed on NP. In both conditions, the expected equilibrium was not achieved as the coating layer continued to deteriorate, allowing further swelling on BPC-6C.

138
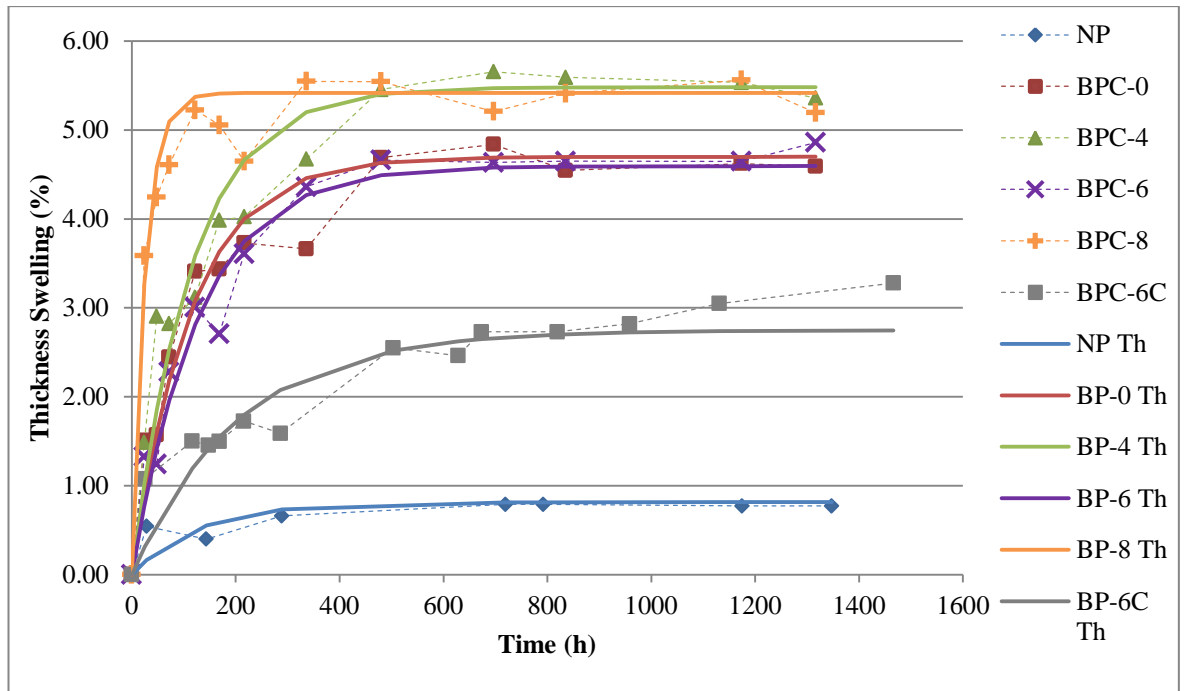
Figure 6.9: Theoretical thickness swelling due to moisture absorption at room temperature
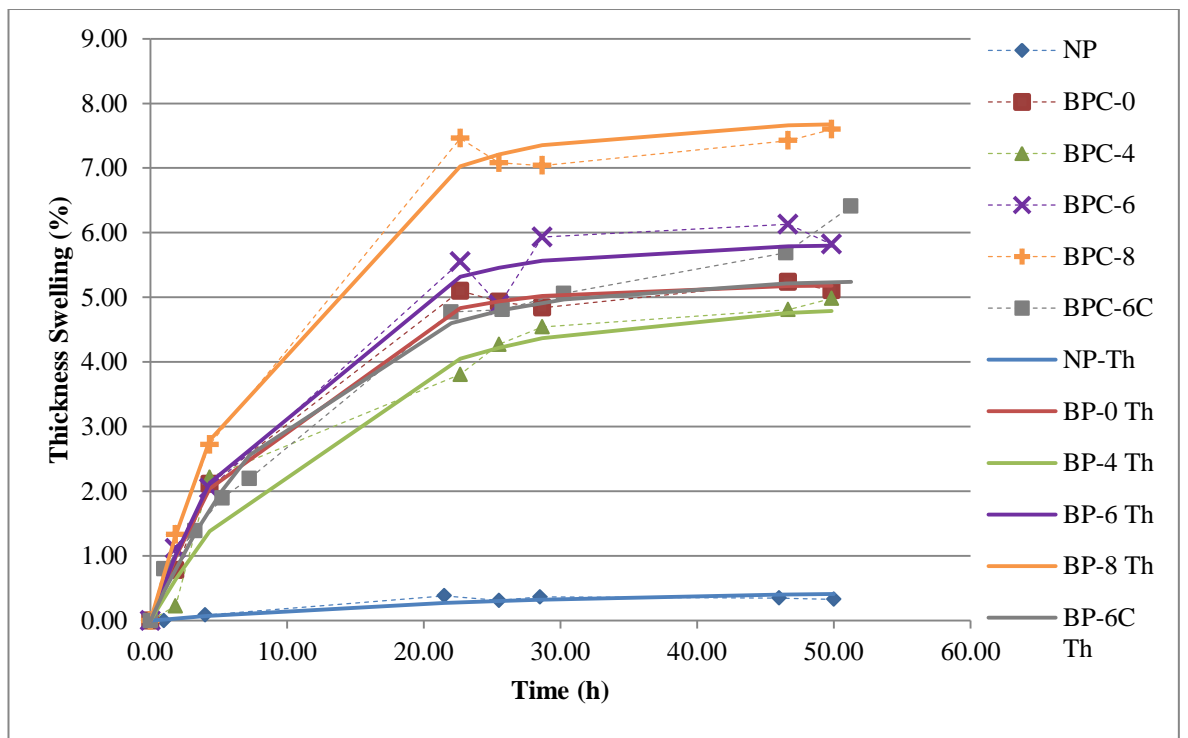
Figure 6.10: Theoretical thickness swelling due to moisture absorption at 80⁰C

From the non-linear regression curve fitting, the swelling rate parameter (K_{SR}) values were obtained and are presented in Table 6.2. The accuracy of the graph fitting can also be evaluated through the R^2 values. As mentioned earlier, the least precision was for the coated samples, and this is reflected by the lower R^2 values at both temperatures. The most satisfactory fit was for BPC-0 at 80⁰C with R^2=1.

139

Table 6.2: Measured TS and predicted K_{SR} for bamboo fibre/polyester composites

Sample	Max. TS (%)		K_{SR} (h^{-1})		R^2	
	RT	80°C	RT	80°C	RT	80°C
BPC-0	4.62	5.24	0.0090	0.1200	0.95	1.00
BPC-4	5.54	4.98	0.0090	0.0800	0.94	0.97
BPC-6	4.65	6.59	0.0080	0.1100	0.97	0.98
BPC-8	5.56	7.60	0.0400	0.1100	0.95	0.99
BPC-6C	3.28	6.41	0.0050	0.0950	0.88	0.93

The swelling rate parameter, K_{SR}, represents the rate at which a composite reaches equilibrium TS after being sufficiently immersed in water. A higher K_{SR} value signifies a higher rate of swelling with a shorter time to reach equilibrium TS. K_{SR} is dependent on both the initial rate of swelling and the equilibrium TS of the composites (Shi & Gardner 2006). From Table 6.2, it can be observed that the K_{SR} value for all the composites at 80°C was higher than at room temperature. This implies that at higher temperatures, the swelling process is expedited, similar to the behaviour of moisture gain. Therefore, a higher rate of absorption will correspond to a faster rate of swelling. BPC-8 can be seen to experience highest swelling rate at room temperature, with a K_{SR} value much higher than the rest of the samples, while BPC-6C has the lowest swelling rate. The rate for BPC-0, BPC-4 and BPC-6 is nearly equivalent. Interestingly, the rate of swelling at 80°C is comparable for all composites, as the values are relatively closer to one another. The effect of alkalisation and improved fibre/matrix interface, as well as the presence of a coating layer, may not be influential in changes of thickness for moisture degraded composites at elevated temperatures.

The TS behaviour of natural fibre composites have been studied and discussed by some researchers, although the literature on this topic is less available compared to the study on moisture absorption behaviour. A recent study by Zabihzadeh et al. (2011) on rapeseed stem/polypropylene composites showed that an increase in the filler content caused higher TS. This was attributed to the swelling of fibres caused by moisture build up within its cell walls, particularly in the direction of the fibre thickness. The magnitude of K_{SR} was from 1.25×10^{-3} to 13.43×10^{-3} h^{-1} for 30% to 60% of filler volume fraction. Thus, the dimensional instability of natural fibre composites depends greatly on the fibre contents, rather than the polymer, which was apparent in the TS graphs of this study. Adhikary et al. (2008) reported a decrease in the equilibrium TS of MAPP coupled Pinus radiata sawdust composites. This was also reflected in the reduction in K_{SR} values of coupled composites, which were attributed to improved compatibility between polymer and wood flour through esterification. However, the improved bamboo fibre-polyester compatibility through alkalisation in this study did not seem to produce the same outcome. Hygrothermal effect on TS of WF/polymer composites studied by Shi and Gardner (2006) was

reported to have a similar response to the bamboo fibre/polyester composites. The time to reach equilibrium TS was shortened as the temperature rose from 40°C to 80°C. However, the maximum thickness reached was the same at all temperatures, approximately 27%. The authors highlighted that the TS process is more complicated at higher temperatures, as it is not only influenced by the hygroscopic aspect of the materials, but also its thermo expansion properties. Thus, this may explain why the K_{SR} values at 80°C were comparable to one another, without regard to the fibre and coating condition. Without moisture influence, the thickness loss of NP, untreated composites, treated composites, and coated composites was measured after one hour exposure at 80°C. This is presented in Figure 6.11. While only NP was observed to have a relatively significant thickness loss, all composites experienced minor swelling less than 0.5%. From this, we can say that the polyester matrix may have more influence on the dimensional change experienced by composites immersed in water at 80°C, compared to at room temperature.
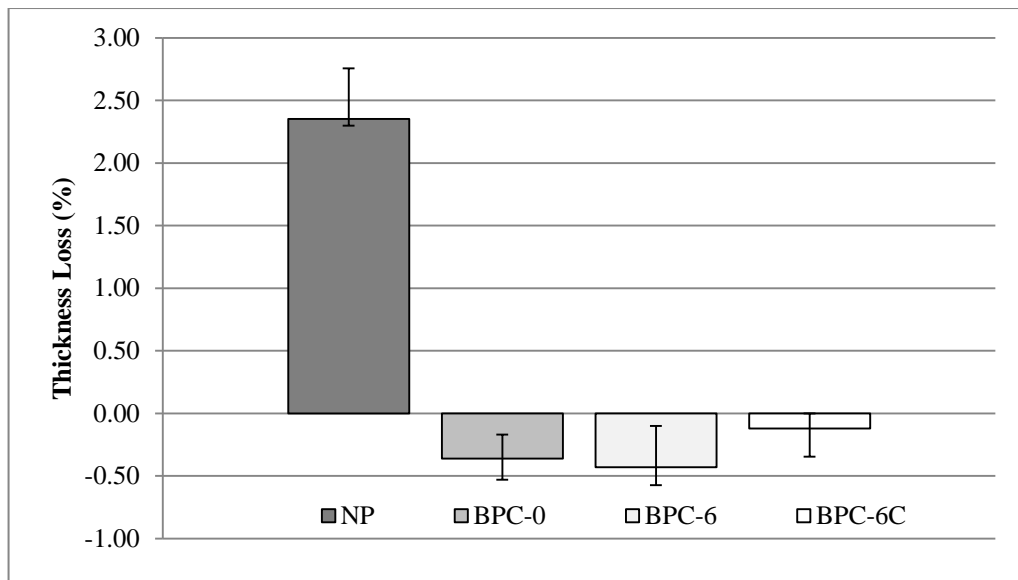
Figure 6.11: Thermo expansion of bamboo fibre/polyester composites at 80°C

The relationship between water absorption and TS has been established, as presented in Figure 6.12 and Figure 6.13. Very good correlations were observed on most of the samples, as presented by the R^2 values. The least conformity was observed on BPC-8 at room temperature, with R^2=0.72. As mentioned before, the swelling rate of BPC-8 is much higher than the other samples, but it did not experience the highest moisture absorption. This inconsistency may have been reflected here. Possibly, the damaged eight per cent NOH treated fibres allowed water to accumulate within its fibrils, pushing the fibrils apart and expanding the dimension of the composite. The linear correlation between water absorption and TS for each composite sample can be expressed by an empirical equation, as given in Table 6.3.

Table 6.3: The relationship between thickness swelling and moisture absorption of bamboo fibre/polyester composites

Samples	Room Temperature		80°C	
	R^2	Empirical equation	R^2	Empirical equation

BPC-0	0.94	$TS=0.48W_a+0.23$	0.99	$TS=0.66W_a-0.03$
BPC-4	0.96	$TS=1.30W_a-0.01$	0.96	$TS=0.68W_a-0.02$
BPC-6	0.94	$TS=1.29W_a-0.29$	0.98	$TS=0.76W_a+0.14$
BPC-8	0.72	$TS=0.67W_a+1.79$	0.98	$TS=1.10W_a+0.34$
BPC-6C	0.98	$TS=0.83W_a-0.06$	0.99	$TS=0.91W_a+0.02$

TS = Thickness swelling, W_a = Water absorption
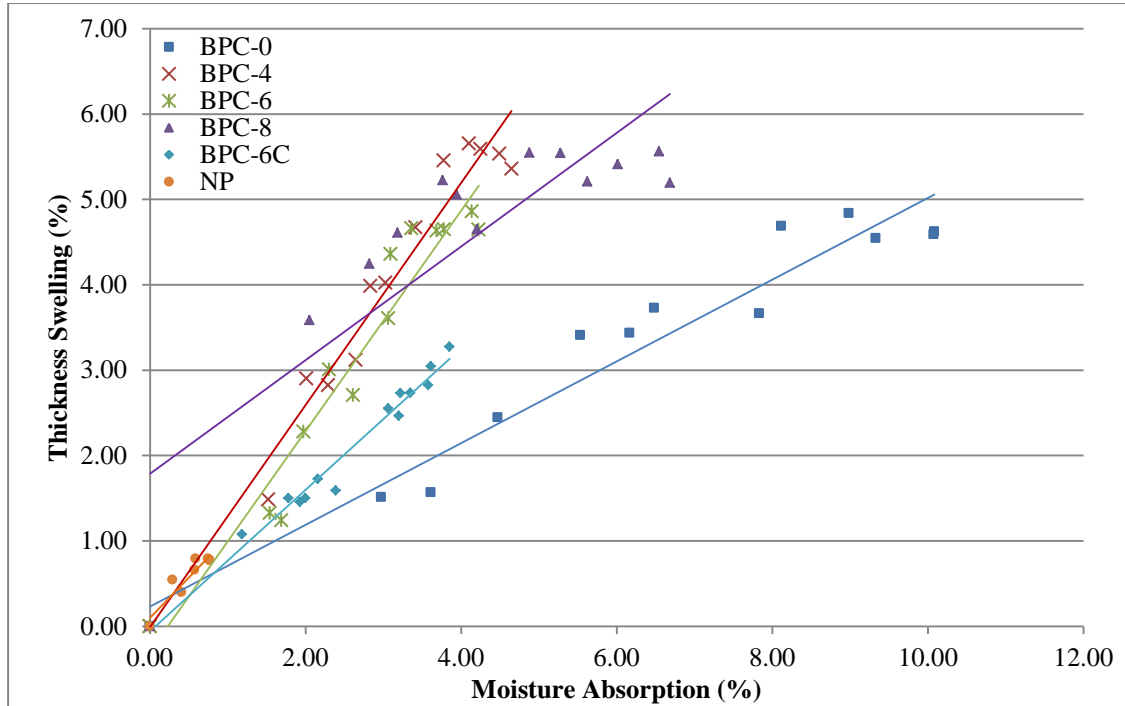
Figure 6.12: Moisture absorption vs. thickness swelling at room temperature
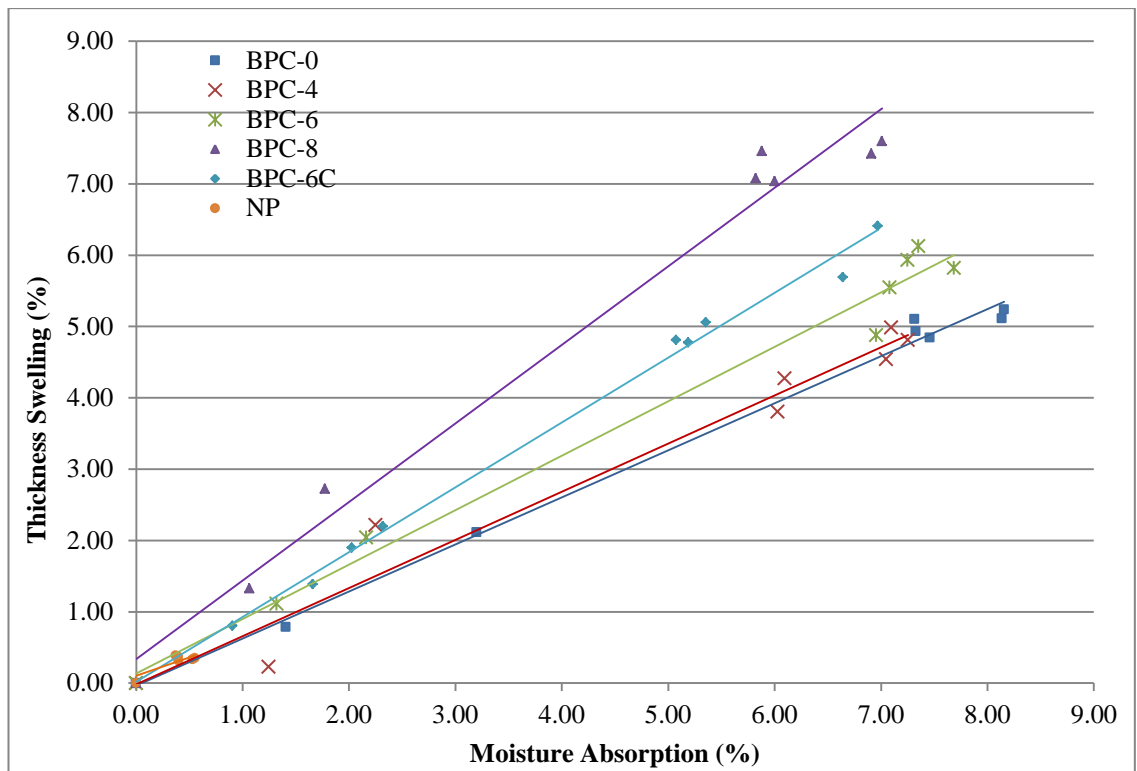
Figure 6.13: Moisture absorption vs. thickness swelling at 80^{0}C

6.5.2 Volume expansion behaviour

The surface area expansions for BPC-0, BPC-4, BPC-6 and BPC-8 were also recorded and are presented in Figure 6.14 and Figure 6.15. Since the swelling in this direction was relatively smaller than the thickness, the exact increase in length of the samples was difficult to measure accurately with a standard vernier calliper; thus, a large experimental scatter can be observed at the initial stage of the experiment. It was observed that within approximately 48 hours, the surface area of the composites had reached maximum expansion without a significant change at the end of the immersion period at room temperature. However, at 80°C, it is harder to interpret whether equilibrium expansion has been reached, although the rate of swelling was found to decrease for all samples after 24 hours. In both cases, the surface area expansion was observed to be much lower than TS. Alkalisation had no influence on this behaviour, as the gain in surface area for all composites was about the same by the end of the experiment; approximately 1.20% at room temperature and 0.96% at 80°C. From this, it is expected that NP will have a very minor surface area change, while coating may not have any impact on this behaviour.
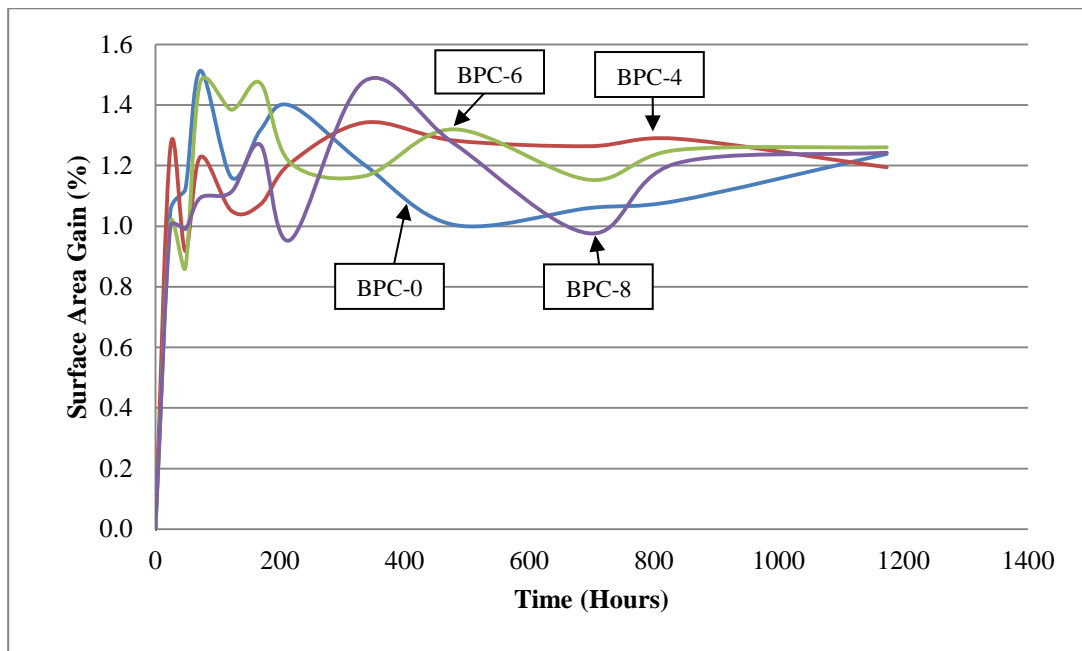
Figure 6.14: Surface area expansion due to moisture absorption at room temperature
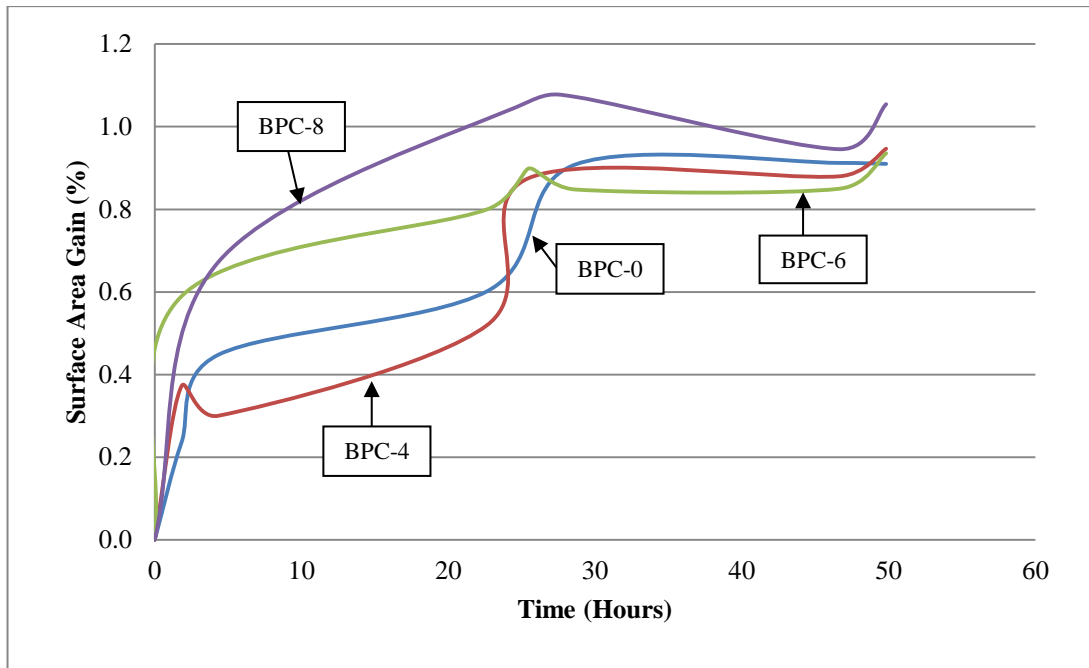
Figure 6.15: Surface area expansion due to moisture absorption at 80⁰C

From the surface area gain and TS data, the volume expansion of the composites was calculated and is presented in Figure 6.16 and Figure 6.17. In both conditions, BPC-8 experienced the highest volume change as expected, possibly due to the swelling of the damaged fibrils as discussed before. The final volume expansion for BPC-0, BPC-4 and BPC-6 are similar. By the end of both tests, the maximum volume gain was approximately 6% for all samples, with a higher rate of expansion with the introduction of heat.
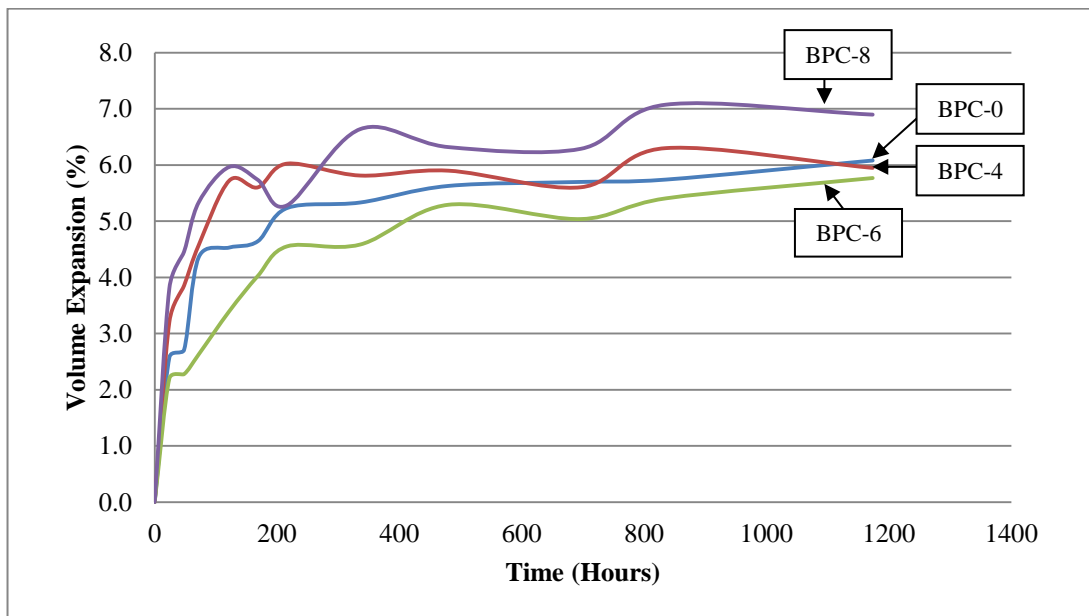
Figure 6.16: Volume expansion due to moisture absorption at room temperature

145
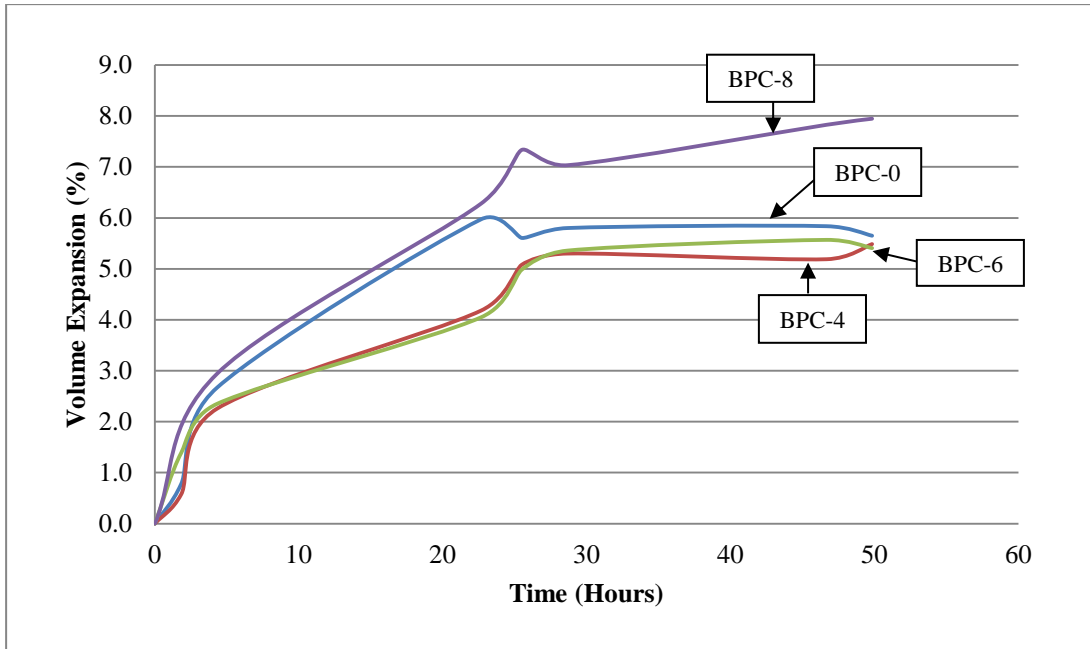
Figure 6.17: Volume expansion due to moisture absorption at 80⁰C

In a polymer resin, the swollen volume of the resin immersed in water is assumed to equal the volume of absorbed water. The resulting volume change can be computed from the following relationship (Mallick 2008):

$$\frac{\Delta V(t)}{V_o} = \frac{\rho_m}{\rho_w} M \qquad \text{Equation 6-5}$$

Where ρ_m, ρ_w and M is the matrix density, water density and moisture content at time t, respectively. The corresponding dilatational (volumetric) strain in the resin is:

$$\varepsilon_m = \frac{1}{3}\frac{\Delta V}{V_0} = \frac{1}{3}\frac{\rho_m}{\rho_w} M \qquad \text{Equation 6-6}$$

The same equation was applied to the bamboo fibre/polyester composites to determine the strain within the samples due to moisture swelling behaviour. Table 6.4 presents the experimental and theoretical strains calculated from Equation 6-6. The experimental strains were obtained from the final volume changes, as shown in Figure 6.16 and Figure 6.17, while the theoretical values were based on the densities and the final moisture content of the composites.

Table 6.4: Dilatational (volumetric) strain due to moisture absorption

Sample	Room Temperature		80⁰C	
	ε Exp	ε Theo	ε Exp	ε Theo
BPC-0	2.03	4.94	1.88	3.99
BPC-4	1.98	2.14	1.83	3.38
BPC-6	1.92	1.98	1.80	3.61
BPC-8	2.30	3.03	2.65	3.25

Generally, the theoretical strains in both temperature conditions are overestimated, as the formula did not consider the higher void contents within the composites, due to the addition of bamboo fibres. The voids caused some release in strain, as the extra space allowed water to accommodate freely in the composites. At higher temperatures, the theoretical strains doubled, but in reality the values are comparable

146

to room temperature. The deterioration of the fibre/matrix adhesion at higher temperatures, which allow more capacity for moisture accommodation, causes lesser strain. Interestingly, the experimental and theoretical strain values for BPC-4 and BPC-6 at room temperatures are very close. This can be attributed to better fibre/matrix interlocking due to the efficiency of the NaOH treatment, which reduces the number of voids within the composites. This results in better consistency with the theoretical prediction. The higher weight gain of BPC-0, but with a relatively lower volume change, caused the experimental strain to be much less than predicted. This may possibly be caused by the presence of wax, hemicellulose or lignin in the fibre, behaving in a way that attracts more water but with less fibre swelling. BPC-8, as discussed before, accommodated more moisture within its damaged fibrils resulting in highest swelling, suffering the worst volumetric strain. However, it can be noted that in practice, swelling is negligible until a threshold moisture concentration in exceeded.

6.6 Tensile properties of moisture degraded bamboo fibre/polyester composites

Tensile tests were performed on the neat polyester (NP), untreated (BPC-0), treated (BPC-6) and coated (BPC-6C) composites after immersion in water for 60 days at room temperature and 2 days at 80^0C. The stress-strain curves were plotted and are presented in Figure 6.18 and Figure 6.19. In both conditions, all samples showed brittle behaviour with sudden failure at maximum load.
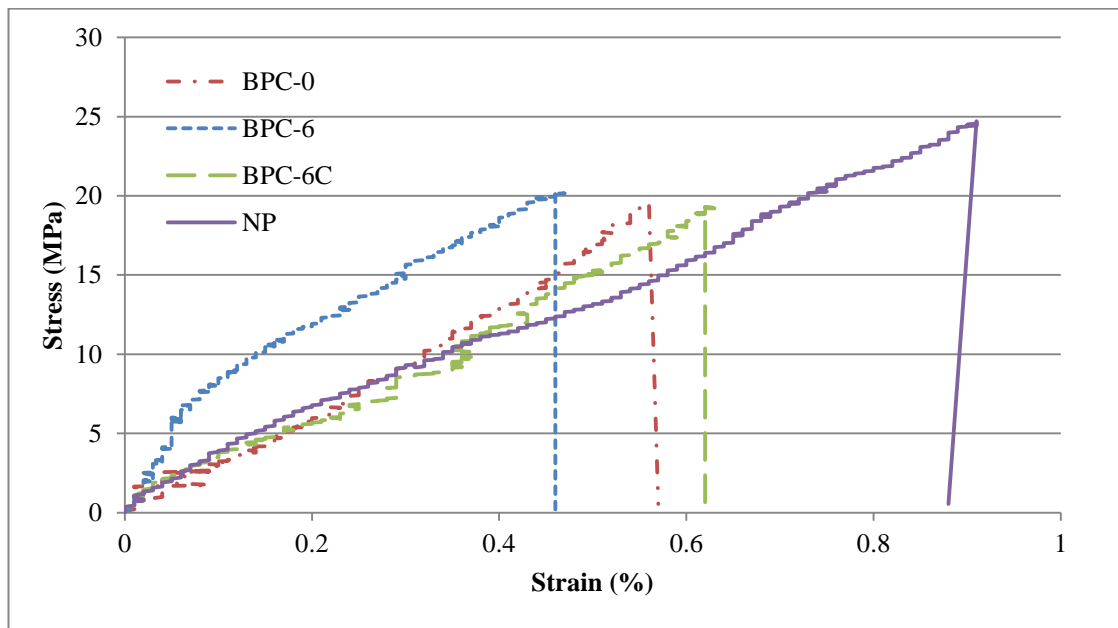
Figure 6.18: Stress-strain curves of moisture degraded samples at room temperature
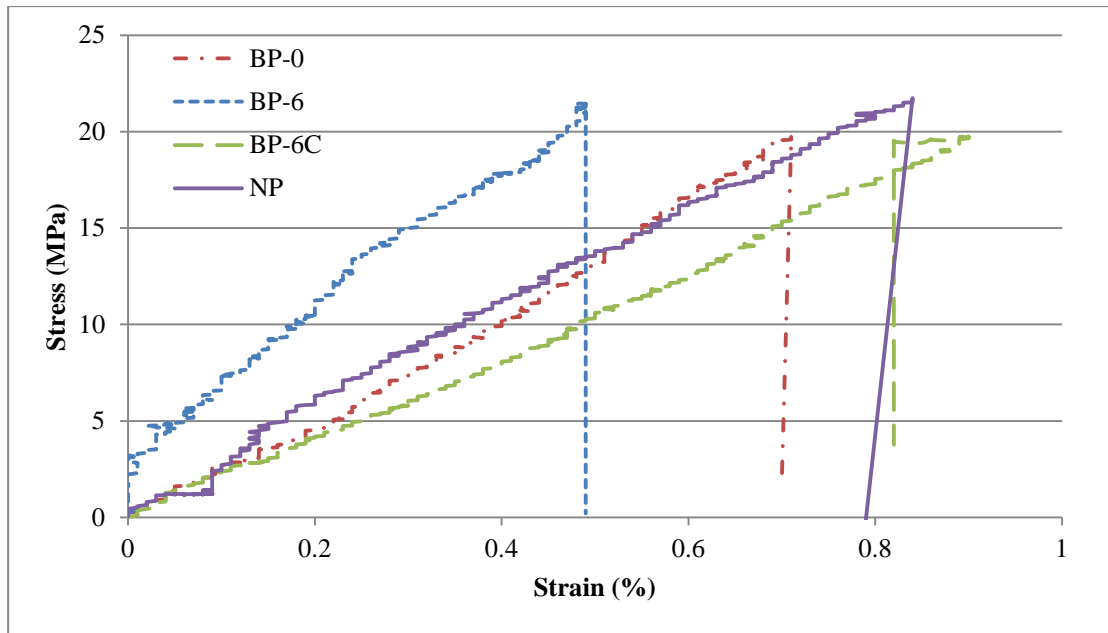
Figure 6.19: Stress-strain curves of moisture degraded samples at 80°C

The maximum tensile strength and elastic modulus of the samples were obtained from the stress-strain curves, and the average values were compared with the initial tensile properties which were obtained at room temperature (RT). The tensile behaviour at 80°C without moisture influence, which was discussed in Chapter Five, was also referred to in order to further understand the hygrothermal effect on the strength of the samples. However, it must be noted that the duration of degradation exposure is different, such that samples were exposed to 80°C without moisture for 1 hour while with moisture, the exposure duration was 2 days. Thus, a precise relationship cannot be established. The difference in tensile properties of the samples at various conditions is presented in Figure 6.20 and Figure 6.21.

	RT	RT-Moisture	80⁰C	80⁰C-Moisture
■ BPC-0	18.97	22.01	22.20	18.75
■ BPC-6	20.03	21.74	24.70	18.64
■ BPC-6C	23.13	21.60	24.57	18.84
■ NP	33.79	25.24	23.83	21.92
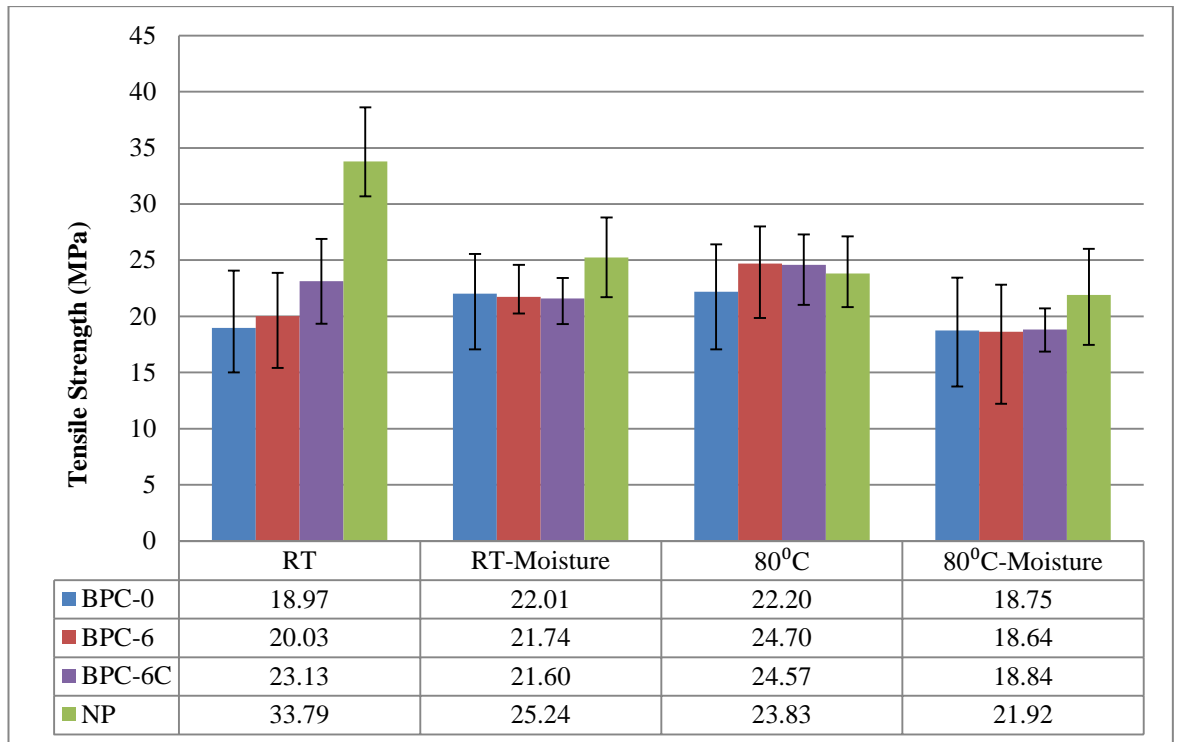
Figure 6.20: Tensile strength at different temperature and moisture condition

	RT	RT-Moisture	80⁰C	80⁰C-Moisture
■ BPC-0	3182.00	2873.75	1233.33	2839.43
■ BPC-6	3813.83	3969.80	1620.50	3555.46
■ BPC-6C	4022.90	2619.25	1715.33	2473.41
■ NP	3348.67	2418.43	1372.17	2323.09
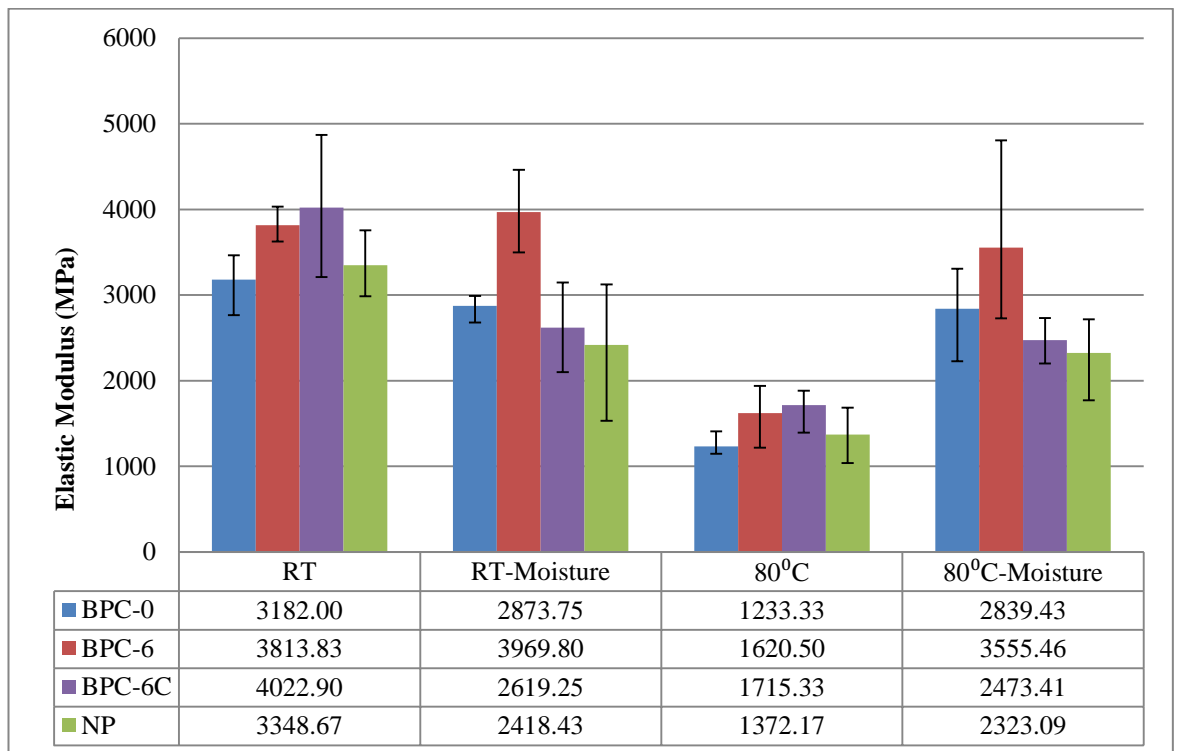
Figure 6.21: Elastic modulus at different temperature and moisture condition

All composite samples were found to reach the same maximum tensile strength after immersion in water at room temperature, which is approximately 22 MPa as shown in Figure 6.20. In comparison with the undegraded samples, about 2% increase was observed for BPC-0 and BPC-6, while BPC-6C showed a very minor decrease. The strength reduction of the coated sample may be due to softening of the coating material, which no longer provided the additional confinement strength observed initially. This ensured the BPC-6C behaved similarly to the uncoated BPC-6 samples. Higher decrement in strength was apparent for NP resin, whereby a 26.6% reduction was observed. It is interesting to note that the tensile strength of moisture soaked bamboo fibre composites were not much affected by the degradation process, unlike the NP. However, the strength of the NP was still higher than the composites after the degradation process. The elastic modulus of BPC-0 and BPC-6 was not overly affected by the moisture, as shown in Figure 6.21. BPC-6C showed a decrease of nearly half of its initial value. The softening of the coating material had caused the tensile machine to record higher deformation, as the grip moved in regards to the softened surface layer, instead of the whole sample. Therefore, the elastic modulus recorded had less influence on the composite sample, but more on the degraded coating layer that behaved separately from the composite, due to failed adhesive bonding. As for the NP, a 27.8% reduction of elastic modulus was observed, similar to its tensile strength.

For water immersion at 80$^\text{o}$C, all composite samples also behaved similarly, with an approximate 18 MPa of tensile strength achieved. All samples saw a 13.6% reduction in strength at 80^{0}C, compared to room temperature immersion. Separately, the effect of water immersion and 80$^\text{o}$C temperature exposure resulted in a slightly higher strength than the initial values for both conditions. However, the combined hygrothetmal effect caused minor strength reductions for coated and uncoated BPC-6 samples, while BPC-0 achieved similar maximum strength to the undegraded sample. At 80$^\text{o}$C without water, the slight softening of the polyester may have produced better interfacial strength, while in water this mechanism was not present. Even from the stress-strain curves and elastic modulus values, the semi-ductile behaviour experienced at 80^{0}C was not observed for the hygrothermal condition. This may be caused by the difference in testing environment, whereby the thermo-mechanical test was performed in an oven, constantly exposing the samples to heat, while the water degraded samples were removed from the degradation environment prior to testing. If any softening of resin occurred, the exposure to room temperature may have re-hardened the samples. However, the elastic modulus of the composites showed similar values to that of moisture degraded samples at room temperature, considering that the composites had physically degraded by 48 hours. The effect of temperature did not seem to be a major influence on the stiffness of the composites immersed in water. For NP, the reduction in stiffness was also comparable to the water immersed samples at room temperature, but with a slightly higher reduction in tensile strength. Nevertheless, without the fibres, the hygrothermal effect at 80^{0}C for the NP still resulted in the highest tensile strength.

The degradation of NP in polar solvents, such as water and aqueous solutions, has been extensively studied and is described in terms of solvolytic reactions, which cause the breaking of C-O or C-N bonds. Polyester is held together by linkages consisting of carboxylic acid ester and the effect of water can be described as (Jones 2001):

$$-\overset{|}{\underset{|}{C}}-\overset{O}{\overset{\|}{C}}-O-\overset{|}{\underset{|}{C}}- \rightarrow -\overset{|}{\underset{|}{C}}\text{-OH} + \text{HO-}\overset{|}{\underset{|}{C}}-$$
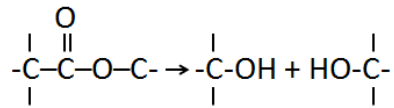
<div align="right">Equation 6-7</div>

Polymers exposed to moisture usually show degradation of mechanical properties, as well as the value of T_g through hydrolytic depolymerisation (Jones 2001). This explains how the NP samples in this study suffered high strength reduction after immersion in water. Similarly, other polymers such as epoxy resins showed lower strength and stiffness in wet conditions at room temperature (Gibson 2011). Interestingly, several researchers have reported some increment in strength for natural fibre/polymer composites subjected to high moisture concentration environments. The reaction of natural fibres to moisture itself was studied by Stamboulis et al. (2001), who reported that green flax fibres gained 20% in strength after being humidified at 90% RH. The authors attributed this to the plasticising effect by some free water molecules, which was advantageous to the strength of cellulose fibres. Chen et al. (2009) observed a slight increase in tensile strength of bamboo/vinyl ester composites exposed to increased RH, while Dhakal et al. (2007) reported a 22% gain in tensile strength for hemp/polyester composites immersed in water at room temperature. However, the hemp/polyester composites showed a relatively lower strength to dry samples at higher fibre contents. The increased in composite strength due to water influence was elaborated by Karmaker et al. (1994). The authors explained that the swelling of fibres due to moisture absorption may have filled the gaps between the fibres and the resin. This could possibly increase the mechanical properties of the composites by improving the shear strength between the fibres and matrix during fracture. However, some researchers have shown contradicting results on the tensile strength of water-aged natural fibre/polymer composites. Athijayamani et al. (2009), Assarar et al. (2011) and Zabihzadeh et al. (2011) have all observed a decrease in mechanical properties for water immersed composites, attributed to the development of shear stress at the fibre/matrix interface, eventually causing ultimate debonding of the fibres, delamination and loss of structural integrity.

The effect of hygrothermal ageing on the mechanical properties of natural fibre/polymer composites have been less studied compared to the effect on the physical and moisture kinetic behaviour. Generally, researchers have mainly agreed that hygrothermally exposed composites suffer reductions in strength and stiffness. Due to the dilatational expansion of the matrix around the fibre, the residual compressive stresses at the fibre/matrix interface was expected to reduce from curing shrinkage, which results in relieved mechanical interlocking between the fibre and the matrix (Mallick 2008). Beg & Pickering (2008) have reported reductions in tensile strength of 33% and elastic modulus of 40% for WF/polypropylene composites immersed in water at 50^0C over a 9-month period, relative to unaged composites. Through SEM, the authors observed loss of adhesion between fibre and matrix after ageing, which was apparent in the presence of voids and fibre pull-out, as well as fibre degradation by water absorption through exposed microfibrils. An exposure to 90% RH at 20^0C and 40^0C for flax/epoxy composite revealed that the tensile strength had a less significant reduction compared to the stiffness. The reduction in strength was explained by a plasticiser effect of water on the matrix (Scida et al. 2013). The effect of improved fibre/matrix adhesion through coupling agent (MAPP) on the hygrothermal ageing of Kraft fibre/polypropylene composites

was studied by Beg & Pickering (2008).With the addition of MAPP, better tensile strength and stiffness were observed for composites immersed in distilled water at 30, 50 and 70^0C, but the tensile properties were reduced as the temperature increased. However, at 70^0C, the tensile strength and stiffness for composites with MAPP were comparable to the untreated composites, meaning that the difference in strength was reduced at higher temperatures. This partially agrees with the current study, as the tensile strength of BPC-6 immersed in water at 80^0C was similar to BPC-0, suggesting that the improved fibre/matrix interlocking may not be significant to the tensile strength of the bamboo/ fibre/polyester composites in a hygrothermal environment. However, it is important to highlight that alkalisation provided better stiffness in this environment, with BPC-6 having much higher elastic modulus than BPC-0.

6.7 Glass transition temperature of moisture degraded bamboo fibre/polyester composite

Another physical effect of moisture absorption, apart from dimensional changes, is a reduction in T_g of the resin. With the reduction of T_g, the mechanical performance of a resin may not be affected at room temperature, but may be severe at elevated temperatures. Epoxy resin suffered a reduction of modulus at 150^0C from 2070 MPa to 20.7 MPa, as its T_g was reduced from 215^0C to 127^0C (Mallick 2008). For a polymeric composite, the same effect is to be expected for its matrix-dominated properties. The visco-elastic properties of samples immersed in water for a period of 60 days were studied using DMA.

6.7.1 Effect of moisture absorption on the storage modulus, loss modulus and damping with temperature

Figure 6.22, Figure 6.23 and Figure 6.24 present the storage modulus, loss modulus and tan delta of moisture immersed bamboo fibre/polyester composites and neat polyester, respectively. In comparison to dry samples, the curves for BPC-0 and BPC-4 clearly show some instability in the data plotted. The data for BPC-6C could not be properly obtained and the test automatically stopped at 140^0C. It was visually observed that the coating layer softened when removed from water and was possibly melted in the DMA machine at 140^0C, as it was found to adhere to the test set-up. Thus, it can be said that the degraded coating had influenced the data acquisition with less information on the behaviour of the whole composite.
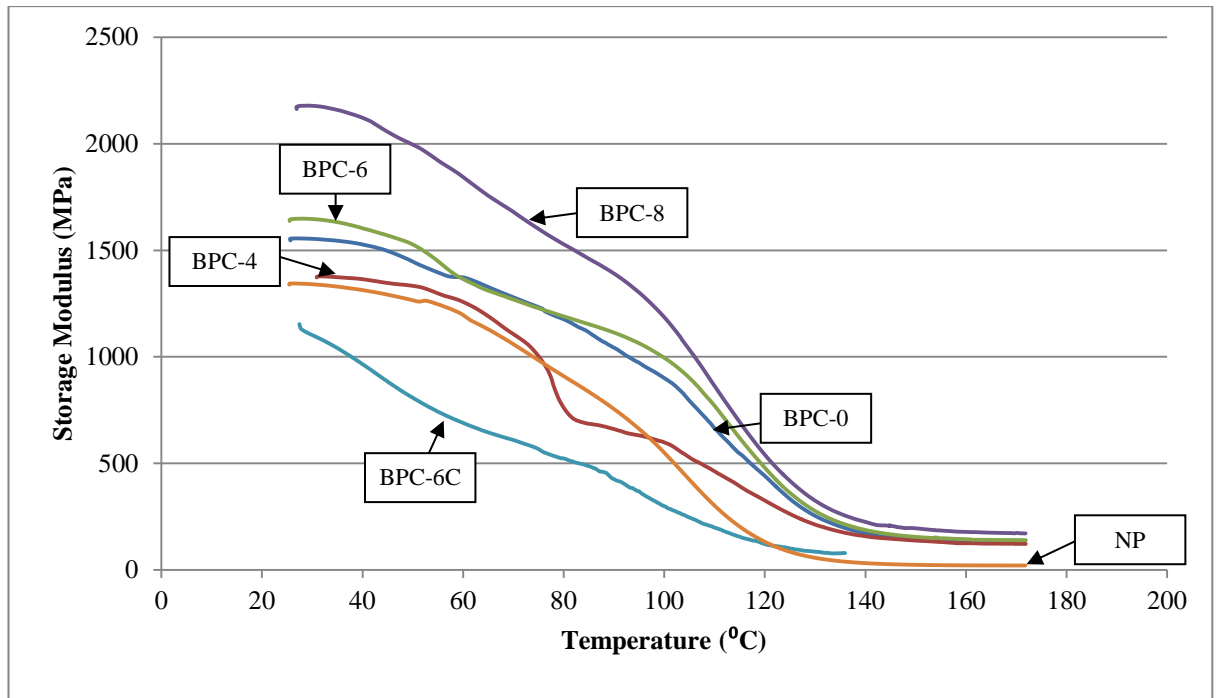
Figure 6.22: Storage modulus of moisture degraded samples
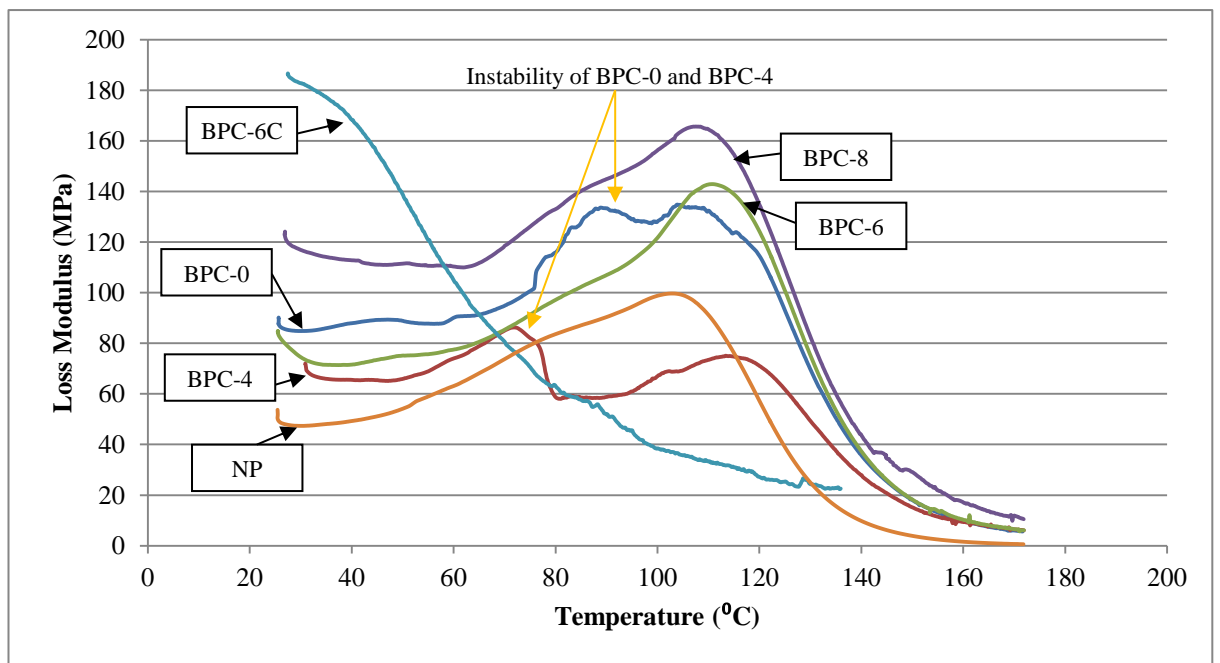
Figure 6.23: Loss modulus of moisture degraded samples

153
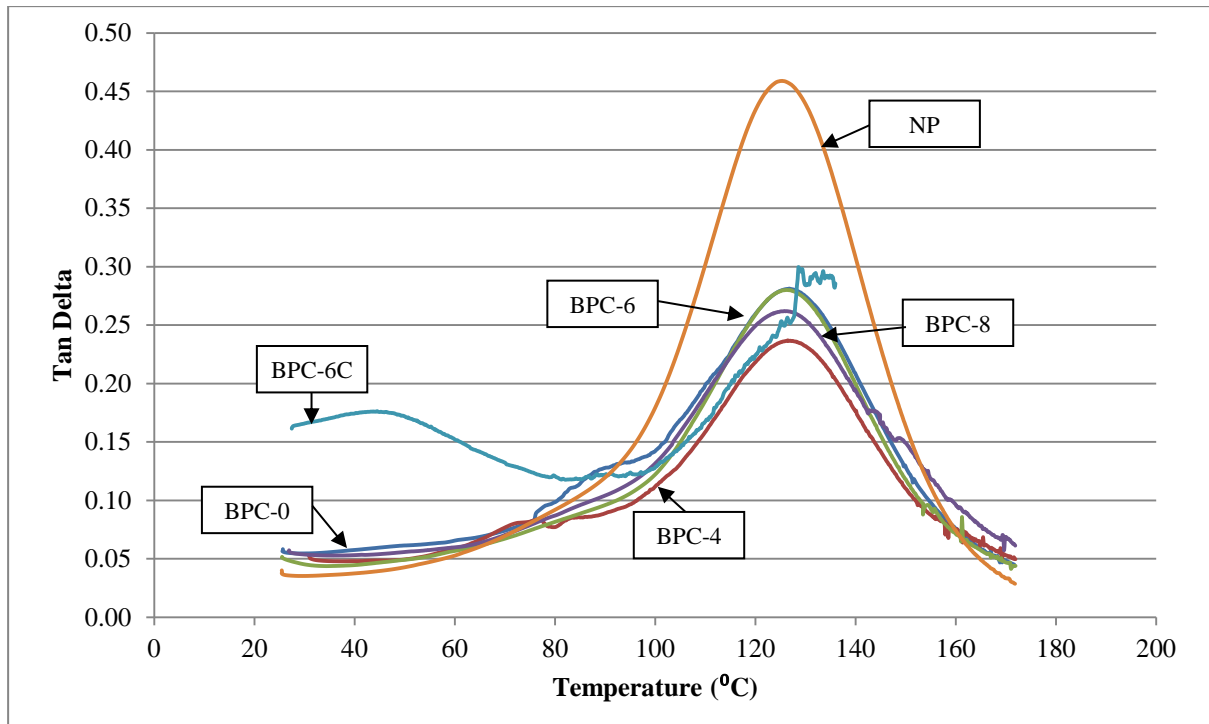
Figure 6.24: Tan delta of moisture degraded samples

Overall, the visco-elastic properties of moisture absorbed NP was observed to have a more obvious impact than the composites with bamboo fibres. All three properties for NP were found to decrease in the plastic region; the temperature below T_g. For dry NP, these properties were higher than all composite samples, indicating better mechanical properties at low temperatures. However, with the presence of moisture, NP had the lowest modulus at all temperature ranges. This coincides with the static tensile testing, which provided lowest elastic modulus for moisture degraded NP samples at both room temperature and at 80^0C. Interestingly, the bamboo fibre/polyester composites generally showed some minor increase in both storage modulus and loss modulus in the plastic region. For example, in the plastic region at 40^0C, moisture saturated BPC-8 had the highest storage and loss modulus, with a 20% and 105% increment, respectively, compared to its dry counterpart. This somehow agrees with the theory discussed earlier on the improvement in some mechanical properties of natural fibre polymeric composites, due to the moisture swelling of fibres providing additional interfacial shear strength. Even without alkali treatment, BPC-0 in wet conditions showed comparable modulus properties with the treated composites. From the tan delta values, it was found that the damping properties were not affected by the presence of moisture within the samples. The comparison of the modulus at 40^0C for dry and wet samples, as well as the maximum tan delta values, are presented in

Table 6.5

Table 6.5: Visco-elastic properties of dry and wet samples

Sample	E' (MPa) at 40°C		E" (MPa) at 40°C		Maximum Tan δ	
	Dry	Wet	Dry	Wet	Dry	Wet
BPC-0	1215	1527	32	88	0.26	0.28
BPC-4	1838	1364	51	66	0.26	0.24
BPC-6	1514	1603	45	72	0.27	0.28
BPC-8	1767	2121	55	113	0.26	0.26
NP	2132	1313	90	49	0.48	0.46

The T_g values for the wet samples were extracted from the peaks of the loss modulus curves and are presented in Table 6.6. It was observed that the hygrothermal effect reduced the T_g for all samples.

Table 6.6: Glass transition temperature (T_g) of dry and wet samples

Sample	T_g from E" Curve ($^{\circ}$C)	
	Dry	Wet
BPC-0	118.17	103.84
BPC-4	114.36	113.39
BPC-6	120.20	110.66
BPC-8	118.25	107.49
NP	112.08	102.81

The T_g of a polymer matrix varies with moisture content (Daniel & Ishai 2006). Jones (2001) summarised that T_g had a strong dependence on the moisture content of the composite, with a 60°C drop observed when the moisture content increased from zero to two per cent. The changes in T_g are said to be a function of the time of exposure to elevated temperatures and moisture, while the extent of degradation of mechanical properties mainly depended on the fraction of the material exhibiting the glass transition, which in this case is the polyester resin. The reduction in T_g is caused by hydrolytic depolymerisation of the NP, wherein the entanglement between long chain molecules (namely ester links), which provides hardness to resin, are cleaved by chemical reaction with water. Water molecules are split into hydrogen cations (H^+) and hydroxide anions (OH^-), which react with the ester links, producing a 'carboxylic acid' group and an 'alcohol' group. The polymer chains now become less entangled, causing the material to soften (Hunter et al. 2000). This chemical reaction is presented in Equation 6-7. Therefore, with the softening of the polyester, we can expect the T_g to reduce, indicating that the polyester and its composites will undergo transition from plastic-state to rubbery-state at a lower temperatures.

6.7.2 Theoretical reduction of mechanical properties due to hygrothermal effect

In the past, theoretical equations have been developed to estimate the properties of polymers and composite systems using synthetic fibres exposed to moisture and heat. However, for natural fibres, not much work could be found in the published literature on this topic. In this section, attempts have been made to apply these empirical formulas to the bamboo fibre/polyester composites to evaluate the difference in

behaviour between natural fibre/polymer composites and their synthetic counterparts in a hygrothermal condition.

The glass transition temperature in wet conditions, T_{gw} can be estimated using the following equation (Gibson 2011; Mallick 2008) :

$$T_{gw} = (0.0050M_r^2 - 0.10M_r + 1.0)T_{gd}$$
<div align="right">Equation 6-8</div>

Where M_r is weight percentage of moisture in the matrix resin and T_{gd} is the glass transition temperature at dry condition. It was noted that Equation 6-8 was used for epoxy matrix composites, but needs validation for other polymeric matrix systems. The theoretical T_{gw} for all samples were calculated using the final moisture content after water immersion at 60 days and are presented in Table 6.7. It can be observed that for NP, the empirical equation gives a very good estimate, only 0.9% higher than the experimental value. However, this is clearly not compatible with natural fibre/polymer composites, as it significantly underestimates the T_{gw}. The high moisture absorption of the bamboo fibres influenced the calculated values; in reality, T_g is more dependent on the polyester resin.

Table 6.7: Theoretical glass transition temperature at wet condition

Sample	Experimental T_g (^{0}C)		Theoretical T_g (^{0}C)
	Dry	**Wet**	**Wet**
NP	112.08	**102.81**	**103.78**
BPC-0	118.17	103.84	59.09
BPC-4	114.36	113.39	74.54
BPC-6	120.20	110.66	80.18
BPC-8	118.25	107.49	66.16

Another empirical equation is used to predict the hygrothermal degradation of composite strength and/or stiffness. It is based on the experimental observation that degradation is gradual until the temperature T approaches T_{gw}, at which point the degradation accelerates. The relationship between T_g and the mechanical properties at wet and dry conditions is presented as follow (Gibson 2011; Mallick 2008):

$$F_m = \frac{P}{P_o} = \left(\frac{T_{gw}-T}{T_{gd}-T_o}\right)^{1/2}$$
<div align="right">Equation 6-9</div>

Where:
F_m = matrix mechanical property retention ratio
P = matrix strength or stiffness after hygrothermal degradation
P_o = reference matrix strength or stiffness before degradation
T = temperature at which is to be predicted (^{0}F)
T_{go} = glass transition temperature for reference dry condition (^{0}F)
T_{gw} = glass transition temperature for wet matrix material at moisture content corresponding to property P (^{0}F)
T_o = test temperature at P_o was measured (^{0}F).

From Equation 6-9, the strength and stiffness after hygrothermal ageing at room temperature and 80^0C for neat polyester, untreated composite, and treated composite were estimated and are presented in Table 6.8. The properties for coated samples could not be calculated due to unavailability of its T_{gw}. Figure 6.25 and Figure 6.26

show the comparison between the calculated tensile strength and elastic modulus, with the experimental results, respectively.

Table 6.8: Theoretical tensile properties of moisture absorbed samples

Sample	Tensile Strength (Mpa)		Elastic Modulus (Mpa)	
	RT-Wet	80^{0}C-Wet	RT-Wet	80^{0}C-Wet
NP	31.94	17.29	3165.41	1713.86
BPC-0	17.45	9.59	2927.09	1609.59
BPC-6	19.00	11.37	3617.70	2164.36

	NP	BPC-0	BPC-6
RT-Experimental	25.24	22.01	21.74
RT-Theoretical	31.94	17.45	19.00
80^{0}C-Experimental	21.92	18.75	18.64
80^{0}C-Theoretical	17.29	9.59	11.37
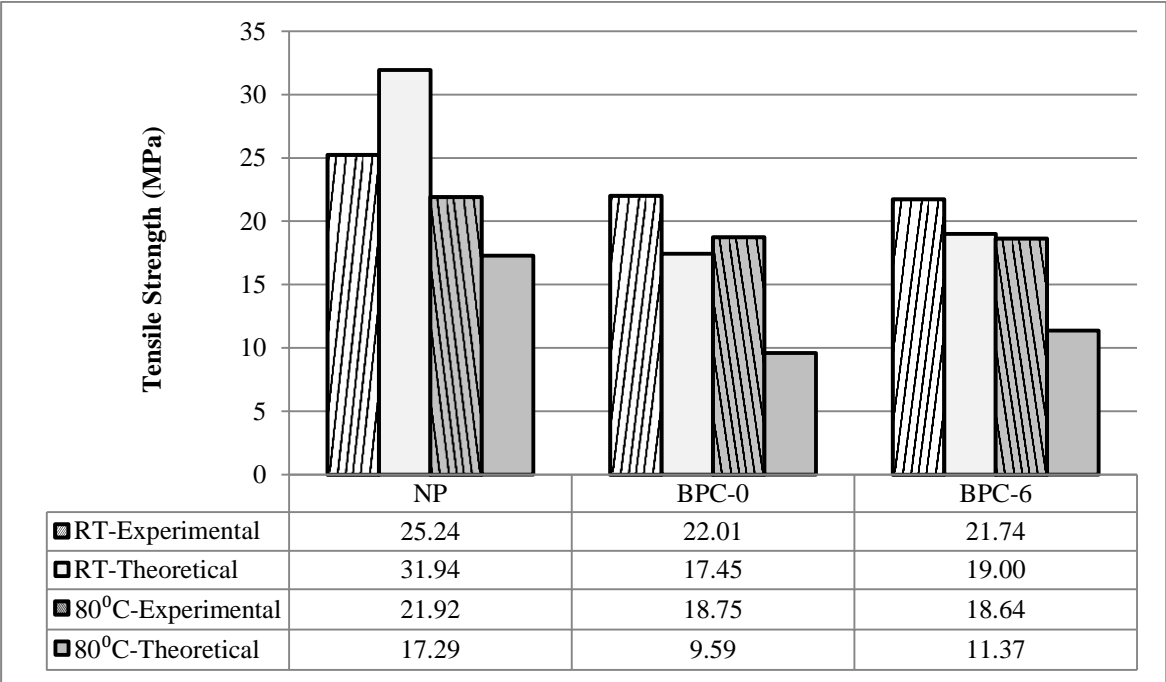
Figure 6.25: Comparison of experimental and theoretical tensile strength of hygrothermally aged samples

	NP	BPC-0	BPC-6
▨ RT-Experimental	2418.43	2873.75	3969.80
▢ RT-Theoretical	3165.41	2927.09	3617.70
▨ 80^{0}C-Experimental	2323.09	2839.43	3555.46
▢ 80^{0}C-Theoretical	1713.86	1609.59	2164.36
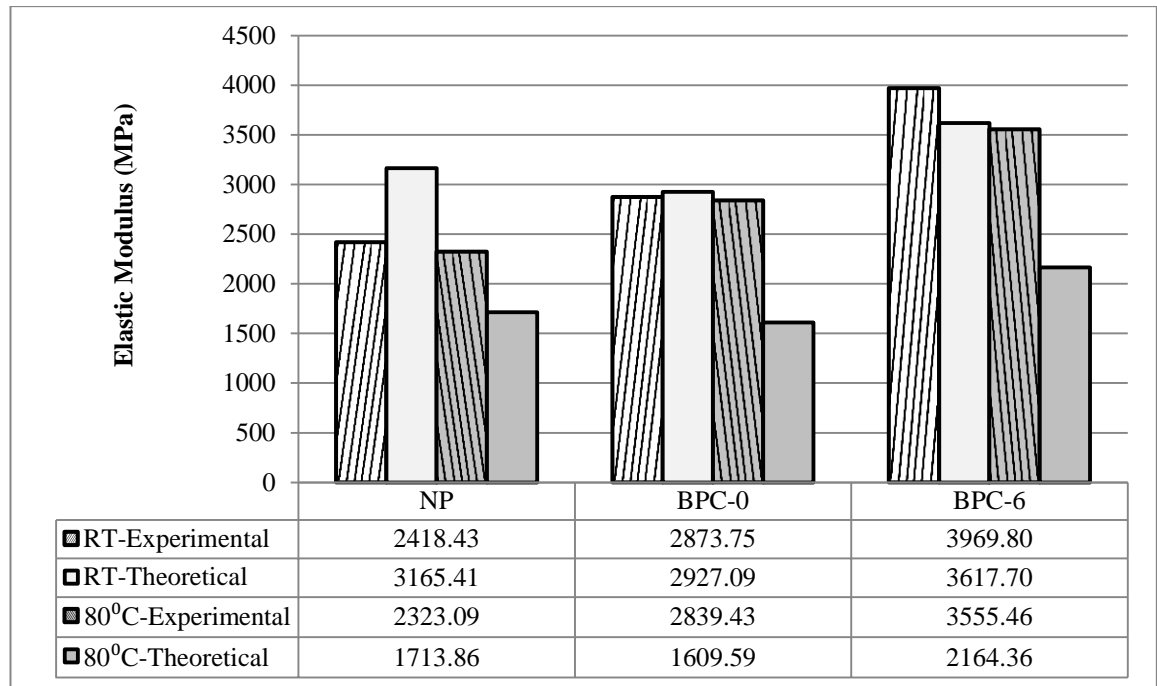
Figure 6.26: Comparison of experimental and theoretical elastic modulus of hygrothermally aged samples

It can be observed that for NP, the tensile strength and stiffness at room temperature under wet conditions yielded an average of 29% higher values than the experimental results, and approximately 23% less at 80^{0}C. Gibson (2011) suggested to validate Equation 6-9 for other polymeric composites, as it was found to have good agreement with epoxy composites. For the bamboo fibre/polyester composites, better estimations were obtained at room temperature, especially for the elastic modulus, whereby differences of 2% and 9% from the experimental values were calculated for BPC-0 and BPC-6, respectively. However, for 80^{0}C, the equation underestimates both tensile properties up to 40 to 48% from the actual values. It must be noted that the equation considers a decrease in strength of the composites due to the effect of moisture on the resin. As observed in this study, the presence of moisture in the bamboo fibre/polyester composites somehow provided added strength, which may outweigh the effect of hydrolysis on the polyester. Thus, the prediction may only be suitable for synthetic fibre/epoxy composites, where fibre swelling due to moisture absorption is less significant. It is expected that synthetic fibres are the least sensitive to environment, causing hygrothermal effects to be most noticeable in matrix-dominated properties. For example, the torsional stiffness of carbon/epoxy composites was reduced from 0.96 GPa in ambient air to 0.90 GPa in room temperature water, to a lower 0.70 GPa in 74^{0}C water (Daniel & Ishai 2006).

6.8   Morphology observation of moisture degraded samples

The fibre/matrix interfaces for BPC-0, BPC-6 and BPC-8 after immersion in water at room temperature and at 80^{0}C were observed using scanning electron microscopy. The micrographs of the degraded non-loaded samples are presented in Figure 6.27. In Figure 6.27 (a), for untreated bamboo fibre/polyester composites after immersion at room temperature, there are apparent voids observed between the fibres and the polyester. This shows weak interfacial adhesion between the two materials. For BPC-

6 and BPC-8, some areas show better adhesion of matrix into the fibres. However, gaps can also be observed on areas, with dense fibre concentration on BPC-6, while BPC-8 shows micro pores between fibrils. The higher weight gain of BPC-0 may reflect the higher amount of voids due to this weak fibre/matrix bonding, compared to the treated samples. The pores observed between the fibrils for BPC-8 may imply that with a lack of hemicellulose and lignin, more voids may be present within the fibres, causing higher moisture accommodation than BPC-6, but lower moisture gain than BPC-0.

At 80^0C, it is clear from the micrographs that all samples experienced fibre debonding, whereby voids were observed to separate the fibres from the matrix. The condition of the fibre/matrix interface for all cases is very similar and this may result in comparable gain in weight for all samples at 80^0C. The shrinkage of matrix and the dissolved particles from the fibres due to the hygrothermal effect may contribute to fibre debonding. The micrograph of BPC-0 shows fibre fibrillation, indicating that the fibres were damaged by the high temperature. Untreated fibres contain hemicelluloses and lignin, which are soluble in water. These substances leached from the fibres due to the effect of water (Joseph et al. 2002), which causes the fibres to be separated into individual fibrils. Hemicelluloses and lignin were partially removed through alkalisation; thus, this effect is less expected in treated fibres. Additionally, micro cracks can be observed on the BPC-8 specimen. The presence of these micro cracks may be one reason for the rate of water absorption to expedite at 80^0C. The effect of water on the degradation of the composites is magnified at higher temperatures.

(a) BPC-0 at room temperature

(b) BPC-0 at 80°C

(c) BPC-6 at room temperature

(d) BPC-6 at 80°C

(e) BPC-8 at room temperature

(f) BPC-8 at 80°C
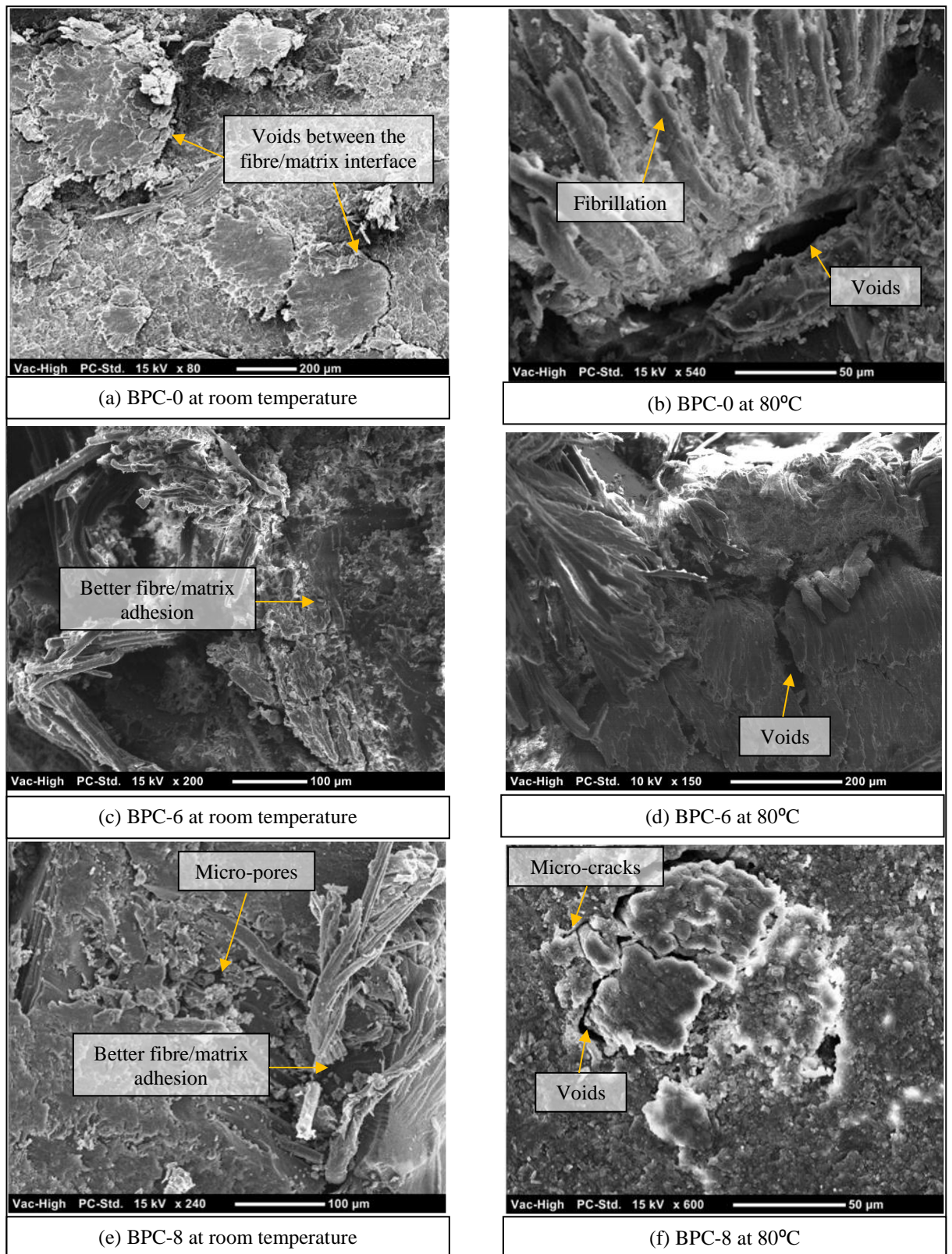
Figure 6.27: Morphology of non-loaded moisture degraded composites

161

The morphology of the fractured surfaces of the tensile tested moisture degraded NP, BPC-0 and BPC-6 samples were observed through SEM and are presented in Figure 6.28. For NP, moisture immersion at room temperature shows a smoother morphology compared to the undegraded samples in Chapter Four. This may imply that hydrolysis of the polyester had occurred, causing softening of the resin. This smoother morphology may be related to the decrease in strength and stiffness, as it shows less resistance to the applied tensile load. However, at 80^0C, obvious polymer melt can be observed throughout the surface. The combined effect of heat with moisture had altered the morphology of the polyester, making it less smooth. At higher magnification, micro cracks were visible and this may indicate a more aggressive moisture attack due to the hygrothermal environment, internally damaging and weakening the resin matrix. It is also possible for the matrix to experience uneven shrinking at high temperatures that may lead to the micro cracks. The initial loss in weight before moisture gain as detailed in Figure 6.3 may support this theory.

Bamboo fibres swell as they absorb moisture and shrink once dried. This process causes internal micro cracks, which will lead to fibre/matrix debonding, reducing the mechanical properties of the composites. For the bamboo fibre/polyester composites, it is noted that treated and untreated fibres showed similar tensile strength at both room temperature and at 80^0C, but better elastic modulus for treated samples. From the SEMs, a comparison between BPC-0 and BPC-6 at room temperature was made. The apparent difference is in the presence of voids between the matrix and the fibres observed on BPC-0. BPC-6 had better fibre/matrix adhesion, even after 60 days of water immersion. Although this is the case, similar tensile strength was achieved for both samples. The SEMs were taken after the samples were dried at room conditions, thus any fibre swelling due to moisture was no longer observed. As discussed before, the gaps between the fibres and the matrix may have been closed by the lateral expansion of the fibres, providing added shear strength during load transfer. Thus, as both treated and untreated fibres swell to their respective maximum moisture content, both would have the same fibre/matrix interface condition, improving the overall composite strength slightly. However, the elastic modulus for BPC-0 was still less than BPC-6, which shows that better stiffness could not be achieved through fibre swelling, and that the actual fibre/matrix adhesion is still responsible for this property. On both samples, pores on the matrix were detected, which were left by fibres after being pulled-out. Figure 6.28 (f) shows a clear view of a pore, still maintaining the shape of the fibre's surface. The surface of the matrix is observed to be smooth due to the softening from the hydrolysis effect, and this may contribute to the failure mechanism of the composites. This suggests that failure is mainly due to fibre pull-out, which after overcoming the shear strength from the swelled fibres, the softened matrix no longer provides a firm grip on the fibres, letting them slip and break. Interestingly, some polyester was still attached to the treated fibres as observed in Figure 6.28 (j), indicating evidence of good fibre/matrix bonding.

At 80^0C, fibre damage was observed on some fibres, as shown in Figure 6.28 (g), whereby exposure and peeling of microfibril surface can be seen. The hygrothermal exposure had caused the fibrils to be eroded, removing some mass. Polymer melt was also obvious on these composites with possible matrix shrinkage, evident by the gap between the treated fibre and matrix, which may be created as the matrix thermally shrunk. This phenomenon had resulted in the decreased tensile strength of the treated

and untreated composites, as both have larger gaps than experienced at room temperature. The failure mechanism for this condition was also through fibre pull-out, with pores from fibrils observed on BPC-0 and a fibre debonded from fractured polyester observed on BPC-6. Lost of resin particles were observed in both room temperature and at 80^0C, as seen in Figure 6.28 (h) and Figure 6.28 (i), acknowledging the capability of moisture in weakening and eroding the resin matrix even at low temperatures.

Observations made on other natural fibre composites were also reported to have similar morphological deterioration. SEMs observations on randomly oriented natural fibres/polyester hybrid composites immersed in water at 30^0C by Athijayamani et al. (2009) showed matrix cracking along the fibre/matrix interface as a result of water molecules attack. The authors attributed this to the shear stress from fibre swelling that ultimately causes debonding. Matrix cracking and lost of resin particles were also observed even at day 5 of immersion. Beg & Pickering (2008) reported that wood polymer composites fractured surfaces after hygrothermal degradation showed a loss of adhesion between fibre and matrix, characterised by the apparition of voids and fibre pull-out. The appearance of microfibrils was clearly observed as a result of fibre degradation by water absorption. Dhakal et al. (2007) highlighted that for randomly oriented fibres, fibre entanglement caused resin-free areas, and acted as reservoirs for moisture accumulation. At boiling point, crack development was observed on the hemp/polyester composites, with lost of resin particles observed due to accelerated ageing.

Sample	Room Temperature	80°C
NP	(a) Smoother surface, matrix softening / (b) Defragmentation	(c) Polymer melt / (d) Defragmentation / Micro-cracks

Sample	Room Temperature	80°C
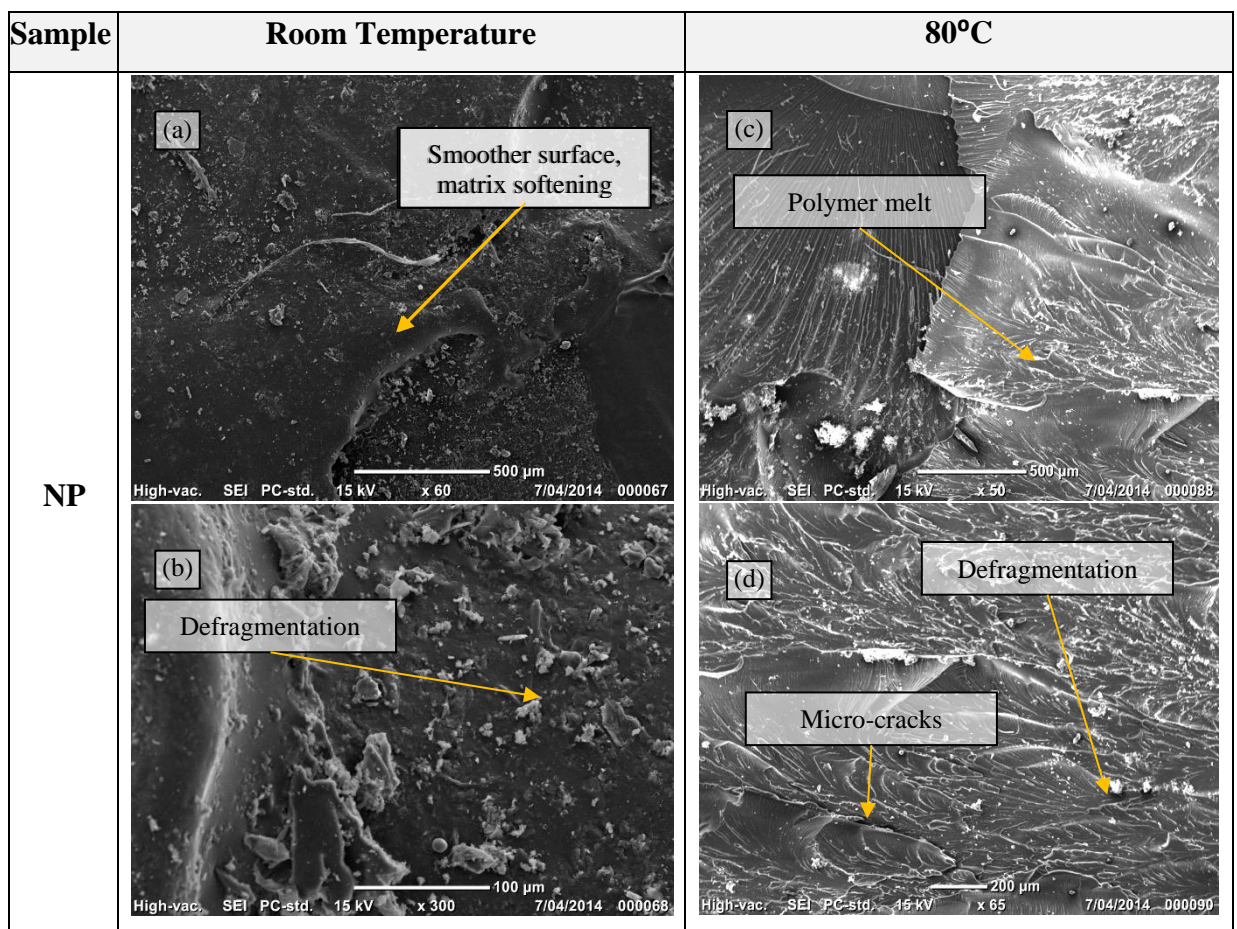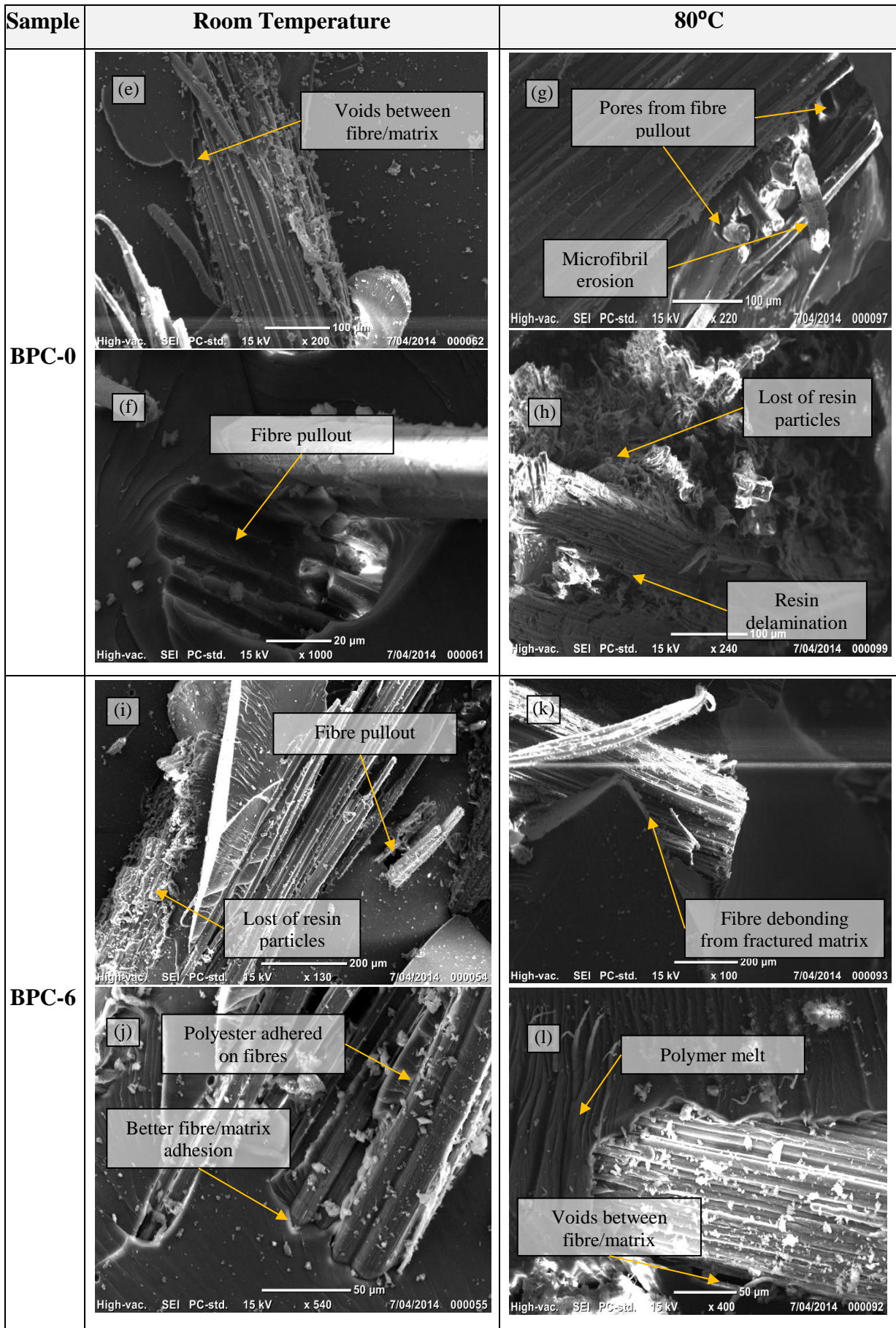
Figure 6.28: Morphology of tensile fractured surfaces of moisture degraded samples

6.9　Chapter summary

The degradation of bamboo fibre/polyester composites subjected to moisture absorption was discussed in this chapter. The percentage gain in weight of bamboo fibres, neat polyester and their composites were measured to represent the amount of water absorbed. The absorption kinetics, physical changes, and mechanical properties of the composites were also evaluated for moisture exposure at room temperature and at 80°C, whereby hygrothermal condition was introduced to the degradation process. The studies have shown that:

1) Bamboo fibres are highly hydrophilic, absorbing moisture from the surrounding environment even when placed in normal room conditions. For all moisture types, untreated fibres were found to absorb the least moisture, with higher absorption observed as the concentration of NaOH treatment increased. 8% NaOH treated fibres exhibit 40% absorption of distilled water in 24 hours, which is 14% more than untreated fibres. This reflects that the voids created by the removal of hemicellulose, lignin and other less stable components are more influential than the presence of hemicellulose itself, which is said to be responsible for the hydrophilicity of natural fibres.

2) NP has the lowest weight gain at both temperature conditions, gaining less than 1% of moisture, indicating that water absorption of composites is mainly due to the presence of bamboo fibres. Alkali treated bamboo fibres produced more water resistance composites compared to untreated fibres. This is especially significant in room temperature conditions. It can be observed that composites with 6% NaOH treated fibres have the highest resistance to water, which may be due to the optimum fibre/matrix adhesion. The 6% NaOH treated composites achieved 60% less moisture gain than untreated composites. The application of acrylic coating was helpful in slowing down the absorptivity of the composites. At 80°C, the rate of absorption increased for all composite samples, reaching an average of 7.5% weight gain on the second day, comparable to room temperature immersion of 60 days. The untreated composites absorbed the most moisture but the difference in weight gain with the treated composites was less substantial. This may suggest that effect of the improved fibre/matrix adhesion was less significant compared to the consequences of heat exposure.

3) The diffusion, solubility and permeability coefficients of the composites both at room temperature and at 80°C were highest for untreated composites. This implies that alkali treatment improves the moisture kinetic behaviour of the composites in terms of resisting moisture attack, which was further improved with the presence of the acrylic coating layer.

4) The physical changes of the samples observed after water immersion were thickness swelling, surface expansion and volumetric expansion. The change in the final thickness of the samples at the end of the immersion period showed that NP had less than 1% gain at both temperature conditions. Untreated composites had comparable thickness swelling with the treated composites, while BPC-8 showed highest rate in swelling. The presence of hemicellulose and lignin may increase moisture absorptivity, but does not affect the swelling in BPC-0, while higher fibrillation in BPC-8 provided more space for expansion. The swelling was suppressed by the presence of the coating layer as it provides 40% additional barrier against thickness swelling. At 80°C, the rate of swelling for all composite samples are higher,

reaching an average of 5.5% gain on the second day, comparable to room temperature immersion of 60 days. The gain in surface area for all composites was observed to be much lower than in the thickness direction, with approximately 1.20% gain at room temperature and 0.96% gain at 80°C. From these two measurements, the volumetric expansion was calculated, giving an approximately 6% final gain for all samples, with a faster rate of expansion at 80°C.

5) Tensile strength achieved for all samples were similar at both temperatures, approximately 22 MPa at room temperature and 18 MPa at 80°C, while NP showed higher strength in both cases. The approximately 2% higher strength achieved for moisture immersed composites at room temperature compared to dry samples can be attributed to the plasticising effect by free water molecules, which was advantageous to the strength of cellulose fibres and also to the increase in interfacial shear strength by fibre swelling, filling the voids at the fibre/matrix interface. All samples saw a 13.6% reduction in strength at 80°C, compared to room temperature immersion. The elastic modulus of untreated and treated composites was not affected much by moisture, even at 80°C. While the stiffness of NP did show a 27.8% reduction at room temperature compared to dry samples, the increase in temperature did not provide any further reduction.

6) The DMA showed that the visco-elastic properties of NP were more affected by moisture than the bamboo fibre/polyester composites, which generally demonstrated minor increase in both storage modulus and loss modulus in the plastic region. In the plastic region at 40°C, moisture saturated 8% NaOH treated composites had the highest storage and loss modulus, with a 20% and 105% increment, respectively, compared to its dry counterpart. Even without alkali treatment, BPC-0 in wet conditions showed comparable modulus properties with the treated composites. However, the damping properties were not affected by the presence of moisture within the samples.

7) The glass transition temperature, T_g for the wet samples were observed to reduce due to the hygrothermal effect. The reduction in T_g was caused by hydrolytic depolymerisation of the NP whereby the entanglement between the ester links were cleaved by chemical reaction with water, reducing its T_g from 112°C to 103°C.

8) The SEMs for the composite samples at room temperature prove that the untreated composites had poor fibre/matrix adhesion, with more voids present. This supports the weight gain results, as more moisture can be accommodated within the untreated composite. Both treated and untreated samples exhibit obvious gaps between the fibre and the matrix at 80°C, due to the damage from heat, with microcracks detected on the NP in some samples. Matrix softening due to hydrolysis was apparent on samples immersed in moisture at room temperature, while polymer melting was evident at 80°C. In both conditions, fibre pull-out was observed on the untreated and treated samples, indicating that the tensile load caused failure through fibre/matrix debonding.

Chapter 7 : Conclusions and Recommendations

7.1   Major conclusions from the study

The current research focused mainly on the degradation of bamboo fibre/polyester composites subjected to moisture and thermal environments. The study was divided into three main parts. The first part aimed to find the optimum NaOH concentration for the treatment of bamboo fibres in providing the best fibre strength and interfacial properties with polyester resin. The second part of the study involved a few approaches in evaluating the thermal response of the fibres and the composites. The last part covered the effects of moisture on the physical and tensile behaviour of the composites, including the effects of a hygrothermal environment. The significant findings were presented at the end of each chapter and are further concluded in this section as follows:

1) The alkali treatment using NaOH on bamboo fibres partially removed the fibre matrix, resulting in a rougher fibre surface and slight decrease in diameter and density. The optimum NaOH concentration was found to be at 6wt. %, which showed optimum mechanical properties, with 181% increment in the fibre tensile strength, 22% increment in the interfacial shear strength with polyester resin and 6% increment in the tensile strength of the bamboo fibre/polyester composite, compared to the untreated samples. The rougher fibre surface provided improved fibre/matrix adhesion and this was evident through SEM with the absence of voids between the fibre and matrix.

2) The increase in NaOH concentration to 8wt.% had an adverse effect on the mechanical properties of both the fibre and the composite, compared to the untreated samples, with 24% and 18% decrement in tensile strength of fibres and composites, respectively. Through SEM, fibrillations due to a high removal of fibre matrix as well as damage to the cellulosic fibrils were observed, which resulted in the deterioration of mechanical properties. However, the rough fibre surface did provide good interfacial adhesion with polyester resin, but the effect was offset by the poor fibre condition.

3) The thermal decomposition of the fibre, resin and composite was studied using TGA. It was observed that alkalisation reduced the thermal stability of fibres, but increased the char production. 8% NaOH treated fibres exhibited the highest change, with 14% reduction in the decomposition temperature and 125% more char than untreated fibres. However, alkalisation did not have much effect on these behaviours in the composite, due to the higher influence of polyester, as resin has a higher volume fraction. The incorporation of the thermally less stable bamboo fibres into the polyester caused approximately 7.7% decrement in thermal stability and about 90% increment in charring, compared to NP.

4) The T_g for the polyester resin used in this study is 112^0C, which increased with the addition of fibres. The maximum was obtained by 6% NaOH treated composite, at 120^0C. Above this temperature, the polyester and the composite will be in a rubbery state with very poor mechanical properties. This was evident on the storage and elastic modulus values for all samples obtained through DMA, which was below 180 MPa and 10 MPa, respectively at the end of the experiment (170^0C). Therefore, the T_g was used as the temperature limit in the thermo-mechanical study.

5) The thermo-mechanical study involves static tensile testing at 40^0C, 80^0C and 120^0C. It was observed that NP had higher initial tensile strength than the composites, which reduced drastically starting from 80^0C onwards. The composites exhibited improved strength up to 80^0C, which may be due to reorientation of the fibres in the direction of the applied load, as observed on the fractured surfaces. The composites had also shown better mechanical performance than the NP at 120^0C. The tensile strength reduction of NP is 29% at 80^0C and 92% at 120^0C, while for the 6% NaOH treated composite, a 23% increment was observed at 80^0C and a reduction of 38% observed at 120^0C. The elastic modulus for all samples was reduced as the temperature rose, due to the softening of the matrix evident through SEM. The softened resin further bonded with the fibres at 40^0C and 80^0C for all composite samples, resulting in improved tensile strength. However, at 120^0C, poor fibre/matrix interlocking can be observed by the presence of voids for all samples, as the elevated temperature causes resin shrinkage and mass loss on both fibre and polyester. This, with polyester softening, degrades the composite strength to half their initial values.

6) Alkalisation causes increased in moisture absorption of bamboo fibres due to the presence of voids by the partial removal of the fibre matrix. The higher the NaOH concentration, the higher the absorptivity of the fibres, with 8% NaOH treated fibres exhibiting 40% absorption of distilled water in 24 hours, which is 14% more than untreated fibres. However, with better fibre/matrix interlocking and polyester dispersion within the voids, the moisture absorptivity and moisture kinetics behaviour improved with NaOH treatment, with optimum results achieved by 6% NaOH treated composites, achieving 60% less moisture gain than untreated composites. It is important to highlight that the NP gained less than 1% of moisture even after 60 days of immersion, implying that the bamboo fibres are highly influential on the composite's hydrophilicity. The thickness swelling of untreated composites showed comparable results with treated composites, indicating that the high gain in moisture due to the presence of hemicellulose did not result in higher swelling.

7) Tensile strength achieved for moisture immersed treated and untreated composites were comparable at 22 MPa, and are approximately 2% higher compared to their respective dry samples. This can be attributed to the plasticising effect by free water molecules, which was advantageous to the strength of cellulose fibres and also to the increased in interfacial shear strength by fibre swelling, filling the voids at the fibre/matrix interface. The elastic modulus of untreated and treated composites was not affected by the moisture. The SEM observations showed that the tensile load caused failure through fibre/matrix debonding, with apparent matrix softening due to hydrolysis.

8) The hygrothermal effect brought by the increased in temperature at 80^oC for 2 days showed an increased rate in moisture absorption and thickness swelling, reaching an average of 7.5% and 5.5% gain, respectively for all composites, which is comparable to room temperature immersion of 60 days. The effect of treatment was less substantial on the moisture absorptivity and thickness swelling, as final weight gain of all composites was comparable. Similar to room temperature moisture immersion, the tensile strength of all composites are comparable and are slightly lower than dry samples at 18

MPa, while the strength of NP is at 22 MPa. All samples saw a 13.6% reduction in strength compared to room temperature immersion. Additionally, the increase in temperature did not provide any further reduction in the stiffness. Through SEM observations, both treated and untreated samples exhibited obvious gaps between the fibre and the matrix, due to damage caused by heat with microcracks and polymer melting detected on the NP. The failure mechanism was also through fibre/matrix debonding.

9) The glass transition temperature, T_g for the wet samples were observed to reduce due to the hygrothermal effect. The reduction in T_g is caused by hydrolytic depolymerisation of the NP, whereby the entanglement between the ester links as cleaved by chemical reaction with water, reducing its T_g from 112^0C to 103^0C.

10) The acrylic coating provided slight improvement in tensile and thermal properties of the coated composite, especially below 80^0C, as it is engineered for extreme outdoor conditions. The coated samples achieved 13% higher strength and 5% higher stiffness than uncoated samples, possibly due to the binding force provided by the coating layer. In the thermo-mechanical study, coated samples exhibited highest stiffness at all temperature settings, which may be enhanced by the restriction to deformation by the coating layer. In terms of moisture protection, the application of acrylic coating was helpful in slowing down the absorptivity of the composite, reducing its moisture kinetic behaviour as well as providing 40% additional barrier against thickness swelling. However, at temperature exposure higher than 80^0C, the coating is no longer effective, as it is damaged by the heat, resulting in similar behaviour to the uncoated samples.

As a final conclusion, it can be highlighted that alkali treatment successfully improved the initial mechanical properties of bamboo fibre/polyester composites. However, after exposure to various natural elements in an outdoor environment, this improvement can be maintained in certain conditions, while in some, alkalisation provided an insignificant influence. Much of the behaviour change depends on how the environment alters the state of the fibre/matrix interface. Other factors to consider include the individual degradation of the composite's constituent, that is, the polymer resin and the reinforcing fibres.

7.2   Recommendations

To ensure the widespread use of natural fibre/polymer composites in outdoor applications, with possible upgrades to load bearing elements in civil engineering, further comprehensive work is required in this field of research. The benefits of natural fibres in providing 'green' materials should be taken advantage of, but the lifespan and cost-effectiveness are concerns for commercialisation. The following aspects are recommendations for further research exploration:

1) The effects of UV rays have been discussed in the literature review, which highlights the degradation process that takes place on the surface of the composite, affecting mostly the resin by photodegradation. UV is unavoidable, especially for outdoor material exposed to direct sunlight. The effects of UV on the physical and mechanical properties of bamboo fibre/polyester composites, as well as in combination with heat and moisture, should be investigated to study the extent of deterioration it can cause.

2) The thermo-mechanical study was performed on samples heated for one hour, which yielded improved in strength at temperatures $\leq 80^0\text{C}$. It is interesting to explore how different durations can affect the mechanical properties of the composite and to obtain a possible limit of exposure time. This is important, as in real conditions, materials may be exposed to prolonged heat.

3) The tensile properties of moisture immersed in water at room temperature for 60 days were not greatly affected, even though significant physical changes were observed. A prolonged immersion with possible tensile evaluation at specific intervals would be beneficial in determining the maximum duration of moisture exposure before any mechanical deterioration is observed. The same can also be applied at hygrothermal condition.

4) Another interesting aspect to explore is the presence of microorganisms in assisting the degradation of natural fibres, which is especially important in high moisture conditions. This recommendation is based on the presence of black spots observed on moisture degraded composites, located along the sides of the composites, where bamboo fibres were not encapsulated with resin.

5) Application of other types of commercially available coating products on bamboo fibre/polyester composites can also be studied to improve durability. A good coating system can potentially assist the development of this type of material. Additives may be preferable, but are harder to incorporate without proper equipment and may also decrease the strength of the composites.

6) If duration of study is not an issue, natural weathering exposure to bamboo fibre/polyester composites should also be considered, as this provides better insight on actual in-service condition. The data obtained should be compared to laboratory environments to evaluate the existing test methods.

References

Aboudzadeh, M, Mirabedini, S & Atai, M 2007, 'Effect of silane-based treatment on the adhesion strength of acrylic lacquers on the PP surfaces', *International journal of adhesion and adhesives*, vol. 27, no. 7, pp. 519-26.

Abu-Sharkh, BF & Hamid, H 2004, 'Degradation study of date palm fibre/polypropylene composites in natural and artificial weathering: mechanical and thermal analysis', *Polymer Degradation and Stability*, vol. 85, no. 3, pp. 967-73.

Adhikary, KB, Pang, S & Staiger, MP 2008, 'Long-term moisture absorption and thickness swelling behaviour of recycled thermoplastics reinforced with Pinus radiata sawdust', *Chemical Engineering Journal*, vol. 142, no. 2, pp. 190-8.

Akay, M 1993, 'Aspects of dynamic mechanical analysis in polymeric composites', *Composites Science and Technology*, vol. 47, no. 4, pp. 419-23.

Akil, H, Omar, M, Mazuki, A, Safiee, S, Ishak, Z & Abu Bakar, A 2011, 'Kenaf fiber reinforced composites: A review', *Materials & Design*, vol. 32, no. 8, pp. 4107-21.

Akil, HM, Santulli, C, Sarasini, F, Tirillò, J & Valente, T 2014, 'Environmental effects on the mechanical behaviour of pultruded jute/glass fibre-reinforced polyester hybrid composites', *Composites Science and Technology.*

Alvarez, VA & Vázquez, A 2004, 'Thermal degradation of cellulose derivatives/starch blends and sisal fibre biocomposites', *Polymer Degradation and Stability*, vol. 84, no. 1, pp. 13-21.

Annie Paul, S, Boudenne, A, Ibos, L, Candau, Y, Joseph, K & Thomas, S 2008, 'Effect of fiber loading and chemical treatments on thermophysical properties of banana fiber/polypropylene commingled composite materials', *Composites Part A: Applied Science and Manufacturing*, vol. 39, no. 9, pp. 1582-8.

Araújo, JR, Waldman, WR & De Paoli, MA 2008, 'Thermal properties of high density polyethylene composites with natural fibres: Coupling agent effect', *Polymer Degradation and Stability*, vol. 93, no. 10, pp. 1770-5,

Assarar, M, Scida, D, El Mahi, A, Poilâne, C & Ayad, R 2011, 'Influence of water ageing on mechanical properties and damage events of two reinforced composite materials: Flax–fibres and glass–fibres', *Materials and Design*, vol. 32, no. 2, pp. 788-95.

ASTM 1989. ASTM D3379-75(1989)e1 *Standard Test Method for Tensile Strength and Young's Modulus for High Modulus Single Filament Materials,* West Conshohocken, PA: ASTM International.

ASTM 2010a. ASTM D638 *Standard Test Method for Tensile Properties of Plastics.*, West Conshohocken, PA: ASTM International.

ASTM 2010b. D570 *Standard Test Methord for Water Absorption of Plastics*, West Conshohocken, PA: ASTM International.

Athijayamani, A, Thiruchitrambalam, M, Natarajan, U & Pazhanivel, B 2009, 'Effect of moisture absorption on the mechanical properties of randomly oriented natural fibers/polyester hybrid composite', *Materials Science and Engineering: A*, vol. 517, no. 1-2, pp. 344-53.

Ayrilmis, N, Akbulut, T, Dundar, T, White, RH, Mengeloglu, F, Buyuksari, U, Candan, Z & Avci, E 2012, 'Effect of boron and phosphate compounds on physical, mechanical, and fire properties of wood–polypropylene composites', *Construction and Building Materials*, vol. 33, pp. 63-9.

Aziz, SH & Ansell, MP 2004, 'The effect of alkalization and fibre alignment on the mechanical and thermal properties of kenaf and hemp bast fibre composites: Part 1 – polyester resin matrix', *Composites Science and Technology*, vol. 64, no. 9, pp. 1219-30.

Baley, C, Morvan, C & Grohens, Y 2005, 'Influence of the absorbed water on the tensile strength of flax fibers', paper presented to Macromolecular Symposia.

Bao, LR, Yee, AF & Lee, CYC 2001, 'Moisture absorption hygrothermal aging bismaleimide resin', *Polymer*, vol. 42, no. 17, pp. 7327-33.

Beckermann, G & Pickering, KL 2008, 'Engineering and evaluation of hemp fibre reinforced polypropylene composites: fibre treatment and matrix modification', *Composites Part A: Applied Science and Manufacturing*, vol. 39, no. 6, pp. 979-88.

Beg, M & Pickering, K 2008, 'Mechanical performance of Kraft fibre reinforced polypropylene composites: Influence of fibre length, fibre beating and hygrothermal ageing', *Composites Part A: Applied Science and Manufacturing*, vol. 39, no. 11, pp. 1748-55.

Beg, MDH & Pickering, KL 2008, 'Reprocessing of wood fibre reinforced polypropylene composites. Part II: Hygrothermal ageing and its effects', *Composites Part A: Applied Science and Manufacturing*, vol. 39, no. 9, pp. 1565-71.

Beg, MDH & Pickering, KL 2008, 'Accelerated weathering of unbleached and bleached Kraft wood fibre reinforced polypropylene composites', *Polymer Degradation and Stability*, vol. 93, no. 10, pp. 1939-46.

Beninia, KCCC, Voorwald, HJC & Cioffi, MOH 2011, 'Mechanical properties of HIPS/sugarcane bagasse fiber composites after accelerated weathering', *Procedia Engineering*, vol. 10, pp. 3246-51.

Bessadok, A, Marais, S, Roudesli, S, Lixon, C & Métayer, M 2008, 'Influence of chemical modifications on water-sorption and mechanical properties of Agave fibres', *Composites Part A: Applied Science and Manufacturing*, vol. 39, no. 1, pp. 29-45.

Boopathi, L, Sampath, PS & Mylsamy, K 2012, 'Investigation of physical, chemical and mechanical properties of raw and alkali treated Borassus fruit fiber', *Composites Part B: Engineering*, vol. 43, no. 8, pp. 3044-52.

Brown, AM 2001, 'A step-by-step guide to non-linear regression analysis of experimental data using a Microsoft Excel spreadsheet', *Computer methods and programs in biomedicine*, vol. 65, no. 3, pp. 191-200.

Butylina, S, Hyvärinen, M & Kärki, T 2012, 'A study of surface changes of wood-polypropylene composites as the result of exterior weathering', *Polymer Degradation and Stability*, vol. 97, no. 3, pp. 337-45.

Campos, A, Marconcini, JM, Martins-Franchetti, SM & Mattoso, LHC 2011, 'The influence of UV-C irradiation on the properties of thermoplastic starch and polycaprolactone biocomposite with sisal bleached fibers', *Polymer Degradation and Stability,* vol. 97, no. 10, pp. 1948-55.

Carter, HG & Kibler, KG 1978, 'Langmuir-type model for anomalous moisture diffusion in composite resins', *Journal of Composite Materials*, vol. 12, no. 2, pp. 118-31.

Carus, M, Eder, DA, Dammer, L, Korte, DH, Scholz, L, Essel, R & Breitmayer, E 2014, *Wood-Plastic Composites (WPC) and Natural Fibre Composites (NFC): European and Global Markets 2012 and Future Trends*, Nova-Institut GmbH, Huerth, Germany.

Chen, D, Li, J & Ren, J 2011, 'Influence of fiber surface-treatment on interfacial property of poly (l-lactic acid)/ramie fabric biocomposites under UV-irradiation hydrothermal aging', *Materials Chemistry and Physics*, vol. 126, no. 3, pp. 524-31.

Chen, H, Miao, M & Ding, X 2009, 'Influence of moisture absorption on the interfacial strength of bamboo/vinyl ester composites', *Composites Part A: Applied Science and Manufacturing*, vol. 40, no. 12, pp. 2013-9.

Daniel, IM & Ishai, O 2006, *Engineering mechanics of composite materials*, Second Edition edn, Oxford University Press.

Defoirdt, N, Biswas, S, Vriese, LD, Tran, LQN, Acker, JV, Ahsan, Q, Gorbatikh, L, Vuure, AV & Verpoest, I 2010, 'Assessment of the tensile properties of coir, bamboo and jute fibre', *Composites Part A: Applied Science and Manufacturing*, vol. 41, no. 5, pp. 588-95.

Dhakal, H, Zhang, Z & Richardson, M 2007, 'Effect of water absorption on the mechanical properties of hemp fibre reinforced unsaturated polyester composites', *Composites Science and Technology*, vol. 67, no. 7-8, pp. 1674-83.

Di Franco, CR, Cyras, VP, Busalmen, JP, Ruseckaite, RA & Vázquez, A 2004, 'Degradation of polycaprolactone/starch blends and composites with sisal fibre', *Polymer Degradation and Stability*, vol. 86, no. 1, pp. 95-103.

Dittenber, DB & GangaRao, HVS 2012, 'Critical review of recent publications on use of natural composites in infrastructure', *Composites Part A: Applied Science and Manufacturing*, vol. 43, no. 8, pp. 1419-29.

Elenga, RG, Djemia, P, Tingaud, D, Chauveau, T, Maniongui, JG & Dirras, G 2013, 'Effects of Alkali Treatment on the Microstructure, Composition, and Properties of the Raffia textilis Fiber', *BioResources*, vol. 8, no. 2, pp. 2934-49.

Essabir, H, Elkhaoulani, A, Benmoussa, K, Bouhfid, R, Arrakhiz, F & Qaiss, A 2013, 'Dynamic mechanical thermal behavior analysis of doum fibers reinforced polypropylene composites', *Materials & Design*, vol. 51, pp. 780-88.

Ezekiel, N, Ndazi, B, Nyahumwa, C & Karlsson, S 2011, 'Effect of temperature and durations of heating on coir fibers', *Industrial Crops and Products*, vol. 33, no. 3, pp. 638-43.

Fabiyi, JS, McDonald, AG, Wolcott, MP & Griffiths, PR 2008, 'Wood plastic composites weathering: Visual appearance and chemical changes', *Polymer Degradation and Stability*, vol. 93, no. 8, pp. 1405-14.

Fatima, S & Mohanty, AR 2011, 'Acoustical and fire-retardant properties of jute composite materials', *Applied Acoustics*, vol. 72, no. 2-3, pp. 108-14.

García, M, Hidalgo, J, Garmendia, I & García-Jaca, J 2009, 'Wood–plastics composites with better fire retardancy and durability performance', *Composites Part A: Applied Science and Manufacturing*, vol. 40, no. 11, pp. 1772-6.

Geethamma, V, Kalaprasad, G, Groeninckx, G & Thomas, S 2005, 'Dynamic mechanical behavior of short coir fiber reinforced natural rubber composites', *Composites Part A: Applied Science and Manufacturing*, vol. 36, no. 11, pp. 1499-506.

George, J, Bhagawan, S & Thomas, S 1998, 'Effects of environment on the properties of low-density polyethylene composites reinforced with pineapple-leaf fibre', *Composites Science and Technology*, vol. 58, no. 9, pp. 1471-85.

Ghavami, K 2005, 'Bamboo as reinforcement in structural concrete elements', *Cement and Concrete Composites*, vol. 27, no. 6, pp. 637-49.

Gibson, A 2007, *Fire properties of polymer composite materials*, vol. 143, Springer.

Gibson, RF 2011, *Principles of composite material mechanics*, CRC Press.

Goriparthi, BK, Suman, K & Mohan Rao, N 2012, 'Effect of fiber surface treatments on mechanical and abrasive wear performance of polylactide/jute composites', *Composites Part A: Applied Science and Manufacturing*, vol. 43, no. 10, pp. 1800-8.

Hamid, MRY, Ab Ghani, MH & Ahmad, S 2012, 'Effect of antioxidants and fire retardants as mineral fillers on the physical and mechanical properties of high

loading hybrid biocomposites reinforced with rice husks and sawdust', *Industrial Crops and Products*, vol. 40, pp. 96-102.

Hejazi, SM, Sheikhzadeh, M, Abtahi, SM & Zadhoush, A 2012, 'A simple review of soil reinforcement by using natural and synthetic fibers', *Construction and Building Materials*, vol. 30, pp. 100-16.

Ho, M-p, Wang, H, Lee, J-H, Ho, C-k, Lau, K-t, Leng, J & Hui, D 2012, 'Critical factors on manufacturing processes of natural fibre composites', *Composites Part B: Engineering*, vol. 43, no. 8, pp. 3549-62.

Hollaway, LC 2010, 'A review of the present and future utilisation of FRP composites in the civil infrastructure with reference to their important in-service properties', *Construction and Building Materials*, vol. 24, no. 12, pp. 2419-45.

Hossain, MK, Hossain, ME, Hosur, M & Jeelani, S 2009, 'Mechanical and Thermal Characterization of CNF-Filled Polyester Nanophased Composite', paper presented to International Conference of Mechanical Engineering, Dakha, Bangladesh.

Hu, R-H, Sun, M-y & Lim, J-K 2010, 'Moisture absorption, tensile strength and microstructure evolution of short jute fiber/polylactide composite in hygrothermal environment', *Materials and Design*, vol. 31, no. 7, pp. 3167-73.

Hunter, LW, White, JW, Cohen, PH & Biermann, PJ 2000, 'A materials aging problem in theory and practice', *Johns Hopkins APL Technical Digest*, vol. 21, no. 4, pp. 575-81.

HunterLab 2008, *CIE L*a*b* Color Scale*, 8, Virginia, USA, Applications Note.

Huston, R, Chan, YC, Chapman, H, Gardner, T & Shaw, G 2012, 'Source apportionment of heavy metals and ionic contaminants in rainwater tanks in a subtropical urban area in Australia', *Water Res*, vol. 46, no. 4, pp. 1121-32.

Idicula, M, Boudenne, A, Umadevi, L, Ibos, L, Candau, Y & Thomas, S 2006, 'Thermophysical properties of natural fibre reinforced polyester composites', *Composites Science and Technology*, vol. 66, no. 15, pp. 2719-25.

Jacob, M, Francis, B, Thomas, S & Varughese, K 2006, 'Dynamical mechanical analysis of sisal/oil palm hybrid fiber-reinforced natural rubber composites', *Polymer Composites*, vol. 27, no. 6, pp. 671-80.

John, M & Thomas, S 2008, 'Biofibres and biocomposites', *Carbohydrate Polymers*, vol. 71, no. 3, pp. 343-64.

Jones, RH 2001, *Environmental effects on engineered materials*, CRC Press.

Joseph, PV, Rabello, MS, Mattoso, LHC, Joseph, K & Thomas, S 2002, 'Environmental effects on the degradation behaviour of sisal fibre reinforced polypropylene composites', *Composites Science and Technology*, vol. 62, pp. 1357–72.

Kabir, M, Wang, H, Cardona, F & Aravinthan, T 2011, 'Effect of chemical treatment on the mechanical and thermal properties of hemp fibre reinforced thermoset sandwich composites', paper presented to Proceedings of the 21st Australasian Conference on the Mechanics of Structures and Materials (ACMSM 21).

Kalia, S, Kaith, BS & Kaur, I 2009, 'Pretreatments of natural fibers and their application as reinforcing material in polymer composites-A review', *Polymer Engineering & Science*, vol. 49, no. 7, pp. 1253-72.

Karmaker, A, Hoffmann, A & Hinrichsen, G 1994, 'Influence of water uptake on the mechanical properties of jute fiber-reinforced polypropylene', *Journal of Applied Polymer Science*, vol. 54, no. 12, pp. 1803-7.

Kelly, A & Tyson, W 1965, 'Tensile properties of fibre-reinforced metals: copper/tungsten and copper/molybdenum', *Journal of the Mechanics and Physics of Solids*, vol. 13, no. 6, pp. 329-50.

Khan, F & Ahmad, S 1996, 'Chemical modification and spectroscopic analysis of jute fibre', *Polymer Degradation and Stability*, vol. 52, no. 3, pp. 335-40.

Khedari, J, Watsanasathaporn, P & Hirunlabh, J 2005, 'Development of fibre-based soil–cement block with low thermal conductivity', *Cement and Concrete Composites*, vol. 27, no. 1, pp. 111-6.

Krenchel, H 1964, *Fibre Reinforcement Akademisk Forlag Copenhagen*, Denmark.

Ku, H, Wang, H, Pattarachaiyakoop, N & Trada, M 2011, 'A review on the tensile properties of natural fiber reinforced polymer composites', *Composites Part B: Engineering*, vol. 42, no. 4, pp. 856-73.

Laner, D, Crest, M, Scharff, H, Morris, JW & Barlaz, MA 2012, 'A review of approaches for the long-term management of municipal solid waste landfills', *Waste Manag*, vol. 32, no. 3, pp. 498-512, item: 22188873.

Laoubi, K, Hamadi, Z, Ahmed Benyahia, A, Serier, A & Azari, Z 2014, 'Thermal behavior of E-glass fiber-reinforced unsaturated polyester composites', *Composites Part B: Engineering*, vol. 56, pp. 520-6.

Lee, S-H & Wang, S 2006, 'Biodegradable polymers/bamboo fiber biocomposite with bio-based coupling agent', *Composites Part A: Applied Science and Manufacturing*, vol. 37, no. 1, pp. 80-91.

Liu, K, Takagi, H, Osugi, R & Yang, Z 2012, 'Effect of lumen size on the effective transverse thermal conductivity of unidirectional natural fiber composites', *Composites Science and Technology*, vol. 72, no. 5, pp. 633-9.

Lorenz, R 2011, Chemistry and chemical technology of unsaturated polyester resins and related resins, Fachhochschule Munster University of Applied Sciences.

Lu, N & Oza, S 2013, 'Thermal stability and thermo-mechanical properties of hemp-high density polyethylene composites: Effect of two different chemical modifications', *Composites Part B: Engineering*, vol. 44, no. 1, pp. 484-90.

Mallick, PK 2008, *Fiber-reinforced composites: materials, manufacturing, and design*, 3rd Edition edn, CRC press.

Manalo, AC, Karunasena, W & Lau, KT, 2013, 'Mechanical properties of bamboo-fiber polyester composites', paper presented to Proceedings of the 22nd Australasian Conference on the Mechanics of Structures and Materials (ACMSM 22).

Manfredi, LB, Rodríguez, ES, Wladyka-Przybylak, M & Vázquez, A 2006, 'Thermal degradation and fire resistance of unsaturated polyester, modified acrylic resins and their composites with natural fibres', *Polymer Degradation and Stability*, vol. 91, no. 2, pp. 255-61.

Martínez-Hernández, A, Velasco-Santos, C, De-Icaza, M & Castano, VM 2007, 'Dynamical–mechanical and thermal analysis of polymeric composites reinforced with keratin biofibers from chicken feathers', *Composites Part B: Engineering*, vol. 38, no. 3, pp. 405-10.

Matuana, LM, Jin, S & Stark, NM 2011, 'Ultraviolet weathering of HDPE/wood-flour composites coextruded with a clear HDPE cap layer', *Polymer Degradation and Stability*, vol. 96, no. 1, pp. 97-106.

Menard, KP 2008, *Dynamic mechanical analysis: a practical introduction*, CRC press.

Methacanon, P, Weerawatsophon, U, Sumransin, N, Prahsarn, C & Bergado, DT 2010, 'Properties and potential application of the selected natural fibers as limited life geotextiles', *Carbohydrate Polymers*, vol. 82, no. 4, pp. 1090-6.

Michel, AT & Billington, SL 2012, 'Characterization of poly-hydroxybutyrate films and hemp fiber reinforced composites exposed to accelerated weathering', *Polymer Degradation and Stability*, vol. 97, no. 6, pp. 870-8.

Milanese, AC, Cioffi, MOH & Voorwald, HJC 2012, 'Thermal and mechanical behaviour of sisal/phenolic composites', *Composites Part B: Engineering*, vol. 43, no. 7, pp. 2843-50.

Mohanty, A, Misra, M & Hinrichsen, G 2000, 'Biofibres, biodegradable polymers and biocomposites: an overview', *Macromolecular Materials and Engineering*, vol. 276, no. 1, pp. 1-24.

Monteiro, SN, Calado, V, Rodriguez, RJS & Margem, FM 2012, 'Thermogravimetric behavior of natural fibers reinforced polymer composites—An overview', *Materials Science and Engineering: A*, vol. 557, pp. 17-28.

Mukhopadhyay, S & Srikanta, R 2008, 'Effect of ageing of sisal fibres on properties of sisal – Polypropylene composites', *Polymer Degradation and Stability*, vol. 93, no. 11, pp. 2048-51.

Mwaikambo, L 2009, *Sustainable Composite Materials: Exploitation of Plant Resourced Materials for Industrial Application*, VDM Publishing.

Nam, TH, Ogihara, S, Tung, NH & Kobayashi, S 2011, 'Effect of alkali treatment on interfacial and mechanical properties of coir fiber reinforced poly(butylene succinate) biodegradable composites', *Composites Part B: Engineering*, vol. 42, no. 6, pp. 1648-56.

Norul Izani, MA, Paridah, MT, Anwar, UMK, Mohd Nor, MY & H'ng, PS 2013, 'Effects of fiber treatment on morphology, tensile and thermogravimetric analysis of oil palm empty fruit bunches fibers', *Composites Part B: Engineering*, vol. 45, no. 1, pp. 1251-7.

Obi Reddy, K, Uma Maheswari, C, Shukla, M, Song, JI & Varada Rajulu, A 2013, 'Tensile and structural characterization of alkali treated Borassus fruit fine fibers', *Composites Part B: Engineering*, vol. 44, no. 1, pp. 433-8.

Placet, V 2009, 'Characterization of the thermo-mechanical behaviour of Hemp fibres intended for the manufacturing of high performance composites', *Composites Part A: Applied Science and Manufacturing*, vol. 40, no. 8, pp. 1111-8.

Pochiraju, KV, Tandon, GP & Schoeppner, GA 2012, *Long-term durability of polymeric matrix composites*, Springer.

Randell, P, Pickin, J & Grant, B 2014, *Waste generation and resource recovery in Australia Reporting period 2010/11*, Department of Sustainability, Environment, Water, Population and Communities, Vic, Australia.

Ratna Prasad, AV & Mohana Rao, K 2011, 'Mechanical properties of natural fibre reinforced polyester composites: Jowar, sisal and bamboo', *Materials and Design*, vol. 32, no. 8-9, pp. 4658-63.

Romanzini, D, Lavoratti, A, Ornaghi Jr, HL, Amico, SC & Zattera, AJ 2013, 'Influence of fiber content on the mechanical and dynamic mechanical properties of glass/ramie polymer composites', *Materials & Design*, vol. 47, pp. 9-15.

Rong, MZ, Zhang, MQ, Liu, YL, Yang, GC & Zeng, HM 2001, 'The effect of fiber treatment on the mechanical properties of unidirectional sisal-reinforced epoxy composites', *Composites Science and Technology*, vol. 61, pp. 1437-47.

Rout, J, Misra, M, Tripathy, SS, Nayak, SK & Mohanty, AK 2001, 'The influence of fibre treatment on the performance of coir-polyester composites', *Composites Science and Technology*, vol. 61, pp. 1303-10.

Sain, M, Park, SH, Suhara, F & Law, S 2004, 'Flame retardant and mechanical properties of natural fibre–PP composites containing magnesium hydroxide', *Polymer Degradation and Stability*, vol. 83, no. 2, pp. 363-7.

Saravanakumar, SS, Kumaravel, A, Nagarajan, T, Sudhakar, P & Baskaran, R 2013, 'Characterization of a novel natural cellulosic fiber from Prosopis juliflora bark', *Carbohydr Polym*, vol. 92, no. 2, pp. 1928-33, item: 23399239.

Sawpan, MA, Pickering, KL & Fernyhough, A 2011, 'Effect of various chemical treatments on the fibre structure and tensile properties of industrial hemp fibres', *Composites Part A: Applied Science and Manufacturing*, vol. 42, no. 8, pp. 888-95.

Scida, D, Assarar, M, Poilâne, C & Ayad, R 2013, 'Influence of hygrothermal ageing on the damage mechanisms of flax-fibre reinforced epoxy composite', *Composites Part B: Engineering*, vol. 48, pp. 51-8.

Sen, T & Reddy, H 2011, 'Application of Sisal, Bamboo, Coir and Jute Natural Composites in Structural Upgradation', *International Journal of Innovation, Management and Technology*, vol. 2, no. 3, pp. 186-91.

Shanmugam, D & Thiruchitrambalam, M 2013, 'Static and dynamic mechanical properties of alkali treated unidirectional continuous Palmyra Palm Leaf Stalk Fiber/jute fiber reinforced hybrid polyester composites', *Materials & Design*, vol. 50, pp. 533-42.

Shao, S, Wen, G & Jin, Z 2008, 'Changes in chemical characteristics of bamboo (Phyllostachys pubescens) components during steam explosion', *Wood Science and Technology*, vol. 42, no. 6, pp. 439-51.

Shi, SQ & Gardner, DJ 2006, 'Hygroscopic thickness swelling rate of compression molded wood fiberboard and wood fiber/polymer composites', *Composites Part A: Applied Science and Manufacturing*, vol. 37, no. 9, pp. 1276-85.

Shih, Y-F 2007, 'Mechanical and thermal properties of waste water bamboo husk fiber reinforced epoxy composites', *Materials Science and Engineering: A*, vol. 445-446, pp. 289-95.

Shinoj, S, Visvanathan, R, Panigrahi, S & Varadharaju, N 2011, 'Dynamic mechanical properties of oil palm fibre (OPF)-linear low density polyethylene (LLDPE) biocomposites and study of fibre–matrix interactions', *Biosystems Engineering*, vol. 109, no. 2, pp. 99-107.

Shubhra, QTH, Alam, AKMM & Beg, MDH 2011, 'Mechanical and degradation characteristics of natural silk fiber reinforced gelatin composites', *Materials Letters*, vol. 65, no. 2, pp. 333-6.

Shubhra, QTH, Alam, AKMM, Khan, MA, Saha, M, Saha, D & Gafur, MA 2010, 'Study on the mechanical properties, environmental effect, degradation characteristics and ionizing radiation effect on silk reinforced polypropylene/natural

rubber composites', *Composites Part A: Applied Science and Manufacturing*, vol. 41, no. 11, pp. 1587-96.

Shukor, F, Hassan, A, Saiful Islam, M, Mokhtar, M & Hasan, M 2014, 'Effect of ammonium polyphosphate on flame retardancy, thermal stability and mechanical properties of alkali treated kenaf fiber filled PLA biocomposites', *Materials & Design*, vol. 54, pp. 425-9.

Silva, FdA, Filho, RDT, Filho, JdAM & Fairbairn, EdMR 2010, 'Physical and mechanical properties of durable sisal fiber–cement composites', *Construction and Building Materials*, vol. 24, no. 5, pp. 777-85.

Spinacé, MAS, Lambert, CS, Fermoselli, KKG & De Paoli, M-A 2009, 'Characterization of lignocellulosic curaua fibres', *Carbohydrate Polymers*, vol. 77, no. 1, pp. 47-53.

Stamboulis, A, Baillie, C & Peijs, T 2001, 'Effects of environmental conditions on mechanical and physical properties of flax fibers', *Composites Part A: Applied Science and Manufacturing*, vol. 32, no. 8, pp. 1105-15.

Stark, NM & Matuana, LM 2004, 'Surface chemistry changes of weathered HDPE/wood-flour composites studied by XPS and FTIR spectroscopy', *Polymer Degradation and Stability*, vol. 86, no. 1, pp. 1-9.

Stark, NM, White, RH, Mueller, SA & Osswald, TA 2010, 'Evaluation of various fire retardants for use in wood flour–polyethylene composites', *Polymer Degradation and Stability*, vol. 95, no. 9, pp. 1903-10.

Suardana, NPG, Ku, MS & Lim, JK 2011, 'Effects of diammonium phosphate on the flammability and mechanical properties of bio-composites', *Materials and Design*, vol. 32, no. 4, pp. 1990-9.

Summerscales, J, Dissanayake, NPJ, Virk, AS & Hall, W 2010, 'A review of bast fibres and their composites. Part 1 – Fibres as reinforcements', *Composites Part A: Applied Science and Manufacturing*, vol. 41, no. 10, pp. 1329-35.

Sydenstricker, THD, Mochnaz, S & Amico, SC 2003, 'Pull-out and other evaluations in sisal-reinforced polyester biocomposites', *Polymer Testing*, vol. 22, no. 4, pp. 375-80.

Thwe, MM & Liao, K 2002, 'Effects of environmental aging on the mechanical properties of bamboo–glass fiber reinforced polymer matrix hybrid composites', *Composites: Part A*, vol. 33, pp. 43-52.

Thwe, MM & Liao, K 2003, 'Durability of bamboo-glass fiber reinforced polymer matrix hybrid composites', *Composites Science and Technology*, vol. 63, no. 3, pp. 375-87.

Tibiletti, L, Longuet, C, Ferry, L, Coutelen, P, Mas, A, Robin, J-J & Lopez-Cuesta, J-M 2011, 'Thermal degradation and fire behaviour of unsaturated polyesters filled with metallic oxides', *Polymer Degradation and Stability*, vol. 96, no. 1, pp. 67-75.

Tong, J, Ma, Y, Chen, D, Sun, J & Ren, L 2005, 'Effects of vascular fiber content on abrasive wear of bamboo', *Wear*, vol. 259, no. 1-6, pp. 78-83.

Truong, M, Zhong, W, Boyko, S & Alcock, M 2009, 'A comparative study on natural fibre density measurement', *Journal of The Textile Institute*, vol. 100, no. 6, pp. 525-9.

Wambua, P, Ivens, J & Verpoest, I 2003, 'Natural fibres: can they replace glass in fibre reinforced plastics?', *Composites Science and Technology*, vol. 63, no. 9, pp. 1259-64.

Wang, W, Sain, M & Cooper, PA 2005, 'Hygrothermal weathering of rice hull/HDPE composites under extreme climatic conditions', *Polymer Degradation and Stability*, vol. 90, no. 3, pp. 540-5.

Wang, W, Sain, M & Cooper, P 2006, 'Study of moisture absorption in natural fiber plastic composites', *Composites Science and Technology*, vol. 66, no. 3-4, pp. 379-86.

Wang, X, Hu, Y, Song, L, Xing, W & Lu, H 2011, 'Thermal degradation mechanism of flame retarded epoxy resins with a DOPO-substitued organophosphorus oligomer by TG-FTIR and DP-MS', *Journal of Analytical and Applied Pyrolysis*, vol. 92, no. 1, pp. 164-70.

Wielage, B, Lampke, T, Utschick, H & Soergel, F 2003, 'Processing of natural-fibre reinforced polymers and the resulting dynamic–mechanical properties', *Journal of materials processing technology*, vol. 139, no. 1, pp. 140-6.

Wong, KJ, Yousif, BF & Low, KO 2010, 'Effects of Alkali Treatment on the Interfacial Adhesion of Bamboo Fibres', *J. Mater Des. Appl.*, vol. 224, pp. 139-48.

Wong, KJ, Zahi, S, Low, KO & Lim, CC 2010, 'Fracture characterisation of short bamboo fibre reinforced polyester composites', *Materials and Design*, vol. 31, no. 9, pp. 4147-54.

WorldBank 2012, *What a waste: A global review of solid waste management*, World Bank.

Xie, Y, Hill, CAS, Xiao, Z, Militz, H & Mai, C 2010, 'Silane coupling agents used for natural fiber/polymer composites: A review', *Composites Part A: Applied Science and Manufacturing*, vol. 41, no. 7, pp. 806-19.

Yao, F, Wu, Q, Lei, Y, Guo, W & Xu, Y 2008, 'Thermal decomposition kinetics of natural fibers: Activation energy with dynamic thermogravimetric analysis', *Polymer Degradation and Stability*, vol. 93, no. 1, pp. 90-8.

Yew, M, Ramli Sulong, N, Yew, M, Amalina, M & Johan, M 2013, 'The formulation and study of the thermal stability and mechanical properties of an acrylic coating using chicken eggshell as a novel bio-filler', *Progress in Organic Coatings*, vol. 76, no. 11, pp. 1549-55.

Yousif, BF & El-Tayeb, NSM 2009, 'Mechanical and wear properties of oil palm and glass fibres reinforced polyester composites', *International Journal of Precision Technology*, vol. 1, no. 2, pp. 213-22.

Yousif, BF & Ku, H 2012, 'Suitability of using coir fiber/polymeric composite for the design of liquid storage tanks', *Materials & Design*, vol. 36, no. 0, pp. 847-53.

Yousif, BF, Shalwan, A, Chin, CW & Ming, KC 2012, 'Flexural properties of treated and untreated kenaf/epoxy composites', *Materials & Design*, vol. 40, no. 0, pp. 378-85.

Zabihzadeh, SM, Omidvar, A, Marandi, MAB, Dastoorian, F & Mirmehdi, SM 2011, 'Effect of filler loading on physical and flexural properties of rapeseed stem/PP composites', *BioResources*, vol. 6, no. 2, pp. 1475-83.

Zhang, ZX, Zhang, J, Lu, B-X, Xin, ZX, Kang, CK & Kim, JK 2012, 'Effect of flame retardants on mechanical properties, flammability and foamability of PP/wood–fiber composites', *Composites Part B: Engineering*, vol. 43, no. 2, pp. 150-8.

Zou, L, Jin, H, Lu, W-Y & Li, X 2009, 'Nanoscale structural and mechanical characterization of the cell wall of bamboo fibers', *Materials Science and Engineering: C*, vol. 29, no. 4, pp. 1375-9.

Appendix A: Acrylic Coating Technical Data Sheet

TECHNICAL DATA SHEET

PRODUCT NAME	Ultralast™ WEATHER PROTECT	
PRODUCT CODE – UWP		Data Sheet No. TDS-UWP001

DESCRIPTION

Ultralast WEATHER PROTECT is non-hazardous water based acrylic clear electrometric coating engineered for maximum durability while staying safe and easy to apply. It is an excellent weather resistant topcoat system that leaves an alluring optically clear wet look finish. This unique Zero-VOC technology provides ultra durable protection against UV rays, micro organisms, moisture, rotting, abrasion and chemical exposure while allowing to flex to resist minor cracking compared to conventional oil based coatings.

WHERE TO USE

Ultralast WEATHER PROTECT has been developed to be used on any and all substrates that require that extra WEATHER PROTECTION. Ideal for interior and exterior timber, concrete, brick, sandstone, terracotta tiles , mild steel , plastic, glass, etc.....

FINISH/APPEARANCE

Optically Clear, wet look finish. Available in Low Sheen, Satin and Gloss.

ADVANTAGES

• UV Resistant	• Remains Flexible	• Non-toxic and odourless	• No Cracking
• Waterproofing property	• Heat resistance	• Fire resistance	• Stain Resistance
• Excellent permeability	• No chipping or scaling	• Ani-Graffiti Properties	

SURFACE PREPARATION

General – All surfaces to be COATED with WEATHER PROTECT should be free from oil, fats, flaking or poorly adhering paint and dirt.
Depending on the substrate abrasive sand papers should be used if not sandblasting or high pressure jet washing to ensure the surface is thoroughly rinsed off prior to application. Bulk concrete would Usually have to cure for 28 days minimum prior to coating.
Please refer to **ULTRALAST** Surface Preparation information for specific substrates.

DATA SHEET	Ultralast WEATHER PROTECT	Product Code	UWP
Data Sheet No.	TDS-UWP001	Date Revised	21/05/13
Contact	+61 2 8338 9997	Page No.	1 of 3

A-1

ultralast
E C O A T I N G   S Y S T E M

TECHNICAL DATA SHEET

PRODUCT NAME   Ultralast™ WEATHER PROTECT

PRODUCT CODE – UCG   **Data Sheet No. TDS-UCG001**

APPLICATION PROCEDURE

Stir or shake contents thoroughly prior to application. Allow to settle for ten minutes for bubbles to minimise before commencing application.

Supplied readily thinned and suitable for application by conventional paint brush, roller, lambs wool or synthetic applicator pad or spray. On Highly Porous substrates you require to apply one coat of Ultralast **BOND**, lightly sand after dry then apply the required two to three coats of Ultralast **WEATHER PROTECT**. On Non-Porous substrates such as previously painted surfaces, we suggest to remove as much of the coating with 80 grit sandpaper, then sand smooth with fine before commencing application. Always ensure previous coat is thoroughly dry and tack-free before applying the next coat.

We recommend that a small test area is tested for product and application suitability prior to any large projects being undertaken. Please refer to **ULTRALAST** Application and data information for specific applications.

STORAGE AND APPLICATION

STORAGE	APPLICATION	SUBSTRATE	ENVIROMENT
Store in a cool dry Shaded Area	MAX 25°C in direct Sunlight.	Min 5°C above dew Point	Relative Humidity
5°C - 25°C	5°C - 40°C	5°C - 40°C	MAX 85%

PACK SIZE

1 lt	5 lt	10 lt	15 lt	20 lt

TYPICAL PROPERTIES AND APPLICATION DATA

COLOUR	Wet - Milky White Dry - Optically Clear	THINNER	Can thin with MAX 10% Ultralast BOND.
TOUCH DRY	20-30 min @ 21°C Recoat 1 hour.	% SOLID BY VOLUME	41%
NUMBER OF COATS	2-3 coats. Number of coats will be determined by substrate & required finish.	APPLICATION METHOD	Paint brush, roller, lambs wool or synthetic applicator pad or spray
COAT OVER Bond	Within 12 hrs.	CLEAN UP	Water
SHELF LIFE	7 *Years.	TOXICITY	Non-Toxic
APPROX DRY FILM PER COAT	25-35 microns	SPECIFIC GRAVITY	1.02*
FINISH	Satin	ODOUR	Odourless
FLASH POINT	Water borne- not flammable	COMPONENTS	ONE PART
VEHICLE TYPE	Acrylic	SPREAD RATE	12-14m² / litre per coat*

DATA SHEET	Ultralast WEATHER PROTECT	Product Code	UWP
Data Sheet No.	TDS-UWP001	Date Revised	21/05/13
Contact	+61 2 8338 9997	Page No.	2 of 3

ultralast
E C O A T I N G   S Y S T E M

TECHNICAL DATA SHEET

PRODUCT NAME   **Ultralast™ WEATHER PROTECT**

PRODUCT CODE – UCG | **Data Sheet No. TDS-UCG001**

HEALTH AND SAFETY

Health Effects
For detailed information refer to the product label and the current Material Safety Data Sheet available through Customer Service. Splashes to the eye may cause eye irritation.
When spraying, inhalation of mists may produce respiratory irritation.
Protective Equipment
Wear eye protection and when spraying wear a dust mask.

In the case of emergency please call your local emergency line.

PRECAUTIONS AND LIMITATIONS

Do not use at temperatures below 5°C, or when the temperature of surface may fall below 5°C during the drying period.

Avoid exposure to steam, water heavy foot traffic for at least three days. The product will fully cure within seven days.

Ensure that Ultralast **WEATHER PROTECT** is thoroughly stirred or shaken before use.

Ultralast **WEATHER PROTECT** may be diluted or thinned with MAX 10% Ultralast **BOND**.

Ultralast **WEATHER PROTECT** may go milky white if being exposed to water for a period of time i.e. continuous rain, ingress of water or has been applied on a surface that is damp. This effect does not alter the performance of the product and 'spotting' will disappear once product has dried or cured back to its natural state.

Note:
- The recommendations contained in these data sheets are based on results obtained from tests and experience. It is believed to be reliable, but is given as a guide only.
- No guarantee is implied by the recommendations contained herein since conditions of use, method of application and preparation of the substrate prior to painting are beyond our control.
- Our technical section should be contacted to clarify recommendations and specifications for projects, either of a specific or general nature.
- This * represents the approximate within 0.1-1% in values.

Please note that this document is only valid for 60 days from date revised.

DATA SHEET	Ultralast WEATHER PROTECT	Product Code	UWP
Data Sheet No.	TDS-UWP001	Date Revised	21/05/13
Contact	+61 2 8338 9997	Page No.	3 of 3

Appendix B: Preliminary Study on the Thermal Degradation of Kenaf Fibre/Epoxy Composite

A preliminary work was performed to study the degradability behaviour of natural fibre/polymer composite exposed to high temperature. The findings were used to draft the experimental work for Chapter Five. The study was performed on kenaf fibre/epoxy composites and neat epoxy. The effect of alkalisation treatment on the thermal degradation of kenaf fibre/epoxy composite was also observed.

B.1   Thermo Gravimetric Analysis

Figures B1 and B2 shows the TGA and DTA curves obtained from the runs.
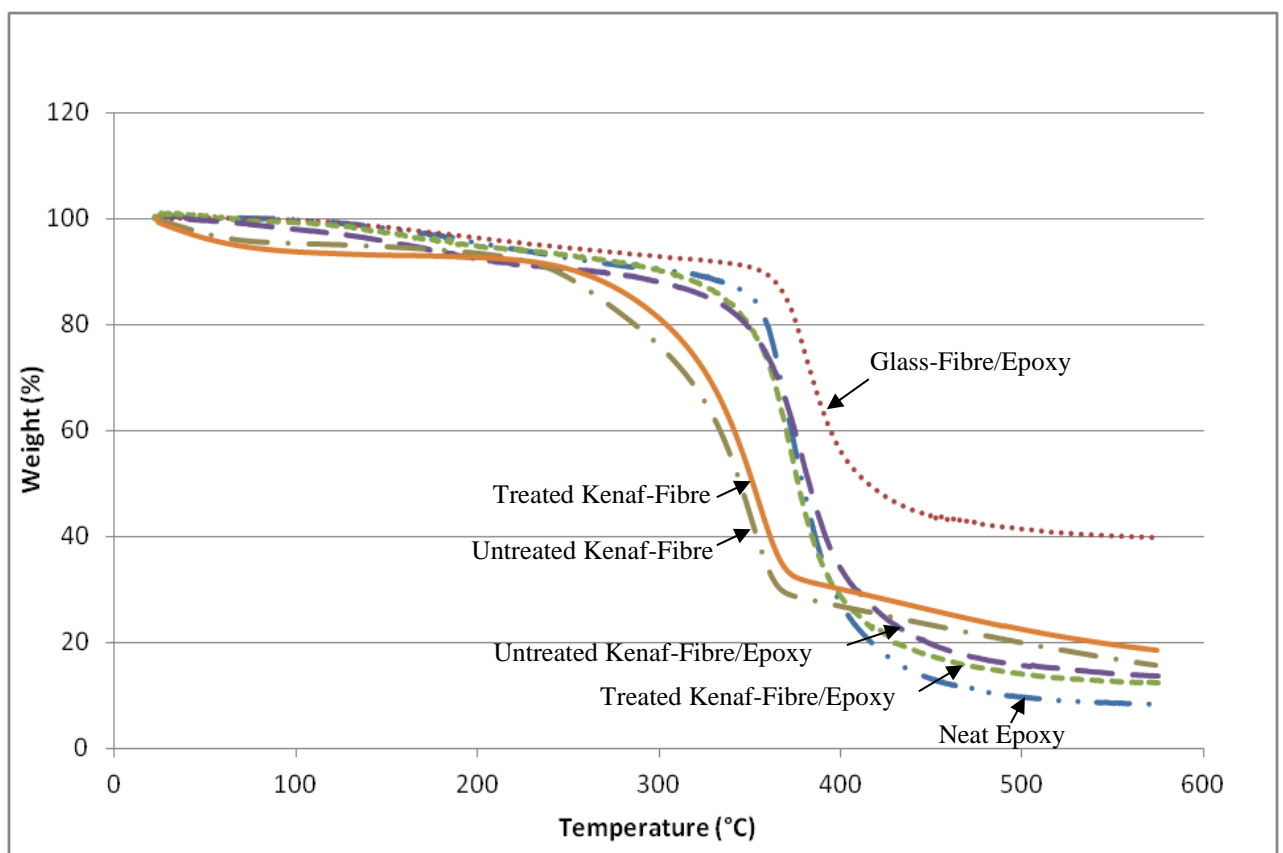
Figure B1: Thermo Gravimetric Analysis (TGA) curves
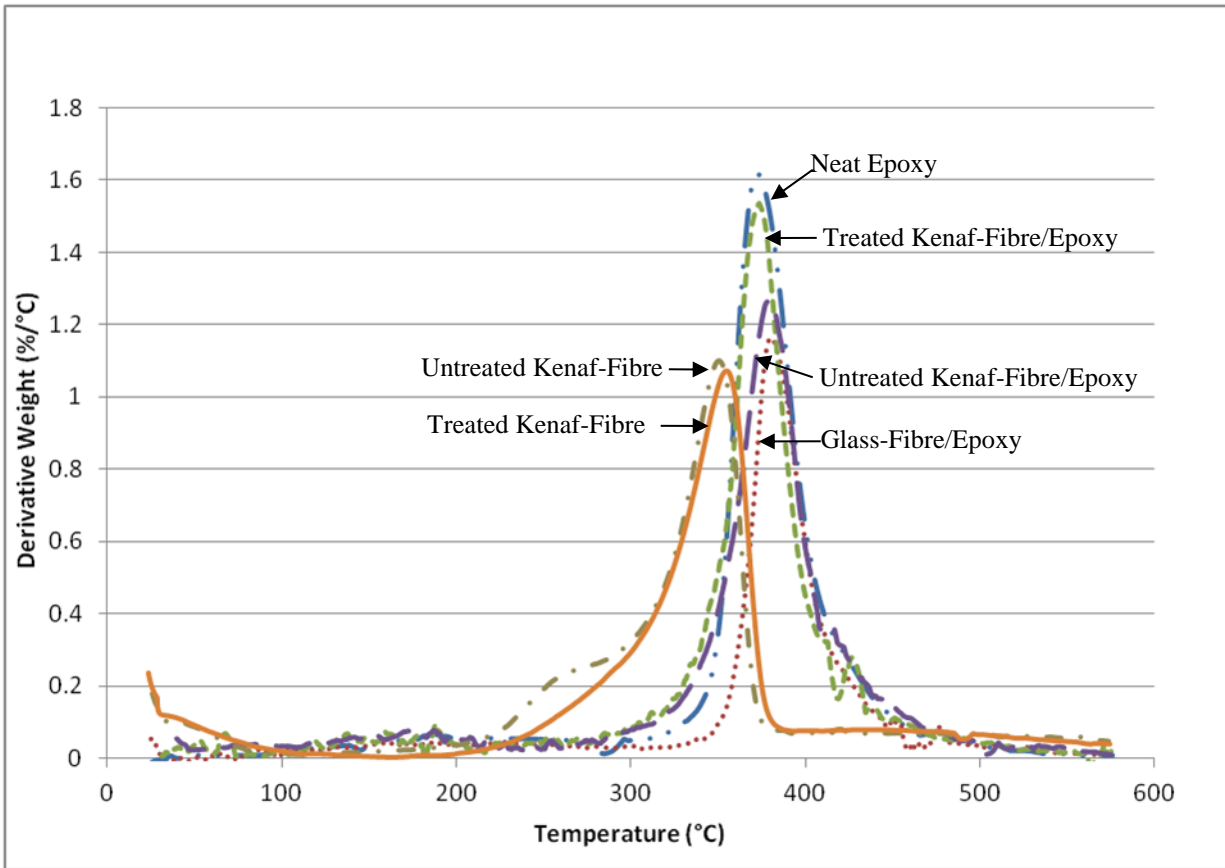
Figure B2: Differential Thermal Analysis (DTA) curves

The data from both curves were extracted and presented in Table B1. From Figure B.1, it can be seen that the untreated kenaf/epoxy composite starts to lose weight earlier than the other samples. This may be attributed to the higher moisture content of untreated fibres whereby, the presence of hemicelluloses has caused higher moisture absorption of the composite. It has been reported in many studies that untreated fibres do not effectively bond with polymer. The porous space between the fibre/matrix interfaces is a possible area for moisture to reside. Moisture evaporates from the sample starting at 80°C. Based on Monteiro et al. (2012), this initial drop in the TGA graph is usually ignored or overlooked by most. Total elimination of water in a natural fibre composite is impossible, even with oven drying prior to fabrication. The hydrophilic nature of the kenaf fibres can be observed for both treated and untreated fibres as they show a much higher early weight loss.

Alkali Treatment (wt.%)	Epoxy	Glass Fibre/ Epoxy	Treated Kenaf-Fibre/Epoxy	Untreated Kenaf-Fibre/Epoxy	Treated Kenaf-Fibre	Untreated Kenaf-Fibre
Decomposition Temperature (°C)	372	380	373	378	350	346
Final Weight after Decomposition (%)	8.29	39.83	12.46	13.67	18.96	16.21
Increment in Thermal Stability from Epoxy (%)	-	2.19	0.40	1.79	-	-
Increment in Char Production from Epoxy (%)	-	380.46	50.30	64.90	-	-

The percentage of weight reduction at 500°C reflects the amount of residues left after the composites were degraded. Epoxy has the lowest residue due to the absence of char. Treated kenaf/epoxy composite had lower residue than untreated kenaf/epoxy composite. Some researchers believed that his is due to the removal of lignin through alkalisation. Lignin in natural fibre is responsible for charring thus untreated kenaf/epoxy composite will have more char (Beg & Pickering 2008; Kabir et al. 2012; Norul Izani et al. 2013). However, based on the TGA graphs of the fibres, treated fibres were observed to leave more chars. This was also observed by Elenga et al. (2013) on Raffia textilis fibres, where 5 and 10% NaOH treated fibres left more residues at the end of the TGA run. The authors suggested that more analysis should be performed on the residues and the gases emitted during heating in order to further understand this behaviour.

The peaks of the DTA curves correspond to the decomposition temperature of each constituent of the composites. However, from Figure B2, only one peak is obvious for all composites due to the overlapping peaks of the fibres and epoxy. It seems that neat epoxy has the lowest decomposition temperature at 372°C while the addition of fibres had shifted the curves to higher temperatures. For the untreated kenaf fibre, two obvious peaks can be observed. The first peek at 260°C corresponds to the decomposition of hemicelluloses while the second peak at 346°C is due to the decomposition of cellulose. With alkalisation, partial removal of hemicelluloses is expected and this is reflected on the decrease in the first peak of the DTA curve for treated kenaf fibres, while the second peak is observed to increase to 350°C. In engineering applications, the first DTA peak which corresponds to the initiation of the decomposition of the material is more important than the subsequent peaks at higher temperatures (Monteiro et al. 2012). Thus from here, we can say that with the removal of hemicelluloses, the decomposition of kenaf fibres were initiated at a higher temperature.

However, as a composite, the treated kenaf-fibre/epoxy is decomposed at a slightly lower temperature than the untreated ones. This contradicts some studies that states that with the reduction of hemicelluloses and lignin from fibre treatment, thermal stability is increased (Beg & Pickering 2008; Methacanon et al. 2010). The minor difference in decomposition temperatures between treated and untreated kenaf fibres and their composites is about ±5°C, which is within the experimental error of most TGA equipment thus from these results, the improvement or decrement in thermal

stability of kenaf fibres due to alkalization on its polymeric composites cannot be clearly observed and may have insignificant influence.

From these results, it can be highlighted that the thermal stability of kenaf fibre/epoxy may not only be dependable on the chemical composition of the fibres alone. However, it is noteworthy that through alkalisation, some parts of the fibre itself may experience partial removal of hemicelluloses and lignin, while some parts may experience total removal with some effect on the cellulosic component. The removal of cell walls of fibres and some cellulose may also have an effect on the thermal protection of the kenaf fibres. As expected, glass fibre improved the thermal resistance of the composite the most and gives a charring structure at the end of the test.

B.2   Weight Loss of Samples at Different Temperatures

The graphs in Figure B3 were yielded from the furnace pyrolysis method. Through this method, the behaviour of the samples at a certain temperature can be evaluated more thoroughly. It can be seen that on average, the weight loss for neat epoxy is the lowest for all four temperature settings. The thermal degradation of epoxy causes decrease in mass due to the production of gaseous products like methane, carbon monoxide, carbon dioxide and water vapour (Wang et al. 2011). Kenaf fibres have lower thermal stability thus it loses more weight than epoxy even at lower temperature. Voids at the fibre/matrix interfaces that are present on the composites after degradation do not apply to neat epoxy, thus this may be attributed to the relatively lesser weight reduction. A review done by Monteiro et al. (2012) had highlighted that Kenaf fibres lose 50 wt.% of its original weight at 341°C while neat epoxy lose 50 wt.% of its original weight at 398°C.
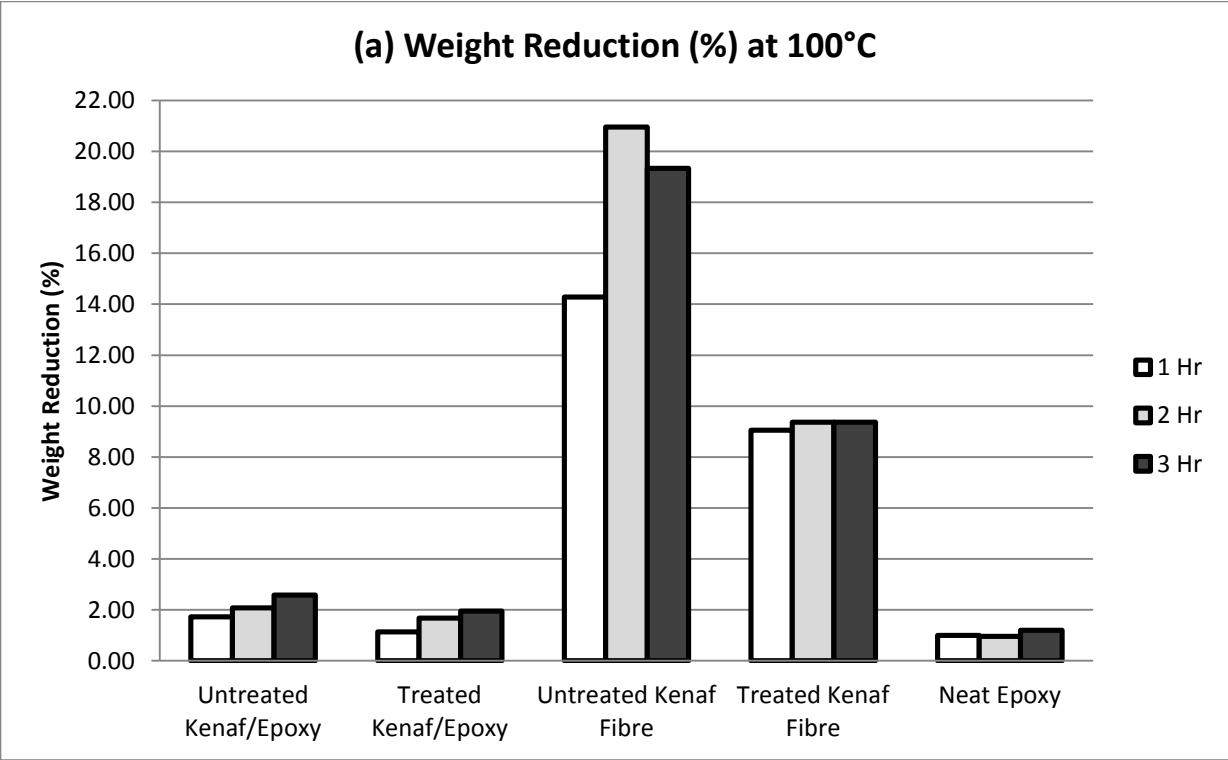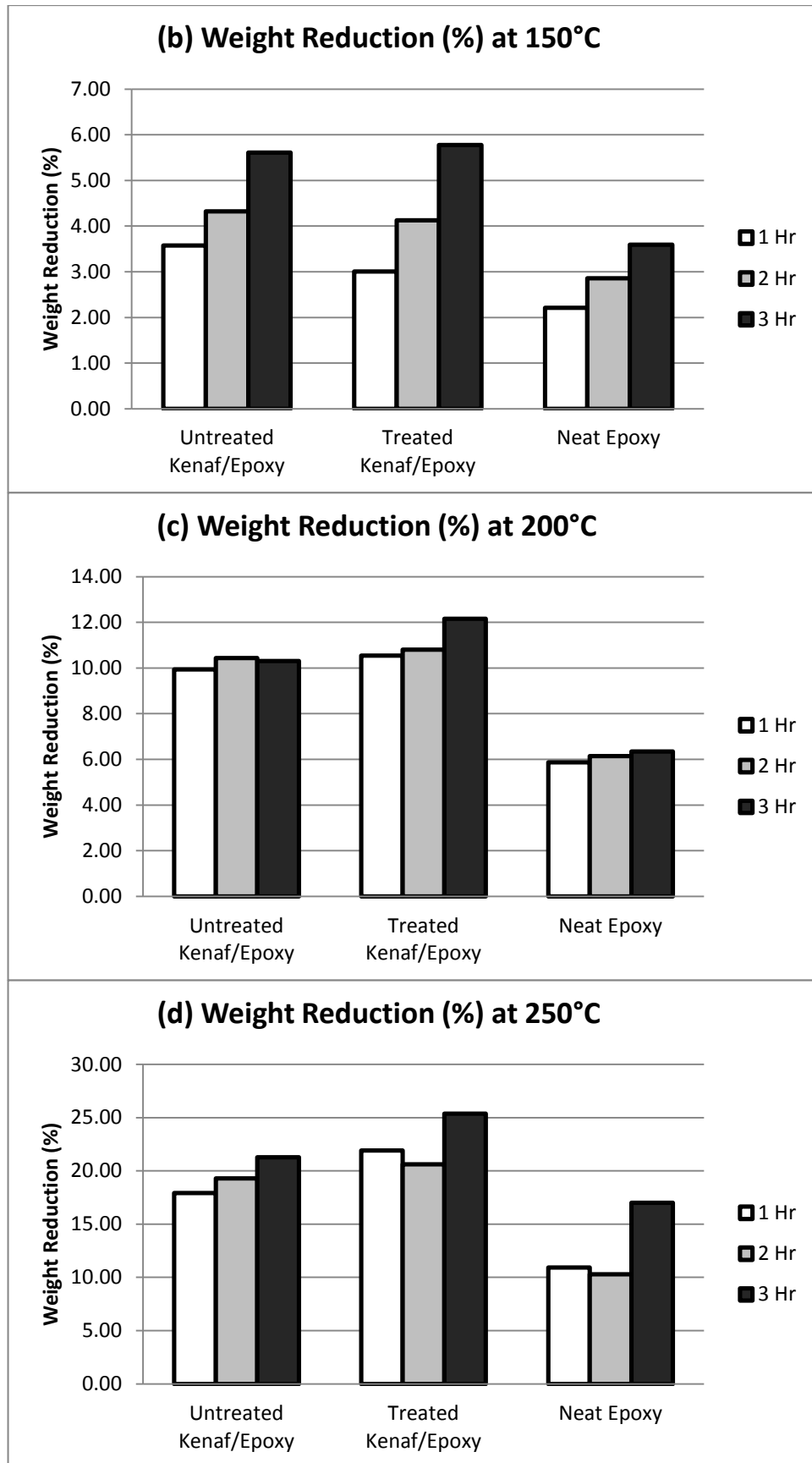
Figure B3: Weight loss of samples at different temperatures

Treated kenaf/epoxy composite experienced lower weight loss than untreated kenaf/epoxy composite only up to 100°C, whereby, its weight loss becomes similar to untreated kenaf/epoxy composite at 150, 200, and 250°C. This may be attributed to the higher moisture content present in untreated kenaf fibres. At room temperature, the untreated kenaf fibres have a moisture content of 6.38%, which is nearly twice the moisture in treated fibres which is 3.85%. Moisture is removed through evaporation at 100ºC, whereby, a 14% weight reduction was observed at 1 hour exposure and 20% weight reduction at longer hours. The weight reduction in treated fibres for all duration of exposures was less than 10%. Due to the significantly higher weight loss of the fibres, test for fibres was conducted only at 100ºC. In a composite form, poor interfacial adhesion between untreated kenaf fibre and epoxy causes void spaces in the composites which may also lead to higher water uptake (Hamid et al. 2012). This behaviour can be further investigated using scanning electron microscopy.

In general, the duration of exposure plays an influential role on the weight loss of the samples only up to 150ºC. Although this weight loss due to moisture evaporation is small, however, the voids caused by the evaporated moisture might have an impact on the mechanical strength of the composites (Monteiro et al. 2012). At higher temperatures, the increased length of duration after 1 hour has lesser effect on the weight loss. It can be concluded that at temperature higher than 150ºC, the rate of thermal degradation is increased and the weight loss process is faster for all samples.

B.3   Physical and Morphological Changes

The physical appearances of the samples were observed and are presented in Figure B4. Both the kenaf composites and neat epoxy still maintain the same appearance at 100ºC. At 150 to 200ºC, all samples darkened, with fine cracks observed on treated and untreated kenaf composites. The occurrence of these cracks may be attributed to the debonding at the fibre/matrix interface that progress as cracks to the composite surface. The samples experienced shrinkage at 250ºC as the epoxy dehydrates. The surfaces of the kenaf composites were uneven due to the protrusion of the fibres as the epoxy and the fibres shrink at a different rate.
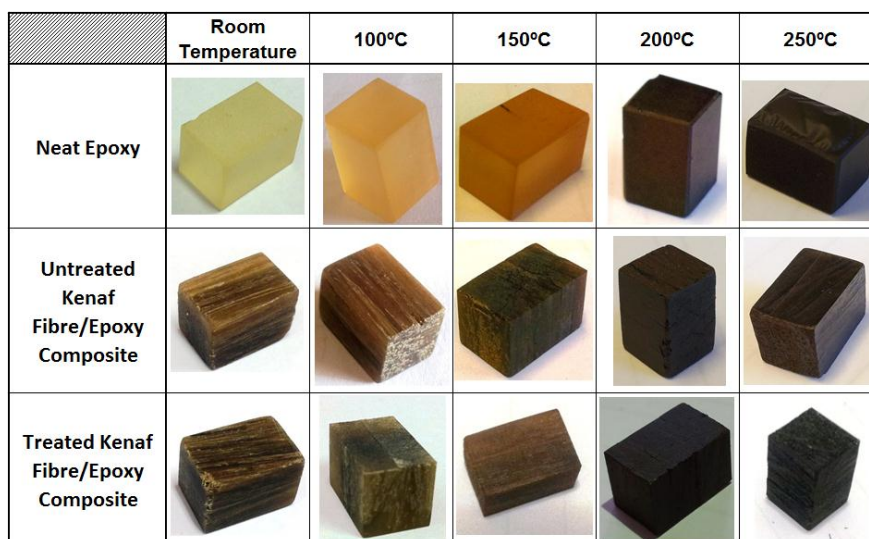
Figure B4: Physical observation of kenaf/epoxy composite and neat epoxy at different temperature exposure

Using SEM, the morphology of the degraded samples was studied. The SEM observations reflect the results of the weight loss of the samples as discussed earlier. Neat epoxy basically experience some polymer melts and defragmentations as shown in Figure B.5. It can be seen that no voids are present, even at 200ºC.
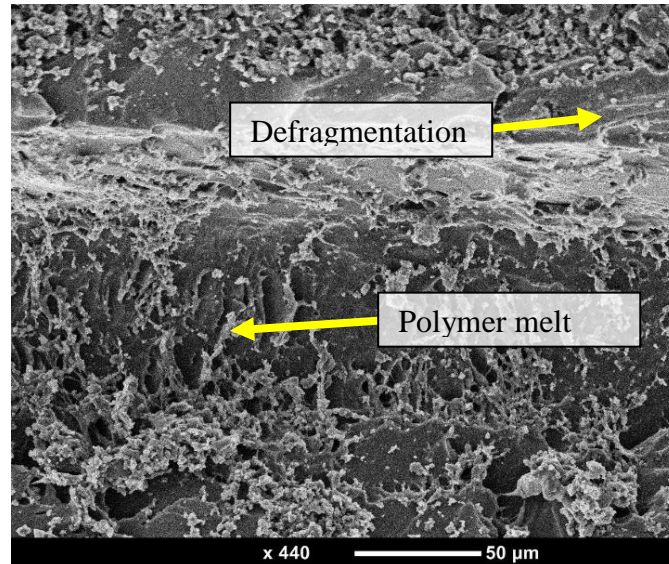
Figure B5: SEM of epoxy at 200 ºC

For the untreated kenaf-fibre/epoxy composites, it is obvious that more voids are present along the fibre-matrix interface, as can be seen at 100ºC, suggesting weak interfacial adhesion. These areas provide spaces for moisture to occupy thus making untreated kenaf composites more vulnerable to moisture attack as compared to the treated ones, which explains its higher initial weight loss. At lower temperature, treated kenaf-fibre/epoxy composite has better fibre/matrix bonding due to the removal of hydrophobic components of the fibre, allowing better compatibility between the kenaf fibre and the epoxy. However, at higher temperatures, both composites suffer fibre/matrix debonding and fibre fibrillation due to the degradation of less stable components of the kenaf fibres as well as shrinkage of the epoxy. These two composites have similar morphologies at 250ºC as shown in Figure B6. The cavities present may represent the high percentage of weight reduction as compared to the neat epoxy. An observation by Ezekiel et al. (2011) on the SEM of heated coir fibres revealed that coir fibres experienced microcracks and open micropores when heated at 150ºC for 20 min. Microfibrils collapsed was apparent when heated at 200ºC for 30 min. Cooled molten liquid pouring out from these micropores may be hemicelluloses or other low molecular weight components. From here, we can say that the leaching of these components from the kenaf fibres may also contribute to the weight loss of the composites.

Untreated Kenaf/Epoxy Composite	Treated Kenaf/Epoxy Composite
100 ºC	

200 ºC	

250 ºC	
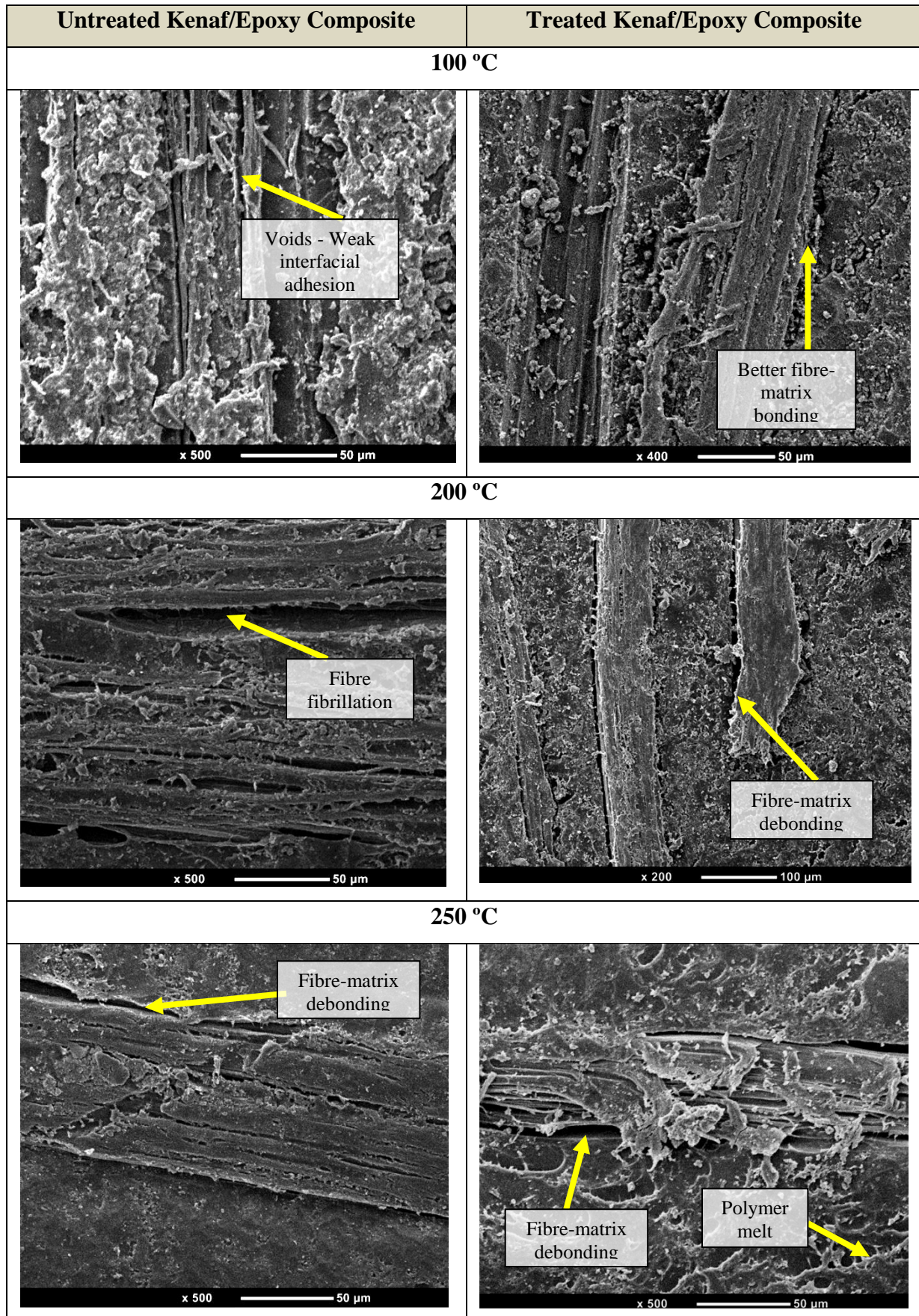
Figure B6: SEM of treated and untreated kenaf/epoxy composite at different temperature exposure

B-8

B.4   Conclusion

Treated and untreated kenaf-fibre/epoxy composites were subjected to thermal degradation by means of Thermo Gravimetric Analysis (TGA) and furnace pyrolysis. From this study, it can be concluded that:

1) Untreated kenaf fibres have higher moisture content than treated fibres, 6.38% and 3.85%, respectively. This influence the weight loss behaviour of the kenaf fibres itself, as well as their corresponding composites. Treatment has helped lessen the percentage weight loss of the fibres and the composites due to heat exposure. With less voids and hemicelluloses on treated composites, moisture is not able to reside within the composites. Untreated fibres have shown lower decomposition temperature and lesser residues at the end of the TGA run. Higher residues for untreated fibres were observed by some researchers that was attributed to higher lignin of raw fibres (Beg & Pickering 2008; Norul Izani et al. 2013). However, this study agrees with Elenga et al. (2013) who noticed higher residues for treated fibres and recommends further analysis on the gaseous and residue content of the decomposed fibres.

2) The addition of fibres into the epoxy composites improves the thermal stability of the composites as well as its charring capability. However, alkalisation reduces the decomposition temperature of the kenaf-fibre/epoxy composite and produces lesser char than untreated composite. From some reported works, the removal of lignin through fibre treatment will increase the decomposition temperature of the composite (Beg & Pickering 2008; Kabir et al. 2012). However, the current study contradicts this and a slightly lower decomposition temperature was observed for treated composites. Further investigation on the contribution of the chemical components of the fibres to these behaviours is highly recommended.

3) From the furnace pyrolysis test, the exposure temperature up to 250°C causes kenaf-fibre/epoxy composites to experience weight loss due to the release of gaseous components from the polymer such as CO, CO_2 and H_2O and the evaporation of moisture and degradation of lower molecular weight components such as hemicellulose from the fibre. It was observed that increased exposure time for more than 1 hour generally causes more weight loss of the composites only up to the temperature of 150ºC. At higher temperatures, the rate of weight loss is faster thus the increased exposure time has lesser influence on the weight loss process. Also, it can be highlighted that at lower temperatures, the weight loss is mainly due to evaporation of water. Once all water molecules are removed, the composites will be fairly stable until approximately 300ºC (as seen on the TGA curves), whereby decomposition of the main components of the composites start to take place.

4) The samples physically experience shrinkage at 250ºC with kenaf-fibre/epoxy composites demonstrates fine cracks starting at 150ºC, which is attributed to the fibre/matrix debonding. Thus it is expected that kenaf-fibre/epoxy composites will suffer a great reduction of its mechanical properties at this temperature.

B.5   References

Beg, MDH & Pickering, KL 2008, 'Accelerated weathering of unbleached and bleached Kraft wood fibre reinforced polypropylene composites', *Polymer Degradation and Stability*, vol. 93, no. 10, pp. 1939-46.

Elenga, RG, Djemia, P, Tingaud, D, Chauveau, T, Maniongui, JG & Dirras, G 2013, 'Effects of Alkali Treatment on the Microstructure, Composition, and Properties of the Raffia textilis Fiber', *BioResources*, vol. 8, no. 2, pp. 2934-49.

Ezekiel, N, Ndazi, B, Nyahumwa, C & Karlsson, S 2011, 'Effect of temperature and durations of heating on coir fibers', *Industrial Crops and Products*, vol. 33, no. 3, pp. 638-43.

Hamid, MRY, Ab Ghani, MH & Ahmad, S 2012, 'Effect of antioxidants and fire retardants as mineral fillers on the physical and mechanical properties of high loading hybrid biocomposites reinforced with rice husks and sawdust', *Industrial Crops and Products*, vol. 40, pp. 96-102.

Kabir, MM, Wang, H, Lau, KT, Cardona, F & Aravinthan, T 2012, 'Mechanical properties of chemically-treated hemp fibre reinforced sandwich composites', *Composites Part B: Engineering*, vol. 43, no. 2, pp. 159-69.

Methacanon, P, Weerawatsophon, U, Sumransin, N, Prahsarn, C & Bergado, DT 2010, 'Properties and potential application of the selected natural fibers as limited life geotextiles', *Carbohydrate Polymers*, vol. 82, no. 4, pp. 1090-6.

Monteiro, SN, Calado, V, Rodriguez, RJS & Margem, FM 2012, 'Thermogravimetric behavior of natural fibers reinforced polymer composites—An overview', *Materials Science and Engineering: A*, vol. 557, pp. 17-28.

Norul Izani, MA, Paridah, MT, Anwar, UMK, Mohd Nor, MY & H'ng, PS 2013, 'Effects of fiber treatment on morphology, tensile and thermogravimetric analysis of oil palm empty fruit bunches fibers', *Composites Part B: Engineering*, vol. 45, no. 1, pp. 1251-7.

Wang, X, Hu, Y, Song, L, Xing, W & Lu, H 2011, 'Thermal degradation mechanism of flame retarded epoxy resins with a DOPO-substitued organophosphorus oligomer by TG-FTIR and DP-MS', *Journal of Analytical and Applied Pyrolysis*, vol. 92, no. 1, pp. 164-70.